STUDIES ON TRANSITION METAL TETRAAZA MACROCYCLIC COMPLEXES

Timothy I Hyde

Ph.D. Thesis

University of Edinburgh

1987

Declaration

Except where specific reference is made to other sources, the work presented in this thesis is the original work of the author. It has not been submitted, in whole or in part, for any other degree. Certain of the results have already been published.

T.I. Hyde

"It has been said that we need three bones in our lives - a backbone to have courage and purposefulness, a wishbone to follow the dreams in our hearts, and a funny bone to be able to laugh when the going gets tough"

Acknowledgements

The author wishes to thank Dr. M. Schröder for his help and encouragement throughout the course of this work. I wish to express my gratitude to Drs. R.O. Gould and A.J. Blake for all their crystallographic determinations. I also wish to thank Dr. R.B.A. Pardy and Dr. A.J. Lavery for their invaluable contributions to this study. In addition, I am grateful to Dr. D. Reed, Mr. J.R.A. Millar and Mr. L.H. Bell for recording ^{13}C and ^{1}H n.m.r. spectra, to Mrs. E. MacDougall for performing microanalytical measurements, Mr. A.T. Taylor for recording all mass spectral data and to B.P. Chemicals, Saltend, Hull for the use of their laboratory facilities.

I am deeply indebted to B.P. Chemicals and the S.E.R.C. for their financial support, and to the University of Edinburgh for the use of their facilities. Finally my thanks to Mrs. Christian Ranken for typing this thesis.

ABSTRACT

Chapter 1

An introduction to the work in the thesis is given. A survey of the literature describes general methods of synthesis of transition metal macrocycles and porphyrins and their relevance to substrate binding and activation. The aims of this study are introduced.

Chapter 2

The synthesis and characterization of four neutral 14-membered tetraaza 2,6-pyridyl macrocycles L^1-L^4 with varying carbon and nitrogen alkylation is described. Extensive ^1H and ^{13}C n.m.r. studies in combination with a single X-ray crystal structure of the free ligand $L^1.H_2O$ were undertaken. The free ligand was found to adopt a puckered arrangement in order to minimise nitrogen donor lone pair interactions.

Chapter 3

The insertion of the platinum metals Ru(II), Rh(III), Ir(III), Pd(II), and Pt(II) into the tetraaza macrocyclic ligands L^1-L^4 is described. All new compounds were fully characterized by n.m.r., infrared and mass spectral techniques and by the X-ray crystal structures of *cis*$[RuL^3(CO)Cl]BPh_4$, *trans*$[RhL^2Cl_2]PF_6$, *cis*$[IrL^4(H)Cl]PF_6$ and $[PdL^1](BPh_4)_2$. The Rh(III) and Pd(II) structures both show the macrocyclic ligands bound to four equatorial sites around each metal centre. In contrast the Ir(III) and Ru(II) complexes display folded ligand structures with one nitrogen

donor, N(7), bent away to occupy an apical position to give *cis* coordination of the remaining two ligands. ^{1}H and ^{13}C n.m.r. studies indicated that in most cases several ligand isomers were present in solution.

Chapter 4

The X-ray crystal structure of the square planar $[Pd(TMC)]^{2+}$ cation shows the macrocycle to adopt the R.S.R.S. conformation.

The complex shows a fully reversible one electron reduction process in acetonitrile at $E_{\frac{1}{2}}$ = -1.45V vs. Ag/Ag^{+}, ΔEp=65mV at Pt electrodes. Controlled potential electrolysis of $[Pd(TMC)]^{2+}$ at -1.50V in acetonitrile afforded a reduction product which was assigned as a d^9, Pd(I) complex $[Pd(TMC)]^{+}$, (g_{11}=2.302, $g_{\perp}$=2.076) with coupling to ^{105}Pd (22.2%, I=5/2), A_{11}=53, $A_{\perp}$=40G. From an investigation of TMC and six other tetraaza macrocyclic complexes, the Pd(II)/(I) redox couple was found to occur at potentials on average 300mV more cathodic than the corresponding Ni(II)/(I) couples. No Pd(II)/(III) redox process was observed within the anodic range of the acetonitrile solvent; this contrasts with the corresponding nickel macrocyclic complexes which all show Ni(II)/(III) redox couples in the range +0.68→+1.33V.

Chapter 5

A comparison of the redox chemistry of the square planar nickel diiminopyridyl macrocyclic complexes $[Ni(n_3X)]^{2+}$ was investigated. (X = n,p where n_4, n_3p are respective tetraaza and triazaphosphorus donor sets). Both complexes show two

reversible one electron reductions. Characterization of the first reduction product by e.s.r. spectroscopy shows the reduction of $[Ni(n_4)]^{2+}$ to be ligand based, whereas for $[Ni(n_3p)]^{2+}$ the reduction was found to be metal based. The binding of CO, phosphines and related ligands to the monovalent complex is described. The single crystal X-ray structure of $[Ni(n_3p)](PF_6)_2$ was determined confirming the square planar nickel geometry.

A structural investigation of the monohalo derivatives $[Ni(n_3X)Cl]^+$, (X = p,s, where n_3s is a triazathia donor set) was undertaken. $[Ni(n_3p)Cl]^+$ shows a 5 coordinate square based pyramidal geometry around Ni(II) analogous to the previously reported $[Ni(n_4)Br]^+$ complex. In contrast a dimeric structure with dichloro bridges between octahedral nickel(II) centres is found for the sulphur analogue $[Ni(n_3s)Cl]_2^{2+}$.

Chapter 6

Parallel studies were instigated into the isoelectronic reactions of $[NiL]^+$ with dioxygen and $[NiL]^{2+}$ with superoxide ion in acetonitrile at 230K (L = TMC, C-*rac* HMC). The product of the reactions was a reactive paramagnetic pale green solution with an anisotropic e.s.r. signal, $g_{\perp}=2.195$, $g_{\parallel}=2.056$. ^{61}Ni labelling experiments confirmed the predominantly metal based radical nature of the species of proposed stoichiometry $[NiL(O_2)]^+$. A respective one or two electron transfer from nickel to superoxide or dioxygen is proposed to form a reactive, formal nickel(III) - peroxo complex. A rhombic e.s.r. signal from a paramagnetic green solution for L=TMC is also assigned as a nickel(III) - peroxo species.

Contents Page

List of Tables and Figures

Page

CHAPTER 1

Introduction

Introduction

1.1 The Thermodynamics of Macrocyclic Chemistry

The greater stability observed in a series of copper(II) tetraaza macrocyclic complexes when compared to linear polydentate ligand analogues was first described by Margerum and Cabbiness and termed the "macrocyclic effect"[1]. The macrocyclic effect is linked to the Gibbs energy term, ΔG, referring to the metathetical reaction [1].

$$\underset{\text{(non-cyclic)}}{[ML]^{n+}} + \underset{\text{(macrocyclic)}}{L^m} \rightarrow \underset{\text{(macrocyclic)}}{[ML^m]^{n+}} + \underset{\text{(non-cyclic)}}{L} \qquad [1]$$

The enhanced stability of the macrocyclic complex has aroused much debate as to its thermodynamic origins with both entropic[2,3], enthalpic[4,5] or a combination of both terms[6,7,8] proposed. Recent results on an extensive series of copper(II) tetraaza macrocycles with 12-16 membered ring size and their open chain analogues suggest the origin is mainly entropic[8]. Clay,[8] in agreement with Kimura and Kodama[3] concluded that the enhanced stability arose from favourable changes in ΔS arising from the increased number of particles in solution [2].

$$[M(H_2O)_6]^{2+} + L^m \rightarrow [ML^m]^{2+} + 6H_2O \qquad [2]$$

A relatively small but usually favourable enthalpic contribution, due to the difference in solvation terms of the free ligands L, L^m is also observed. The more compact, cyclic ligand is generally less solvated than the non-cyclic

analogue and therefore less energy is expended in its desolvation step[4].

Metal complexes of macrocyclic ligands therefore typically show;

i) a marked kinetic inertness towards <u>both</u> complex formation and dissociation[9]. Cabbiness and Margerum found that under equivalent conditions rates of formation of Cu(II) cyclic tetraaza complexes are *ca.* 10^6 slower than open chain analogues. Rates of decomposition 10^7 slower than open chain analogues impart a greater stability to the cyclic complex[9].

ii) A high thermodynamic stability which is reflected in stability constants several orders of magnitude larger than corresponding complexes with linear ligands[1].

iii) Strong metal-donor atom interactions within the macrocycle result in large in-plane ligand field values[10].

The macrocyclic ligand normally allows for the stereochemistry of the complex to be maintained during a change in oxidation state of the central metal ion.

The macrocycle can therefore be regarded as a protecting group for the metal centre controlling its stereochemical, electronic and redox properties. These factors are required in the function of many natural product systems. Consequently the macrocyclic moiety, usually in the form of a 14-16 membered tetrapyrrolic unit, is found in a diverse array of biological systems.

1.2 Biological Aspects and Substrate Binding

Examples of the function of various essential transition metal macrocycles *in vivo* include; oxygen carriers (Fe - hemoglobins)[152], electron transport (eg. cytochrome c-(Fe))[11], substrate modification (Co - vitamin B_{12})[11] and CO_2 reduction (Ni - coenzyme P430)[12]. The biologically occurring metal macrocycles are considered to represent the ultimate in metal ion control.[11] This is accomplished through (i) intricate modification to the basic tetrapyrrolic framework, (ii) changes to the peripheral substituents on the ligand, and (iii) subtle environmental effects from the tertiary structure of the metalloprotein or enzyme, eg., highly specific base paired hydrogen bonding interactions[11]. The natural product porphyrin systems have stimulated a great deal of interest in model macrocyclic systems containing tetraaza donor sets with the biologically important first row transition metals Fe,Co, Ni,Cu and Zn.

Numerous research groups have attempted to mimic the *in vivo* metal ion control such as substrate binding and activation of biological macrocycles *in vitro*. A representative example of substrate binding is provided by Busch and coworkers in their work with lacunar macrobicyclic complexes of general structure (3)[13,14].

$R^1 = CH_2C_6H_5CH_2$

$= CH_2CH_2CH_2$

$R^2 = R^3 = Me$

M = Co(II), Ni(II), Fe(II)

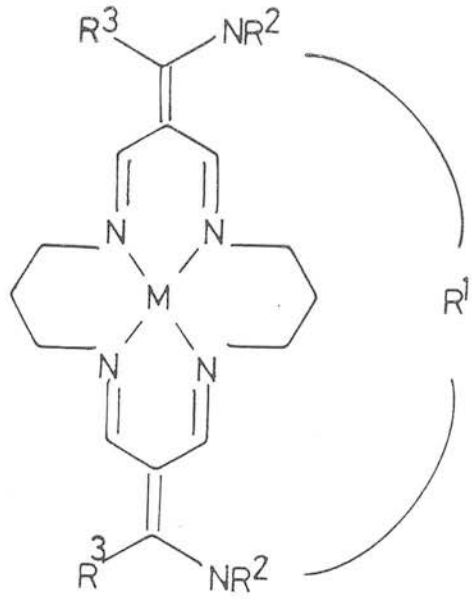

[3]

The Fe(II) complex was chosen for further study as its Fe(II)/(III) redox properties closely match those found in biological heme moieties. The observed reversible dioxygen binding to M=Fe(II) and Co(II) was found to be very sensitive to the nature of the R^1 bridge. By providing a tight, sterically demanding cavity, $R^1 = -CH_2C_6H_4CH_2-$, reversible oxygen binding without irreversible side reactions was observed[13]. Using the smaller propylene bridge, $-CH_2CH_2CH_2-$, an autoxidation reaction was observed with no reversible binding being detected[14].

Other significant contributions to the field of substrate binding and activation have been provided by the research groups of notably Baldwin[15], Collman[16] and Groves[17]. 'Capped' and 'picket fence' porphyrins are two examples of modified porphyrins for specific activity towards a coordinating axial ligand synthesised by the Baldwin and Collman research groups respectively.

1.3 Factors Influencing Metal-Macrocycle Redox Properties

Many variations in compound stability, redox or magnetic properties may be rationalised with respect to the in-plane ligand field (Dq^{xy}). Macrocyclic ligands often produce stronger ligand fields than comparable non-macrocyclic ligands owing to a constraining or constrictive effect. This property leads to ground state electronic configurations that are observed only in the presence of macrocyclic ligands. Factors known to influence the central metal ion include macrocyclic (i) ring size, (ii) saturation, (iii) stereochemistry, (iv) donor atom type and (v) substituents on the macrocycle.

For a series of Ni(II) tetraaza macrocycles, Busch[18] and Barefield[19] were able to quantify the factors that stabilize the Ni(I), Ni(III) and Fe(III) oxidation states. Examples of experimentally derived contributions to the reversible Ni(II)/(I) half wave potential include[18,19].

	$\Delta E_{\frac{1}{2}}$/mV
Ring size increase: 14→15 member	+225
Ring size increase: 14→16 member	+375
Delocalized charge on macrocycle	-430
Saturation: introduction of α-diimine function	+170
Substitution: NMe group for NH	+140

An example of the ability of variations in macrocyclic ring size and stereochemistry to stabilize unusual oxidation states is illustrated by the homoleptic complexes (4)-(6).

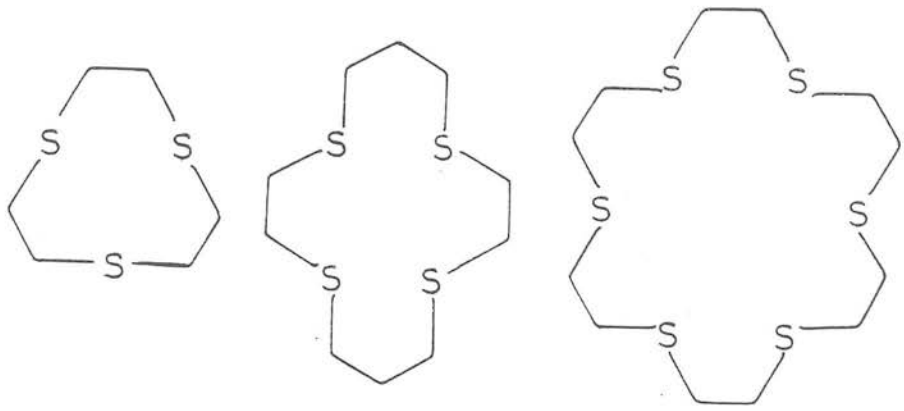

(4) (5) (6)

To form the formal metal(III) complexes $[M(4)_2]^{3+}$, M=Pd,Pt, by chemical or electrochemical oxidation of the d^8,M(II) precursors, octahedral coordination around the d^7 metal ion is required[20-22]. The complexes $[M(L)]^{2+}$ M=Pd,Pt, L=(5) or (6) show no oxidative redox processes. The inactivity of the two macrocyclic complexes may be rationalised by the inability to form octahedral complexes with (5) or (6). Ligand (6) may be regarded as being too small to fully encapsulate octahedrally the relatively large Pd(II), Pt(II) metal ions. Therefore the coordinative flexibility of (4) in this system appears crucial in stabilizing the d^7 metal centre.

Fabbrizzi[23] has recently presented results into the investigation of variation of donor atom type on nickel redox couples. Using macrocycles L=(7)-(9) with 'N_3', 'N_2O', 'N_2S'

donor sets octahedral complexes of stoichiometry $[Ni(L)_2]^{2+}$ were synthesised and the effect of introducing axial O,S donor heteroatoms on the Ni(II)/(III) redox couple investigated.

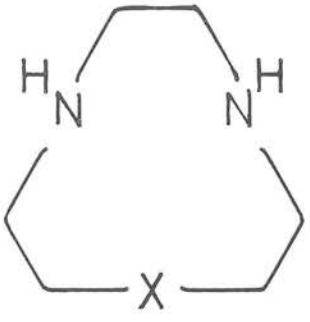

X = NH : (7)
O : (8)
S : (9)

The examples described above illustrate the ability of macrocycles to form activated species via unusual coordination or redox properties by fine 'tuning' of the gross redox properties of the central metal ion with variation in macrocyclic design. These adjustments are often essential if the activated species is to be reactive towards small molecules and organic substrates in catalytic reactions.

1.4 Catalytic Aspects

For the design of an efficient catalytically active metal complex the protection or blocking of certain coordination sites and the parallel incorporation of specific labile positions at the metal centre is desirable. Porphyrins and macrocycles that stabilize a wide range of transition metal oxidation states in reversible multi-redox processes while simultaneously occupying usually four coordination sites of a metal are ideally suited for catalytic investigation.

Therefore the activation of small molecule substrates such as ethylene, NO, NO_3^-, CO, CO_2, O_2, N_2 and H_2 by metallo-porphyrins and macrocycles has received considerable attention[24-34]. The four electron reduction of O_2 to H_2O has received impetus with the importance of fuel cells and air batteries[24,25]. The covalently linked 'face to face' Co porphyrin dimers, [10] and interestingly the iridium monomer Ir(OEP)H[32] adsorbed on graphite electrodes exhibit unusually high catalytic activity towards the reduction of O_2 to H_2O without production of significant H_2O_2 concentrations in aqueous acidic media.

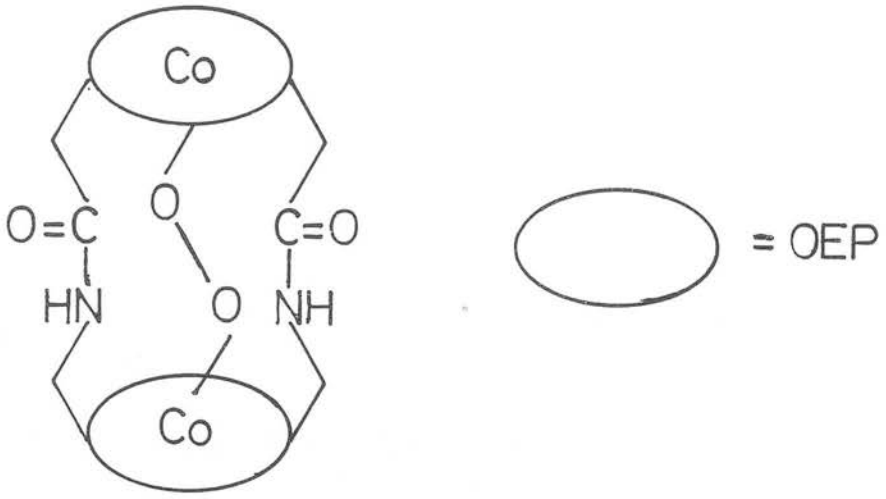

(10)

Wayland and coworkers[35] have recently catalytically produced methanol and formaldehyde from H_2 and CO using $[Rh(OEP)]_2$ by irradiation at 350nm.

Several groups have studied the electrocatalytic reduction of CO_2 using tetraaza macrocycles such as cyclam or (11), or the porphyrins OEP^{2-}, TPP^{2-}. The reduction was found to proceed to CO[27-29], oxalate[30] or formate[27] depending on the

metal and the reaction conditions employed. $[Ni(cyclam)]^{2+}$ has been found to be a remarkably efficient and selective catalyst for the reduction of CO_2 to CO in aqueous solution without the production of appreciable amounts of H_2 from the competing reaction of the electroreduction of water [28,29]. It is believed that the Ni(I) species $[Ni(cyclam)-CO]^+$ is present in solution during the electrocatalytic process.

High valent iron and manganese porphyrins have been used as alkane and alkene epoxidation and hydroxylation catalysts, successfully mimicking the behavior of cytochrome P450, an iron heme based family of monooxygenase enzymes[17].

Low valent, electron rich metal centres such as Co(I), Rh(I) and Ni(I) can undergo oxidative addition[36-38] or electron transfer reactions[39]. Using tetraaza or tetrathia macrocycles as a protecting group, species such as $[Rh(12)(C_3H_6Br)I]$, $[Rh(5)(C_6H_5CO)Cl]^+$ and $[Ni(TMC)CH_3]^+$ are formed on reaction of low valent metal centres with alkyl or acyl halides.

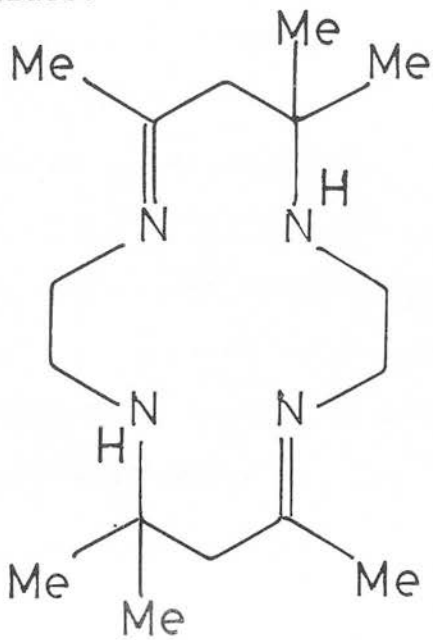

(11)

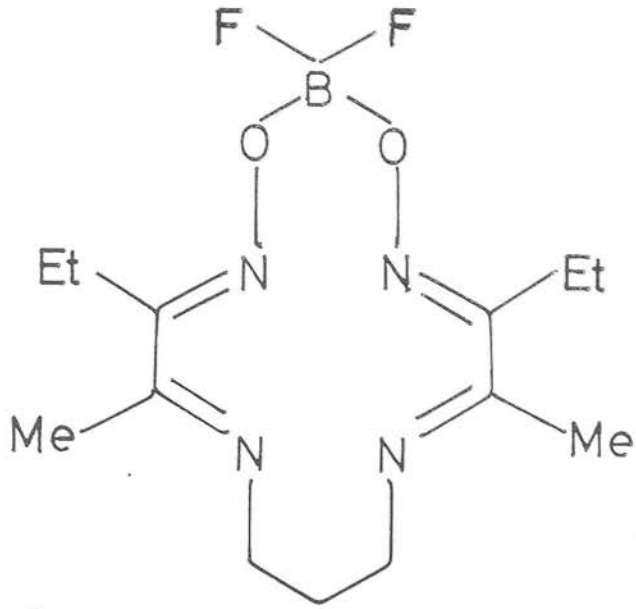

(12)

A recent development in macrocyclic chemistry has been the synthesis of metalloporphyrin and macrocyclic complexes containing metal carbon σ bonds in axial coordination sites. In addition to the alkyl and acyl examples described above, carbene, vinyl, vinylidiene and acetylene species have also been prepared[40,41] while hydrido[35,42], dinitrogen[31] and dioxygen[43] complexes that may be considered as catalytic intermediates have also been prepared.

The double bonded metalloporphyrin dimers $[M(por)]_2$, (M=Ru(II), Os(II), Ir(II), Rh(II), por = OEP^{2-},TPP^{2-}) have been utilized as a convenient reagent for many insertion or binding reactions. A representative summary of recent work of Collman and coworkers[40] for the diruthenium species $[Ru(OEP)]_2$ is illustrated below (Figure 1.4.I.).

Figure 1.4.I. A Summary of Collman's Work on Reaction of $[Ru(OEP)]_2$

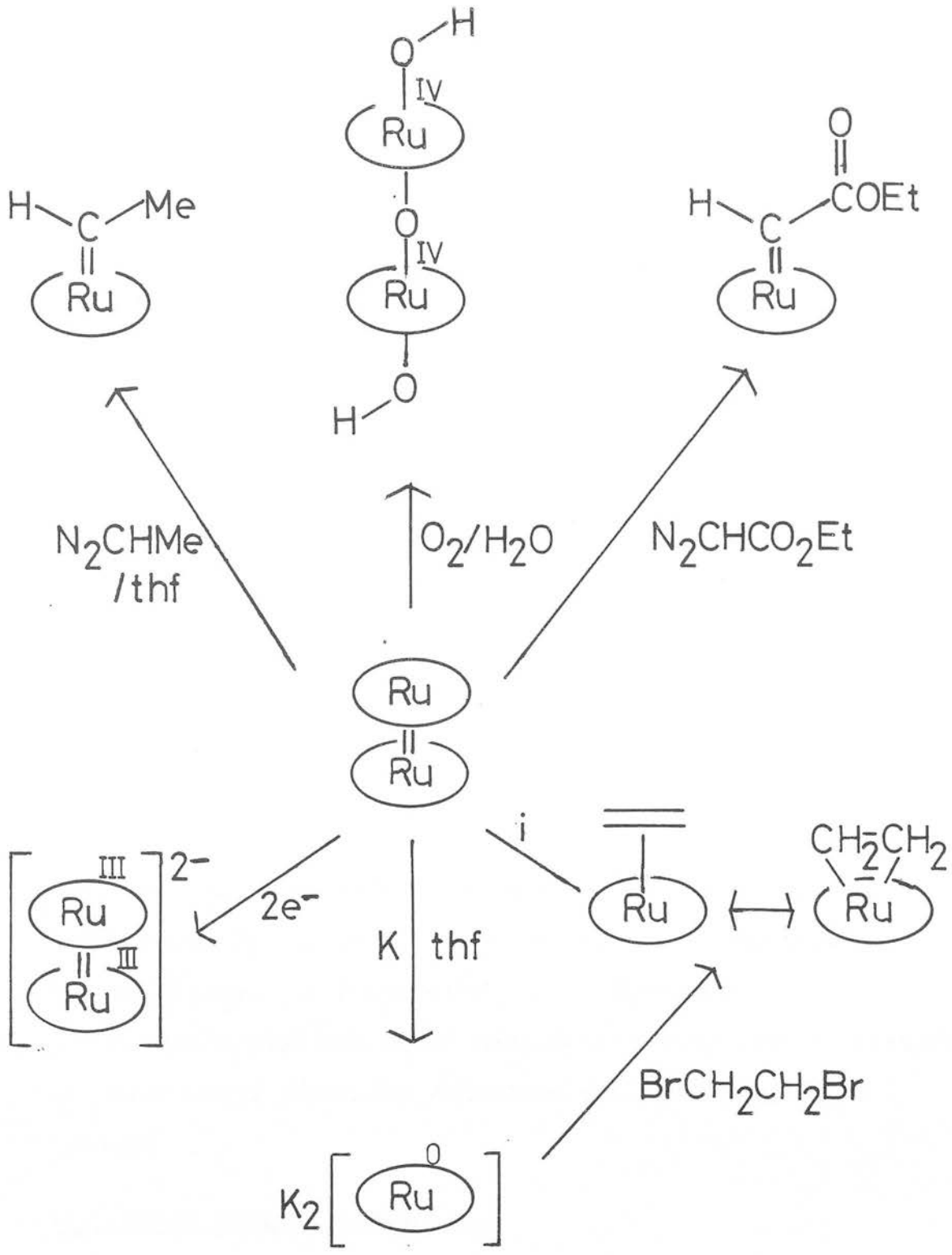

1.5 General Methods of Synthesis

i. Template reactions

Since the discovery by Curtis[44] and Busch[45] of the transition metal-mediated template synthesis of macrocyclic ligands, an immense number of complexes have been synthesised. Most are based on 14-membered macrocycles with tetraaza donor groups due to their relevance to biological systems and their relative ease of synthesis. The first row transition metals Ni(II), Zn(II) and Cu(II) have been found experimentally to be the most effective template centres. (Section 3.1.I). Second and third row platinum group metal ions are generally considered poor centres for template reactions due to their kinetic non-lability. Metal phthalocyanine complexes with the second and third row platinum metals are however formed by template reactions. Condensation around a metal salt is achieved by heating at elevated temperatures (*ca.* 250°C) in the presence of excess σ-cyanobenzamide or phthalonitrile[46]. The mild conditions employed for the successful Schiff base template reactions with first row transition metals are insufficiently vigorous to form analogous second and third row complexes. Our approach to the synthesis of non-porphyrinoid platinum metal macrocyclic complexes therefore involved metal insertion reactions into preformed free ligands.

ii. Metal Insertion Reactions

As described above, many macrocycles are efficiently formed in high yield around Cu(II) or Ni(II) metal centres.

Demetallation to give the free ligand for use in subsequent metal insertion reactions is effected with aqueous cyanide for Ni(II)[47] or Na_2S for Cu(II)[48]. Other first row transition metal ions can then be readily inserted into these preformed ligands in high yields[48,51,57]. To date, few examples of the insertion of second or third row transition metal ions using a similar methodology have been reported[49] (Section 3.1.2). By analogy to the well established synthesis of platinum metal porphyrin complexes[50], it would be expected that vigorous conditions would be required. For example, platinum metal ions can be readily inserted into a porphyrin free ligand, H_2por, in refluxing dimethylformamide (dmf) or glacial acetic acid (boiling points 153° and 118°C respectively) [13].

$$M^{n+} + H_2por \overset{\Delta}{\rightleftharpoons} [M(por)]^{(n-2)+} + 2H^+ \qquad [13]$$

M=Ru(II), Ru(III), Os(II), Rh(III), Ir(III), Pd(II), Pt(II).

1.6 Aims of Work

The use of macrocyclic complexes in coordination as protecting groups for metal centres is well established. The multi-redox and catalytic behavior observed for second and third row transition metal porphyrin complexes has been extensively studied by other workers[32,40,41]. However there remains a general paucity of analogous non-porphyrinoid second and third row macrocyclic complexes, due primarily to difficulties encountered in their synthesis. We therefore

undertook a study on the synthesis and redox properties of a series of non-porphyrinoid tetraaza macrocyclic complexes. Four neutral tetraaza 2,6-pyridyl ligands with varying carbon and nitrogen alkylation (L^1-L^4, see Figure 1.6.I) were synthesised via the Ni(II) mediated template reaction (Chapter 2). The insertion and subsequent characterization of the platinum metal complexes with L^1-L^4 is described in Chapter 3. The redox activation of platinum metal porphyrin complexes and their reactivity with small molecule substrates provides a continuing area of investigation (Section 1.4). The redox behavior of a series of seven square planar Ni(II) and Pd(II) tetraaza macrocycles complexes were investigated with the aim of studying their reactions with small molecule substrates. Although factors that influence the stability and reactivity of homoleptic metal macrocyclic complexes are often well established, fewer studies on mixed donor macrocyclic species have been undertaken, due to complexities often involved in their synthesis[66,138]. A study was therefore initiated on the structural and redox properties of a series of 2,6-diiminopyridyl macrocycles with tetraaza, triazaphosphorus and triazathia donor sets (Chapter 5). The reduction of dioxygen by transition metal porphyrin complexes may be of industrial importance in the development of new fuel cells[24,25,32]. The reaction of dioxygen and superoxide with two square planar nickel tetraaza macrocycles was therefore studied by e.s.r. spectroscopy (Chapter 6).

Figure 1.6.I. Principle Macrocyclic Ligands (with Atomic Numbering and Nomenclature) Discussed in this Work

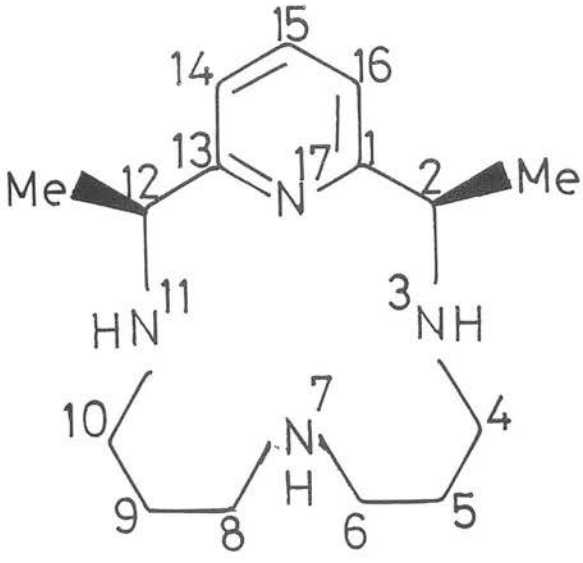

L^1

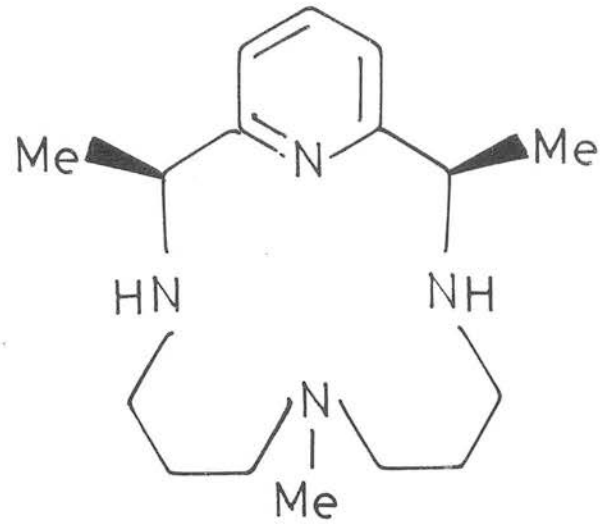

L^3

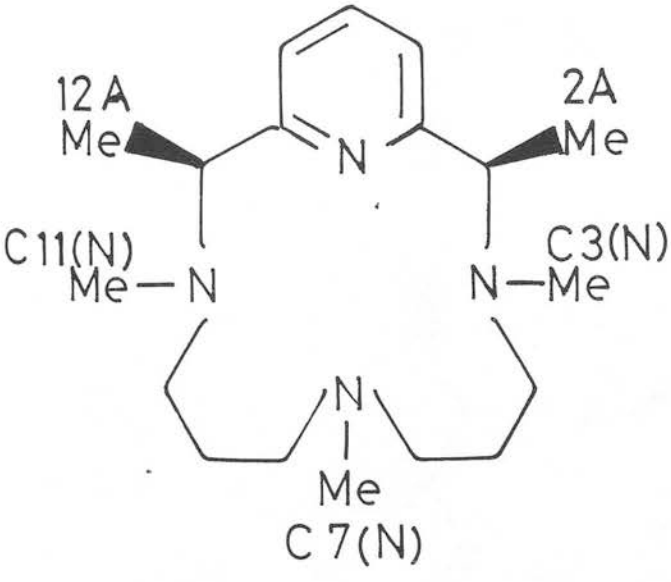

L^2

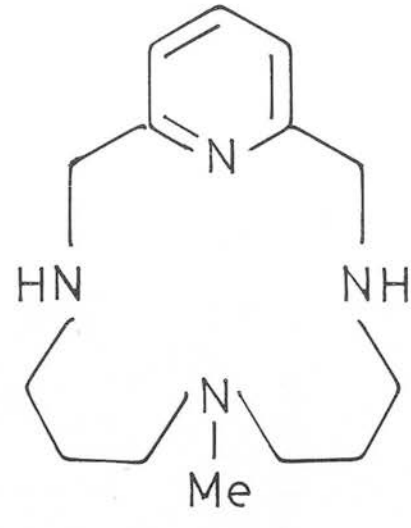

L^4

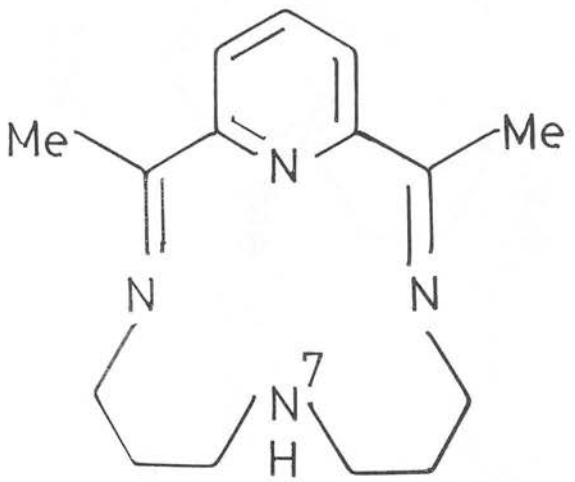

n_4

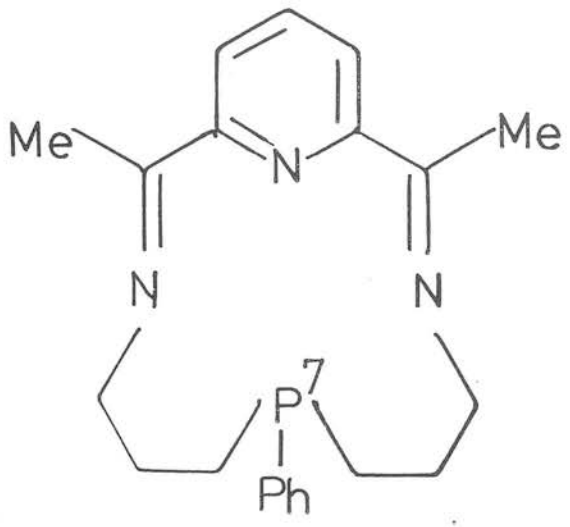

n_3p

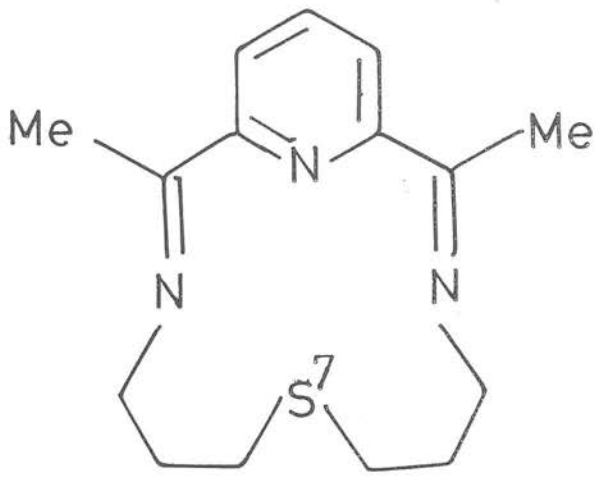

n_3s

Figure 1.6.I (cont.)

Figure 1.6.I (cont.)

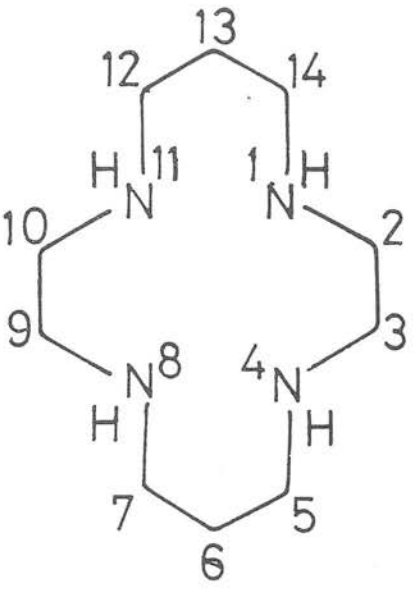

cyclam

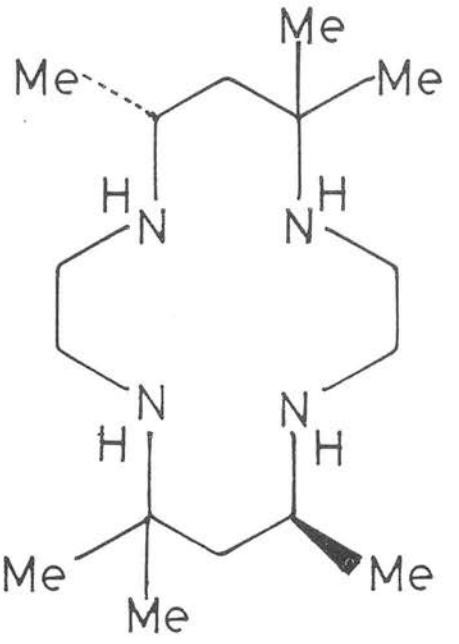

C-meso-HMC

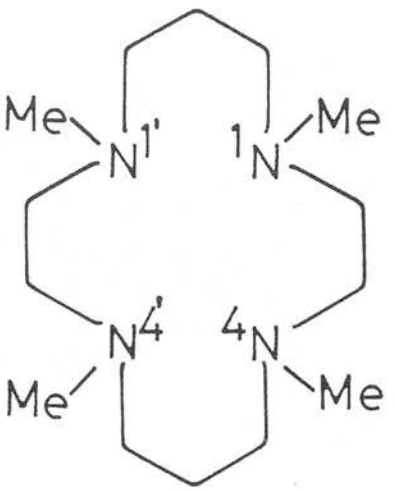

TMC

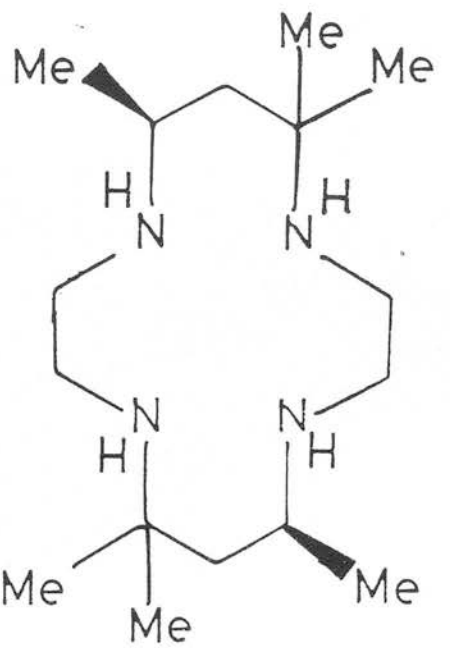

C-rac-HMC

C H A P T E R 2

Synthesis and Characterization of 2,6-Pyridyl Tetraaza Macrocycles with Varying C-and N-Alkylation

2.1 Introduction

The 2,6-pyridyl tetraaza macrocycle L^1 can be readily synthesised in good yield using the nickel-mediated template method[47]. Extraction of the nickel template centre and insertion of other first row transition metals Fe(II), Co(III), Cu(II) and Zn(II) into the free macrocycle L^1, has been accomplished by several groups of workers[51,52]. The synthesis of L^1 and derivatives, L^2-L^4, with varying C- and N-alkylation was undertaken to extend the range of

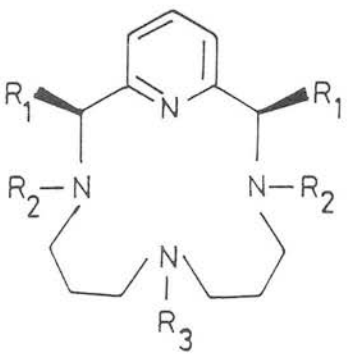

[14]

L^1 : $R_1 = Me$; $R_2 = R_3 = H$

L^2 : $R_1 = R_2 = R_3 = Me$

L^3 : $R_1 = R_3 = Me$; $R_2 = H$

L^4 : $R_1 = R_2 = H$; $R_3 = Me$

ligands available for reaction with the platinum group metal ions. A characteristic reaction of some transition metal amine species especially iron[53] and ruthenium[54] is oxidative dehydrogenation at the C-N function to form an α--imine species [15].

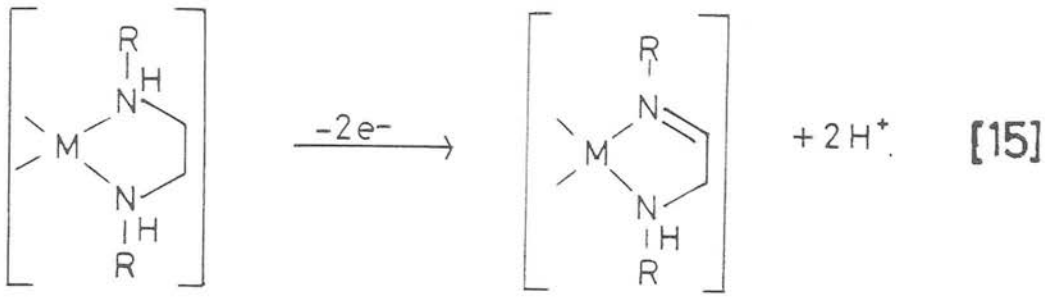

[15]

Removal of all secondary amine protons of the free ligand by alkylation with formic acid/formaldehyde would be expected to block this reaction pathway thereby facilitating the isolation of metal complexes.

With control of the environment of the central macrocyclic cavity by alkylation or substitution of pendant ligating groups for the secondary amine groups, a route to the stabilization of a wide range of metal oxidation states was envisaged. The incorporation of pendant ligating groups into macrocyclic ionophores has been reported by several groups. These include functionalization of aza macrocycles by $-CH_2CH_2N(CH_3)_2$,[55,56] $-CH_2CH_2OH$[55], $-CH_2C_5H_4N$[58,57], $-CH_2C_6H_5$[57] and $-CH_2COOH$[59] moieties [16]-[19].

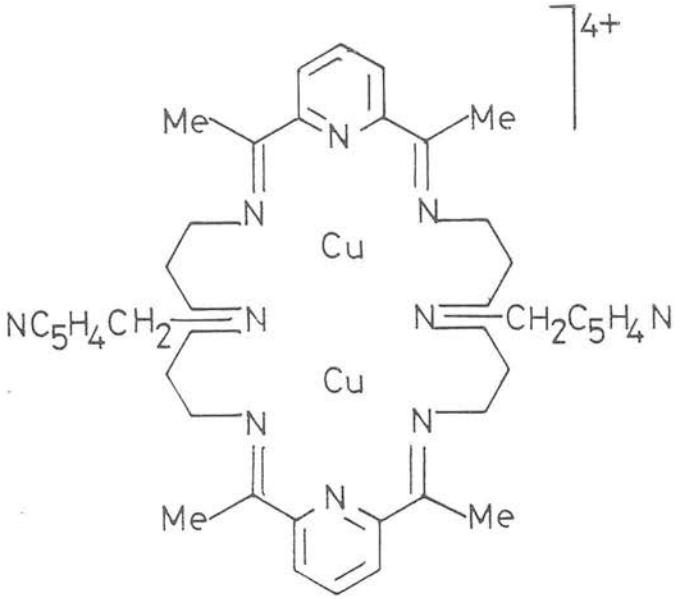
4+
Me
N
Me
N
N
Cu
NC5H4CH2
N
N
CH2C5H4N
Cu
N
N
Me
N
Me

(16)

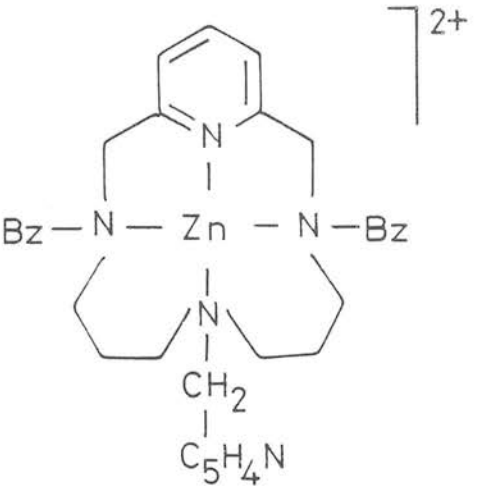
2+
N
Bz — N — Zn — N — Bz
N
CH2
C5H4N

(17)

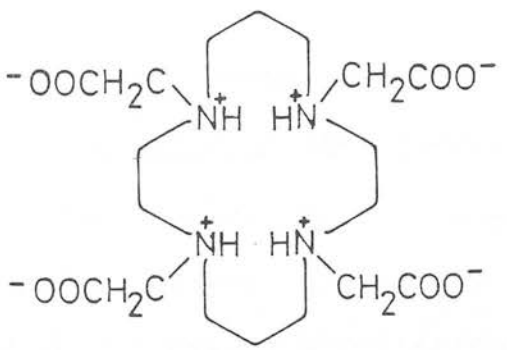
-OOCH2C
NH
HN
CH2COO-
NH
HN
-OOCH2C
CH2COO-

(18)

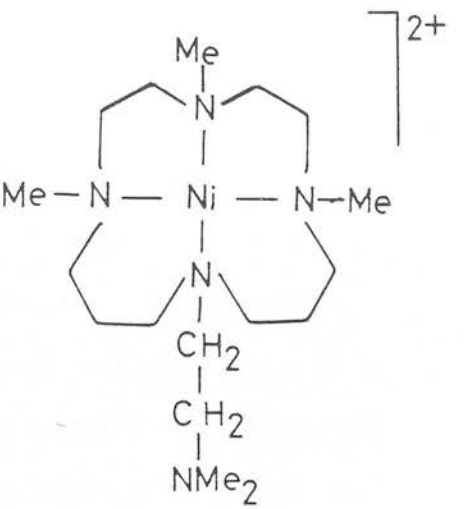
2+
Me
N
Me — N — Ni — N — Me
N
CH2
CH2
NMe2

(19)

2.2 Stereochemistry of Macrocycles L^1-L^4

With three chiral N and two chiral C centres on complexation of L^1-L^3 with a metal ion, 24 isomers including 10 pairs of optical isomers are possible[60]. The isomers of L^1-L^3 are divided into C-*meso* and C-*rac* isomers. The 16 C-*rac* isomers (with the two CMe groups on opposite sides of the tetraaza macrocyclic plane) are 8 pairs of enantiomers. The 8 C-*meso* isomers (with CMe groups on the same side of the macrocyclic plane) include two pairs of enantiomers. The six stereoisomers with C-*meso* geometry are represented diagrammatically in Figure 2.2.I [60].

Usually, not all of these isomers are observed experimentally. Busch[51], predicted an order of stability of the six configurations by considering bond angle strain and steric repulsions and proposed an order of decreasing stability I (most stable) >II>III>IV>V>VI (least stable).

Results and Discussion

2.3 Synthesis of the Free Ligands L^1-L^4

Macrocycles L^1,L^3,L^4 were prepared by the acid catalysed template condensation around Ni(II) using the appropriate pyridine diketone and diamino propylamine, following with a few minor modifications, the general synthetic procedure of Karn and Busch[47]. A summary of the synthesis is given in Figure 2.3.I; full details are given in the experimental section. Step ii, the borohydride reduction of the diimine function of $[Ni(n_4)]^{2+}$ to form the saturated macrocycle

Figure 2.2.I Representation of the C-*meso* Configurational Isomers of L^1

Key: □ represents methyl groups and ○ NH groups,

'+' represents group above the macrocyclic plane,

'-' below the plane.

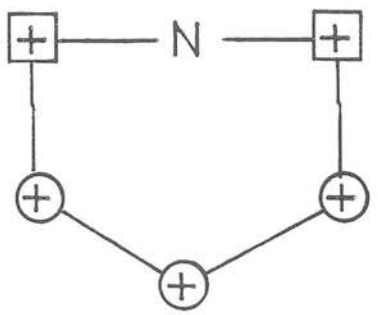

I

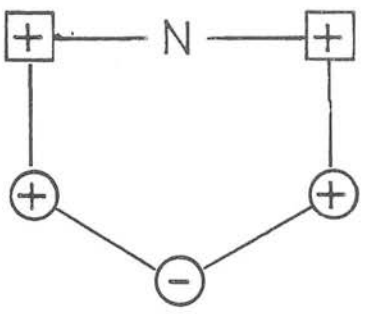

II

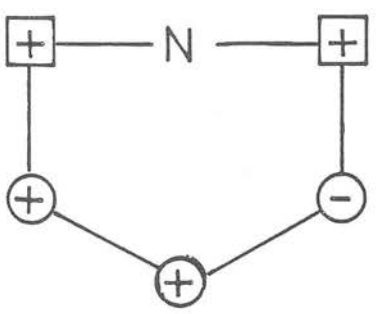

III

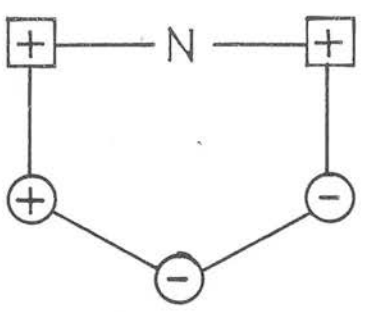

IV

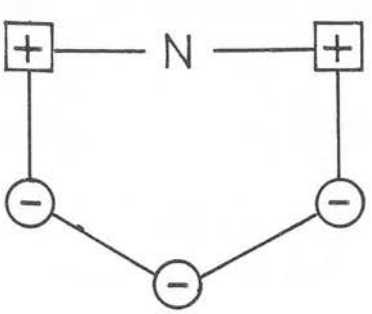

V

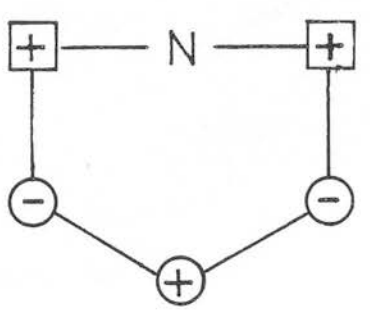

VI

Figure 2.3.I. Synthesis of the Free Ligands L^1-L^4

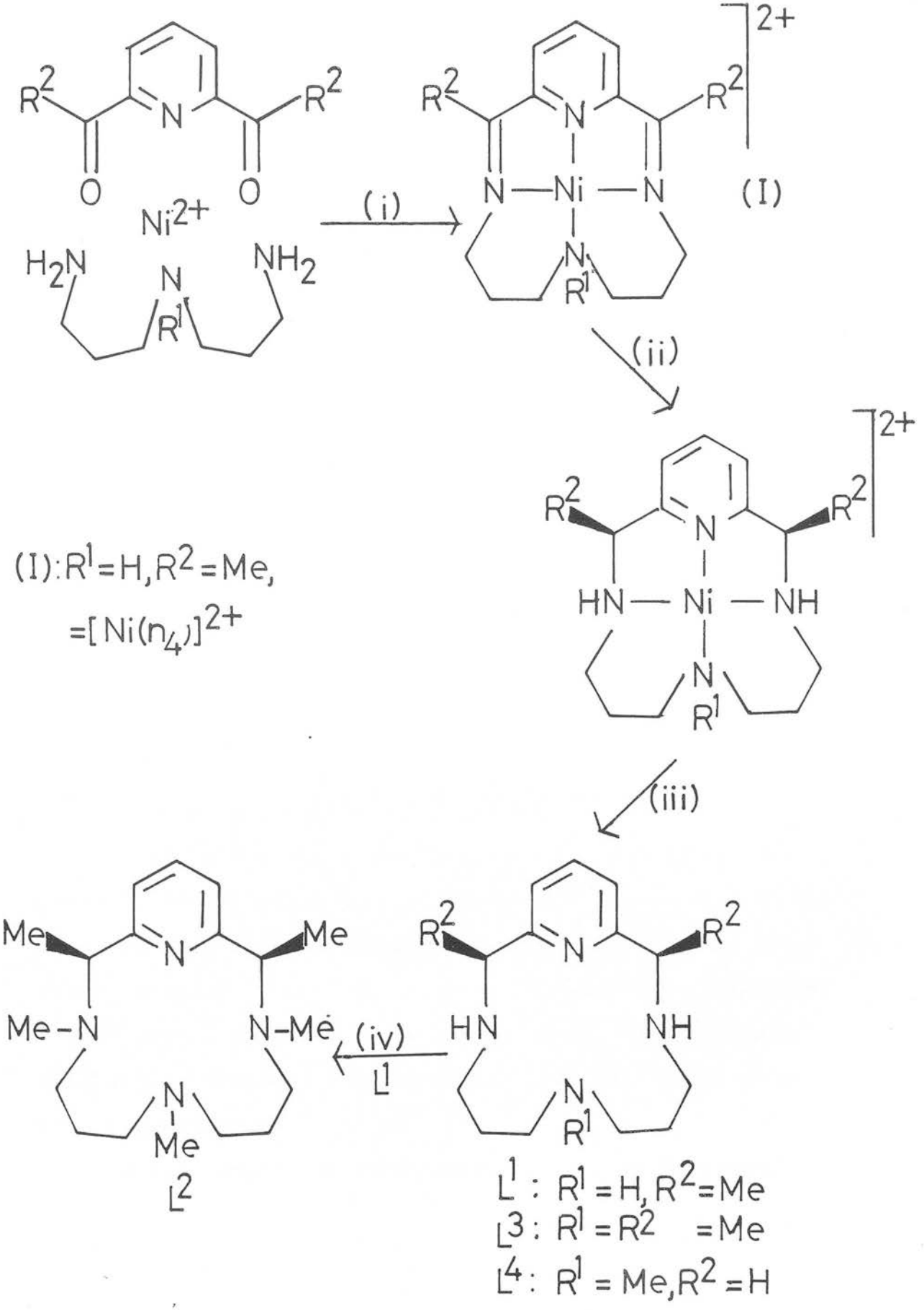

enables the removal of the metal ion from the macrocyclic core. Metal abstraction from the unreduced diimine ligand would cause hydrolysis of the metal free macrocycle under the aqueous conditions of the experiment. Reduction of the diimine function of $[Ni(n_4)]^{2+}$ leads to the formation of two chiral carbon centres giving rise to C-*meso* (*syn* Me groups) and C-*rac* (*anti* Me groups) isomers. Busch[47] found that on reduction using Pt/H_2 the C-*meso* isomer was predominantly formed in a ratio of 10:1 over the C-*rac* isomer. In our hands, for the borohydride reduction for L^1,L^3 the ratio was approximately 15:1.

With careful recrystallization from diethyl ether the pure C-*meso* isomer can be obtained, as judged by ^1H n.m.r. (Figure 2.3.II) and ^{13}C n.m.r. spectroscopy (Table 2.3.III) and supported by a single crystal X-ray structural analysis (Figure 2.4.II).

Overall yields for the synthesis of ligands L^1,L^3,L^4 based on initial diketone are approximately 20%. An improved synthetic procedure using Cu(II) as a template, followed by demetallation with Na_2S, to give an overall yield of 46% has been recently reported by Barefield[48].

To reduce the potential number of stereoisomers, the ligand L^4 was synthesised. Loss of chirality at the ortho carbon position reduces dramatically the possible number of isomers from 24 to 4. These are represented by structures I,II,III,IV of Figure 2.2.I with ' + ' now representing a non chiral C-H group. Structures III,IV are therefore a pair of enantiomers.

The new ligand L^2, which includes no secondary amine

Figure 2.3.II. ^{1}H N.m.r. of $L^{1}.H_2O$ (360MHz, $CDCl_3$)

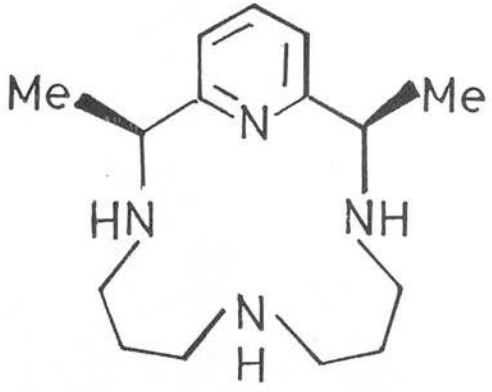

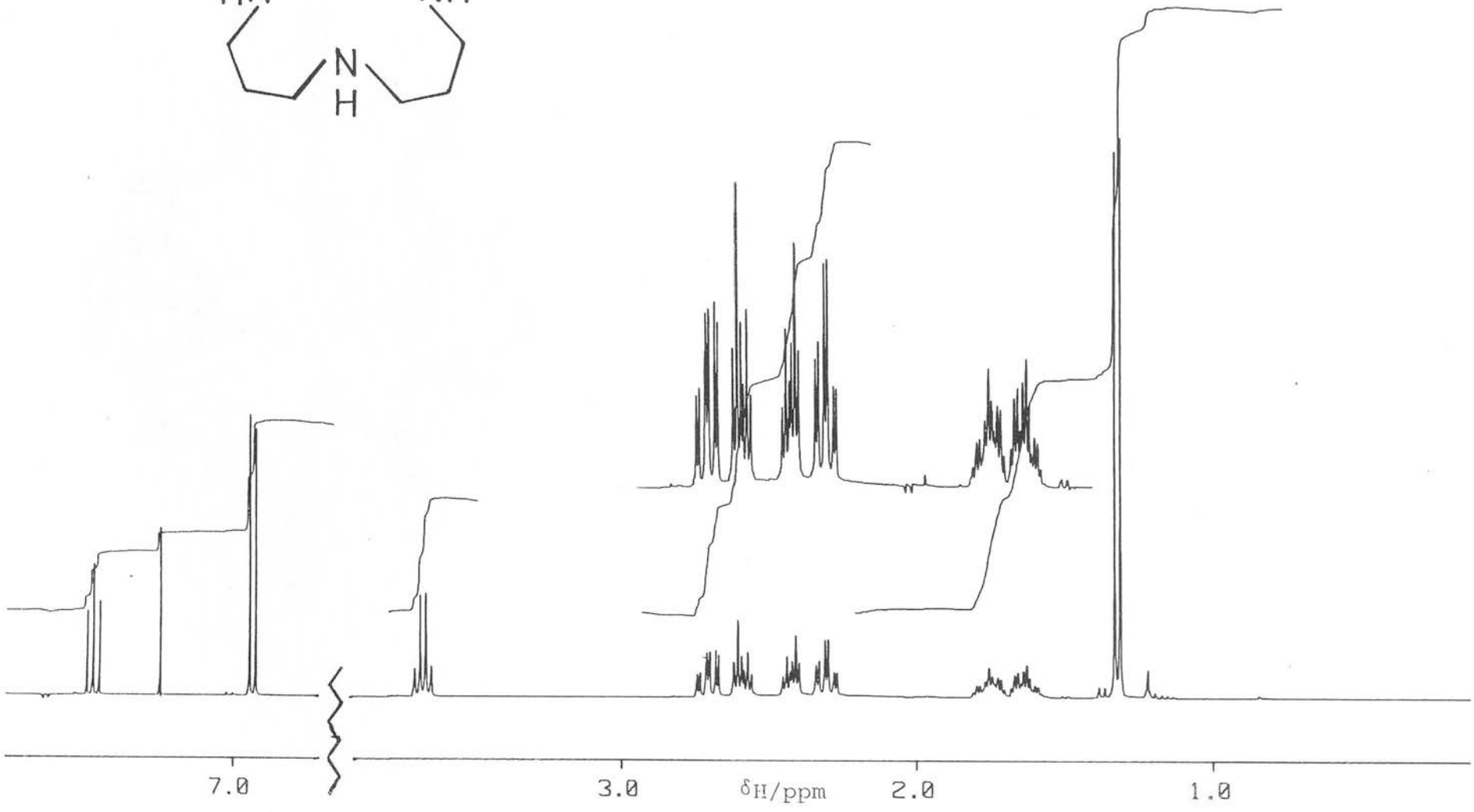

Table 2.3.III. Summary of ^{13}C D.E.P.T. n.m.r. data for L^1-L^4. [a]

Carbon	L^1	L^2	L^3	L^4
C15	136.05	136.24	135.90	136.23
C14,16	120.54	120.69	120.13	120.26
C2,12	58.99	65.11	59.17	54.32
C6,8	45.66	54.79	54.63	56.11
C4,10	43.82	51.80	44.56	46.47
C7(N)	-	42.53	41.13	40.73
C3(N),11(N)	-	39.28	-	-
C5,9	28.37	24.57	26.95	26.93
C2A,12A	23.39	16.54	23.66	-

[a] at 50.32MHz in $CDCl_3$ solvent δc/ppm

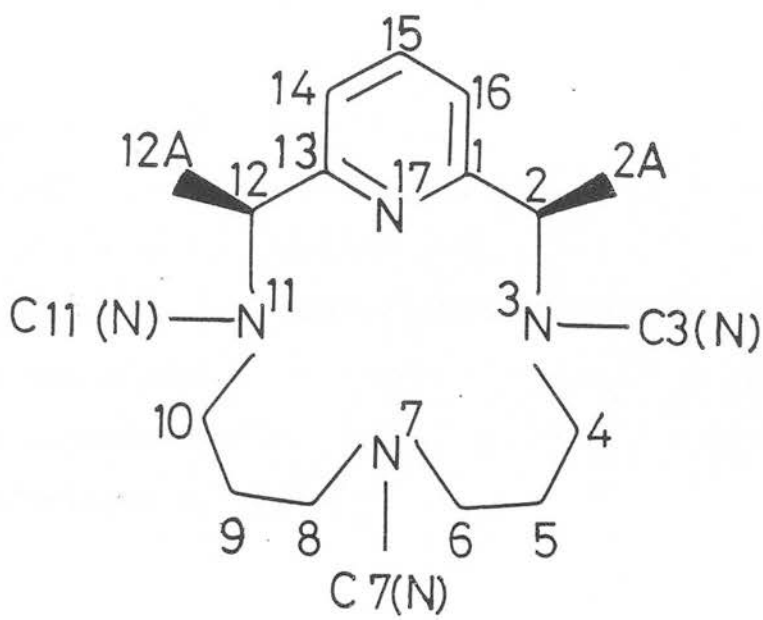

functions was synthesised in order to prevent potential ligand oxidative dehydrogenation reactions from occurring. The reaction of $L^1.H_2O$ with a mixture of formic acid and formaldehyde solution[61] gave the tri-N-methylated product L^2 in an essentially quantitative yield as a viscous, near colourless oil at room temperature. It is believed that the reduced capability for intermolecular hydrogen bonding of L^2 in comparison with the crystalline solids $L^1.H_2O$, $L^3.H_2O$ and L^4 is responsible for its physical form. The reaction mechanism takes place in two stages, with i) an initial attack by formaldehyde, followed by ii) reduction with formic acid[62].

$$>NH + HCOH + H^{\cdot} \xrightarrow{i} H_2O + >\dot{N}=CH_2 \xrightarrow{ii} N-CH_3 \qquad [20]$$

The absence of secondary amine groups in the product was determined by a combination of infrared, ^1H and ^{13}C n.m.r. and mass spectral techniques.

A comprehensive ^1H and ^{13}C n.m.r. study on ligands L^1-L^4 was carried out. Characterization by n.m.r. not only demonstrates the isomeric purity of the free ligands, (Figure 2.3.II), but also aids in the elucidation of the structures of the metal inserted complexes. ^{13}C D.E.P.T. n.m.r. spectroscopy, by distinguishing between CH, CH_2 and CH_3 carbons has proven to be especially useful in assignment of the free ligands (Table 2.3.III) and metal inserted complexes (Sections 3.4 and 3.6).

2.4 The Single Crystal X-Ray Structure of $L^1.H_2O$

In order to confirm the proposed C-*meso* geometry at the ortho-carbon position, a single crystal X-ray structure was undertaken. It was also of interest to ascertain the conformational characteristics of the metal-free ligand to compare with corresponding parameters for the metal inserted complexes (see Chapter 3). A crystal of size 0.6x0.6x0.5mm suitable for X-ray analysis was obtained on slow evaporation of a diethyl ether solution.

Crystal Data

$C_{15}H_{26}N_4.H_2O$, M = 280.4, orthorhombic, space group *Pbca*, a = 17.715(3), b = 14.342(4), c = 13.385(5)Å; U = 3400.7Å^3, Dc = 1.095 g cm^{-3}, Z = 8, $F(000)$ = 1216, μ(Mo-Kα) = 0.66 cm^{-1} λ(Mo-Kα) = 0.71069Å. At convergence R,Rw = 0.060, 0.076 respectively for 1520 data.

Selected bond lengths and angles are given in Table 2.4.I and two views of the free macrocycle are shown in Figures 2.4.II and 2.4.III.

The crystal structure shows the ligand to adopt a puckered rectangular conformation of the 14 membered ring in order to minimise lone pair interactions between nitrogen atoms. Deviations of -0.30, +0.21, -0.31, +0.39Å of N(x), x = 3,7,11 and 17 respectively from the best least squares tetraaza plane illustrates the distortion from planarity of the tetraaza donor set. The most significant observation from the crystal structure is that the pyridine ring makes a dihedral angle of 65.6° to the least squares tetraaza plane.

Table 2.4.I. Selected bond lengths and angles (with e.s.d's) for $L^1.H_2O$

Bond lengths (Å)

N(17) - C(1)	1.337(4)	N(7) - C(8)	1.462(6)
N(17) - C(13)	1.338(4)	C(8) - C(9)	1.498(6)
C(1) - C(2)	1.524(5)	C(9) - C(10)	1.522(6)
C(1) - C(16)	1.397(5)	C(10) - N(11)	1.471(5)
C(2) - N(3)	1.486(5)	N(11) - C(12)	1.482(5)
C(2) - C(2A)	1.521(5)	C(12) - C(13)	1.519(5)
N(3) - C(4)	1.472(5)	C(12) - C(12A)	1.511(5)
C(4) - C(5)	1.525(6)	C(13) - C(14)	1.396(4)
C(5) - C(6)	1.507(6)	C(14) - C(15)	1.384(5)
C(6) - N(7)	1.458(5)	C(15) - C(16)	1.379(5)

Bond angles (°)

C(1) - C(2) - N(3)	113.0(3)
C(1) - C(2) - C(2A)	110.1(3)
C(1) - N(17) - C(13)	118.4(3)
N(17) - C(1) - C(2)	115.6(3)
N(17) - C(1) - C(16)	122.4(3)
C(2) - C(1) - C(16)	121.9(3)

Figure 2.4.II View of the Single Crystal X-ray Structure of L^1

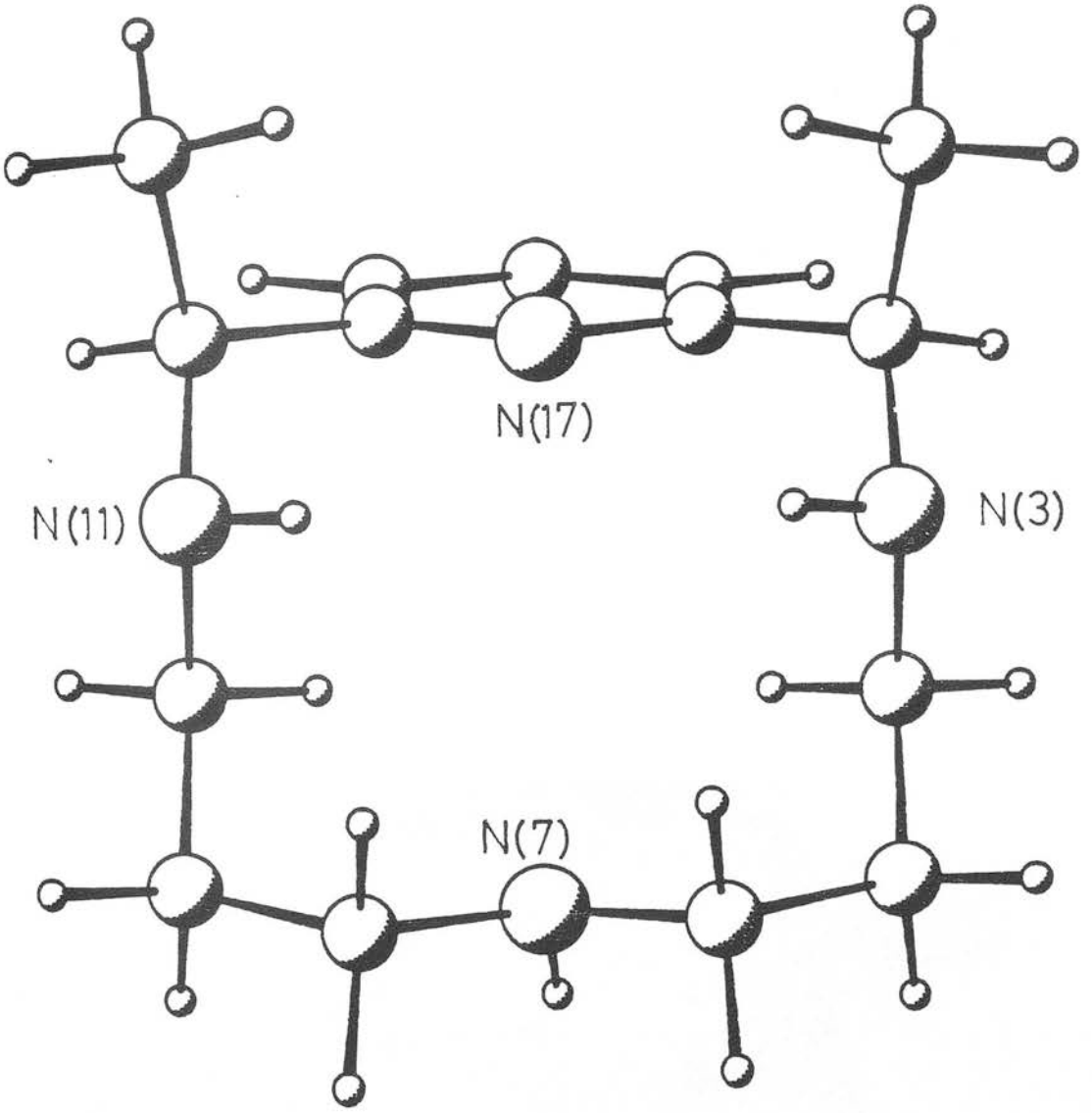

Figure 2.4.III. View of the Single Crystal X-ray Structure of L^1

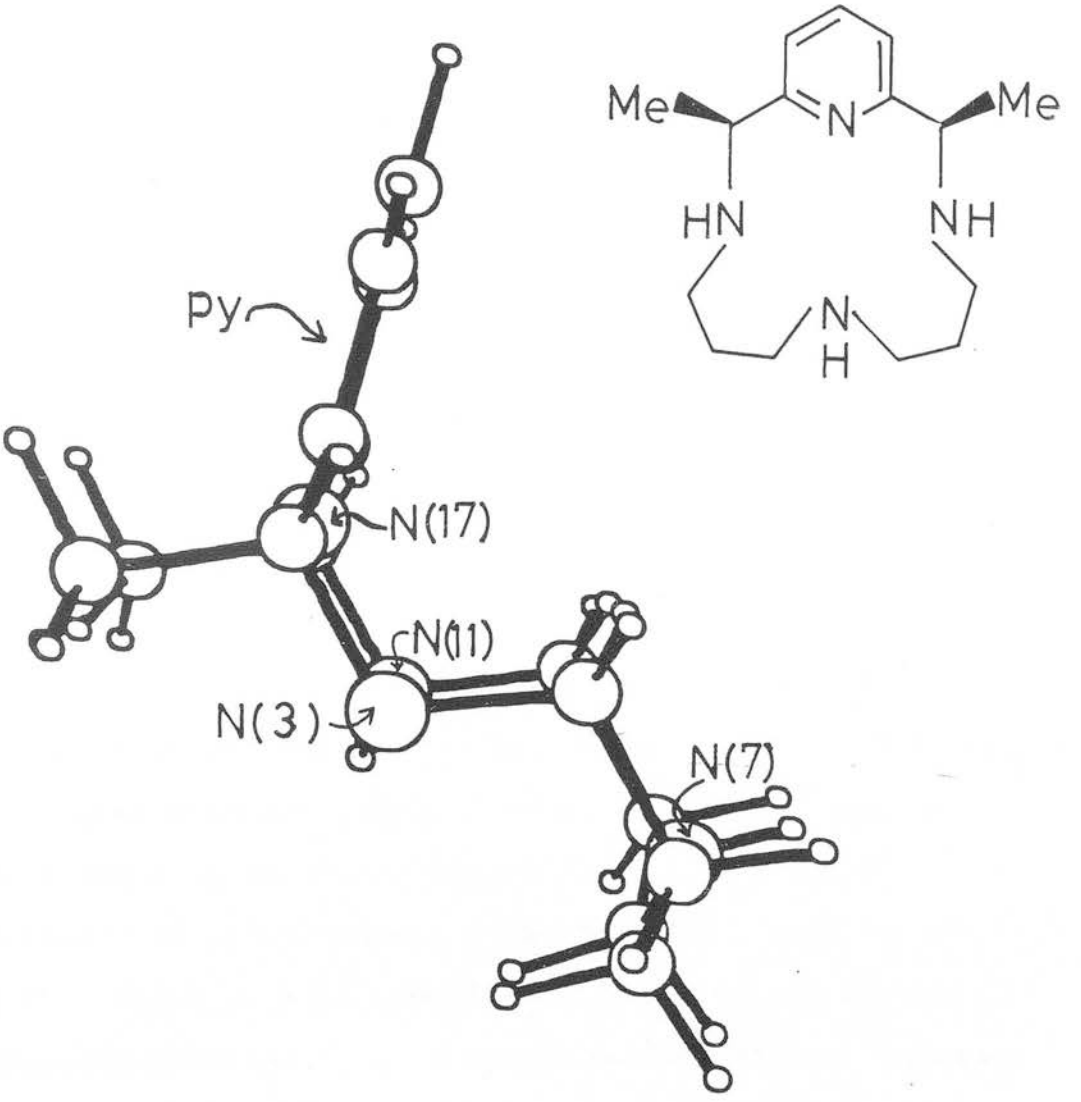

This compares with a comparable angle of *ca.*5° for the metal inserted complexes (see Chapter 3). The solid state structure confirms the C-*meso* geometry with the ligand adopting structure II of Figure 2.2.I. The secondary amine protons of N(3), N(11) are on the same side of the macrocyclic tetraaza plane as the two C-*meso* methyl groups with the proton on N(7) *anti* to N(3), N(11). Transannular donor N-N distances of 4.024(4) and 4.895(4)Å respectively are observed for N(7)-N(17) and N(3)-N(11).

After this structure had been solved, a single crystal X-ray structure of unsolvated L^1 was reported by Drew and coworkers[63]. This shows the ligand adopting structure I of Figure 2.2.I with all three secondary amine protons on the same side as the CMe groups. Torsion angles around N(7) therefore differ with -60.2° for C(4) C(5) C(6) N(7) and -68.7° for C(6) N(7) C(8) C(9) compared to +55.3° and +171.4° for the respective corresponding torsions for our structure. Drew found that the conformation of the macrocycle with structure I is considerably more planar with a maximum deviation of ±0.08Å for a nitrogen donor group from the best least squares tetraaza plane; the pyridine ring makes a dihedral angle of 49.2° to this plane. The water molecule associated with our structure forms hydrogen bonds to N(3) and N(11), (but not N(7)) which presumably influences the conformation obtained. No intermolecular hydrogen bonding is observed in comparison to the structure of C-*rac*-HMC.H_2O, where weak inter- (and intramolecular) hydrogen bonding was noted.[64]

Drew notes that from Molecular Mechanics calculations

that L^1 is not at its lowest energy conformation[63]. Differences between the six possible conformations are at maximum 2.5kJ mol^{-1}. This small value would be expected considering the flexibility of the 14 membered ring which allows for the facile interconversion about the secondary amine nitrogen donor atoms.

It therefore seems likely that the conformation of the free macrocycle is a low energy form and that the conformations observed for the metal complexes in Chapter 3 are higher energy forms due to the demands of metal coordination.

2.5 Experimental

Infrared spectra (4000-250 cm^{-1}) were recorded on a Perkin-Elmer 598 spectrometer using the KBr disc method. ^{1}H n.m.r. were obtained on Brucker WP200 and WH360 instruments operating at 200.13 and 360.13MHz respectively. ^{13}C D.E.P.T. n.m.r. were recorded at 50.32MHz using the Brucker WP200 spectrometer. Electron impact mass spectrometry was carried out using a Kratos MS902 spectrometer. Microanalyses were preformed by the Chemistry Department, University of Edinburgh. Melting points (uncorrected) were determined with a Kofler hot-stage microscope.

Reagents

All solvents were purified according to standard procedures [65]. 2,6-Diacetylpyridine, 4-methyl-4-aza-heptane-1,7-diamine (Aldrich) and 4-aza-heptane-1,7-diamine (Fluka) were used as supplied without further purification. 2,6-Pyridinedicarbaldehyde was synthesised by selenium dioxide oxidation of 2,6-pyridinedimethanol. A typical preparation of one of the free ligands, $L^{1}.H_2O$, is given below.

C-*meso*-2,12-dimethyl-3,7,11,17-tetraazabicyclo[11,3,1]-heptadeca-1,(17),13,15-triene monohydrate, $L^{1}.H_2O$

The nickel mediated template condensation of 2,6-diacetylpyridine and 4-azaheptane-1,7-diamine forming the tetraaza diimino unsaturated macrocycle precursor $[Ni(n_4)](ClO_4)_2$ was prepared by the method of Karn

and Busch[47] in 56% yield. $[NiL^1](ClO_4)_2$ was prepared by borohydride reduction of $[Ni(n_4)](ClO_4)_2$. $[Ni(n_4)](ClO_4)_2$ (11.60 g, 0.023 mol) in methanol (300 cm^3) was heated to 60°C. A slow addition of sodium tetrahydroborate (2.13 g, 0.056 mol) over 1 hour was followed by stirring for 3 hours at 60°C. A slow addition of 60% $HClO_4$ and cooling overnight to 0°C gave $[NiL^1](ClO_4)_2$ as orange crystals [Yield 5.6 g, 0.011 mol (48%)].

Removal of Ni^{2+} from the ligand L^1 was achieved with aqueous cyanide. A solution of $[NiL^1](ClO_4)_2$ (3.00 g, 5.77 mmol) in water (120 ml) was heated to 80°C and KCN (2.25 g, 0.035 mol) added. After stirring for 1 hour the solution was made strongly basic with KOH (4.5 g). On cooling the solution was extracted with chloroform (15x10 ml) and dried ($MgSO_4$). The extracts were evaporated to dryness to give a pale yellow oil and redissolved in diethyl ether (20 ml) from which crystals of the C *meso* isomer were obtained by slow evaporation.

Yield: 1.28 g, 4.56 mmol, (79%)

M.pt. 85-88°C, M^+ (electron impact) = found (calculated);
262 (262)

Analysis: Required for $C_{15}H_{26}N_4.H_2O$:
C 64.25 H 10.06 N 19.98%
Found C 64.26 H 10.08 N 20.15%

Infrared: ν_{max}=3280 (N-H stretch), 3048, 1591, 1572 cm^{-1} (pyridyl)

^1H nmr. $\delta_H[CDCl_3]$ 7.47(1H, t, py-*H*, J=7.6Hz); 6.93(2H, d, py-*H*, J=7.6Hz); 3.67(2H, q, C*H*CH_3, J=6.7Hz); 2.70(2H, d of t, J=11.3, 3.5Hz); 2.59(2H, d of t, J=11.9, 4.6Hz); 2.42(2H, d of t, J=11.1, 4.3Hz); 2.30(2H, d of t, J=11.1, 3.5Hz); 1.68(4H, m, CH_2-C*H*$_2$-CH_2); 1.32(6H, d, CHC*H*$_3$, J=6.7Hz).

C-*meso*-2,7,12-trimethyl-3,7,11,17-tetraazabicyclo[11,3,1]-heptadeca-1(17),13,15-triene monohydrate, $L^3.H_2O$

This was similarly prepared using 4-methyl-4-azaheptane-1,7-diamine as the precursor linear triamine.

M.pt. 77-80°C M^+ (electron impact) 276(276)

Analysis: Required for $C_{16}H_{28}N_4.H_2O$:

C 65.27 H 10.27 N 19.03%

Found C 65.56 H 10.22 N 19.12%

I.r.: ν_{max}=3286 (N-H stretch), 3059, 1590, 1571 cm^{-1} (pyridyl)

^1H n.m.r. $\delta_H[CDCl_3]$ 7.49(1H, t, py-*H*, J=7.6Hz); 6.90(2H, d, py-*H*, J=7.5Hz); 3.64(2H, q, C*H*CH_3, J=6.7Hz); 2.54(2H, s, N*H*); 2.30(8H, m); 1.99(3H, s, N-C*H*$_3$); 1.65(4H, m); 1.34(6H, d, CHC*H*$_3$, J=6.7Hz).

7-Methyl-3,7,11,17-tetraazabicyclo[11,3,1]heptadeca-1(17),13,15 triene, L^4

The free ligand was prepared in a similar manner using 2,6-pyridinedicarbaldehyde and 4-methyl-4-azaheptane-1,7-diamine as the respective source of dicarbonyl and triamine.

M.pt. 82-85°C M^+ (electron impact) = 248(248)

Analysis: Required for $C_{14}H_{24}N_4$:

C 66.70 H 9.74 N 22.56%

Found C 66.67 H 9.76 N 22.13%

I.r. ν_{max}=3300 (N-H stretch) 3030, 1593, 1574 cm^{-1} (pyridyl)

^1H n.m.r. $\delta_H[CDCl_3]$ 7.49(1H, t, py-*H*, J=7.6Hz); 6.95(2H, d, py-*H*, J=7.6Hz); 3.82(4H, s, CC*H*$_2$N); 2.90(2H, s, N*H*); 2.50(4H, t, J=5.7Hz); 2.33(4H, t, J=5.8Hz); 2.01(3H, s, N-C*H*$_3$), 1.68(4H, m, NCH$_2$-C*H*$_2$-CH$_2$-N).

C-*meso*-2,3,7,11,12-pentamethyl-3,7,11,17-tetraazabicyclo-[11,3,1]heptadeca-1(17),13,15-triene, L^2

The ligand was prepared by N-methylation of $L^1.H_2O$ with a formic acid/formaldehyde solution[61]. $L^1.H_2O$ (0.24 g, 8.5 mmol) was refluxed for 24 hours at 90°C in 98% formic acid (3 ml)/40% formaldehyde (8 ml) under nitrogen. On cooling to room temperature 15% NaOH (17 ml) was added giving a pH of *ca.* 10. Extracting with chloroform (8x8 ml), drying ($MgSO_4$), removal of the solvent and recrystallizing from diethyl ether gave a colourless oil.

M^+ (electron impact) = 304(304)

I.r. ν_{max}=3060, 1588, 1575 cm^{-1} (pyridyl)

^1H n.m.r. $\delta_H[CDCl_3]$ 7.54(1H, t, py-*H*, J=7.6Hz); 7.09(2H, py-*H*), d, J=7.7Hz); 3.68(2H, q, C*H*CH_3, J=6.5Hz); 2.50(4H, m); 2.31(6H, s, N-C*H*$_3$); 2.17(4H, m); 1.94(3H, s, N-C*H*$_3$); 1.44(4H, m, CH_2-C*H*$_2$-CH_2); 1.39(6H, d, CHC*H*$_3$, J=6.8Hz).

C H A P T E R 3

Insertion of the Platinum Metals into 2,6-Pyridyl Tetraaza Macrocycles

Introduction

3.1 General Methods of Synthesis

3.1.1 Template reaction

For a metal centre to act as an effective template its properties must include (i) kinetic lability, (ii) the ability to direct the mechanism to cyclic rather than oligomeric or polymeric products, and (ii) the ability to stabilize the macrocycle once formed. These criteria are met for the first row transition metals such as Ni(II), Cu(II) and Zn(II)[66]. However, due to their relative kinetic non lability, second and third row platinum group metal ions are generally considered to be poor centres for template macrocyclic synthesis.

The template condensation of the platinum metals with 1,2-dicycanobenzene or o-cyanobenzamide at elevated temperatures of *ca.* 250°C forming metallophthalocyanine complexes, is well established[46].

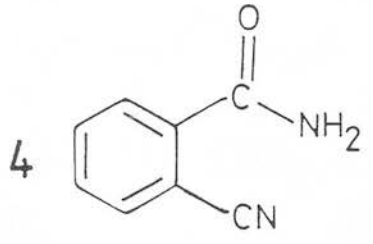

$$4\ \mathrm{L} + MCl_3 \longrightarrow [M(Pc)ClL] \qquad [21]$$

L

M = Ru(III), Rh(III)

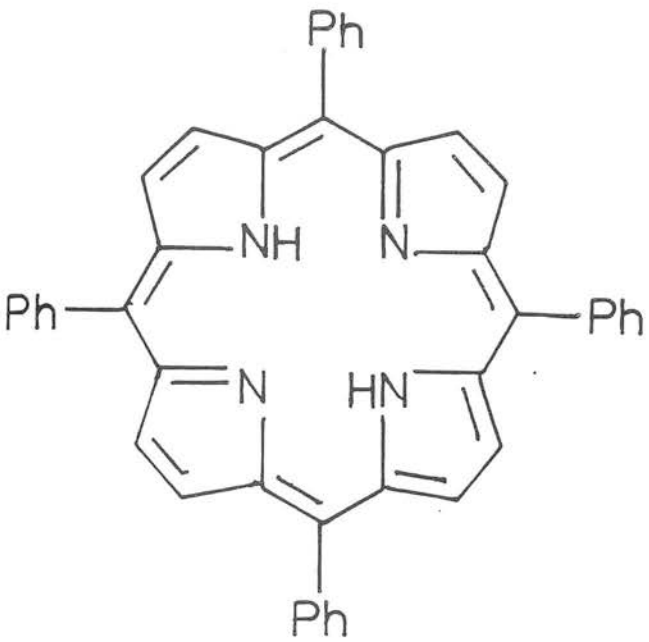

H_2TPP

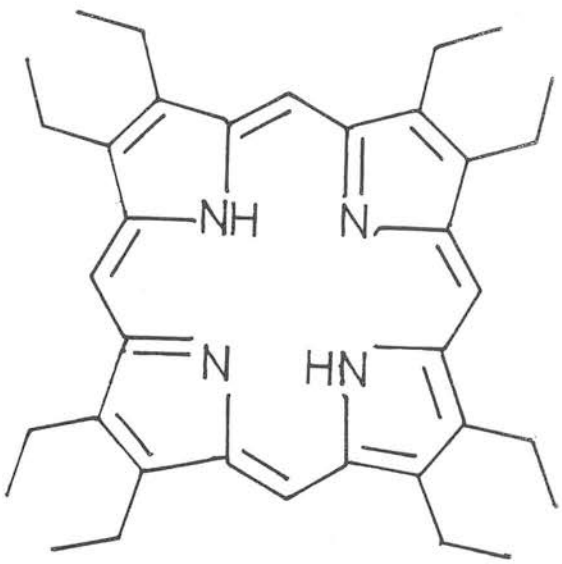

H_2OEP

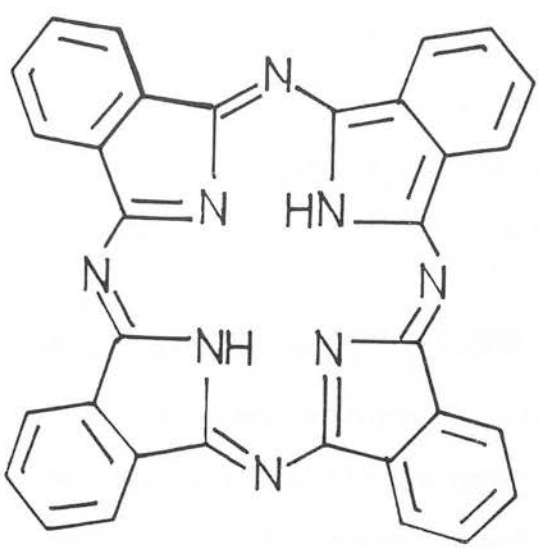

H_2Pc

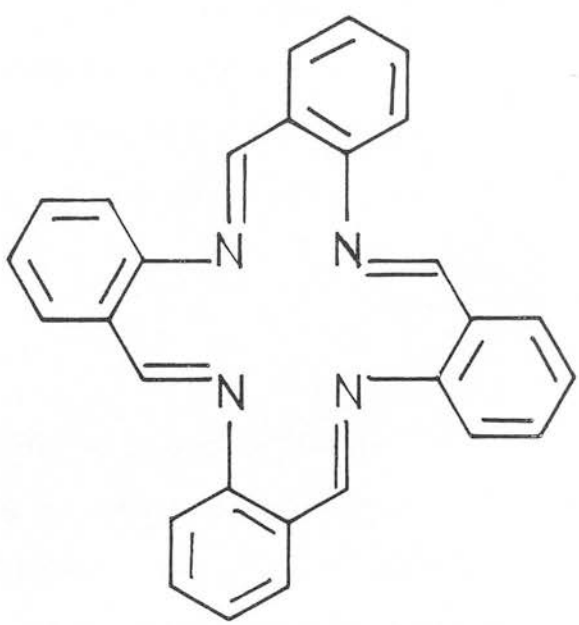

(22)

This method of synthesis has been extended to use o-amino-benzaldehyde to prepare the Pt,Pd complexes of the 16 membered macrocycle,[67] (22).

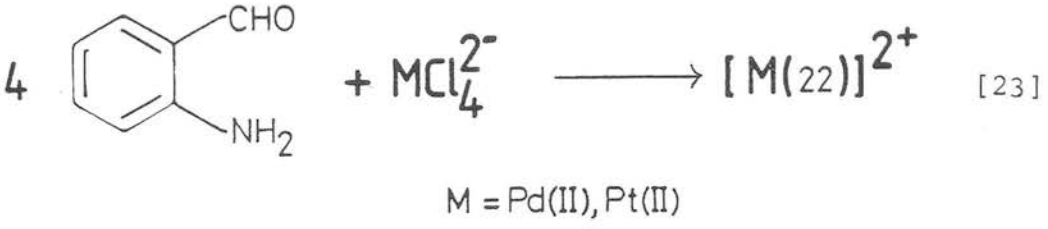

However, few other examples of platinum metal mediated template reactions have been reported. Using Ru(III) as template Poon and Che[68] claimed to have prepared a Ru(II) pyridyl tetraaza macrocyclic complex, $[Ru(n_4)(H_2O)_2]^{2+}$, under mild conditions by refluxing 2,6-diacetylpyridine with *mer*$[Ru(N_3)Cl_3]$, (N_3 = 4-azaheptane-1,7-diamine) in aqueous ethanol. In view of its importance to the synthesis of new platinum metal tetraaza macrocycles, we initiated our study by trying to reprepare the ruthenium species $[Ru(n_4)(H_2O)_2]^{2+}$, and also to extend the range of metals utilized in template reactions to include other platinum metals.

3.1.2 Metal Insertion Reactions

The most successful preparations of platinum metal macrocyclic complexes generally employ metal insertion reactions into a preformed free ligand. The rate of metal insertion however is often slow. These problems are further

aggravated on attempted insertion of the third row metal ion due to their enhanced kinetic inertness over their second row analogues[69].

Rh(III) has been inserted in high yield into saturated tetraamines or ring size varying from 12 to 16[70-72], and a range of 14 membered tetraaza macrocycles with varying ligand saturation and substitution on ring carbons[38,73-75] e.g. *trans*[Rh(12)(Me)I], *cis*[Rh(24)Cl_2]$^+$, *cis* or *trans*-[Rh(L)Cl_2]$^+$, L = cyclam, C-*meso*-or C-*rac*-HMC.

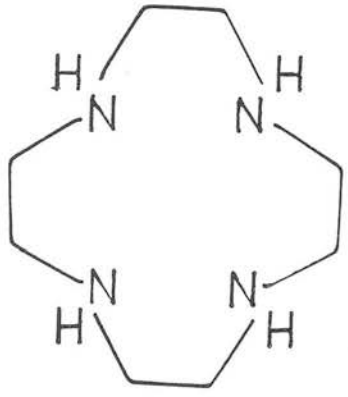

(24)

To date, only one literature report of the corresponding d^6, Ir(III) complex has been published. Poon[76], prepared in moderate yields *cis*[Ir(L)X_2]$^+$, L = HMC or cyclam, X = Br,Cl by a controlled rate of addition of an alcoholic solution of L to refluxing $K_2[IrX_6]$ in methanol or ethanol.

In the same manner Poon has produced a reliable method

of inserting Ru(III) to form *trans*$[Ru(L)X_2]^+$, L = cyclam, TMC, HMC, X = Br,Cl by controlled addition of L to refluxing $K_2[RuX_5(H_2O)]$[77,78].

By controlled electrochemical and chemical oxidation of the TMC product, the ruthenium IV,[79] V[80] and VI[81] species *trans*$[Ru(TMC)(O)(CH_3CN)]^{2+}$, *trans*$[Ru(TMC)(O)_2]^{2+/+}$ have been isolated. The authors noted difficulties in the synthesis of Ru(II) tetraaza macrocyclic complexes; on reduction of the Ru(III) cyclam species they were unable to isolate stable Ru(II) products, decomposition was attributed to ligand oxidative dehydrogenation[77]. Similarly Os(III) was inserted in low yields forming *trans*$[Os(L)X_2]^+$ by reacting $[OsX_6]^{2-}$ with L in methanol, L = cyclam[49], TMC, X = Cl,Br. For the cyclam complex oxidative dehydrogenation was noted as a competing side reaction. H_2O_2 oxidation of the TMC product gives *trans*$[Os(VI)TMC(O)_2]^+$ in a similar manner to ruthenium[82]. This complex can be electrochemically reduced to produce a rare example of a stable Os(V) product[83].

A greater number of Pd tetraaza macrocycles have been prepared than Pt, although in both cases examples are vastly outnumbered by their square planar Ni analogues. The square planar $[Pd\ cyclam]^{2+}$ and octahedral $[Pd(IV)(cyclam)Cl_2]^{2+}$ have been prepared and structurally characterized[84]. The fully inserted Pt analogues are to date unreported.

Kimura[85] has recently isolated a platinum complex of the cyclam derivative, (25), under surprisingly mild conditions.

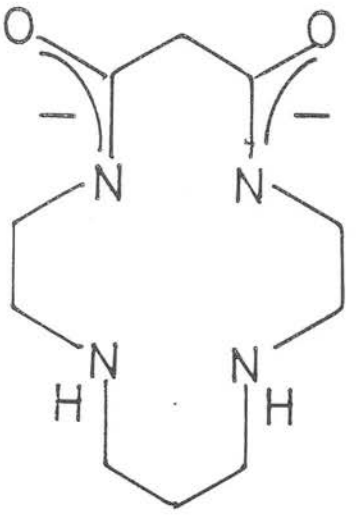

(25)

Gentle warming for 6 hours of [H_2(25)] with K_2PtCl_4 in water in the presence of the reducing agent $Na_2S_2O_3.5H_2O$ gave the neutral species [Pt(25)] in high yield. Without the reductant complexation to the kinetically inert Pt(II) centre is dramatically reduced.

Using syntheses often analogous to those described above, an attempt to systematically insert the platinum metals into L^1-L^4 to form new platinum metal-non porphyrinoid analogues was undertaken. It was expected that insertion of the platinum metals into the pyridyl ligands would proceed more efficiently than into a 'cyclam' type analogue due to the greater nucleophilic nature of the pyridyl function over a secondary or tertiary amine function.

Results and Discussion

3.2 Ruthenium

3.2.1 Synthesis

i. Template methods

Poon and Che[68] have reported the synthesis of a macrocyclic Schiff base complex formulated as $[Ru(II)(n_4)(H_2O)_2]^{2+}$, [26] in 65% yield by condensation of 2,6-diacetylpyridine with *mer*$[Ru(N_3)Cl_3]$, (N_3 = 4-aza-heptane, 1,7-diamine) in aqueous ethanol.

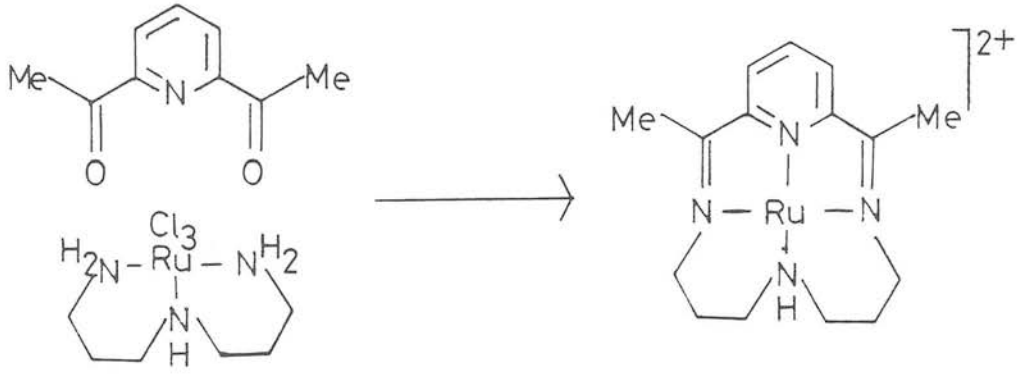

[26]

The assignment of a Ru(II) macrocyclic complex was based only upon magnetic, UV/vis and elemental analysis data. In view of the potential significance for a general synthetic route to platinum metal macrocycles a thorough investigation of the unusual reaction was initiated.

Repeated attempts to resynthesise the compound by the published procedure outlined above were unsuccessful. Solids isolated from the preparation gave bands in the infrared

spectrum assignable to $\nu_{C=O}$ and ν_{NH} stretching vibrations of non-cyclised products. Attempted template reactions around $[Ru(CH_3CN)_4Cl_2]$ or $K_2[RuCl_5(OH_2)]$ respectively led, in our hands, to products involving incomplete macrocyclic condensation. It is believed that intermediates with strong metal-nitrogen bonds are formed, their non-lability inhibiting the possible ring closure step.

ii. Metal Insertion Reactions

With the failure to isolate macrocyclic products by template methods, insertion reactions of Ru(II) into the pyridyl macrocycle L^3 were attempted. Initial experiments using *trans*$[Ru(CH_3CN)_4Cl_2]$ suggested that lengthy reflux times in high boiling point solvents were required for metal insertion. A product with a poorly resolved infrared spectrum was isolated from the reaction of *trans*$[Ru(CH_3CN)_4Cl_2]$ with L^3 using 2-ethoxyethanol as solvent. Of note was a medium intensity band at 1943 cm^{-1} suggesting terminally bound carbonyl, presumably derived from the solvent which is a known carbonylating medium. The reaction was therefore repeated under a CO atmosphere in various solvents. Optimum conditions were found on treating *trans*$[Ru(CH_3CN)_4Cl_2]$ with L^3 in refluxing ethanol under CO for 24 hours. Further reflux for 24 hours under N_2 gave a dark orange solution and addition of NH_4PF_6 or $NaBPh_4$ yielded the corresponding salts of $[Ru(II)L^3(CO)Cl]^+$ in up to 60% yield [87]. Infrared, conductivity and f.a.b. mass spectral evidence suggest the above stoichiometry ($\nu_{C\equiv O}$ = 1930, $\nu_{(Ru-Cl)}$ = 301 cm^{-1}; 1:1 electrolyte in CH_3NO_2; $[^{102}RuL^3(CO)Cl]^+$ M(calculated) 441,

found 441).

No attempt was made to prepare complexes with ligands L^1,L^4 although it would be expected that complexes of similar stoichiometry to $[RuL^3(CO)Cl]^+$ could be prepared. The higher basicity[88] and added steric bulk of the tertiary amine functions of L^2 are factors that contribute to the failure to prepare $[RuL^2(CO)Cl]^+$ by an analogous route.

3.2.2 The Single Crystal X-ray Structure of *cis*$[RuL^3(CO)Cl]BPh_4$

A single crystal X-ray study was undertaken on a red-brown plate (0.5x0.34x0.07mm), obtained from slow evaporation of a nitromethane solution in order to confirm the stereochemistry about the ruthenium centre.

Crystal Data

$C_{17}H_{28}ClN_4ORu^+.C_{24}H_{20}B^-$, M = 760.2, triclinic, space group $P\bar{1}$, a = 9.9854(17), b = 11.6723(22) c = 16.558(3)Å, α = 72.124(19), β = 89.210(15), γ = 82.200(15)°, U = 1818.9Å^3, Dc = 1.388 g cm^{-3}, Z = 2, $F(000)$ = 792, μ(Mo-Kα) = 5.00 cm^{-1} λ(Mo-Kα) = 0.71069Å. At convergence R,Rw = 0.067, 0.0948 respectively for 3757 data.

Selected bond lengths and angles are given in Table 3.2.I and two views of the cation are shown in Figures 3.2.II and 3.2.III.

The structure shows octahedral Ru(II) coordinated to the macrocycle in a folded configuration[87]. Ruthenium is coordinated to all four nitrogen donors of L^3, three are bound

Table 3.2.I. Selected bond lengths and angles (with e.s.d's) for $[RuL^3(CO)Cl]BPh_4$

Bond lengths (Å)

Ru - N(17)	2.038(8)
Ru - N(3)	2.116(9)
Ru - N(7)	2.138(8)
Ru - N(11)	2.106(9)
Ru - Cl	2.422(3)
Ru - C	1.830(10)
C - O(1)	1.167(13)

Bond angles (°)

Cl - Ru - N(17)	85.9(2)
Cl - Ru - N(3)	86.6(2)
Cl - Ru - N(7)	179.2(2)
Cl - Ru - N(11)	87.5(2)
Cl - Ru - C	88.6(3)
N(17) - Ru - N(7)	93.4(3)
N(17) - Ru - C	174.4(4)
N(3) - Ru - N(11)	159.3(3)
Ru - C - O(1)	175.2(9)

Figure 3.2.II View of the Single Crystal X-ray Structure of $[RuL^3(CO)Cl]^+$

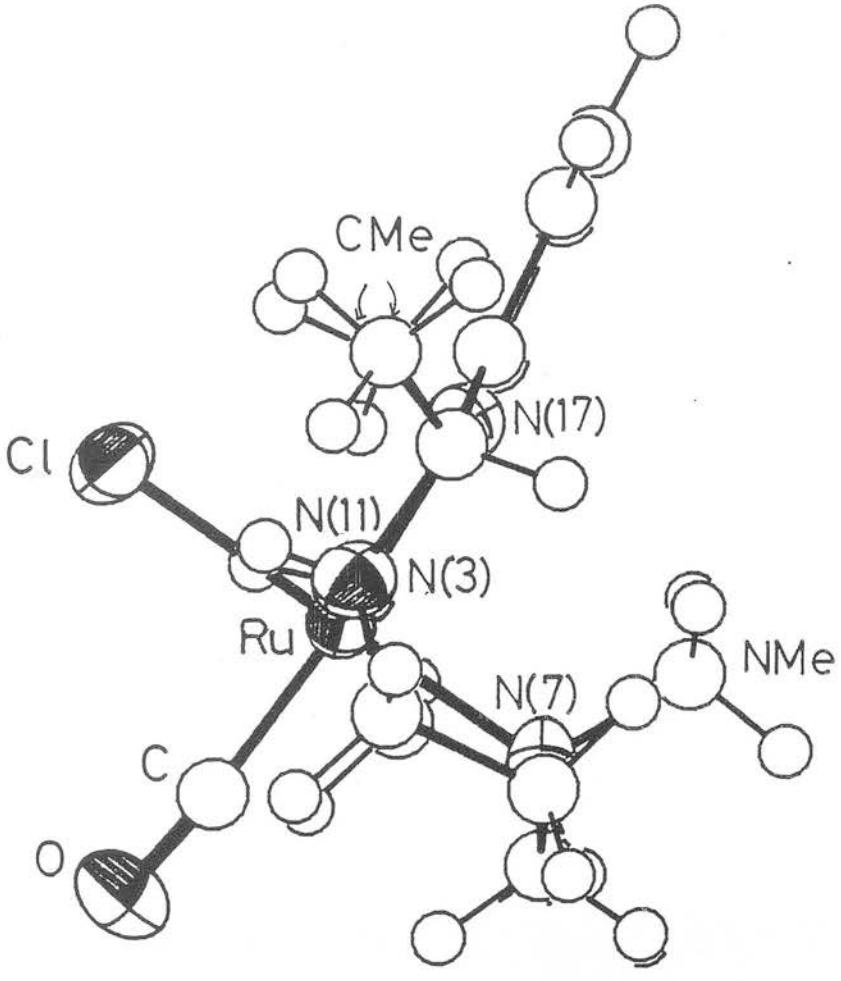

Figure 3.2.III View of the Single Crystal X-ray Structure of $[RuL^3(CO)Cl]^+$

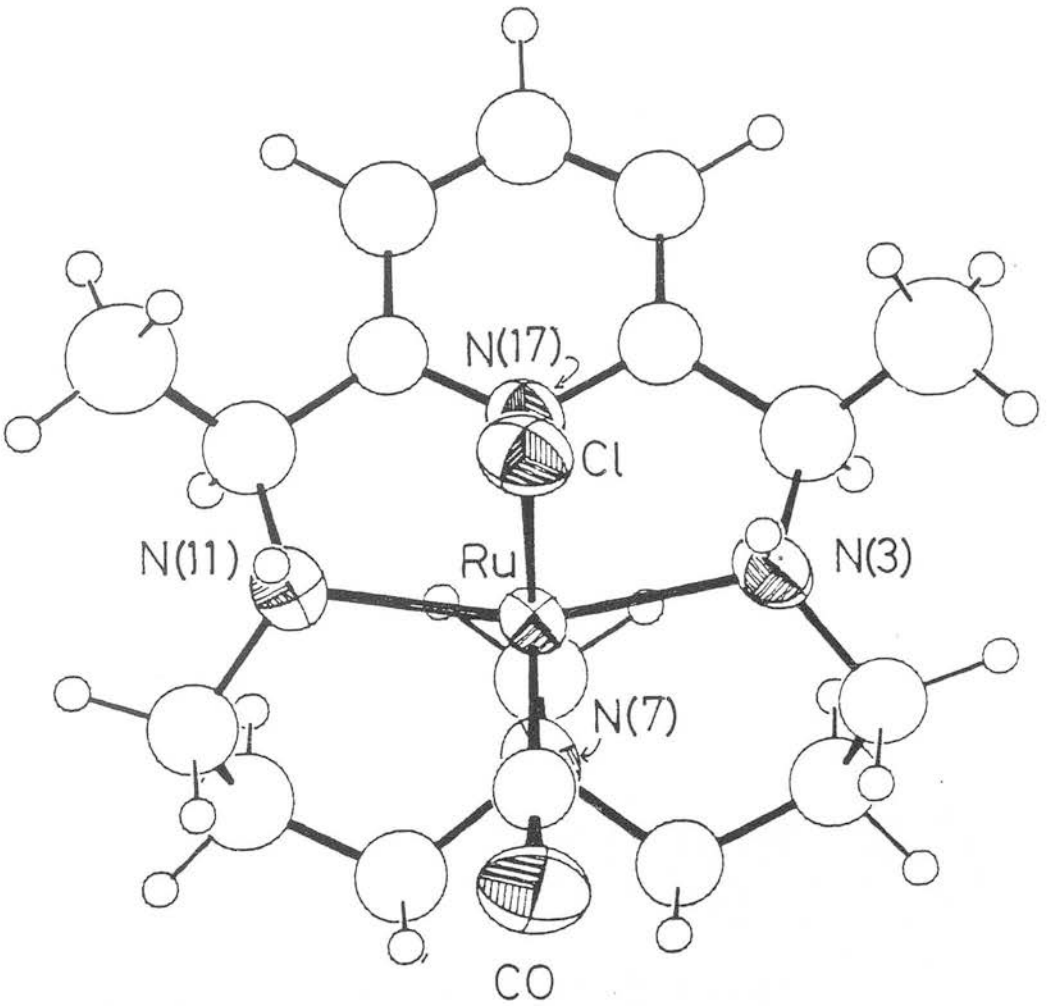

equatorally; Ru-N(3) = 2.116(9), Ru-N(11) = 2.106(9), Ru-N(17) = 2.038(8)Å, and the fourth donor, N(7), is bent away to bind in an axial position, Ru-N(7) = 2.138(8)Å. Mutually *cis* chloro and carbonyl ligands, Ru-Cl = 2.433(3), Ru-C = 1.830(10)Å, complete the essentially octahedral coordination around Ru. The CO ligand is *trans* to the pyridyl N(17) donor and the Cl is *trans* to N(7), <N(17)-Ru-C = 174.4(4)°, <Cl-Ru-N(7) = 179.2(2)°. The Ru atom lies 0.098Å out of the triaza plane defined by N(17), N(3), N(11) towards N(7). The best least squares plane of the pyridine ring makes a dihedral angle of 7.9° to this 'RuN_3' plane.

The *cis* chloro carbonyl moiety represents a coordination mode not previously observed for ruthenium macrocycles, although related species have been proposed, but not confirmed, for ruthenium phthalocyanine or porphyrin complexes[89]. The moiety is not unique for ruthenium-nitrogen donor chemistry as the well established *cis* Ru(II) 2,2'-bipyridyl, (bipy), complex $[Ru(bipy)_2(CO)Cl]^+$ has been structurally characterized[90].

3.2.3 Discussion

The folded macrocyclic conformation found in the solid state structure of $[RuL^3(CO)Cl]^+$ may be explained by considering the 'fit' of the metal ion into the cavity of the planar macrocycle. Nelson and coworkers[91] calculated that metal ions of ionic radius 0.84Å or less would 'fit' into the more rigid unsaturated macrocycle n_4 without any distortion of the macrocycle from planarity. Octahedral Ru(II) of ionic

radius 0.78Å [92], would therefore be expected to be accommodated into the more flexible derivative of n_4, L^3, without distortion from planarity. This fact suggests that the folded structure observed may represent the kinetic rather than the thermodynamic product of the reaction.

The mechanism of the reaction is uncertain. On repeating the synthesis under equivalent conditions but substituting N_2 for a CO atmosphere gave no pure isolatable products. This observation demonstrates the importance of π acceptor ligands such as CO in the formation and stabilization of Ru(II) tetraaza macrocyclic complexes. Taube and Walker[93] prepared an air stable Ru(II) cyclam complex of stoichiometry $[Ru(cyclam)PPh_3Cl]Cl.H_2O$ using $[RuCl_2(PPh_3)_3]$ as the source of Ru(II).

One example of the use of ruthenium(II) carbonyl complexes in catalysis is illustrated by the catalysis of the Water Gas Shift Reaction by $[Ru(bipy)_2(CO)Cl]^+$ (bipy = 2,2'-bipyridine) [94,95]. The Water Gas Shift reaction [27]

$$CO + H_2O \rightarrow CO_2 + H_2 \qquad [27]$$

catalysed by transition metal complexes in alkaline media has been suggested to involve nucleophilic attack of OH^- or H_2O on the carbon atom of the M-CO moiety giving a hydroxcarbonyl complex [28]. Thermal decarboxylation of [28] produces CO_2 and a metal hydride [29] which subsequently reacts with protons and water evolving H_2.

$$Ru\text{-}CO + OH^- \rightarrow Ru\text{-}COOH \qquad [28]$$

$$Ru\text{-}COOH \rightarrow RuH + CO_2 \qquad [29]$$

All the proposed intermediates have been detected by Tanaka and coworkers[95] using *cis*$[Ru(bipy)_2(CO)Cl]^+$ in mild alkaline conditions.

No assessment of the potential catalytic properties of $[RuL^3(CO)Cl]^+$ by the detection of intermediates such as [28] and [29] has to date been initiated.

3.3 Osmium

3.3.1 Synthesis

To date, no osmium tetraaza pyridyl macrocycles have been successfully synthesised. An attempt to insert osmium in an analogous manner to that used in the successful insertion of ruthenium was undertaken. Refluxing $(NH_4)_2[OsCl_6]$ with L^1 under CO in ethanol for 24 hours resulted in a yellow green solid precipitating from a dark orange solution. The product, which is insoluble in all common solvents has bands at 1603 and 1574 cm^{-1} due to the coordinated macrocycle. No bands from coordinated carbon monoxide were observed but a strong ν(Os-Cl) band is seen at 314 cm^{-1}. Solubility data in combination with elemental analysis figures suggest a polymeric formulation. Repeating the reaction using methanol as solvent resulted in a similar orange solution. On work up of the solution dark brown decomposition products were obtained.

Very recently an example of an osmium(III) tetraaza macrocycle, *trans*$[Os(TMC)Cl_2]^+$ has been prepared by Che[82,83]. The synthetic procedure described above was used although tin plates were used as the reducing agent.

3.4 Rhodium

3.4.1 Synthesis

i. Template methods

Rhodium-mediated template reactions were attempted using $RhCl_3.3H_2O$, $[Rh(CH_3CN)_4Cl_2]^+$ or $[Rh(H_2O)_6]^{3+}$ in an analogous manner to those described for ruthenium. Using $RhCl_3.3H_2O$, an isolated product was proven to be the intermediate $[Rh(N_3)Cl_3]$ (N_3 = 4-aza-heptane-1,7-diamine) by microanalytical and infrared analysis. No evidence for a further reaction with 2,6-diacetylpyridine to form the pyridyl macrocycle was obtained on further reflux. The d^8, Rh(I) centre would be expected to behave as a more effective template for these reactions than d^6, Rh(III). With the success of metal insertion reactions of Rh(III) into the free ligands L^n (see below) its feasibility was not persued.

ii. Metal Insertion Reactions

Rhodium(III) complexes with L^1-L^4 were prepared by addition of a methanolic solution of $RhCl_3.3H_2O$ to a refluxing solution of the respective free ligand. A solution colour change from pale red to yellow/orange occurs over a period of 4 hours. On addition of NH_4PF_6 pale yellow solids of stoichiometry $[RhL^nCl_2]PF_6$ were isolated in yields ranging from 60-80% after recrystallization from methanol. A combination of spectroscopic evidence suggested the above stoichiometry eg., $[RhL^1Cl_2]PF_6$. F.a.b. mass spectrum $[^{103}RhL^1Cl_2]^+$, M (calc) 436 (found (435)); $[^{103}RhL^1Cl]^+$, 400(400); $[RhL^1]^+$, 365(363); 1:1 electrolyte in CH_3NO_2;[86] i.r. pyridyl ν(C=C), (C=N) = 1600, 1580, ν(Rh-Cl) = 338 cm^{-1}.

3.4.2 The Single Crystal X-ray Structure of $[RhL^2Cl_2]PF_6$

In order to confirm the stereochemistry and ligand conformation of the complex and in view of the paucity of Rh(III) tetraaza macrocycles that have been characterized crystallographically a single crystal analysis was undertaken. A yellow plate (0.5x0.2x0.1mm) suitable for a structural determination was obtained by slow evaporation of a nitromethane solution.

Crystal data

$C_{18}H_{32}Cl_2N_4Rh^+.PF_6^-$, M = 623.2, triclinic, space group $P\bar{1}$, a = 7.949(7), b = 11.067(12), c = 14.116(13)Å, α = 74.22(8), β = 86.36(7), γ = 84.67(8)°, U = 1188.7Å^3, Dc = 1.741 g cm^{-3}, Z = 2, $F(000)$ = 632, μ(Mo-Kα) = 11.2 cm^{-1}, λ(Mo-Kα) = 0.71069Å. At convergence R,Rw = 0.065, 0.081 respectively for 2292 data.

Selected bond lengths and angles are given in Table 3.4.I and two views of the cation are shown in Figures 2.4.II and 3.4.III.

The structure shows that the rhodium atom is octahedrally coordinated with two *trans* dichloro ligands (Rh-Cl = 2.343(3), 2.350(3)Å) and four equatorially bound N donors (Rh-N = 2.138(9), 2.141(9), 2.164(9) and 1.967(8)Å of the planar macrocycle completing the coordination.

All three of the macrocyclic NMe groups are on the same side of the macrocyclic plane with the two CMe groups on the opposite side (Figure 3.4.II). With the two propylene chains forming symmetry related 6 membered chair configurations, these three features combine to minimise methylene and methyl

Table 3.4.I. Selected bond lengths and angles (with e.s.d's) for $[RhL^2Cl_2]PF_6$

Bond lengths (Å)

Rh - N(17)	1.967(8)
Rh - N(3)	2.138(9)
Rh - N(7)	2.141(9)
Rh - N(11)	2.164(9)
Rh - Cl(1)	2.343(3)
Rh - Cl(2)	2.350(3)

Bond angles (°)

Cl(1) - Rh - N(17)	86.77(25)
Cl(1) - Rh - N(3)	91.26(24)
Cl(1) - Rh - N(7)	89.05(25)
Cl(1) - Rh - N(11)	91.42(24)
Cl(1) - Rh - Cl(2)	175.53(11)
N(3) - Rh - N(11)	164.7 (3)
N(7) - Rh - N(17)	175.8 (3)

Figure 3.4.II. View of the Single Crystal X-ray Structure of $[RhL^2Cl_2]^+$

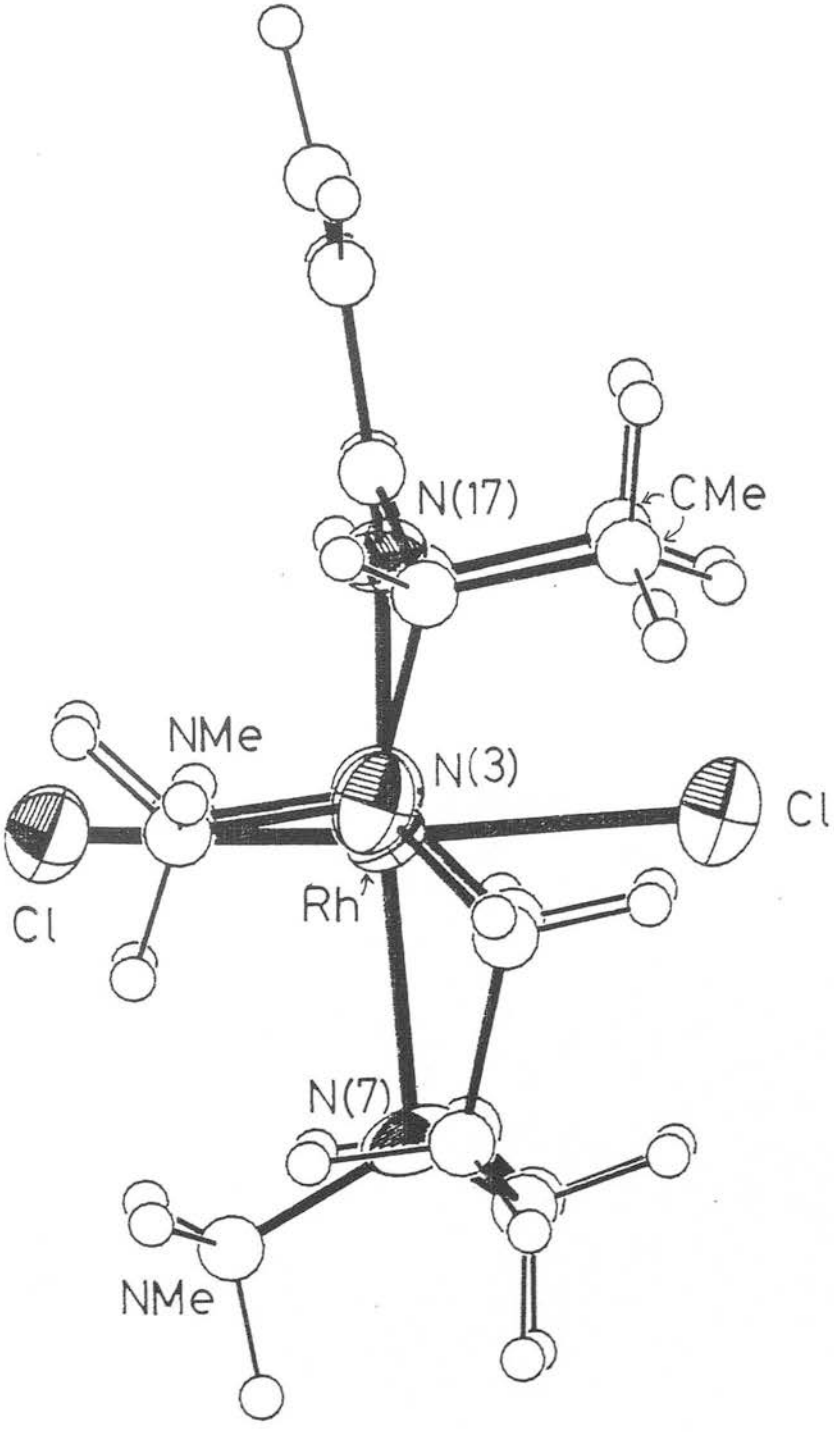

Figure 3.4.III. View of the Single Crystal X-ray Structure of $[RhL^2Cl_2]^+$

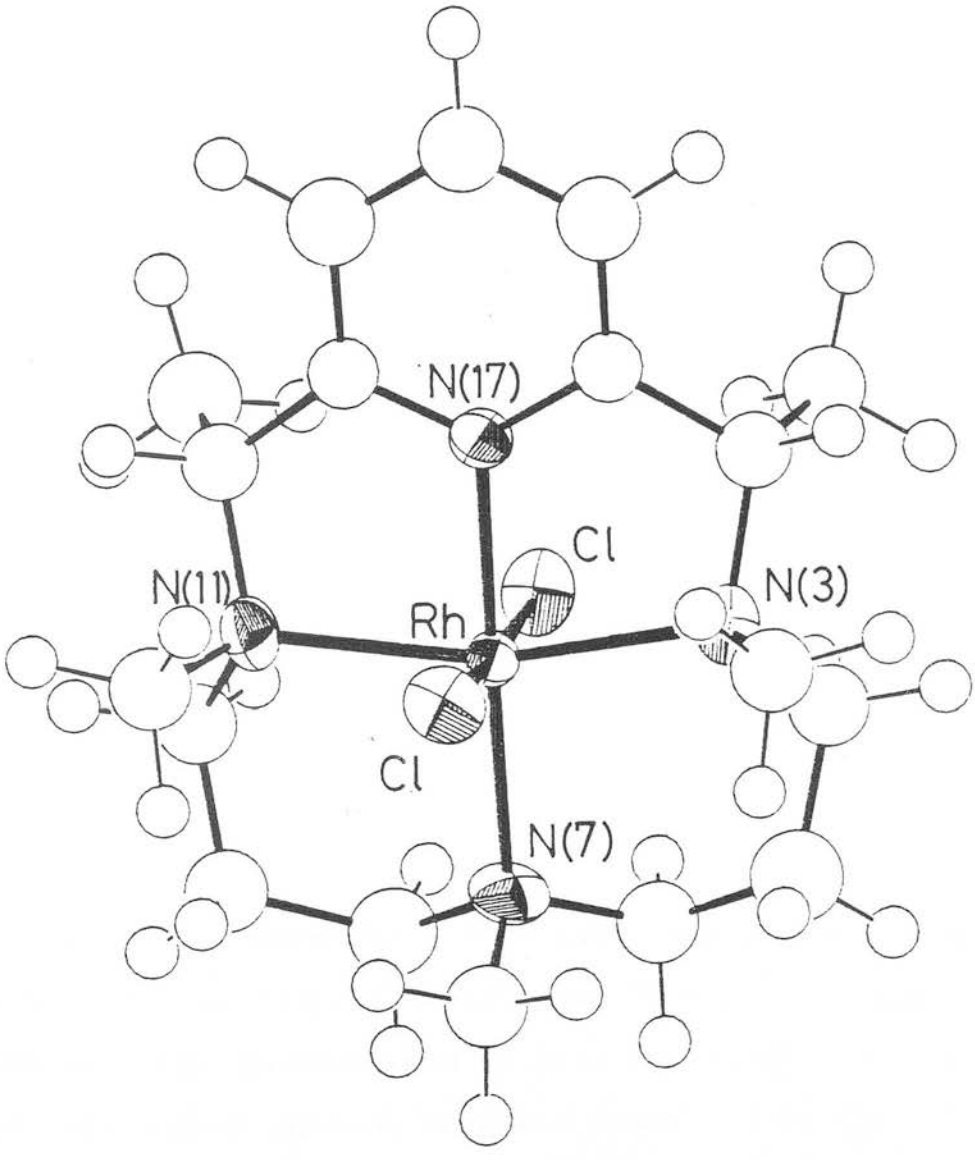

group interactions. One other example of a tri-N-methylated pyridyl macrocycle has been structurally characterized[48]. Barefield has reported the same ligand configuration with the N-bound methyl groups on the same side for $[Ni(30)]^{2+}$ consistent with the steric argument for the observed ligand configuration.

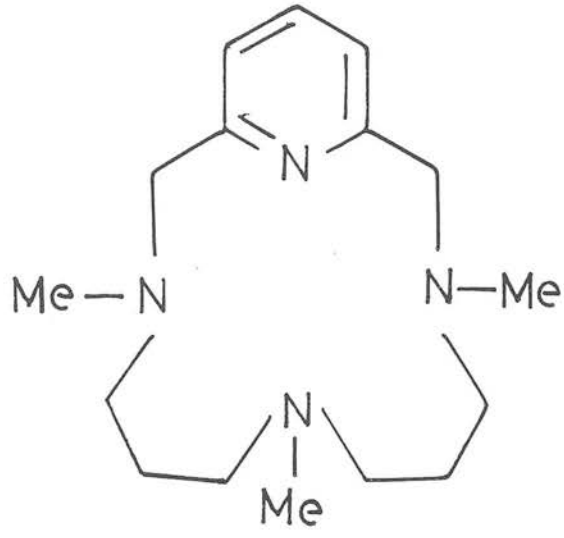

(30)

Coordination around the rhodium is only approximately octahedral as shown by N-Rh-N and Cl-Rh-Cl interatomic angles of 164.7(3), 175.8(3) and 175.53(11)° respectively. However, the rhodium atom is only displaced by 0.01Å from the best least squares tetraaza plane. Distances of relevant atoms from this plane are: Rh -0.01, N(3) -0.06; N(7) 0.05; N(11) -0.06; N(17) 0.075Å. The MN_4 atoms are therefore considerably more planar in $[RhL^2Cl_2]^+$ than C *meso* $[NiL^1](ClO_4)_2$ in which nickel deviates by -0.09Å and nitrogen between -0.08 and 0.11Å from the best tetraaza plane[96].

To encompass the rhodium ion little sign of distortion

of the macrocycle is noted. No increase in macrocyclic bond lengths or angles of L^2 when compared with comparable parameters of L^1 are observed. To accommodate the octahedral geometry of Rh(III) the pyridine ring of L^2 makes a dihedral angle of 6.06° to the best least squares tetraaza plane in comparison to the 65.6° found for the free ligand structure $L^1.H_2O$.

3.4.3 NMR Studies

On obtaining analytically pure samples of $[RhL^nCl_2]^+$, ^1H n.m.r. studies indicated in all cases that a mixture of isomers in varying amounts was present. A further investigation of the ligand isomers was studied utilizing ^{13}C D.E.P.T. n.m.r. spectroscopy. From ^{13}C D.E.P.T. n.m.r. experiments the free ligands L^2,L^4 show the expected respective 9 and 7 resonances due to non-quaternary carbons of the ligands (Table 3.4.IV). On insertion of Rh(III) into L^4 forming $[RhL^4Cl_2]^+$, four resonances for each carbon C(5) and C(14) are present in CD_3NO_2 due to the presence in solution of all four possible isomers. From integration (of carbon atoms with assumed similar relaxation times) for the four species an approximate ratio of 5:2:2:1 was determined for its isomeric composition. At other unique carbon centres overlapping chemical shifts reduce the number of resonances observed. Analysis of $[RhL^2Cl_2]^+$ by ^1H and ^{13}C D.E.P.T. n.m.r. in CD_3NO_2 however shows that not all the expected six configurational isomers are present. A maximum of three isomers are present in any detectable amount.

Table 3.4.I. ^{13}C D.E.P.T. n.m.r. of L^2,L^4 and their Rh complexes

Assignment	δC/ppm L^{2a}	δC/ppm $[RhL^2Cl_2]^{+\ b,c}$	δC/ppm Other resonances	δC/ppm L^{4a}	δC/ppm $[RhL^4Cl_2]^{+\ b,c}$	δC/ppm Other resonances
C15	136.24	139.45	139.75	136.23	139.96	139.16
C14,16	120.69	121.07	120.24	120.26	120.45	120.20, 119.94, 119.57
C2,12	65.11	80.75	80.98, 80.42	54.32	58.40	56.42
C6,8	54.79	62.92	62.28, 61.84	56.11	61.98	61.69
C4,10	51.80	58.17	57.60, 56.94	46.47	47.36	51.03, 45.51
C7N	42.53	47.79	48.17	40.73	45.94	45.94
C3N,11N	39.28	57.86	67.19	-	-	-
C5,9	24.57	22.70	24.73, 22.31	26.93	19.85	25.20, 24.93, 22.15
C2A,12A	16.54	19.77	19.43, 18.04	-	-	-

a $CDCl_3$ solution

b CD_3NO_2 solution

c major isomer

Figure 3.4.V ^{13}C D.E.P.T. n.m.r. of $[RhL^4Cl_2]^+$ in CD_3NO_2

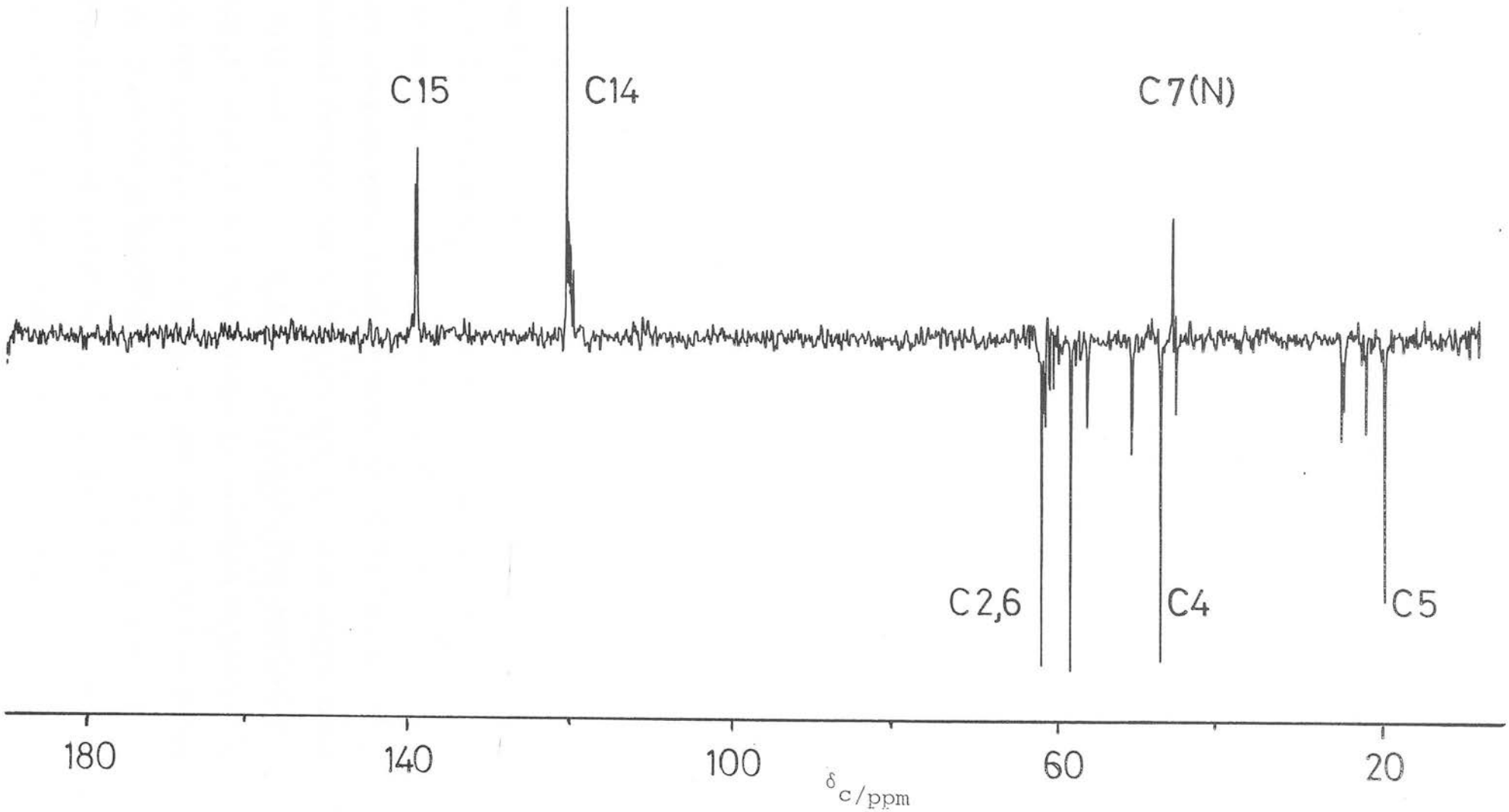

One symmetric isomer is present in greater than 90% abundance, as judged by ^1H n.m.r. integration of the NMe protons. The steric bulk of the four extra methyl groups at C(2), C(12) and N(3), N(11) of L^2 when compared with L^4 is suggested to impose a preferred ligand stereochemistry. For L^2,L^4 it is tentatively proposed that the major species present in solution is the symmetric species with all NH or NMe groups on the same side of the macrocycle. For L^2, C-*meso* CMe groups *anti* to the tertiary amine groups are also predicted from steric arguments. This conclusion has been supported by the single crystal X-ray structure of *trans*$[RhL^2Cl_2]PF_6$ (Figure 3.4.II).

3.4.4 Electronic and Infrared Spectra of $[RhL^nCl_2]^+$ Complexes

Cis and *trans* isomers have been differentiated from analysis of the electronic spectra of octahedral rhodium(III) tetraaza macrocycles with ring size varying from 12-16 members. Fourteen membered rings have been shown to form both *cis* and *trans* isomers whereas 12,13 and 15,16 membered rings form only *cis* and only *trans* isomers respectively[70]. Differentiation is possible due to the higher extinction coefficients and a shifting of the lowest energy band to lower wave length for the *cis* complex when compared with the *trans* isomer. For octahedral Rh(III) there are two spin allowed transitions $\nu_1(^1T_1g \leftarrow {}^1A_1g)$ and $\nu_2(^1T_2g \leftarrow {}^1A_1g)$. In general the complexes *trans*$[RhLCl_2]^+$ where L = a tetraamine or tetraaza macrocycle, have ν_1 in the range 406-411 nm (ε75-120) and ν_2 in the range 310-340 nm (ε=80-160 $dm^3mol^{-1}cm^{-1}$). For *cis* complexes ν_1 ranges from 350-360 nm (ε200-250 $dm^3mol^{-1}cm^{-1}$)[70,75]. The electronic spectra of the pyridyl macrocyclic Rh(III)

Table 3.4.VI. Electronic and Infrared Spectral Data for Selected Octahedral Rh(III) Tetraamine Complexes

Complex	λ_{max}/nm (ε /dm^3 mol^{-1} cm^{-1}) [a]			ν(Rh-Cl) [b]	Ref
	ν_1	ν_2			
trans[RhL^{1}Cl$_2$]PF$_6$	404(138)	324(764)sh [c]	269(4050)	338	this work
trans[RhL^{2}Cl$_2$]PF$_6$	426(144)	348(705)sh	271(4485)	353	this work
trans[RhL^{3}Cl$_2$]PF$_6$	406(146)	324(463)sh	260(3175)	353	this work
trans[RhL^{4}Cl$_2$]PF$_6$	404(126)	326(467)sh	267(3540)	348	this work
trans[Rh(en)$_2$Cl$_2$]$^+$ [d]	406(75)	286(130)			72
trans[Rh(cyclam)Cl$_2$]$^+$	406(78)	310(80)sh	242(3300)		70
trans[Rh(TMC)Cl$_2$]PF$_6$	452(63)	324(242)			73
cis[RhL^{4}Cl$_2$]PF$_6$	372(250)sh		270(3585)	302 245	this work
cis[Rh(en)$_2$Cl$_2$]$^+$ [d]	352(155)	295(180)			75
cis[Rh(cyclam)Cl$_2$]$^+$	355(223)	300(365)	260(685)		70,71

[a] in CH_3CN

[b] as KBr discs

[c] sh = shoulder

[d] en = ethane-1,2-diamine

complexes $[RhL^nCl_2]^+$, n = 1-4, resemble those of previously reported tetraamine complexes. The ν_1 band at 406-411 nm has however a larger extinction coefficient (ε=120-150 $dm^3 mol^{-1}cm^{-1}$) than simple amine or fully saturated macrocycles. A high energy ligand→Rh charge transfer band is also observed in the range 260-270 nm (Table 3.4.VI). Evidence for both *cis* and *trans* isomers is observed for L^4, the ligand with least steric crowding. Separate samples isolated from different preparations showed not only the characteristic ν_1 band at 404 nm (ε=126) of the *trans* complex but a higher intensity band at 372 nm (ε=250) assigned to the *cis* complex. Further evidence for the *cis* assignment was obtained from the far infrared spectrum. Two strong bands at 302 and 245 cm^{-1} may be assigned tentatively to Rh-Cl stretching vibrations predicted for a *cis* ML_4X_2 complex[97]. The far infrared spectrum of the rhodium complexes with ligands L^1-L^4 all have a single moderately strong band at *ca.*350 cm^{-1} consistent with a *trans* structure. The reduction in the in-plane ligand field is witnessed by a shift of *ca.*20 nm for the ν_1,ν_2 bands to lower energy for the Rh complex of L^2 when compared with L^n n = 1,3,4. A shift in the lowest energy band of the palladium complex $[PdL^2]^{2+}$ of approximately the same magnitude is also observed when compared with $[PdL^n]^{2+}$, n = 1,3,4 (Section 3.9).

3.5 Iridium

3.5.1 Synthesis

In comparison with rhodium macrocycles of which several

examples are now known, only one method of synthesis of an iridium tetraaza macrocycle has been described in the literature[76]. Poon and coworkers prepared *cis*$[IrLX_2]^+$, L = HMC or cyclam, X = Br,Cl by a controlled rate of addition of an alcoholic solution of L to refluxing $K_2[IrX_6]$ in methanol. It is well established that the synthesis of Ir(III) amine complexes are not straightforward and yields are often low due to substitutionally inert starting materials and competing hydrolysis and redox side reactions. We therefore utilized long reflux times under vigorous conditions in attempts to prepare Ir(III) pyridyl macrocycles.

Reaction of $IrCl_3.xH_2O$ with L^4 in a refluxing aqueous ethanol solution for 72 hours allowed the isolation of a pale brown solid in moderate yield (36%) on addition of PF_6^- counter anion. The spectacular feature of the infrared spectrum is a very strong sharp band at 2138 cm^{-1} assigned as an iridium hydride stretching vibration, ν_{Ir-H}. Iridium hydride stretching vibrations are generally found to fall within the range 2200-2000 cm^{-1} [97].

A singlet at -22.25 p.p.m. in the ^1H n.m.r. spectrum confirmed the hydride assignment. A metal chloride stretch, $\nu_{(Ir-Cl)}$ at 283 cm^{-1} in the infrared spectrum was also observed; this, together with elemental analysis figures, suggested a stoichiometry of $[IrL^4(H)Cl]PF_6$. F.a.b. mass spectral data were in agreement with the proposed stoichiometry; $[^{193}IrL^4(H)Cl]^+$ M.(calc) 478 (found 478); $[^{193}IrL^4Cl]^+$ 477(476); $[^{193}IrL^4]^+$ 441(438). From the above data however the stereochemistry of the product cannot be assigned. For the complex $[HIr(piperidine)_4Cl]^+$, a *trans* geometry has been

assigned by analysis of the infrared spectrum with $\nu_{(Ir-H)}$ and $\nu_{(Ir-Cl)}$ stretching vibrations occurring at 2198 and 241 cm^{-1} respectively[98].

Jenkins and Shaw[99] have investigated chloroiridium(III) octahedral complexes and found that iridium(III)-chloride stretching modes were in the region 249-246 cm^{-1} for *trans* hydride but 320-303 cm^{-1} for *trans* chloride, a ligand of lower *trans* influence. For our macrocyclic product $[IrL^4(H)Cl]^+$ the $\nu_{(Ir-Cl)}$ stretching vibration was observed at 283 cm^{-1} which may be consistent with mutual *cis*-chlorohydrido ligands.

3.5.2 The Single Crystal X-ray Structure of $[IrL^4(H)Cl]PF_6$

In view of the fact that no Ir(III) tetraaza macrocycles or hydrido Ir(III) tetraamine complexes have been structurally characterized, and in order to investigate the proposed *cis* conformation for the $[IrL^4(H)Cl]^+$ complex, a single crystal X-ray study was carried out. A pale brown crystal (0.35x0.12x0.10 mm) suitable for X-ray analysis was obtained by slow evaporation of a nitromethane solution.

Crystal Data

$C_{14}H_{25}ClIrN_4^+.PF_6^-$ M = 622.0 triclinic, space group $P2_1/c$, a = 10.028(4), b = 11.926(6) c = 16.539(9)Å, β = 99.23(4)°, U = 1952.4Å^3, Dc = 2.116 g cm^{-3}, Z = 4, $F(000)$ = 1200, μ(Mo-Kα) = 70.93 cm^{-1}, λ(Mo-Kα) = 0.71069Å. At convergence R,Rw = 0.0305, 0.0312 respectively for 1548 data.

Selected bond lengths and angles are given in Table 3.5.I and two views of the cation are shown in Figures 3.5.II

Table 3.5.I. Selected bond lengths and angles (with e.s.d's) for $[Ir(III)L^4(H)Cl]PF_6$

Bond lengths (Å)

Ir - N(17)	1.952(10)
Ir - N(3)	2.080(11)
Ir - N(7)	2.266(11)
Ir - N(11)	2.083(11)
Ir - Cl(1)	2.393(4)
Ir - H(1)	1.57 (13)

Bond angles (°)

Cl - Ir - N(17)	175.7(3)
Cl - Ir - N(3)	97.2(3)
Cl - Ir - N(7)	89.0(3)
Cl - Ir - N(11)	97.4(3)
Cl - Ir - H(1)	98.1(48)
N(17) - Ir - N(7)	95.3(4)
N(3) - Ir - N(11)	164.5(4)
N(17) - Ir - H(1)	77.6(48)
N(7) - Ir - H(1)	172.2(48)
N(3) - Ir - H(1)	82.9(48)
N(11) - Ir - H(1)	89.7(48)

and 3.5.III.

The structure shows octahedral Ir(III) coordinated to the macrocycle, L^4, in a similar folded configuration to $[RuL^3(CO)Cl]^+$. Iridium is coordinated to all four nitrogen donors of L^4, three are bound equatorially, Ir-N(3) = 2.080(11), Ir-N(11) = 2.083(11) and Ir-N(17) = 1.952(10)Å, and the fourth donor, N(7), is bent away to bind in an axial position, Ir-N(7) = 2.266(11)Å. Mutually *cis* chloro and hydride ligands, (Ir-Cl = 2.393(4), Ir-H = 1.57(13)Å) complete the essentially octahedral coordination around Ir. The chloride ligand is *trans* to the pyridine N(17) donor and the hydride *trans* to N(7) , <N(17)-Ir-Cl = 175.7(3)°, <H-Ir-N(7) = 172.2(48)°. The Ir atom lies 0.09Å out of the triaza plane defined by N(17),N(3),N(11) towards N(7), ie. away from the hydride. This plane makes a dihedral angle of 5.29° to the best least squares plane of the pyridine ring. The Ir-H bond was located and fully refined to a value of 1.57(13)Å. This represents a coordination mode not previously observed for macrocyclic compounds, although macrocyclic hydrides have been proposed as intermediates in platinum metal insertion reactions into tetraaza macrocycles[49]. The hydridic *trans* influence is illustrated by the exceptionally long Ir-N(7) bond length. A bond length increase of *ca.* 0.14Å is observed due to the hydride's high *trans* influence in which it directs a large portion of the s character in the σ bond towards itself, weakening the remaining σ bonds, especially the *trans* Ir-N(7) bond. A *trans* influence of similar magnitude is observed in the hydridopentaamine rhodium(III) cation, $[HRh(III)(NH_3)_5]^{2+}$ in which an increase

Figure 3.5.II. View of the Single Crystal X-ray Structure of $[IrL^4(H)Cl]^+$

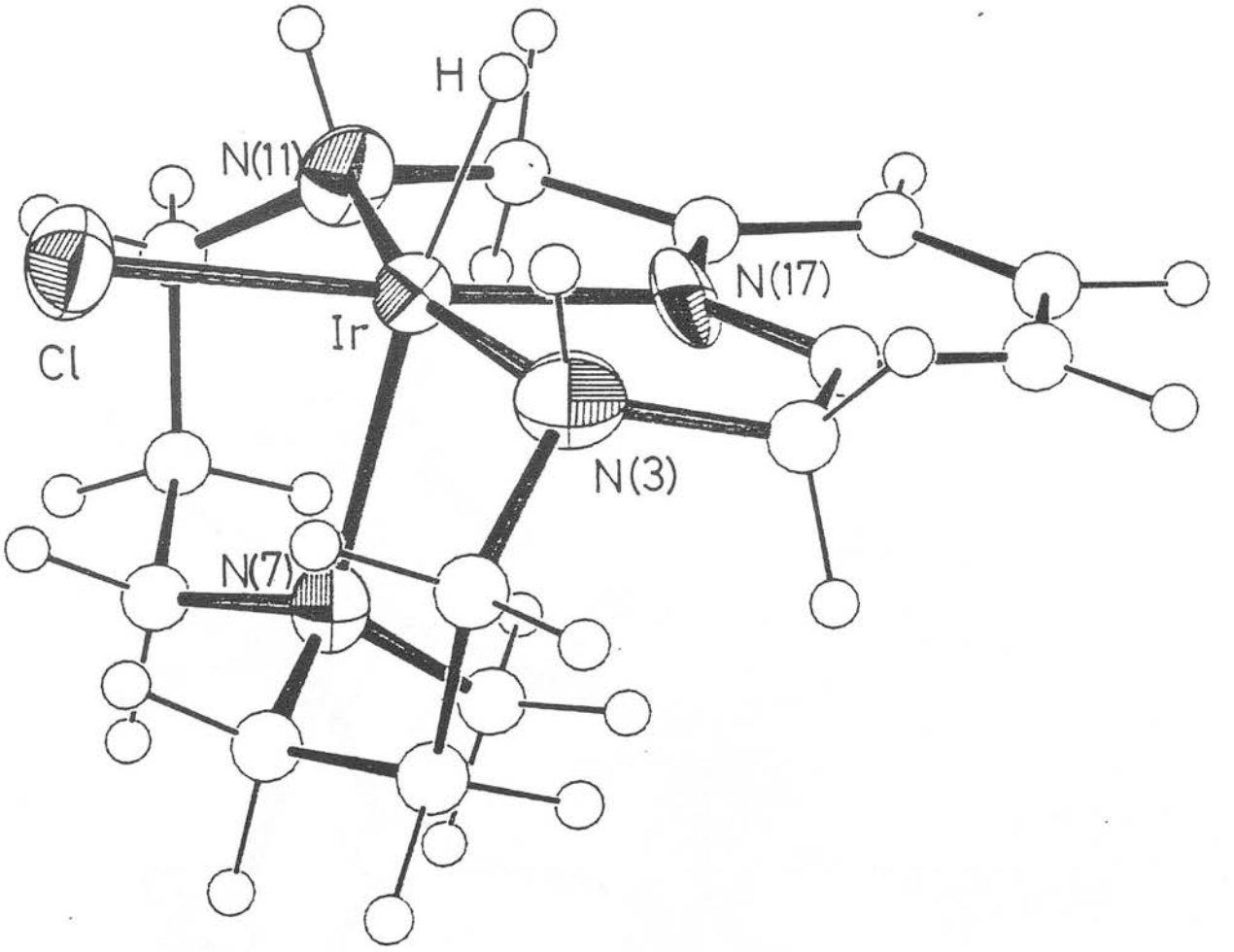

Figure 3.5.III View of the Single Crystal X-ray Structure of $[IrL^4(H)Cl]^+$

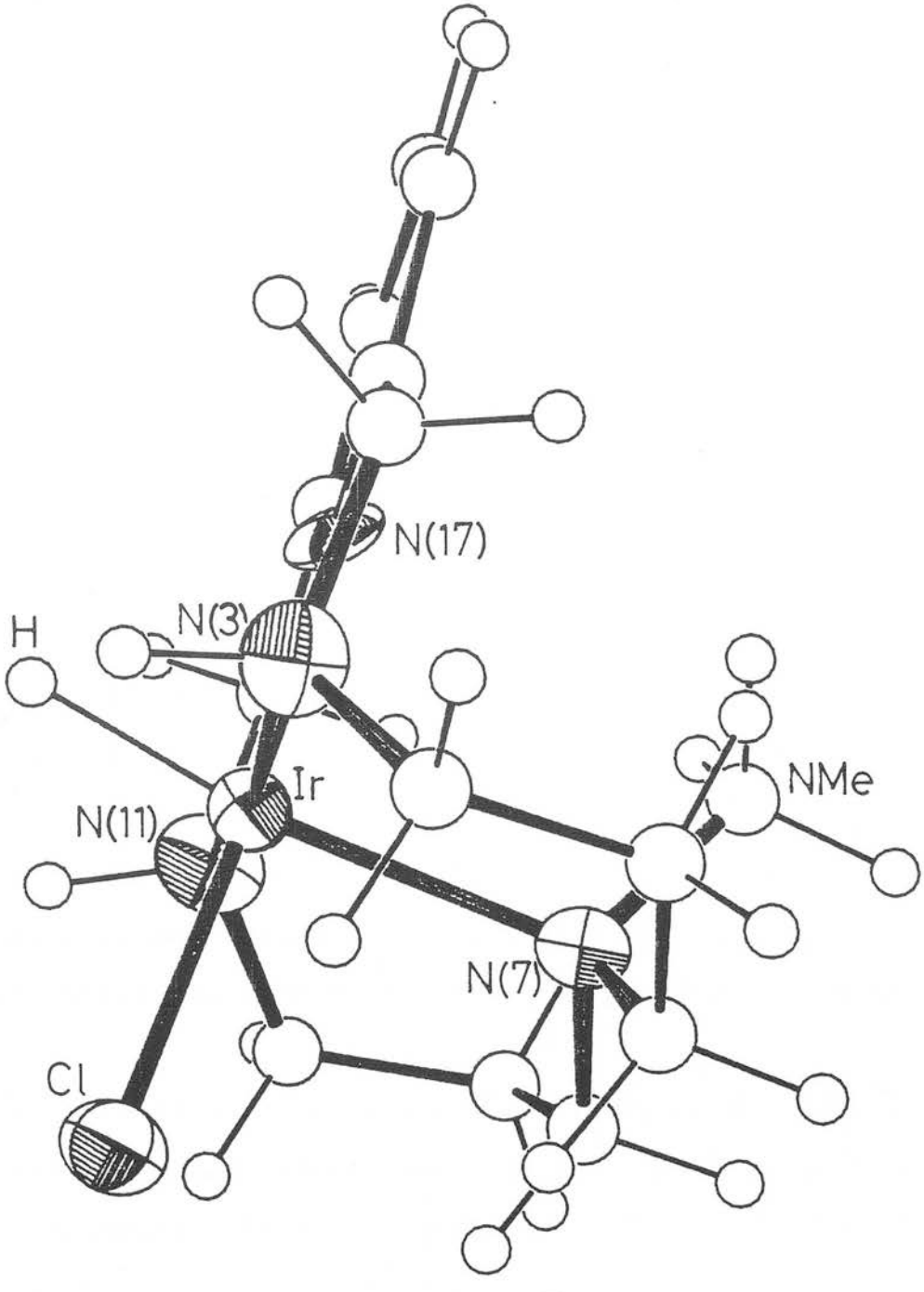

of 0.165Å is noted in the Rh-N bond length *trans* to the hydride, in comparison to the *cis* Rh-N bond length[100]. No apparent significant intermolecular contacts up to a distance of 3.2Å from the hydride are found.

3.5.3 Discussion

The exceptional stability of the hydride iridium tetraaza complex $[IrL^4(H)Cl]^+$ is of interest. Although many stable Ir(III) hydrido complexes are known[101], most utilize one or more π acceptor ligands in their stabilization[102]. Stable hydrido amine Rh(III) complexes have also been prepared[100], but only one example of a hydrido Ir(III) tetraamine complex $[HIr(piperidine)_4Cl]^+$ has been reported. To synthesize hydrido-iridium(III) complexes most preparations use oxidative addition of HX, X = halide or H, to derivatives of Vaskas complex $[Ir(CO)Cl(ER_3)_2]$ (E = P,As, R = (O(alkyl)), alkyl etc.) It is not apparent in the preparation of $[IrL^4(H)Cl]^+$ if the aqueous ethanolic solvent is a powerful enough reducing agent to reduce Ir(III) to Ir(I) for an oxidative addition reaction mechanism to occur.

Several workers have postulated that the mechanism of preparation of Rh(III),Ru(III),Os(III)[49] and Ir(III)[76] ammine, macrocycles or related compounds involve reactive hydrido intermediates when prepared in basic alcoholic solvents.

The Ir(III) ion has an ionic radius of 0.68Å [92] and is therefore sufficiently small to be accommodated in a planar configuration of the pyridyl macrocycle. The *cis* folded macrocyclic configuration found on insertion of Ir(III) into

L^4 was also found by Poon on insertion of Ir(III) into cyclam to form *cis*$[Ir(cyclam)X_2]^+$, X = Cl,Br[76]. Poon was unable to directly prepare the *trans* isomer. Experiments preformed in strongly basic media to induce isomerization suggested that Ir(III) amine complexes are inert to ligand substitution and isomerization reactions.

Transition metal hydrides are important intermediates in many catalytic reactions. Investigated extensively is the addition of a metal hydride across an unsaturated centre. Very often the addition is followed by elimination with isomerization or hydrogenation[102]. In the presence of CO hydroformylation reactions occur [31]. Insertion into the M-H bond of other small molecules such as O_2 gives metallo-hydroperoxide species, M-OOH[103]. The iridium macrocyclic species $[IrL^4(H)Cl]^+$ may also find relevance in the field of catalysis in common with the porphyrin complexes M(por)H, M = Ir,Rh, por = OEP^{2-},TPP^{2-} which show catalytic activity[35,104].

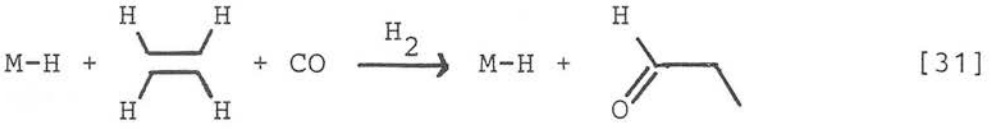

[31]

3.6 Palladium

3.6.1 Synthesis

In an attempt to insert Pd(II) into a wide range of tetraaza macrocycles in high yields, a variety of experimental conditions were employed. Surprisingly, best results were obtained with mild conditions. Stirring L^n, n = 1-4, in

methylene chloride with a solution of the palladium acetate trimer $[Pd(OAc)_2]_3$ for 24 hours allowed for the isolation of pale brown solids of stoichiometry $[PdL^n](PF_6)_2$ on addition of NH_4PF_6. Yields of up to 60% were obtained after recrystallization from methanol. Elemental analysis, infrared, conductivity and f.a.b. mass spectral evidence suggested the above stoichiometry, (eg., $[PdL^1](PF_6)_2$; i.r. pyridyl ν(C=C), ν(C=N) = 1606, 1580 cm^{-1}; 2:1 electrolyte in CH_3NO_2; $[^{106}PdL^1(PF_6)]^+$ M.(calc) 513 ((found)513), $[^{106}PdL^1]^+$ 363, (362)).

3.6.2 The Single Crystal X-ray Structure of $[PdL^1](BPh_4)_2$

In order to investigate the ligand conformation on insertion of Pd(II), the single crystal X-ray structure of $[PdL^1]^{2+}$ was carried out. Results could then be compared directly with the conformation of the free ligand, $L^1.H_2O$ (Section 2.4). A pale brown crystal (0.38x0.13x0.10mm) suitable for X-ray analysis was obtained by slow evaporation of a methanol solution.

Crystal Data

$C_{15}H_{26}N_4Pd^{2+}.B_2C_{48}H_{40}^{2-}$ M = 1007.27, monoclinic, space group $P2_1/a$, a = 16.243(16), b = 26.035(15), c = 12.221(10)Å, β = 103.13(8)°, U = 5033Å^3, Dc = 1.329 g cm^{-3}, Z = 4 $F(000)$ = 2112 μ(Mo-Kα) = 4.06 cm^{-1} λ(Mo-Kα) = 0.71069Å.

A view of the cation is shown in Figure 3.6.I. A square planar geometry is observed around the Pd centre. Extensive disorder is observed throughout the cation

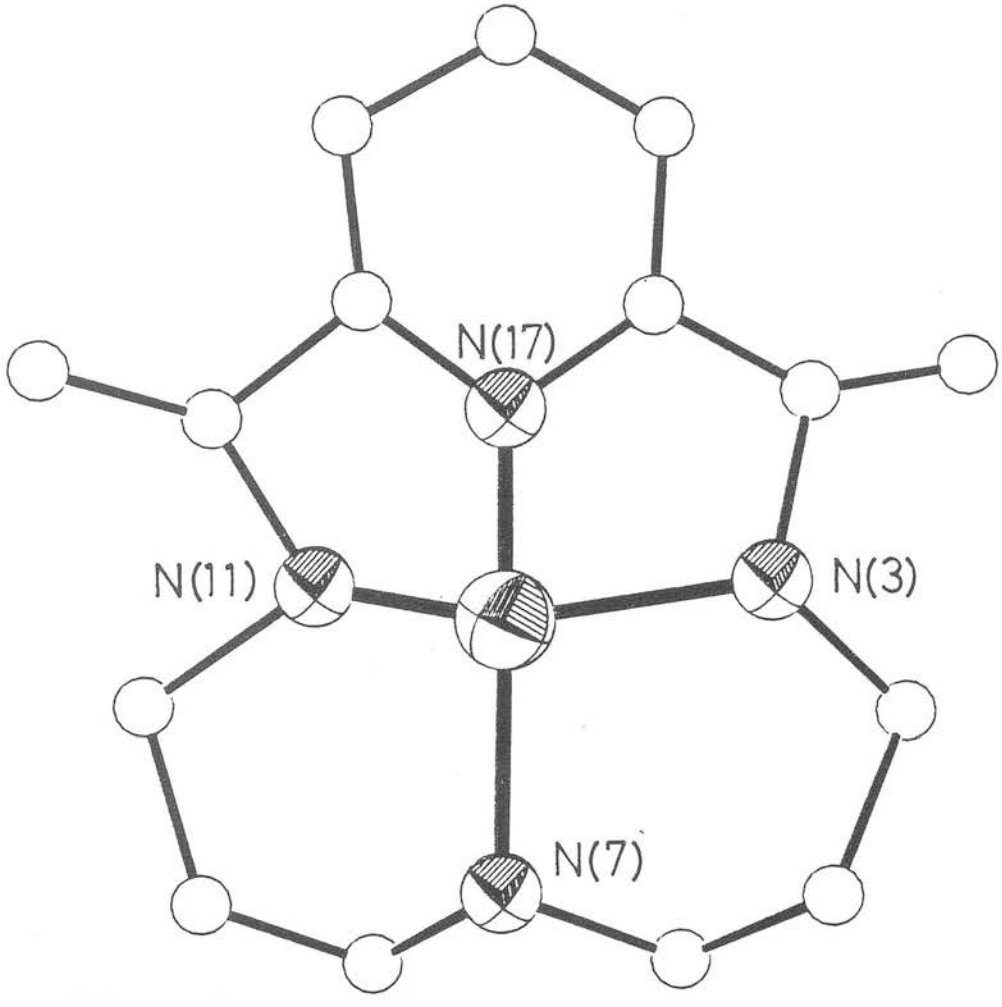

Figure 3.6.I. View of the Single Crystal X-ray Structure of $[PdL^1]^{2+}$

invalidating any direct comparisons with the conformation of the free ligand, $L^1.H_2O$. The two BPh_4^- anions are however ordered and fully located. Currently R = 0.166, Rw = 0.172 for 1844 data. Several ligand isomers present in the single crystal are believed to contribute to the poor quality of the data.

3.6.3 NMR Studies

Characterization of the palladium complexes of L^n, n = 1-4, by ^1H n.m.r. shows the existence in solution of ligand isomers in varying proportions, in a similar manner to rhodium complexes of L^n. As noted by other workers[52], study of the pyridine region, δ_H = 7.5-8.5 p.p.m., is a sensitive probe for the analysis of isomeric products. The proton on the β carbon for L^1,L^3, shows in each case at least five doublets from a maximum of six possible configurational isomers. For L^1, this conclusion is supported by ^{13}C D.E.P.T. n.m.r. (Table 3.6.II) which shows five resonances in the range δ_C 120.7-119.6, characteristic of the β pyridine carbon. Other unique carbons show between two resonances (C15) separated by 0.3 p.p.m. and five resonances (C2A) separated by 4.9 p.p.m. (Figure 3.6.IIIa).

It may be expected that the replacement of secondary amine protons by the more sterically demanding methyl substituents of $[PdL^2]^{2+}$ would impose a preferred ligand conformation. Inspection of the two NMe singlets, N(3)Me, N(7)Me in the ^1H n.m.r. spectrum shows this to be the case with *ca.*92% (by ^1H n.m.r. integration) of the total due to one symmetric species. Two small intensity signals, (*ca.*

Table 3.6.II. ^{13}C D.E.P.T. n.m.r. of L^1, L^4 and their Pd complexes

Assignment	δ_C/ppm L^{1a}	δ_C/ppm $[PdL^1]^{2+}$ b,c	Other resonances	δ_C/ppm L^{4a}	δ_C/ppm $[PdL^4]^{2+}$
C15	136.05	141.30	140.99	136.23	140.88
C14,16	120.54	120.43	120.69, 120.55	120.26	119.08
			120.01, 119.63		
C2,12	58.99	69.35	70.46, 67.26	54.32	62.32
C6,8	45.66	50.80	50.96, 50.57	56.11	61.29
C4,10	43.82	49.28	49.91, 47.32	46.47	51.59
			45.94, 45.76		
C7N	-	-	-	40.73	43.32
C5,9	28.37	26.92	27.02, 26.17	26.93	24.57
C2A,12A	23.39	14.08	18.89, 15.37	-	-
			14.29, 13.96		

a $CDCl_3$ solution

b CD_3NO_2 solution

c major isomer

Figure 3.6.IIIa ^{13}C D.E.P.T. n.m.r. of $[PdL^1]^{2+}$ in CD_3NO_2

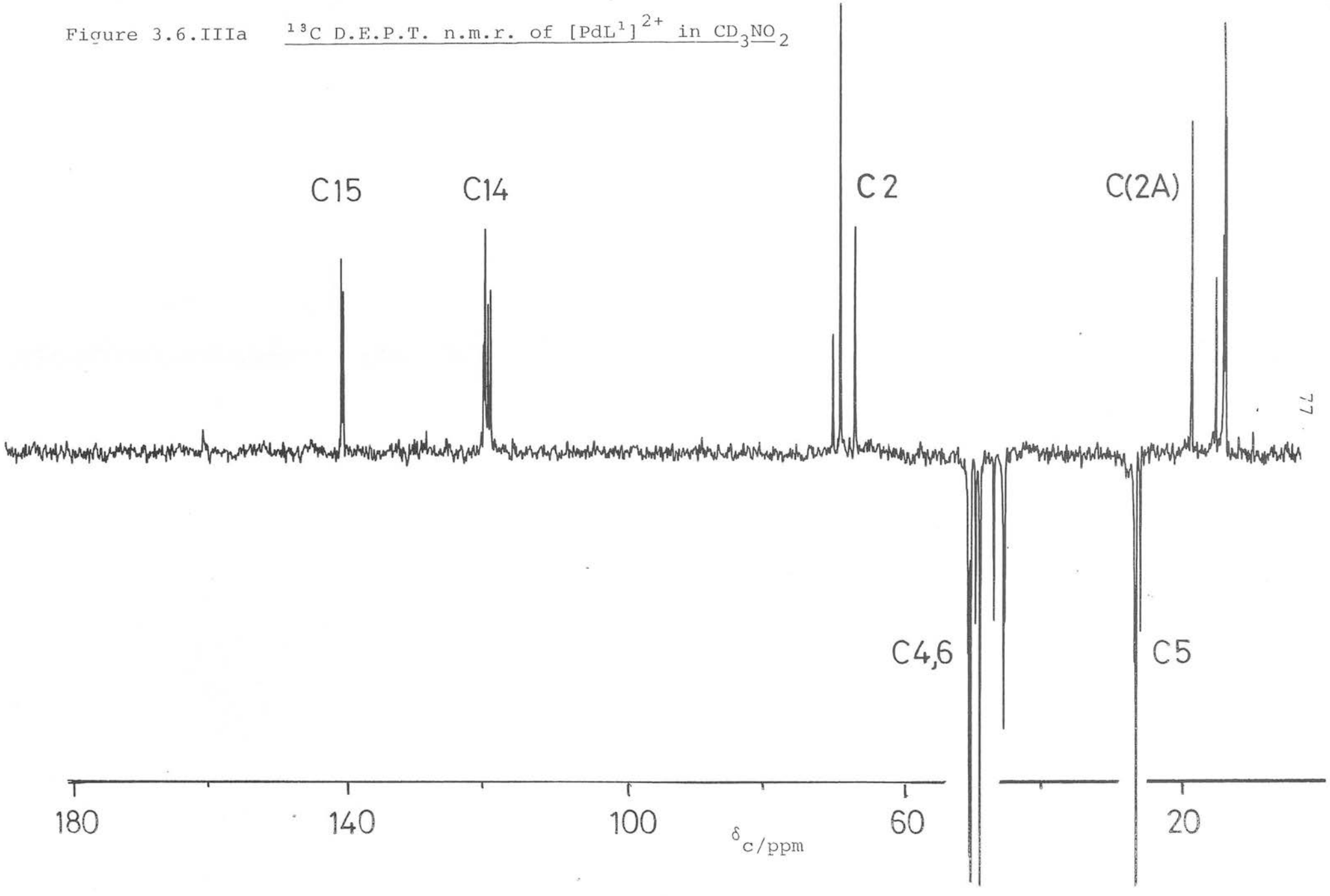

Figure 3.6.IIIb ^{13}C D.E.P.T. n.m.r. of $[PdL^4]^{2+}$ in CD_3NO_2

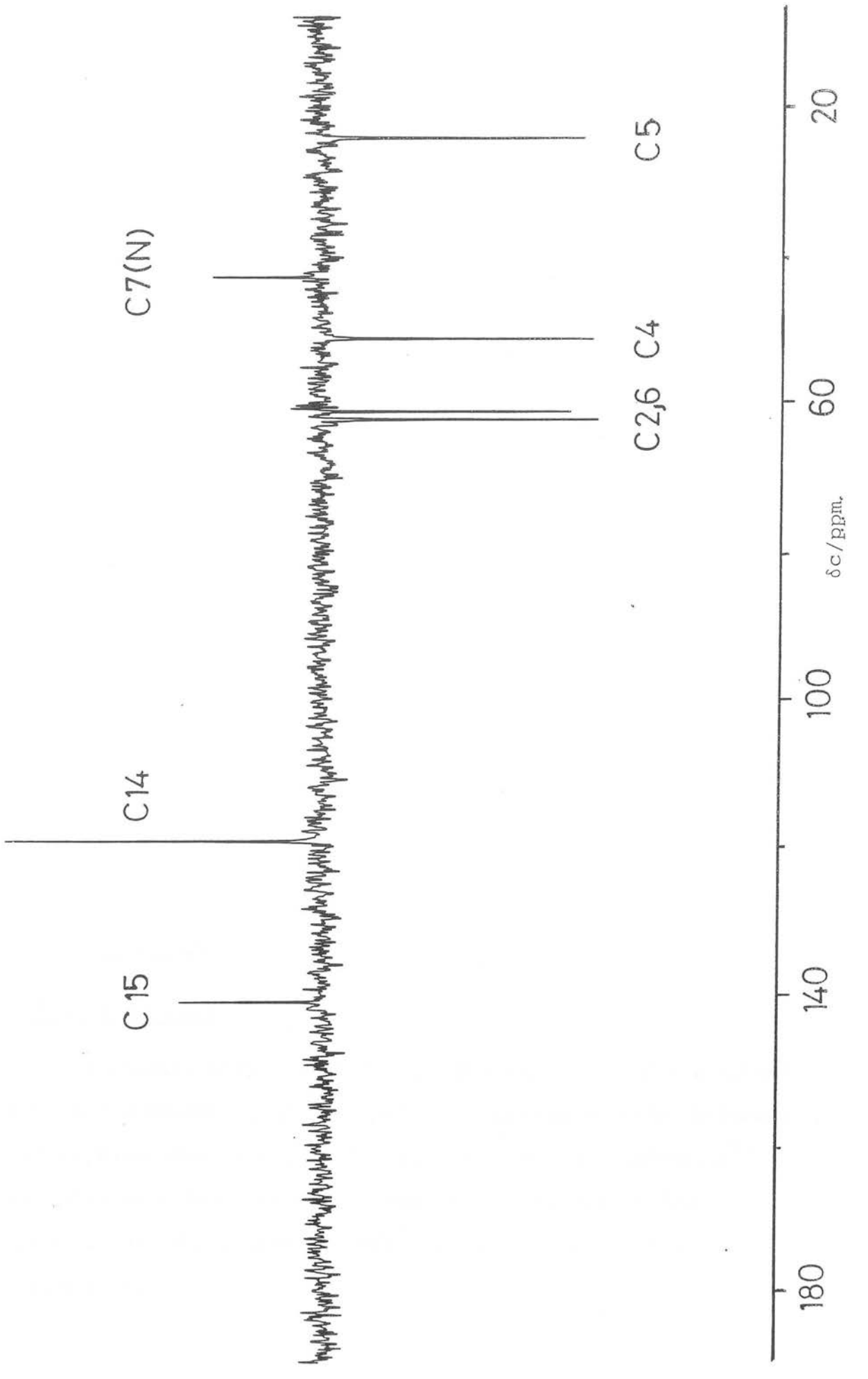

8%) due to the presence of other isomers complete the isomeric mixture. By extrapolating the above results, it would be predicted that L^4 would exist as its Pd complex as all four possible isomers. However in CD_3NO_2, $[PdL^4]^{2+}$ shows seven unique non quaternary resonances due to only one symmetric isomer. Moore *et al.* has prepared the complexes $[ML^4](ClO_4)_2$, M = Ni,Zn. ^{13}C N.m.r. studies also show seven resonances due to one symmetric species[52]. Comparison of ^{13}C chemical shift suggests that the same ligand conformation is present for $[ML^4]^{2+}$, M = Pd,Ni, as the maximum variation of 2.5 p.p.m. is observed for equivalent carbon assignments. It is believed that the ligand conformation has the two secondary amine and NMe group on the same side of the macrocyclic plane. (Figure 3.6.IIIb).

On insertion of palladium into L^4 shifts of between +8.0 and -2.4 p.p.m. are observed in comparison to the free ligand (Table 3.6.II). These magnitudes are comparable to values obtained by Nelson *et al.*[105] for complexation of Pd with open chain pyridyl diimine complexes.

3.7. Platinum

3.7.1 Synthesis

In common with the third row metals Os,Ir, difficulties were encountered in the synthesis of platinum metal tetraaza macrocycles when compared to their second row analogues[69]. For platinum there is not a comparable reagent to the trimeric $[Pd(OAc)_2]_3$ used successfully in the synthesis of Pd macrocycles.

Reaction of $PtCl_2$ in refluxing ethanol with L^4 for 60 hours allowed the isolation of a pale brown solid of stoichiometry $[PtL^4](PF_6)_2$ in low yield (*ca.*5%) on addition of NH_4PF_6. Reflux for an intermediate duration (8 hours) under similar conditions had given a pale yellow solid also in low yield (*ca.*5%). Microanalysis figures were in agreement for a stoichiometry of $[PtL^4Cl]PF_6$. Further evidence to suggest the yellow species is an intermediate in the formation of the fully inserted platinum macrocycle is obtained from the infrared spectrum. In addition to coordinated macrocyclic bands, a medium intensity band at 333 cm^{-1} is assigned to a ν(Pt-Cl) stretching vibration. One possible explanation for the low yields obtained is due to protonation of the NMe group of L^4 from the protic solvent, as tertiary amine macrocycles have been noted to have increased basicity over secondary amine[88]. Reflux in the aprotic solvent mixture CH_3CN/methylene chloride (1:1 v/v) for 48 hours followed by reflux in CH_3CN/ethanol (1:3 v/v) for a further 32 hours allowed for the isolation of the fully metal inserted product, $[PtL^4]^{2+}$, in moderate yields (*ca.*30%).

3.7.2 NMR Studies

The ^1H n.m.r. spectrum of $[PtL^4]^{2+}$ in CD_3NO_2 shows many similarities to that obtained for $[PdL^4]^{2+}$. It can be concluded that the same single ligand conformation found from ^{13}C n.m.r. studies for the Ni(II) and Pd(II) analogues is present for Pt(II). Shifts upfield for all resonances, most noticeably +0.22 and +0.56 p.p.m. for the NCH_3 and NH resonances respectively for the platinum complex are found when compared with the palladium analogue (Table 3.9.II).

3.7.3. F.a.b. Mass Spectral Studies

The technique, first described in 1981 has found use in identification of transition metal macrocyclic compounds[52,106]. Identification of the transition metal macrocyclic compound is proven by the molecular ion, $[ML]^+$, or quasi-molecular ion peaks $[M(LH)]^+$, $[M(L-H)]^+$ with the expected natural abundance isotopic distribution ratios. For $[PtL^4](PF_6)_2$, one molecular fragment centred at m/z = 443 was detected in the positive ion f.a.b. spectra using a glycerol/dmf solvent matrix corresponding to the loss of both PF_6^- anions. For the isostructural palladium complex, $[PdL^4](PF_6)_2$ under equivalent conditions molecular ion peaks corresponding to the sequential loss of PF_6^- anions, $[PdL^4(PF_6)]^+$ and $[PdL^4]^+$ were observed (Table 3.9.IV). Analysis of the isotopic distribution ratios for $[PtL^4]^+$ suggests that a combination of the $[PtL^4]^+$ and $[Pt(L^4-H)]^+$ species are present, with the latter the predominant. This species is derived from loss of HPF_6 from $[PtL^4(PF_6)]^+$. Similar behaviour has been observed by Moore and coworkers[52] for $[NiL^4](ClO_4)_2$ and similarly assigned to loss of $HClO_4$ from $[NiL^4(ClO_4)]^+$ to form the $[Ni(L^4-H)]^+$ species.

3.8 Conclusions

The binding of platinum group metals to macrocyclic ligands to form stable complexes with specific labile sites for substrate coordination and activation is an area of great potential in the development of new catalytic systems. This study has shown the feasibility of inserting Pt(II), Pd(II), Ru(II), Rh(III), Ir(III) into tetradentate macrocycles

Figure 3.7.I. Expansion of the f.a.b. Mass Spectrum of the Fragment Ion $[Pt(L^4-H)]^+$

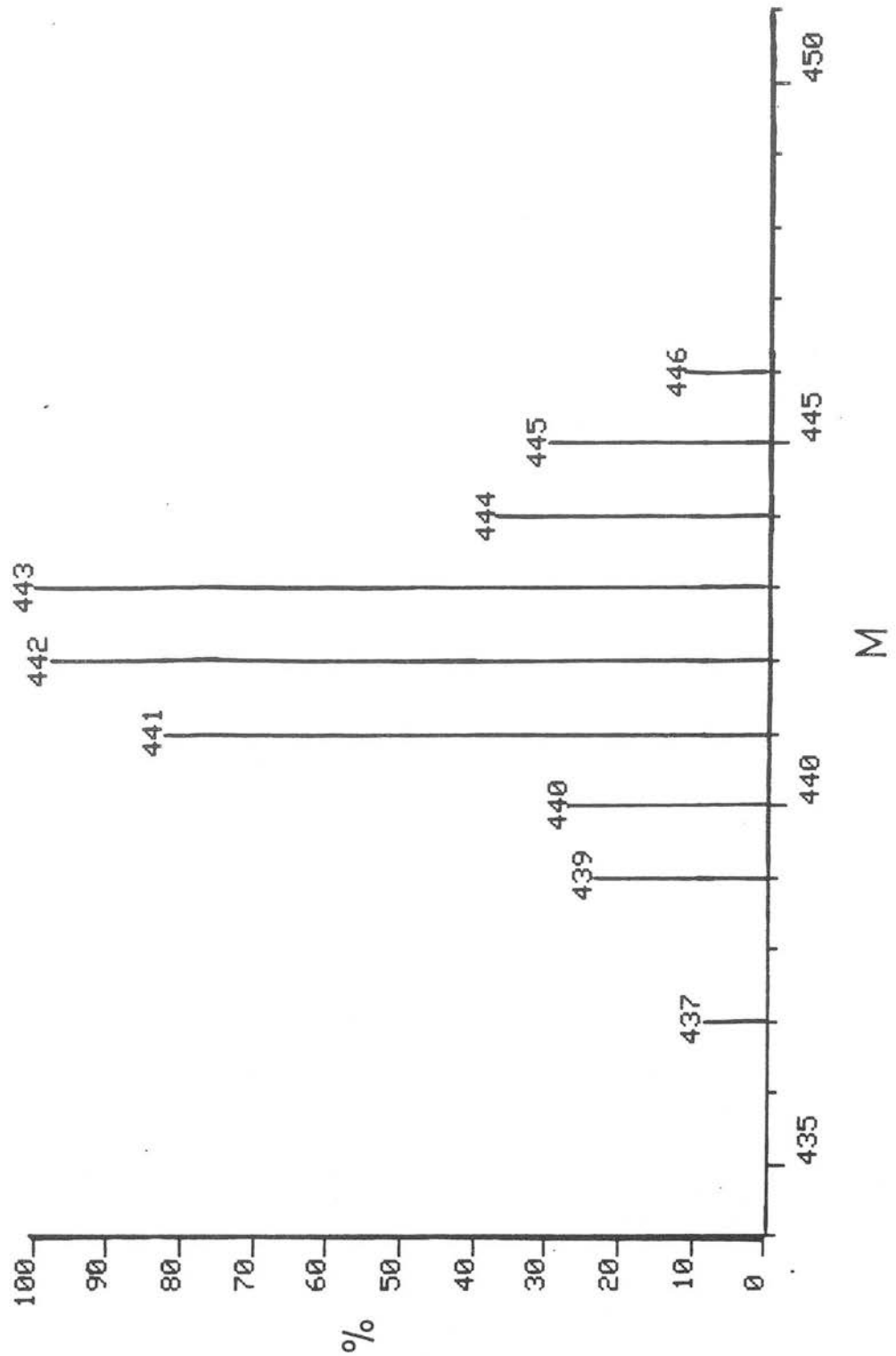

in yields ranging from 30-80% to give the first examples of platinum metal 2,6-pyridyl tetraaza macrocycles. The isolation of the Ir(III), Ru(II) species $[IrL^4(H)Cl]^+$, $[RuL^3(CO)Cl]^+$, may be regarded as potentially useful catalytic macrocyclic species from their coordination of the labile small molecules H^- and CO to metal centres.

3.9 Experimental

Fast atom bombardment (f.a.b.) mass spectra were obtained in glycerol/dmf matrices on a Kratos MS50TC spectrometer. U.v./visible spectra were recorded with a Pye Unicam SP8-400 spectrophotometer. Conductivity measurements were determined with a Portland Electronics Model 310 conductivity bridge. Other physical measurements were carried out as in Chapter 2.

Reagents

The preparation of the free ligands L^1-L^4 is described in Chapter 2. Commercial ruthenium trichloride, rhodium trichloride, platinum dichloride, iridium trichloride and palladium acetate (Johnson Matthey plc) were used as supplied. *trans*$[Ru(MeCN)_4Cl_2]$ was prepared by the method of Wilkinson *et al* [107]. Selected microanalytical, ^1H n.m.r., infrared and f.a.b. mass spectral data are presented in Tables 3.9.I, 3.9.II, 3.9.III and 3.9.IV respectively.

cis$[Ru(II)L^3(CO)Cl]PF_6$

trans$[Ru(MeCN)_4Cl_2]$ (95 mg, 0.28 mmol) was dissolved in dry ethanol (150 cm^3) which had been purged with CO. $L^3.H_2O$ (78 mg, 0.26 mmol) was added and reflux under CO continued for 24 hours in which time a yellow/orange to dark orange colour change occured. Further reflux under N_2 for 24 hours, reduction in the solvent volume and addition of excess NH_4PF_6 gave an air stable pale orange/brown precipitate which was recrystallized from ethanol.

Yield 87 mg, 0.15 mmol, (56%)

Equivalent conductivity: (of BPh_4 salt), slope of $\Lambda_o-\Lambda_e$ vs $c_e^{\frac{1}{2}}$ plot in CH_3NO_2=235

Electronic spectrum: (in CH_3CN, 900-186nm) 299 (ε=2790), 281(2600), 247(4330), 206(1430 $dm^3mol^{-1}cm^{-1}$).

[Rh(III)L^3Cl_2]PF_6

Preparation of the rhodium complex with L^3 is typical for ligands L^1-L^4. To a warmed solution of $L^3.H_2O$ (105 mg, 0.36 mmol) in methanol (50 cm^3) under N_2 was added $RhCl_3.3H_2O$ (95 mg, 0.36 mmol) in methanol (10 cm^3). On refluxing for 6 hours a golden yellow solution colour resulted. Reduction to half the solution volume and addition of excess NH_4PF_6 gave a yellow powder which was recrystallized from methanol.

Yield 187 mg, 0.31 mmol, (88%)

[Ir(III)L^4(H)Cl]PF_6

$IrCl_3.3H_2O$ (138 mg, 0.39 mmol) and L^4 (82 mg, 0.33 mmol) were refluxed in an ethanol (120cm^3)/water (80 cm^3) mixture for 72 hours under nitrogen. After filtration and removal of *ca.* 150 cm^3 a clear yellow solution resulted. Addition of NH_4PF_6 allowed for a pale brown solid to be isolated which was recrystallized from methanol.

Yield *ca.* 75 mg, 0.12 mmol, (36%).

[Pd(II)L^1]$(PF_6)_2$

Preparation of the palladium complex with L^1 is typical for ligands L^1-L^4. To a solution of $L^1.H_2O$ (50 mg, 0.19 mmol)

in dry methylene chloride, (50 cm^3) at room temperature was added $\{Pd(OAc)_2\}_3$ (43 mg, 0.19 mmol) in methylene chloride (20 cm^3). Stirring for 24 hours resulted in a solution colour change from yellow to pale brown. Removal of the solvent at 0°C (vacuum line) and dissolving the residue in methanol (20 cm^3) allowed for a pale brown solid to be isolated on addition of excess NH_4PF_6.

Yield 73 mg, 0.11 mmol (58%)

Electronic spectrum (in CH_3CN 900-186nm) $[PdL^1](PF_6)_2$: 210nm (ε=20,050), 267(4330), 300(1350); $[PdL^2](PF_6)_2$ 206(22900), 272(3300), 310(1450); $[PdL^3](PF_6)_2$ 206(22950), 267(4150), 292(1480); $[PdL^4](PF_6)_2$ 210(19600), 267(3950), 297(1170 $dm^3mol^{-1}cm^{-1}$).

Equivalent conductivity: $[PdL^1](PF_6)_2$ slope of $\Lambda_o-\Lambda_e$ vs $C_e^{\frac{1}{2}}$ plot in CH_3NO_2 = 484. $[PdL^4](PF_6)_2$ = 404.

<u>$[Pt(II)L^4](X)_2$, X=PF_6, BPh_4</u>

$PtCl_2$ (100 mg, 0.38 mmol) and L^4 (93 mg, 0.38 mmol) were refluxed in ethanol (200 cm^3) for 60 hrs under N_2. After filtering off a substantial amount of platinum metal and removal of *ca.* 160 cm^3 of solvent, a brown solid was obtained on addition of NH_4PF_6. Recrystallization twice from ethanol allowed for *ca.* 5% yield of pure product to be isolated.

An improved synthetic route employed $PtCl_2$ (50 mg, 0.19 mmol) and L^4 (47 mg, 0.19 mmol) in CH_3CN (75 cm^3) and CH_2Cl_2 (75 cm^3). After reflux for 44 hours no pure product was isolated. Reflux of the residue for a further 32 hours in CH_3CN (35 cm^3) and ethanol (75 cm^3) gave after filtration a clear yellow solution. Addition of $NaBPh_4$ gave a pale brown powder that was recrystallized from ethanol.

Yield *ca.* 60 mg (30%).

Table 3.9.I. Elemental Analysis Data for $[ML^n]^{x+}$ (M=Rh,Ir,Pd,Pt,Ru, n=1-4)

Complex	%C	%H	%N
$[RuL^3(CO)Cl]BPh_4$	63.3(64.8)	6.5(6.4)	7.0(7.4)
$[RuL^3(CO)Cl]PF_6$	34.0(34.8)	4.7(4.8)	9.3(9.5)
$[RhL^1Cl_2]PF_6$	31.1(31.0)	4.5(4.5)	9.5(9.5)
$[RhL^2Cl_2]PF_6$	35.0(34.7)	5.2(5.2)	8.5(9.0)
$[RhL^3Cl_2]PF_6$	32.0(32.3)	4.9(4.7)	9.2(9.4)
$[RhL^4Cl_2]PF_6$ [b]	30.0(29.7)	4.8(4.3)	9.7(9.9)
$[RhL^4Cl_2]PF_6$ [c]	29.4(29.7)	4.3(4.3)	9.5(9.9)
$[IrL^4(H)Cl]PF_6$	25.5(25.6)	3.9(3.7)	8.4(8.5)
$[PdL^1](PF_6)_2$	27.1(27.3)	4.0(4.0)	8.5(8.5)
$[PdL^1](BPh_4)_2$	74.1(75.1)	6.5(6.6)	5.7(5.6)
$[PdL^2](PF_6)_2$	30.4(30.8)	4.7(4.6)	7.9(8.0)
$[PdL^3](PF_6)_2$	29.3(28.6)	4.3(4.2)	8.3(8.3)
$[PdL^4](PF_6)_2$	26.3(26.1)	3.7(3.7)	8.7(8.7)
$[PtL^4](PF_6)_2$	23.5(23.9)	3.5(3.3)	8.0(7.6)
$[PtL^4](BPh_4)_2$	67.4(68.8)	6.2(6.0)	5.2(5.2)
$[PtL^4Cl]PF_6$	26.3(26.9)	3.9(3.9)	9.0(9.0)

[a] calculated values in parenthesis

[b] *cis* isomer

[c] *trans* isomer

Table 3.9.II. Selected ^1H n.m.r. Data for $[ML^n]^{X+}$ [a] in CD_3NO_2 (M=Rh,Ir,Pd,Pt,Ru, n=1-4)

Complex	δ_H/ppm py-*H*,(t) [b]	py-*H*,(d)	C*H*CH_3,(q)	CH_2,(m)	N(7)CH_3,(s)	C(2)CH_3,(d)	Other, (s)
$[RhL^1Cl_2]^+$	8.13	7.59	c	-	-	1.91	-
$[RhL^2Cl_2]^+$	8.07	7.60	4.67	-	2.80	1.79	2.92[d]
$[RhL^3Cl_2]^+$	8.08	7.59	5.31	-	2.60	c	6.40[e]
$[RhL^4Cl_2]^+$	8.03	7.58	-	4.98	2.64	-	6.20[e]
$[IrL^4(H)Cl]^+$	7.83	7.32	-	4.63	2.36	-	-22.25,[f] 6.51[e]
$[PdL^1]^{2+}$	8.24	7.51	4.71	-	-	1.80	5.54[e]
$[PdL^2]^{2+}$	8.30	7.59	4.82	-	2.71	1.75	3.02[d]
$[PdL^3]^{2+}$	8.21	7.49	4.74	-	2.74	1.82	5.63[e]
$[PdL^4]^{2+}$	8.12	7.52	-	4.87, 4.55	2.75	-	5.22[e]
$[PtL^4]^{2+}$	8.21	7.57	-	5.00, 4.59	2.97	-	5.78[e]
$[RuL^3(CO)Cl]^+$	8.18	7.63	5.10	-	2.10	1.78	-

a, Major isomer only

b, s = singlet, d = doublet, t = triplet, q = quartet, m = multiplet

c, Unresolved

d, δN(3)CH_3

e, δN*H*

f. δIr-*H*

Table 3.9.III. Selected Infrared Data for L^n and $[ML^n]^{x+}$ (M=Rh,Ir,Pd,Pt,Ru, n=1-4)[a]

Complex	ν(N-H) s,m [b]	ν(py-H) w	ν(C=C) m	ν(C=N) m	ν(M-Cl), m	Other
$L^1.H_2O$	3280	3048	1691	1572	-	820, 851, m[e]
$[PdL^1](PF_6)_2$	3258	3120	1606	1580	-	
$[RhL^1Cl_2]PF_6$	h	h	1600	1520	338	
L^2	-	3060	1588	1575	-	825, m[e]
$[PdL^2])PF_6)_2$	-	3096	1601	1580	-	
$[RhL^2Cl_2]PF_6$	-	3098	1600	1580	353	
$L^3.H_2O$	3286	3059	1590	1571	-	835, 854, m[e]
$[PdL^3](PF_6)_2$	3249	3050	1604	1581	-	
$[RhL^3Cl_2]PF_6$	3240, 3219	3090	1600	1580	353	
$[RuL^3(CO)Cl]PF_6$	3180	3100	1592	1573	301	1930, s[f]
L^4	3300	3030	1593	1574	-	830, 854, m[e]
$[PdL^4](PF_6)_2$	3278	3030	1610	1584	-	
$[RhL^4Cl_2]PF_6$ [c]	3268	3082	1609	1583	302, 245	
$[RhL^4Cl_2]PF_6$ [d]	3262, 3243	3080	1600	1580	348	
$[IrL^4(H)Cl]PF_6$	3151	3140	1609	1591	283	2138, s[g]
$[PtL^4](PF_6)_2$	3255	3140	1602	1575	-	

a, KBr discs/cm^{-1} c, cis isomer e, δ(py-H) g, ν(Ir-H)

b, s=strong, m=medium, w=weak d, trans isomer f, ν(C≡O) h, unresolved

Table 3.9.IV. Selected Fast Atom Bombardment (f.a.b.) Mass Spectral Data[a] for $[ML^n]^{x+}$ M=Rh,Ir,Pd,Pt,Ru, n=1-4 (Positive Ion)

Complex	Calculated (Found)[b]		Calculated (Found)		Calculated (Found)
$[RuL^3(CO)Cl]^+$	441(441)[c]	$[RuL^3CO]^+$	406(405)	$[RuL^3]^+$	378(373)
$[RuL^3(CO)Cl]^+$	441(440)[d]	$[RuL^3CO]^+$	406(404)	$[RuL^3]^+$	378(372)
$[RhL^1Cl_2]^+$	436(435)	$[RhL^1Cl]^+$	400(400)	$[RhL^1]^+$	365(363)
$[RhL^2Cl_2]^+$	478(477)	$[RhL^2Cl]^+$	443(441)	$[RhL^2]^+$	407(407)
$[RhL^3Cl_2]^+$	449(450)	$[RhL^3Cl]^+$	414(e)	$[RhL^3]^+$	379(377)
$[RhL^4Cl_2]^+$	422(422)	$[RhL^4Cl]^+$	387(e)	$[RhL^4]^+$	351(349)
$[IrL^4(H)Cl]^+$	478(478)	$[IrL^4Cl]^+$	477(476)	$[IrL^4]^+$	441(438)
$[PdL^1(PF_6)]^+$	513(513)	$[PdL^1]^+$	368(369)		
$[PdL^3(PF_6)]^+$	528(527)	$[PdL^3]^+$	383(381)		
$[PdL^4(PF_6)]^+$	499(499)	$[PdL^4]^+$	354(353)		
$[PtL^4(PF_6)]^+$	588(e)	$[PtL^4]^+$	443(443)		
$[PtL^4(BPh_4)]^+$	762(e)	$[PtL^4]^+$	443(442)		

a, Using glycerol/dmf solvent matrix

b, All data calculated using most abundant natural isotopes

c, PF_6^- salt

d, BPh_4^- salt

e, Not observed/resolved

C H A P T E R 4

Electrochemical Studies of $[M(TMC)]^{2+}$, and Related Tetraaza Macrocycles (M=Ni(II),Pd(II))

4.1 Introduction

The tetraaza macrocycle TMC (1,4,8,11-tetramethyl-1,4,8,11-tetraazacyclotetradecane) can be associated with a wide variety of oxidation states, ranging from d^2 Ru(VI), Os(VI) through to d^{10} Cu(I). Poon and Che[82,108] prepared the high oxidation state complexes $[M(TMC)(O)_2]^{2+}$, M=Ru(VI), Os(VI). Their stability is ascribed to the two coordinating oxo ligands, with the TMC macrocycle acting as a protecting group for the metal centre. In contrast, Meyerstein and coworkers[109,110] have prepared the low oxidation state complexes $[M(TMC)]^{+}$, M=Cu(I), Ni(I), in aqueous solution. The combination of factors attributed to the stabilization of the low oxidation state include (i) an inability for decomposition to occur via ligand oxidative dehydrogenation reactions, (ii) N-alkylation considerably slows down the rate of ligand exchange, and (iii), the weaker ligand field exerted on N-alkylation favours the low oxidation state[111].

In the absence of other ligands, we argued that TMC should stabilize the low valent metal state. The electrochemistry of $[Pd(TMC)]^{2+}$ and other related Pd(II) tetraaza macrocycles was therefore investigated, with a view to the development of new electrocatalytic precursors for the reduction of small molecule substrates[112].

The direct electrochemical reduction of many small molecule substrates such as CO_2 and O_2 at various metal electrodes has a large overpotential, which requires a relatively high input of energy for reduction. Therefore the search for electrocatalysts to mediate small molecule reduction at lower potentials has become an important area

of research[25]. Since the initiation of this work, the Pd(II) porphyrins [Pd(TPP)] and [Pd(OEP)] have been found to display electrocatalytic activity for the reduction of CO_2.[33]

4.2 Stereochemistry of TMC Complexes

When TMC coordinates to four equatorial sites of a square plane metal centre there are 16 possible arrangements for the four methyl groups either above or below the coordination plane. These reduce to five energetically distinct geometries as proposed by Bosnich *et al.*[113] represented in Figure 4.2.I.

The R.S.S.R. isomer is found on N-methylation of R.S.S.R. $[Ni(cyclam)]^{2+}$ [114] whereas the R.S.R.S. isomer is found on insertion of Ni(II) into the preformed ligand[19]. It has been suggested by several authors[115,116] that the R.S.S.R. isomer is the thermodynamically more stable and that the R.S.R.S. isomer is the kinetic product, formed as it is the conformation adopted by the free ligand[116]. It was believed that interconversion between the two to form the thermodynamic isomer was not possible. Moore[115] and Lincoln[117] have recently demonstrated the interconversion of the two isomers via the R.S.R.R. isomer in strongly coordinating solvents. In contrast, for $[NiL]^{2+}$ L=cyclam, C *meso* or C *rac* HMC, interconversion of the secondary amine protons is a facile process in neutral or basic solution and structures with R.S.S.R., R.S.R.S. and R.R.R.R. conformations have been characterized[118-120].

Figure 4.2.I. Diagrammatic representation of the five main isomers of $[M(TMC)]^{n+}$.

Key: The '+' and '-' signs indicate that the attached CH_3 group is above or below the coordination plane respectively.

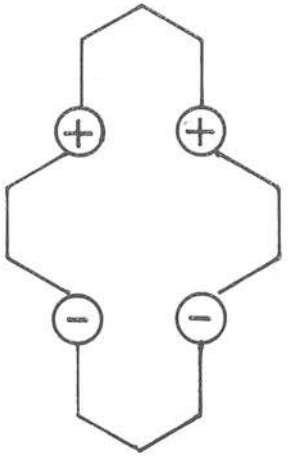

RSSR

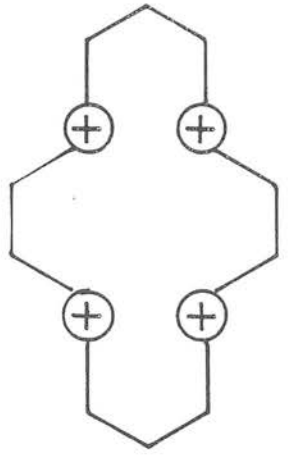

RSRS

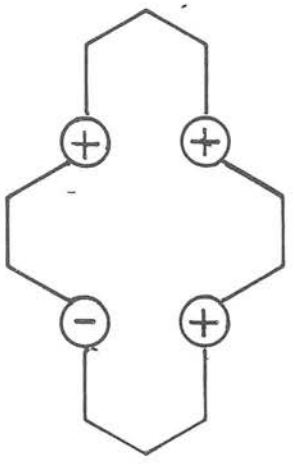

RSRR

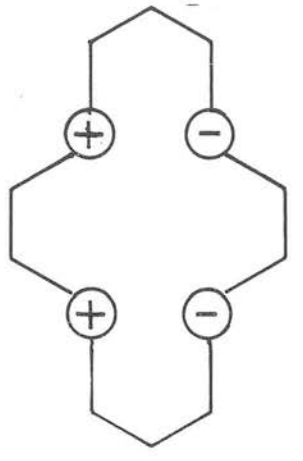

RRSS

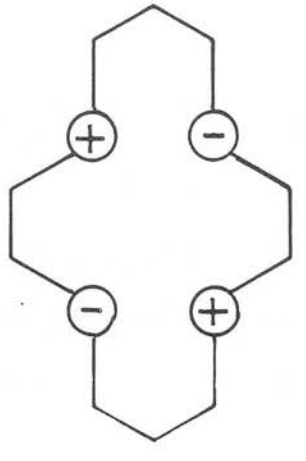

RRRR

Results and Discussion

4.3 Synthesis and Characterization of $[PdL]^{2+}$, L = cyclam, HMC, TMC

Using an analogous method of synthesis to that used for the pyridyl macrocycles L^1-L^4 (Chapter 3), palladium(II) has been inserted into the 'cyclam' type ligands in yields of up to 86%. Pale brown solids of stoichiometry $[PdL](PF_6)_2$, L = cyclam, HMC, TMC, were isolated on addition of NH_4PF_6.

In view of the debate surrounding the isomerization and conformations of $[Ni(TMC)]^{2+}$,[115-117] the configuration of $[Pd(TMC)]^{2+}$ was clearly of interest. The ^1H and ^{13}C n.m.r. spectra of $[Pd(TMC)]^{2+}$ in CD_3NO_2 indicated the presence of only one isomer in solution with one resonance observed for the methyl protons (δ_H=2.8 p.p.m., CH_3, 12H) and for the methyl carbons (δ_C=45.6 p.p.m., CH_3). Close inspection of the resonances of the methylene protons could not differentiate conclusively between the possible R.S.R.S. and R.S.S.R. isomers[112]. To obtain the absolute ligand configuration, a single crystal X-ray study on $[Pd(TMC)]^{2+}$ was carried out.

4.4 The Single Crystal X-Ray Structure of $[Pd(TMC)](PF_6)_2 \cdot CH_3NO_2$

A pale cream crystal (0.6x0.24x0.12mm) suitable for X-ray analysis was obtained by diethyl ether diffusion into a nitromethane solution.

Crystal Data

$C_{14}H_{32}N_4Pd^{2+}.2PF_6^-.CH_3NO_2$, M=713.80, orthorhombic,

space group *Pna2*, a = 18.325(5), b = 15.279(4), c = 9.768(5)Å; U = 2735Å^3, D_c = 1.733 g cm^{-3}, Z=4, F(000) = 1440, μ(Mo-Kα) = 8.86 cm^{-1}, λ(Mo-Kα) = 0.71069Å. At convergence R,Rw = 0.0742, 0.0997 respectively for 1814 data.

Selected bond lengths and angles are given in Table 4.4.I and two views of the cation are shown in Figures 4.4.II and 4.4.III. The Pd is coordinated in a square planar array to N(1), N(4) and their mirror related equivalents N(1') and N(4') with the four N bound methyl groups on the same side of the tetraaza plane in the R.S.R.S. configuration (Pd-N(1) = 2.051(11), Pd-N(4) = 2.066(11)Å. The macrocycle conformation comprises of five membered chelate rings in asymmetric gauche, and six membered chelate rings in chair configurations respectively. An average Pd-N bond length of 2.058Å is close to the ideal value of 2.07Å calculated for the best 'fit' of an ion into a planar 14 membered macrocyclic tetraaza moiety[119]. Chelate angles summing to 359.7° support this calculation (<N(1)-Pd-N(4) = 88.0(4), <N(1)-Pd-N(1') = 92.7(4), <N(4)-Pd-N(4') = 91.0(4)°). The 'bite' of the chelate rings close to 86° for a five membered ring and 92° for a six membered ring as observed in this structure has been found to give the minimum strain conformation[119]. The Pd deviates by only 0.082Å towards the four N bound methyl groups from the essentially planar tetraaza donor set (maximum deviation from the plane ±0.003Å). A deviation to below the tetraaza plane would introduce severe interaction between the four methyl groups. For the square planar R.S.R.S. [Ni(TMC)]$^{2+}$ cation, a puckered

Table 4.4.I. Selected bond lengths and angles (with e.s.d's) for $[Pd(TMC)](PF_6)_2.CH_3NO_2$

Bond lengths (Å)

Pd	- N(1)	2.051(11)
Pd	- N(4)	2.066(11)
N(1)	- C(1N)	1.512(22)
N(1)	- C(2)	1.47 (3)
N(1)	- C(14)	1.47 (3)
C(2)	- C(3)	1.37 (5)
C(3)	- N(4)	1.53 (4)
N(4)	- C(4N)	1.471(22)
N(4)	- C(5)	1.44 (3)
C(5)	- C(6)	1.43 (4)
C(13)	- C(14)	1.35 (4)

Bond angles (°)

N(1)	- Pd - N(4)	88.0(4)
N(1)	- Pd - N(1')	92.7(4)
N(1)	- Pd - N(4')	175.5(4)
N(4)	- Pd - N(4')	91.0(4)

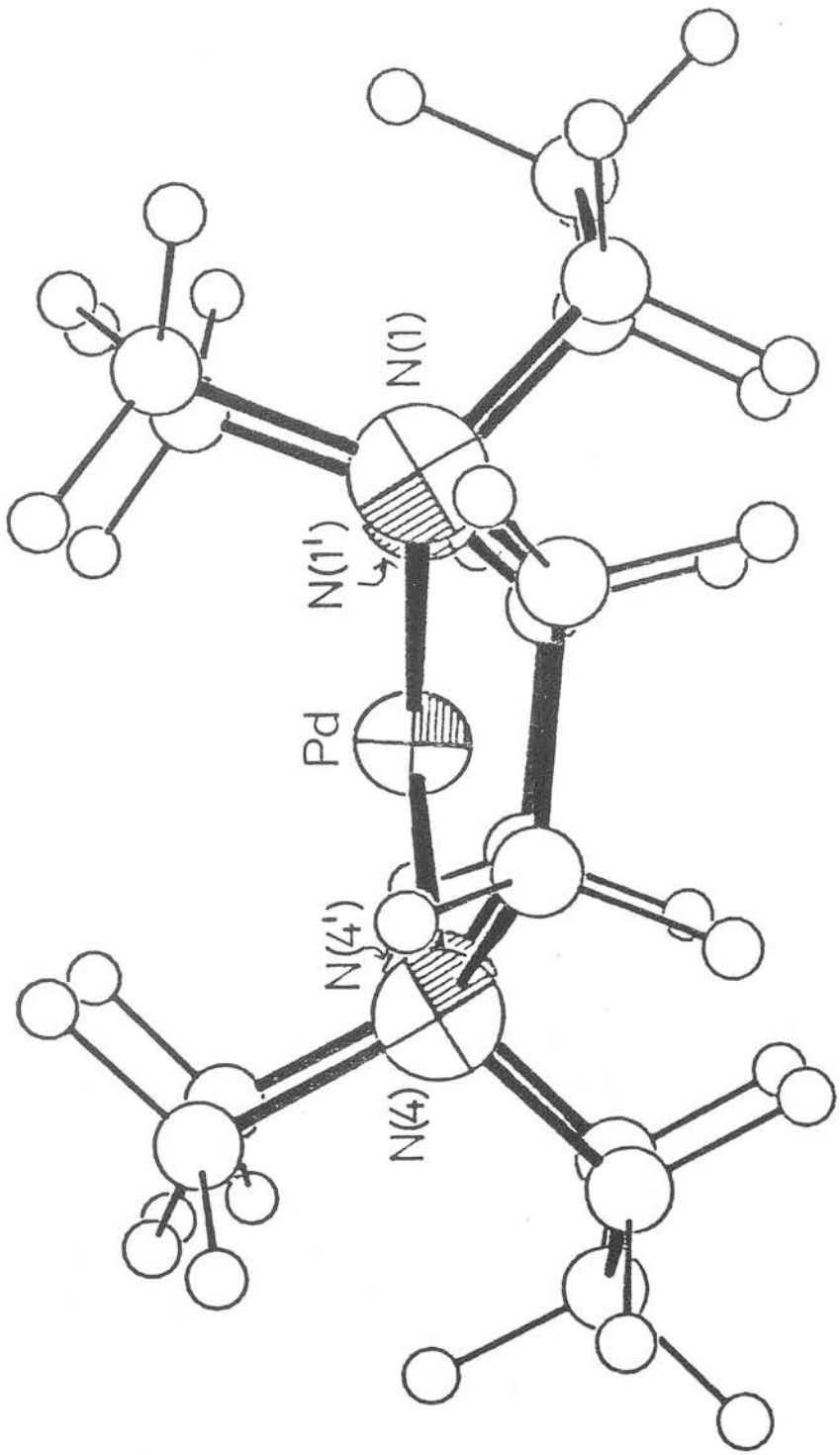

Figure 4.4.II. View of the Single Crystal X-ray Structure of $[Pd(TMC)]^{2+}$

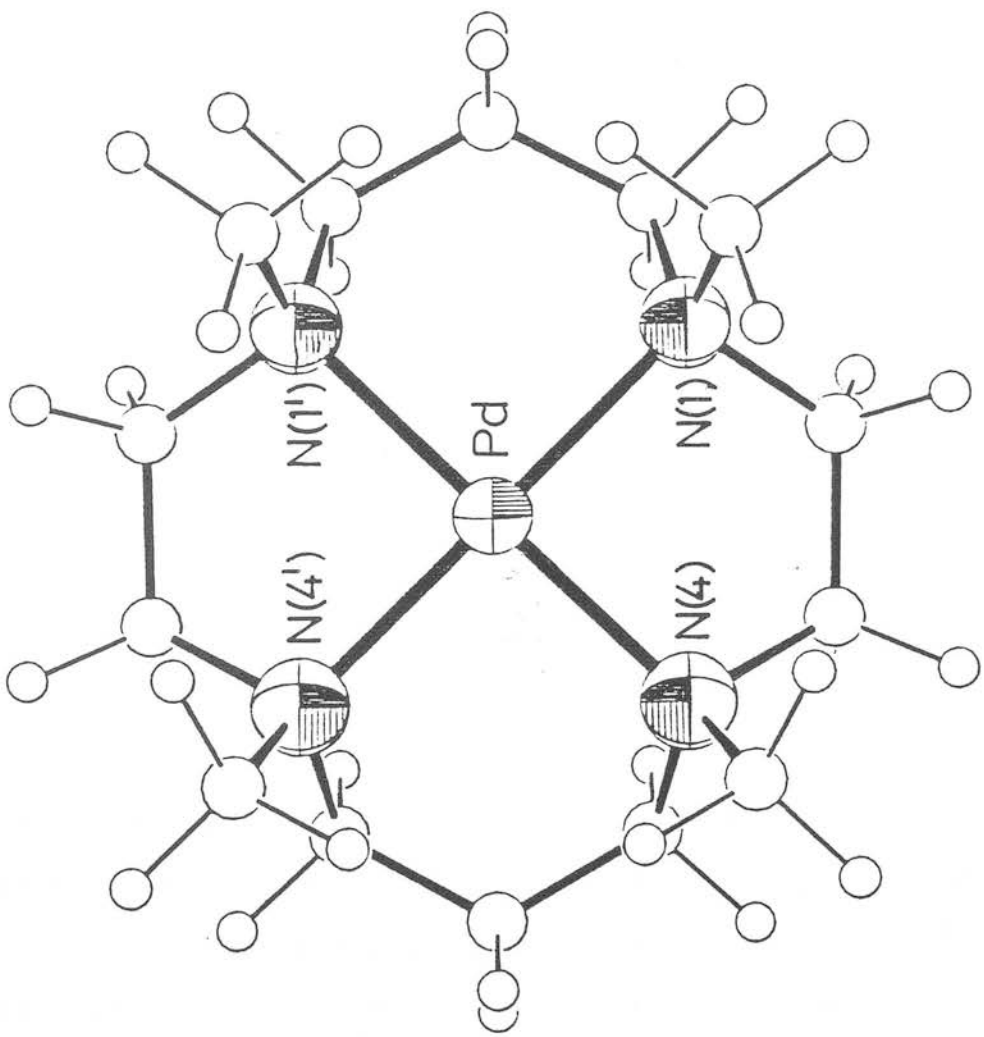

Figure 4.4.III. View of the Single Crystal X-ray Structure of $[Pd(TMC)]^{2+}$

tetraaza plane is observed with deviations of -0.201, -0.192, +0.197 and +0.196Å in N from the best least squares plane[116]. Trans <N(1)-Ni-N(4) angles of 168.2(3), 169.0(3)° are a manifestation of the non planar ligand (*cf.* <N(1)-Pd-N(4) = 175.5(4)°). The differences in the Ni and Pd structures are due to the shorter Ni-N bond lengths by an average 0.075Å (Ni-N(av) = 1.983Å). A puckering of the nitrogen donors is therefore required to accommodate the smaller Ni(II) ion.

The structure of $[Pd(cyclam)]^{2+}$,[84] shows the secondary amine groups with the R.S.S.R. configuration. Pd-N bond lengths of 2.051(5)Å are only 0.007Å shorter than those found in $[Pd(TMC)]^{2+}$, in agreement with shorter Ni-N bond lengths found for $[Ni(cyclam)]^{2+}$ than $[Ni(TMC)]^{2+}$.[19]

4.5 The Electrochemistry of $[Pd(TMC)]^{2+}$

Cyclic voltammetry of $[Pd(TMC)](PF_6)_2$ in CH_3CN (0.1M $TBAPF_6$ supporting electrolyte) at platinum electrodes shows a fully reversible reduction at $E_{\frac{1}{2}}$ = -1.45V vs Ag/Ag^+ (ΔEp= 65mV, Ipa/Ipc = 1.0 at a scan rate of 100mV sec^{-1}) (Fig.4.5.I). No oxidation to Pd(III) or Pd(IV) is seen within the range of the solvent up to +2.2V. Controlled potential electrolysis of $[Pd(TMC)]^{2+}$ at a platinum gauze in CH_3CN at -1.55V under a stream of argon gas at 20°C produces a highly air sensitive, pale brown reactive species, the e.s.r. spectrum of which at 77K as a frozen glass (Figure 4.5.II) shows an anisotropic signal with axial symmetry g_{11}=2.302, $g_{\perp}$=2.076. These spectral features are consistent with the formation of a d^9 palladium(I) species $[Pd(TMC)]^+$. Further confirmation for

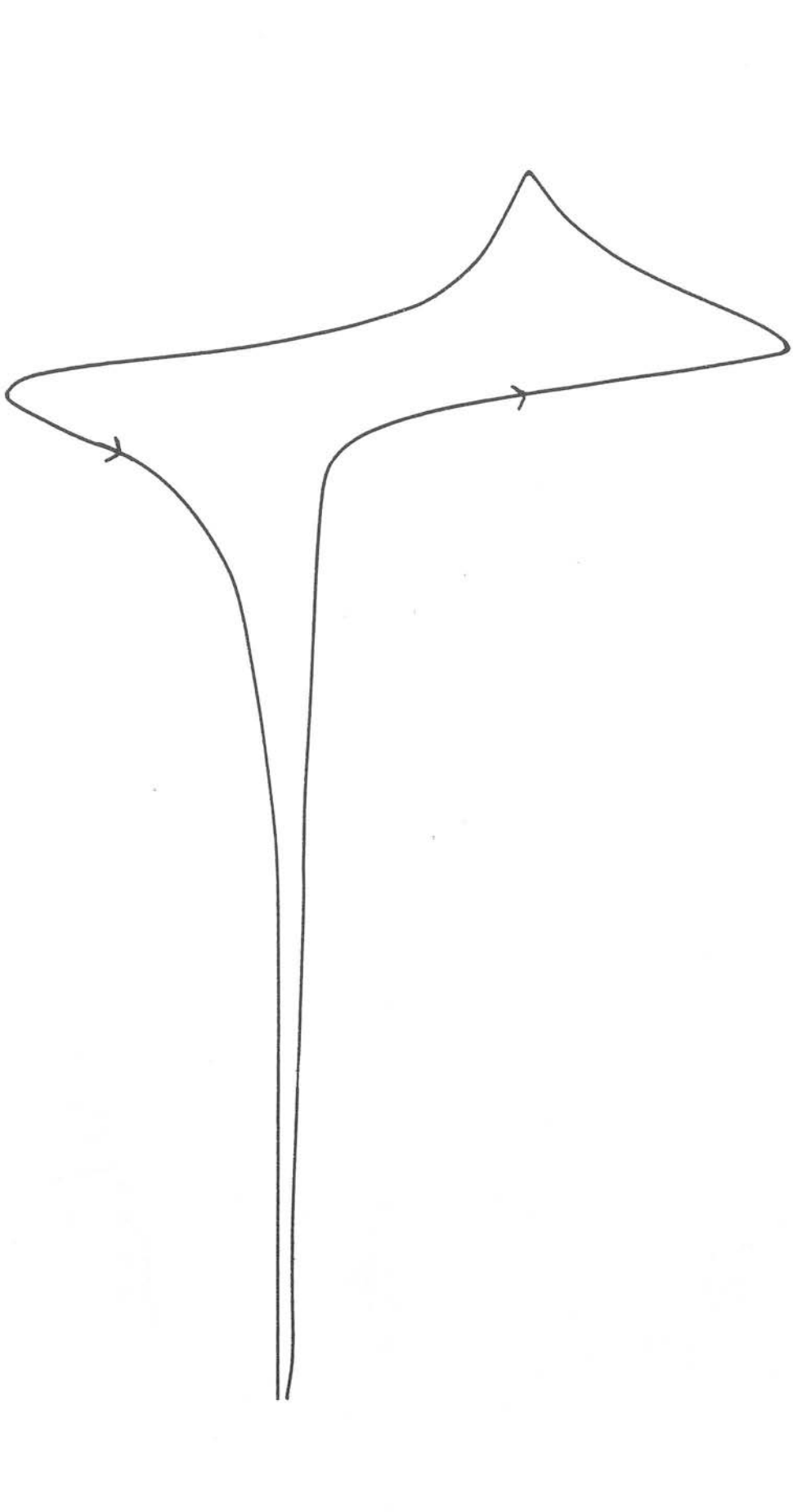

Figure 4.5.I. Cyclic Voltammogram of $[Pd(TMC)]^{2+}$ in CH_3CN/0.1M $TBAPF_6$

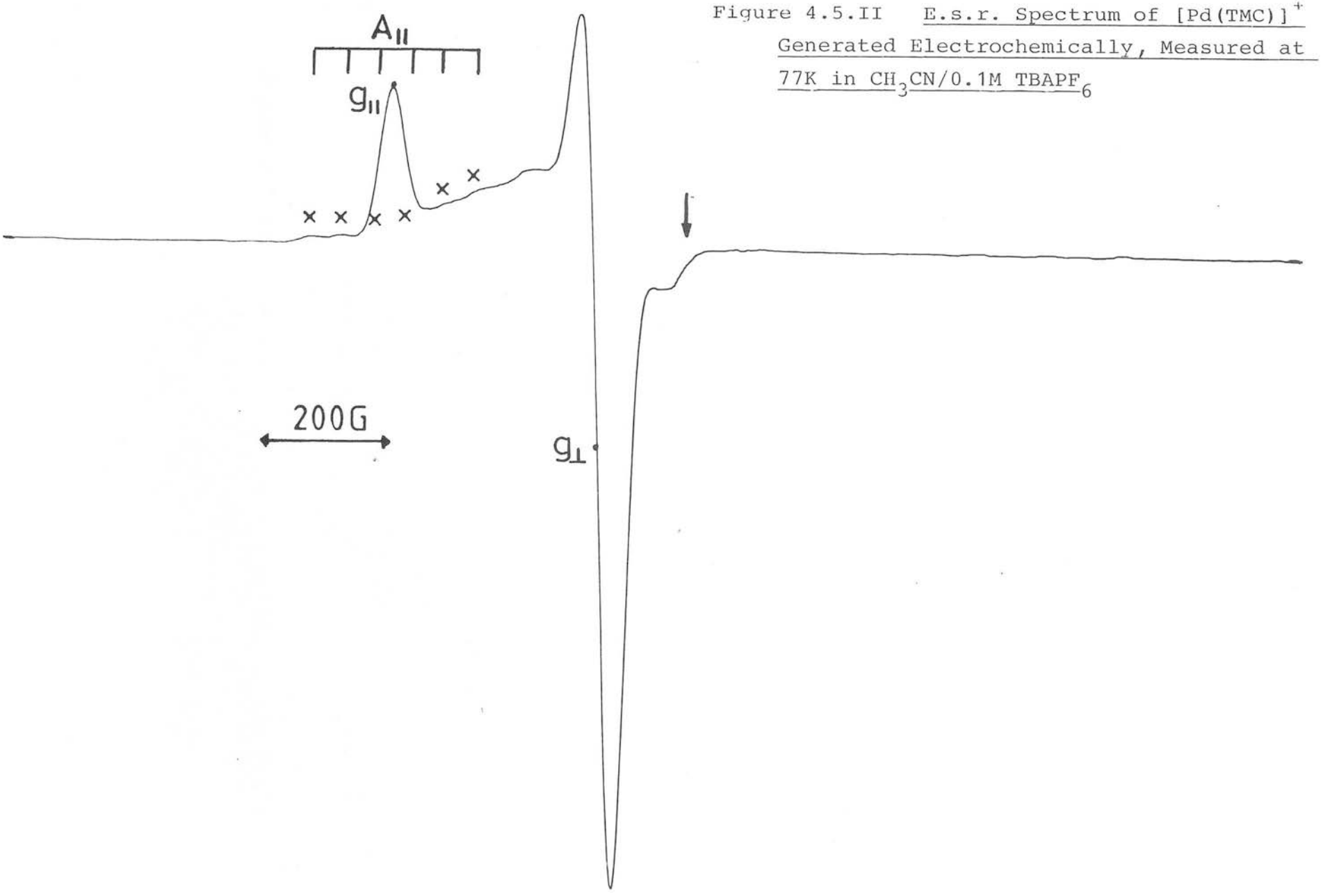

Figure 4.5.II E.s.r. Spectrum of $[Pd(TMC)]^+$ Generated Electrochemically, Measured at 77K in CH_3CN/0.1M $TBAPF_6$

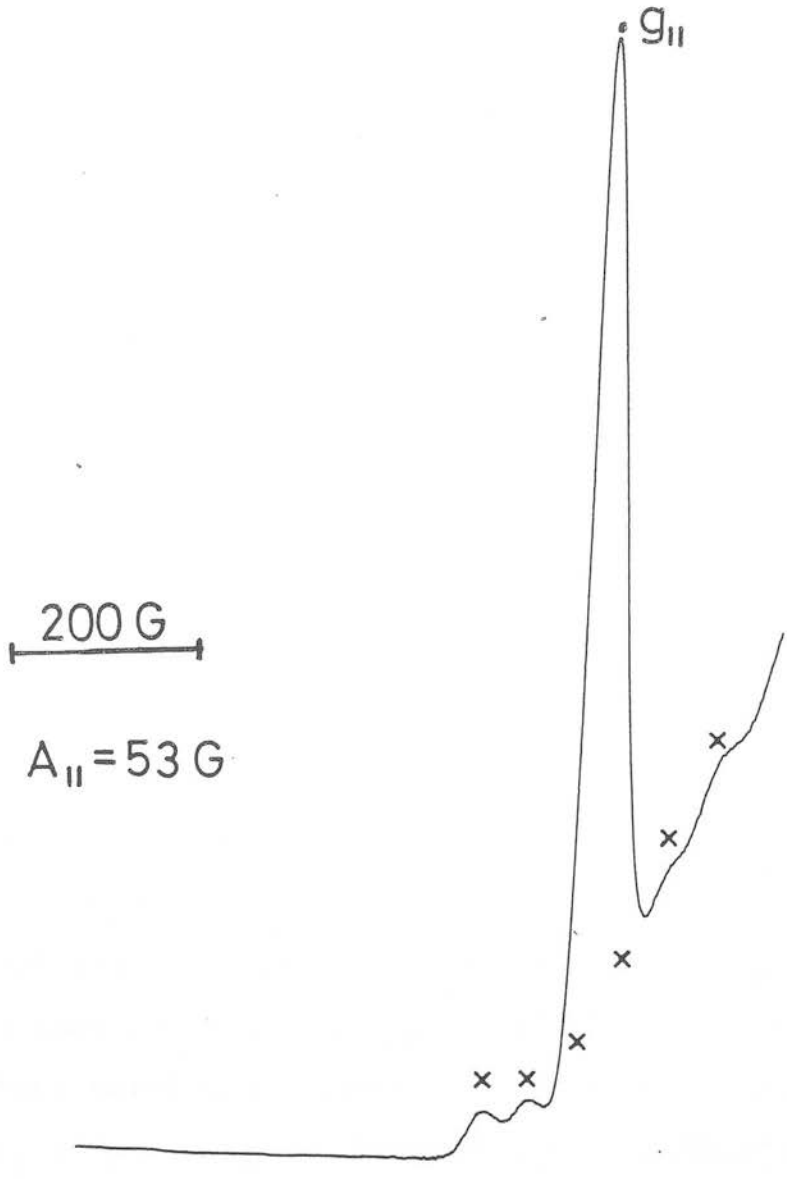

Figure 4.5.III Expansion of the g_{11} Region of the E.S.R. Spectrum of $[Pd(TMC)]^+$ at 77K in CH_3CN/0.1M $TBAPF_6$ Showing Hyperfine Coupling to ^{105}Pd

a predominantly metal based redox process is obtained by the observation of hyperfine coupling to ^{105}Pd (I = 5/2, 22.2%) (Figure 4.5.III). In the g_{11} region the 1st, 2nd, 5th and 6th features are distinguishable allowing a coupling constant, A_{11} of 53G to be estimated. Similarly the 1st and 6th features in the $g_{\perp}$ region are discernible giving the coupling constant $A_{\perp}$=40G. Similar spectral features have been observed for the isoelectronic nickel(I) complex $[Ni(TMC)]^+$.[36] We have measured the e.s.r. spectrum of a sample of ^{61}Ni(I=3/2) enriched $[Ni(TMC)]^+$ at 77K and have observed hyperfine coupling to the metal centre with A_{11}=62G and $A_{\perp}$=27G.[112] (Figure 6.3.II).

Further characterization of the palladium(I) species $[Pd(TMC)]^+$ is impeded by its high reactivity in solution, the complex having a half life of $t_{\frac{1}{2}} \simeq 5$ minutes under the conditions of the electrogeneration in CH_3CN at 20°C.

4.6 Discussion

Several examples of Pd complexes in the formal oxidation state of I are known. However with one exception[121] all characterized Pd(I) complexes are dinuclear or polynuclear diamagnetic species with coupling of unpaired electron density to form direct metal-metal bonds[122]. The palladium dimer $[Pd_2(CNCH_3)_6](PF_6)_2$ with an intermetallic distance of 2.53Å is an extensively studied example[123]. The first example of a Pd(I) mononuclear complex was recently reported[121]. The electrogeneration of the π complex $[Pd(C_5Ph_5)(cod)]$, (cod = cyclooctadiene) was confirmed by e.s.r. spectroscopy by

displaying coupling to ^{105}Pd (A = 25G) confirming the predominantly metal based character of the reduction.

The stability of the palladium(I) macrocyclic species $[Pd(TMC)]^+$ may be rationalised with reference to the TMC ligand. It allows for the metal reduction to occur at a moderate negative potential due to the weaker in-plane ligand field of TMC than macrocycles including secondary amine protons. The methyl groups are also an important factor as decomposition routes via secondary amine proton abstraction are blocked by N-alkylation. Potential dimerization reactions of the radical species are also inhibited by the steric bulk of the four methyl groups of the ligand. A dimerization reaction for the Ni(I) tetraaza macrocyclic complex [Ni(32)] has been recently proposed[124].

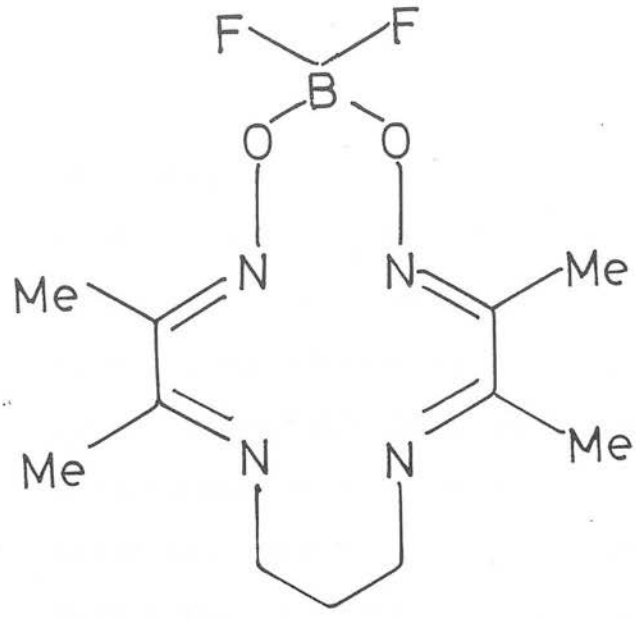

(32)

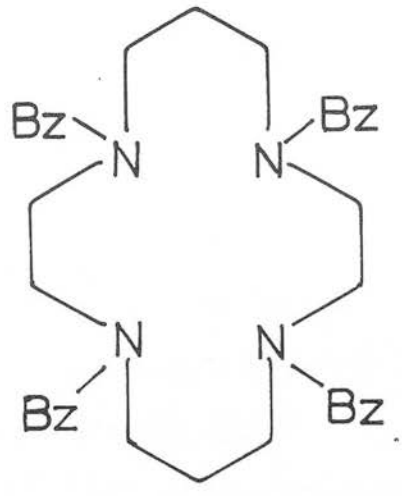

(33)

Further stabilization of the Pd(I) oxidation state may therefore be achieved by substituting the methyl groups of TMC for the more bulky benzyl groups of tetrabenzyl cyclam (33).

4.7 A Comparison with other Related Pd(II), Ni(II) Macrocycles

A series of other palladium macrocyclic complexes, including the pyridyl macrocycles L^1-L^4 were studied in order to compare and contrast their redox behaviour with $[Pd(TMC)]^{2+}$. The corresponding Ni(II) macrocycles have also been prepared for comparative purposes. All results are summarized in Table 4.7.I.

The N-tri-methyl pyridyl macrocyclic complex $[PdL^2]^{2+}$ gave a reversible reduction at the same potential as $[Pd(TMC)]^{2+}$. Attempts to electrogenerate $[PdL^2]^{+}$ were unsuccessful due to its increased reactivity over $[Pd(TMC)]^{+}$. The other Pd species all with two or more macrocyclic secondary amine protons show reductions by cyclic voltammetry at more negative potentials than $[PdL]^{2+}$, $L=L^2$, TMC. Several complexes show quasi-reversible or irreversible reductions to Pd(I) at extreme cathodic potentials. The nickel complexes $[NiL]^{2+}$, $L=L^1$-L^4, HMC, TMC, cyclam, show similar reductive electrochemistry to their Pd analogues. All reductions to Ni(I) are however fully reversible and on average 300mV more anodic in potential than for Pd(I) for the corresponding macrocycle L (Table 4.7.I). In contrast to their nickel(II) analogues which show Ni(II)/(III) redox couples in the range $E_{\frac{1}{2}}$ = +0.68→+1.33V vs. Ag/Ag^+, none of the palladium tetraaza

Table 4.7.I. Redox Data for Pd(II) and Ni(II) Tetraaza Macrocyclic Complexes[+]

	Reduction Potential $E_{\frac{1}{2}}$/V (ΔE/mV)			Oxidation Potential $E_{\frac{1}{2}}$/V (ΔE/mV)	
Complex	Pd	Ni	Δ[a]	Pd	Ni
$[M(TMC)]^{2+}$	-1.45(65)	-1.17(75)	0.28	-[b]	+1.33(106)
C*meso*$[ML^2]^{2+}$	-1.45(70)	-1.15(75)	0.30	-	+1.27(108)
$[ML^4]^{2+}$	-1.66(i)[c]	-1.40(70)	(0.26)	-	+1.03(66)
C*meso*$[ML^3]^{2+}$	-1.70(qr)	-1.39(75)	(0.31)	-	+1.00(78)
C*meso*$[ML^1]^{2+}$	-1.74(i)	-1.48(82)	(0.26)	-	+1.00(81)
C*meso*$[M(HMC)]^{2+}$	-1.91(105)[d]	-1.56(95)	0.35	-	+0.89(109)
$[M(cyclam)]^{2+}$	-2.02(82)[e]	-1.72(90)	0.30	-	+0.68(75)
$[M(\ 7\ )_2]^{2+}$	-1.96(i)			+0.05(150)	+0.69(qr)
$[M(\ 4\ )_2]^{2+}$	-0.77(80)[f]	-0.98(99)		+0.69(84)	+1.06(180)

[+] In CH_3CN with 0.1M $TBAPF_6$ base electrolyte. All potentials vs. Ag/Ag^+ (Fc/Fc^+=+0.08V) Scan rate 100m V/sec unless otherwise stated.

a Difference between Ni,Pd redox couples/V.

b No oxidation to solvent range (+2.2V)

c i = irreversible qr = quasi reversible

d scan rate = 400mV/sec

e scan rate = 1V/sec

f -45°C

macrocycles investigated show any oxidative activity up to +2.2V. Octahedral or distorted octahedral geometry would be required for the stabilization of the Pd(III) (or Pd(IV)) oxidation state[20,21]. The bis-sandwich palladium complexes $[Pd(4)_2]^{2+}$ and $[Pd(7)_2]^{2+}$ show oxidations at mild anodic potentials to yield Pd(III) species. The ability of the macrocycles (4) and (7) to adjust their mode of coordination in response to the oxidation state of the metal is essential for redox activity. The tetraaza complexes $[PdL]^{2+}$, L=L^1-L^4, HMC, TMC, cyclam, are restricted to square planar coordination and are therefore oxidatively inactive.

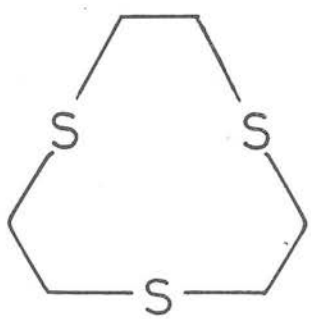

(4)

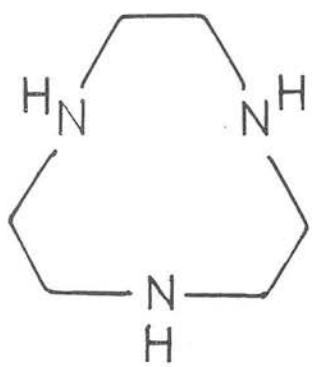

(7)

4.8 Reaction of $[Pd(TMC)]^+$ with Small Molecule Substrates

The direct electrochemical reduction of substrates such as CO_2 often require large overpotentials (more negative than -2.0V vs S.C.E.). An indirect electrochemical reduction involving the initial reduction of a metal complex which subsequently binds and reduces the substrate allows potentials closer to the thermodynamic values to be approached[30].

A preliminary investigation of the potential electrocatalyst $[Pd(TMC)]^+$ with small molecule substrates has therefore been initiated. Cyclic voltammetry experiments were carried out in the presence of PR_3, R=OMe, PPh and the gases O_2,CO,CO_2 and ethylene. CO binds strongly to $[Pd(TMC)]^+$ to give a presumably transient five coordinate species $[Pd(TMC)CO]^+$. No shifts in the cathodic wave are observed on addition of CO to an argon saturated solution. An anodic wave was not observed in the return scan until +0.20V suggesting a strong stabilization of Pd(I) in the presence of CO (Figure 4.7.I). Similar behavior was observed in the presence of $P(OMe)_3$,PPh_3; reoxidation waves occurring at -0.12 and -0.44V respectively. The palladium(II) porphyrins [Pd(por)], por = OEP^{2-},TPP^{2-} have been found to display electrocatalytic activity for the reduction of CO_2 in CH_2Cl_2 with oxalic acid identified as a major product[33]. For $[Pd(TMC)]^{2+}$ in CH_3CN or CH_2Cl_2 in the presence of CO_2 no electrocatalytic activity was observed as in both solvents the Pd(II)/(I) redox couple remained fully reversible. A similar result was obtained in an ethylene saturated acetonitrile solution. The reaction of $[Pd(TMC)]^+$ with dioxygen is proposed to yield a Pd(II) superoxy species $[Pd(TMC)O_2]^+$, as indicated by shifts of *ca.* 350mV in the dioxygen reduction wave in the presence of $[Pd(TMC)]^{2+}$. Such superoxy species have been suggested as active intermediates for the epoxidation of alkenes[125].

Figure 4.8.I. Cyclic Voltammogram of $[Pd(TMC)]^{2+}$ in CH_3CN/0.1M $TBAPF_6$ in the presence of CO

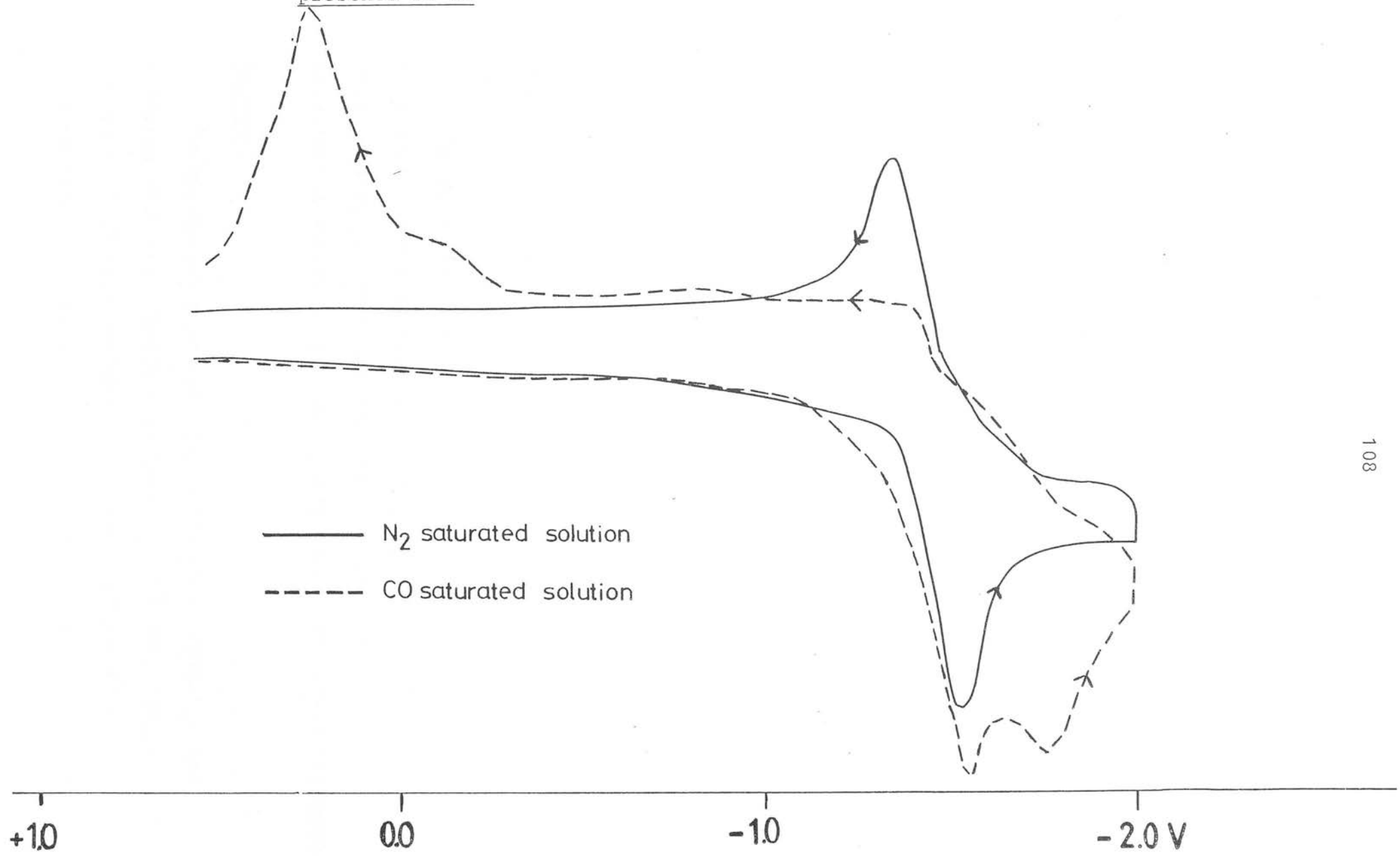

4.9 Experimental

X band electron spin resonance (e.s.r.) spectra were recorded using a Brucker ER-200D spectrometer employing 100 KHz field modulation. All e.s.r. spectra were measured as glasses in acetonitrile at 77K. Electrochemical measurements were recorded on a Brucker 310 Universal Modular Polarograph or Princetown Applied Research Model 173 Potentiostat/Galvanostat with 175 Universal Programmer equipment. Cyclic voltammetric slides were undertaken using a three electrode potentiostatic system in acetonitrile with 0.1M tetrabutylammonium hexafluorophosphate ($TBAPF_6$) present as supporting electrolyte. Platinum button microelectrodes were employed as auxilliary and working electrodes with a $Ag-AgBF_4$ reference electrode (with respect to this reference electrode, ferrocene is oxidized at +0.08V). Controlled potential electrolysis experiments were carried out under a constant stream of argon gas using a platinum gauze and platinum wire as the respective working and auxiliary electrodes, a salt bridge is incorporated to separate oxidized and reduced species.

The electrogenerated solution was transferred by syringe to a modified e.s.r. tube which had been cooled,evacuated, flushed with nitrogen gas and closed with a tap. The transferred solution was immediately frozen in liquid nitrogen.

Reagents

Tetrabutylammonium hexafluorophosphate, ($TBAPF_6$) was prepared from 40% [TBA]OH (Aldrich) and 65% HPF_6 (Strem) and recrystallized from methanol. "Dried, distilled" grade acetonitrile (Fisons) was used without further purification.

The ligands 1,4,8,11-tetraazacyclotetradecane, "cyclam" (Lancaster Synthesis) and 1,4,8,11-tetramethyl-1,4,8,11-tetraazacyclotetradecane, "TMC" (Strem) were used as supplied. C-*meso*-HMC was prepared by the method of Busch and Tait[126].

[PdL](PF$_6$)$_2$, L=cyclam, TMC, C-*meso*-HMC

The compounds were prepared in a similar manner to [Pd(II)L^n](PF$_6$)$_2$, n = 1-4 (Chapter 3).

[Pd(cyclam)](PF$_6$)$_2$

Yield 110 mg, 1.8 mmol, (52%)

Analysis: Required for $C_{10}H_{24}N_4P_2PdF_{12}\cdot H_2O$

C 19.5 H 4.2 N 9.1%

Found C 19.6 H 4.1 N 9.1%

I.r. ν_{max}=3256, 3190 (ν_{NH}), 1619 cm^{-1} (δ_{NH})

Electronic spectrum (in CH_3CN 900-186nm) 275 (ε=464), 207 (14670 dm^{3}mol^{-1}cm^{-1})

F.a.b. Mass Spectrum. Calculated for ^{106}Pd (Found)

[Pd(cyclam)PF$_6$]$^+$ 451(451), [Pd(cyclam)]$^+$ 306(305).

[Pd(TMC)](PF$_6$)$_2$

Yield 220 mg, 0.34 mmol, (86%)

Analysis: Required for $C_{14}H_{32}N_4P_2PdF_{12}$

C 25.8 H 4.9 N 8.6%

Found C 25.8 H 5.1 N 8.4%

Electronic spectrum (in CH_3CN 900-186nm) 307 (ε=1168) 225(20250 dm^{3}mol^{-1}cm^{-1}).

F.a.b. Mass Spectrum. Calculated for ^{106}Pd (Found)
$[Pd(TMC)PF_6]^+$ 508(508), $[Pd(TMC)]^+$ 363(362).
^1H N.m.r. $\delta_H[CD_3NO_2]$ 3.39(4H, d of t, NC*H*(H), J=13.1, Hz); 3.17(8H, m, NCH_2CH_2N); 2.81(12H, s, NCH_3); 2.58 (4H, d of t NCH(*H*), J=13.2, 3.3Hz); 2.05-2.38(4H, m, $-CH_2CH_2CH_2-$).
^{13}C D.E.P.T. n.m.r. $\delta_C[CD_3NO_2]$ 62.0, 59.6 (both N-CH_2-) 45.6 (N-CH_3); 22.6 ($-CH_2CH_2-CH_2-$)

C-*meso* $[Pd(HMC)](PF_6)_2$

Yield 81 mg, 1.2 mmol, (54%)
Analysis Required for $C_{16}H_{36}N_4P_2PdF_{12}$

C 28.2 H 5.3 N 8.2%
Found C 29.3 H 5.5 N 8.0%

I.r. ν_{max}=3240, s, (δ_{NH})
Electronic Spectrum (in CH_3CN 900-186nm) 283 (ε=475) 218(13530 $dm^3mol^{-1}cm^{-1}$)
F.a.b. Mass Spectrum. Calculated for ^{106}Pd (Found)
$[Pd(HMC)PF_6]^+$ 535(535), $[Pd(HMC)]^+$ 390(391).

$[NiL^n]^{2+}$ n=1-4

The nickel(II) pyridyl macrocycles $[NiL^n](ClO_4)_2$ n=1,3,4 were available as intermediates from the synthesis of the free ligands L^n n=1,3,4; their synthesis is described in Section 2.5.

$[NiL^1](ClO_4)_2$ Analysis: required for $C_{15}H_{26}N_4NiCl_2O_8$

C 36.4 H 5.0 N 10.7%
Found C 34.8 H 5.0 N 10.8%

I.r. ν_{max}=3227, 3194 ν(NH), 1614, 1583 cm^{-1}

$[NiL^3](ClO_4)_2$ Analysis: required for $C_{16}H_{28}N_4NiCl_2O_8$

C 36.0 H 5.3 N 10.5%

Found C 36.1 H 5.2 N 10.3%

I.r.: ν_{max}=3212 s,s (ν_{NH}), 1619 cm^{-1}, s,s, (δ_{NH})

$[NiL^4](ClO_4)_2$ Analysis: required for $C_{14}H_{24}N_4NiCl_2O_8$

C 33.2 H 4.8 N 11.1%

Found C 33.8 H 5.0 N 11.0%

I.r.: ν_{max}=3200 s,s (ν_{NH}), 3030, w, (ν_{py-H}), 1618, 1586 cm^{-1}

$[NiL^2](PF_6)_2$

L^2 (33 mg, 0.11 mmol) and $NiNO_3.6H_2O$ (38 mg, 0.11 mmol) were refluxed in methanol (40 cm^3) for 6 hours. Addition of NH_4PF_6 allowed an orange solid to be isolated that was recrystallized from methanol.

Yield 13 mg, 0.02 mmol, 20%

Analysis: required for $C_{18}H_{32}N_4NiP_2F_{12}$

C 33.1 H 4.9 N 8.6%

Found C 32.9 H 4.8 N 8.7%

I.r.: ν_{max}=1614, 1582 cm^{-1}, pyridyl ν(C=C), ν(C=N)

$[NiL]^{2+}$ L = cyclam, HMC, TMC

Synthesis of the complexes $[NiL]^{2+}$ are described in Chapter 6.

C H A P T E R 5

Electrochemical and Structural Studies on Unsaturated Nickel Tetradentate Macrocycles with 'N_3X' Donor Sets (X=N,P,S)

5.1 Introduction

During the last 20 years many studies on the redox properties of first row transition metal macrocycles have been undertaken in order to determine the factors that influence the stability and reactivity of the central metal ion. From these studies, important parameters such as macrocyclic 'hole' size[18,127,128], saturation and charge[18], configurational characteristics, (e.g. *meso/rac*[129], R.S.R.S./R.S.S.R.[19] or cyclam/isocyclam isomers[130]) and macrocyclic design (e.g. introduction of pendant arms[55,131], electron withdrawing/donating substituents[132], and substitution of hetero atoms into the donor set[23,66,133,134]) have been assessed. Least studied due to the synthetic complexities often involved in macrocyclic synthesis is the substitution of hetero atoms into the donor set. Tasker and coworkers prepared and investigated the Mn and Zn complexes of the pentadentate macrocycle (34) containing the 'N_3X_2' donor set, X=NH,S,O[134].

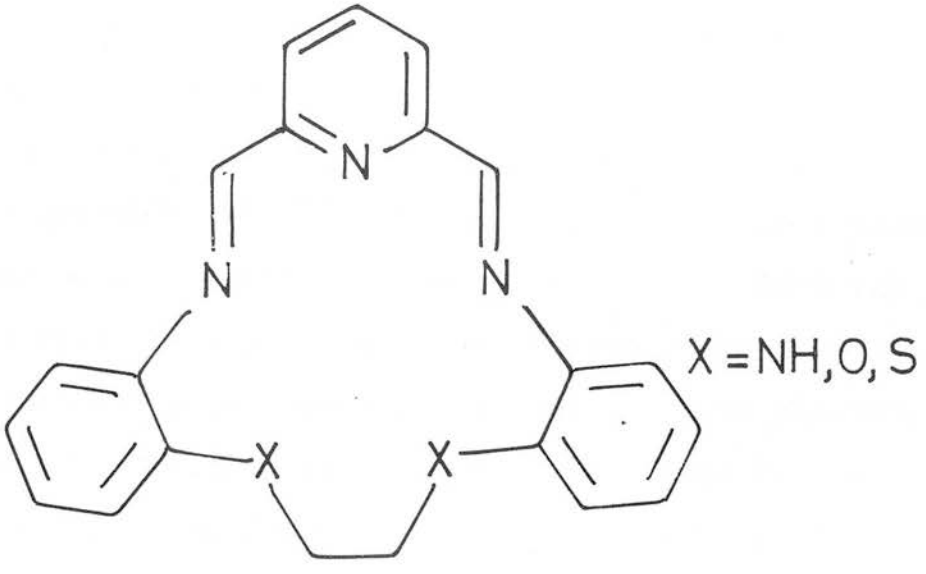

(34)

Although Kaden and coworkers[135,136] have published extensive data on a variety of mixed donor 'N_2S_2' macrocycles, e.g. (35), and Tasker *et al.*[137] and Meek *et al.*[138] have prepared and structurally characterized the only examples of tetradentate 'N_2P_2' macrocycles, few comparisons between the two sets are possible due to their differences in structure.

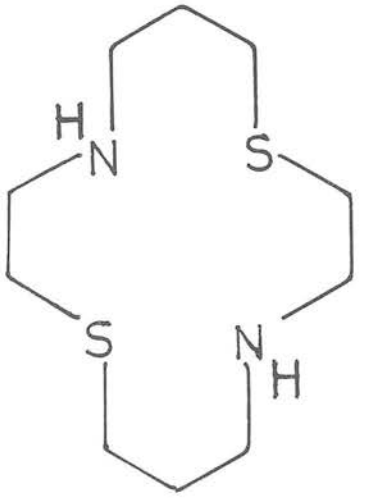

(35)

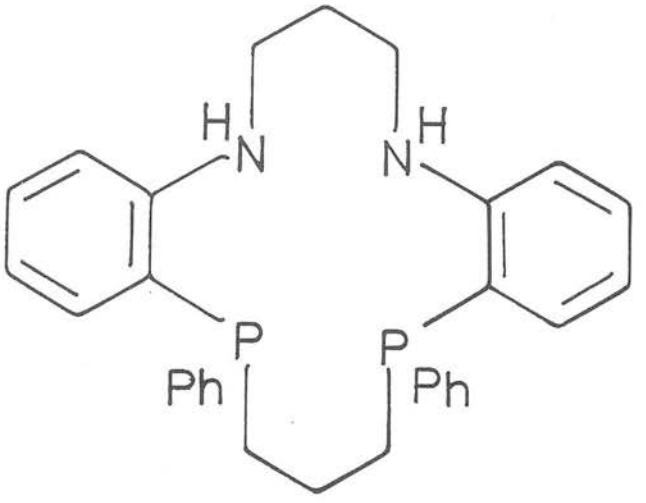

(36)

This problem was addressed by our investigation into the diiminopyridyl macrocycles with 'N_3X' donor sets, X=N,P,S. All three macrocycles, first synthesised by independent groups[47,139,140], by the nickel template method of condensation of 2,6-diacetylpyridine with the appropriate diamino ligand, have been prepared and investigated structurally and electrochemically. Diiminopyridyl macrocycles n_3X, X=n,p,s, are suitable for a comparative study for several reasons. The n_4 and n_3p macrocycles can

be prepared in high yield without complex organic synthesis of ligand precursors. The n_3s macrocycle was prepared by Dr. R.C. Sharma at the University of Edinburgh, and structural data for the nickel complex $[Ni(n_3s)Cl]_2(BF_4)_2$ is included here purely for comparative purposes[141]. The rigid diiminopyridine moiety limits the stereochemistry of the macrocycle so that a direct comparison in variation of one hetero atom donor is possible without changing other structural parameters. Previous redox studies have established a well defined electro-chemistry of the redox active $[Ni(n_4)]^{2+}$ complex[128,142]. It is compared with the results for the n_3p and n_3s macrocycles obtained from this study. For $[Ni(n_4)]^{2+}$ accessible, stable Ni(III) and Ni(I) oxidation states separated by *ca*.2.5V have been characterized. An intramolecular electron transfer from ligand to metal has also been described[18,142] which suggests that $[Ni(n_4)]^{2+}$ and structurally related species may be of use as electron transfer mediators and possible electro-catalysts.

5.1.2 The Interaction of Small Molecules with Ni(I)

The addition of π acid axial ligands to square planar transition metal unsaturated macrocycles has been examined by several groups[142-145]. The stabilization of the low valent oxidation states Co(I), Ni(I), Cu(I) was achieved in several cases. The stability was attributed to the combination of π acceptor properties of the unsaturated macrocycle and the particular axial ligand. Ni(II) complexes with conjugated α-diimine moieties such as (32) and the n_4

macrocycle undergo one electron reductions to give Ni(II) stabilized ligand radicals $[Ni(Mac^{\dot{-}})]^{+}$.

Upon interaction with axial ligands such as CO, these complexes form five coordinate Ni(I) carbonyl complexes [37].

$$[Ni(II)(Mac^{\dot{-}})]^{+} + CO \rightarrow [Ni(I)(Mac)CO]^{+} \qquad [37]$$

Thus an unpaired electron is induced to migrate to a predominantly metal orbital from a predominantly ligand based orbital via a reversible intramolecular electron transfer reaction[142,143].

Results and Discussion

5.2 Synthesis of Diimino Pyridine Macrocyclic Complexes

The nickel diiminopyridine tetraaza macrocyclic complex $[Ni(n_4)]^{2+}$ was readily synthesised by an established method of a Schiff base template condensation of 2,6-diacetylpyridine with 4-azaheptane-1,7-diamine using nickel as a templating centre. Under conditions of 8 hours reflux in aqueous ethanol an acid catalysed condensation gave the brick-red coloured product in 55% yield[47].

To prepare the triazaphosphorus macrocyclic complex $[Ni(n_3p)]^{2+}$ extremely mild template conditions were found to be essential. Condensation of 2,6-diacetylpyridine with bis(3-aminopropyl)phenyl-phosphine in the presence of Ni(II) nitrate was achieved under optimum conditions of gentle warming of an aqueous ethanolic solution to 50°C for one hour,

followed by stirring for 6 hours at room temperature. The complex was isolated as orange-brown crystals in 65-70% yield. To prepare the five coordinate nickel species $[Ni(n_3p)Cl]PF_6$ a 1:1 mixture of nickel dichloride and NH_4PF_6 was used as the source of nickel. The product was isolated as purple crystals in *ca.* 50% yield[139].

5.3 Structural Studies on Nickel Diiminopyridine Macrocycles

5.3.1 Introduction

In conjunction with the electrochemical studies a parallel investigation concerning structural aspects has been undertaken on nickel diiminopyridine macrocycles. In particular the structural and stereochemical effects of systematically varying one hetero atom of the $[Ni(n_3X)(Hal)]^+$ moiety (X=n,p,s, Hal=Br or Cl) has been studied. The crystal structure of $[Ni(n_3p)Cl]^+$ was compared with the published structure of $[Ni(n_4)Br]^+$ [145] and that of $[Ni(n_3s)Cl]_2^{2+}$, recently determined by Blake and Sharma at Edinburgh[141]. The effect of the axial halide substituent can also be assessed with reference to the structures of $[Ni(n_3p)]^{2+}$ and $[Ni(n_3p)Cl]^+$.

5.3.2 The Single Crystal X-Ray Structure of $[Ni(n_3p)](PF_6)_2$

The effect of the introduction of a larger second row element into the 14-membered diiminopyridyl macrocycle fragment was assessed from an X-ray analysis. A deep brown needle (0.24x0.08x0.12mm) suitable for X-ray analysis was obtained

by slow cooling and evaporation of a concentrated solution in water/ethanol (1:1).

Crystal Data

$C_{21}H_{26}N_3NiP^{2+}.2PF_6^-$ M = 700.03, Monoclinic, space group $C2/c$, a = 29.553(9), b = 8.725(8), c = 23.111(4)Å; β = 107.42(2)°, U = 5686Å^3, Dc = 1.635 g cm^{-3}, Z = 8, $F(000)$ = 2832, μ(Mo-Kα) = 9.45 cm^{-1}, λ(Mo-Kα) = 0.71069Å. At convergence **R**,Rw = 0.054, 0.064 respectively for 1944 data.

Selected bond lengths and angles are given in Table 5.3.I and a view of the cation is shown in Figure 5.3.II.

The structure shows a square planar nickel coordination geometry bound to phosphorus and all three nitrogen donors. The diiminopyridine fragment including the triaza donor set is essentially coplanar (maximum deviation from this plane is -0.06 Å) with the nickel atom +0.13Å from this plane. The phosphorus atom is displaced by 0.44Å from the 'N_3' plane. linked to N(3),N(11) by two propylene chains in a mirror related chair configuration. The dihedral angle between the triaza plane (Ni, N(3), N(11), N(17)) and the plane incorporating the phenyl moiety (N(17), Ni, P(7), C(21)) is 89.6°. Whereas Ni-N bond lengths for N(3), N(11) are almost equal in length (1.915(7) and 1.919Å), the pyridine nitrogen-nickel bond, Ni-N(17), is almost 0.1Å shorter, (1.822(7)Å). A similar magnitude of contraction is found for Ni-N(17) for all $[Ni(n_3X)(Hal)]^+$ structures[141,145].

Table 5.3.I. Selected bond lengths and angles (with e.s.d's), for $[Ni(n_3p)](PF_6)_2$ and $[Ni(n_3p)Cl]PF_6$

Bond lengths (Å)	$[Ni(n_3p)](PF_6)_2$	$[Ni(n_3p)Cl]PF_6$
Ni - N(17)	1.822(7)	1.828(5)
Ni - N(3)	1.915(7)	1.903(5)
Ni - P(7)	2.1483(25)	2.1498(18)
Ni - N(11)	1.919(7)	1.909(5)
Ni - Cl	-	2.4124(19)
Bond angles (°)		
N(3) - Ni - P(7)	97.35(21)	96.24(16)
N(3) - Ni - N(11)	164.5 (3)	164.05(22)
N(3) - Ni - N(17)	82.6 (3)	82.04(22)
P(7) - Ni - N(11)	97.47(21)	96.92(17)
P(7) - Ni - N(17)	171.39(22)	153.12(17)
N(11) - Ni - N(17)	82.6 (3)	82.15(23)
Ni - P(7) - C(6)	111.1 (3)	110.88(24)
Ni - P(7) - C(8)	110.3 (3)	110.02(23)
C(6) - P(7) - C(011)	105.9 (4)	105.5 (3)
C(8) - P(7) - C(011)	104.0 (4)	105.1 (3)
Cl - Ni - N(3)	-	94.33(16)
Cl - Ni - P(7)	-	96.96(7)
Cl - Ni - N(11)	-	93.22(17)
Cl - Ni - N(17)	-	110.92(17)

Figure 5.3.II View of the Single Crystal X-ray Structure of $[Ni(n_3p)]^{2+}$

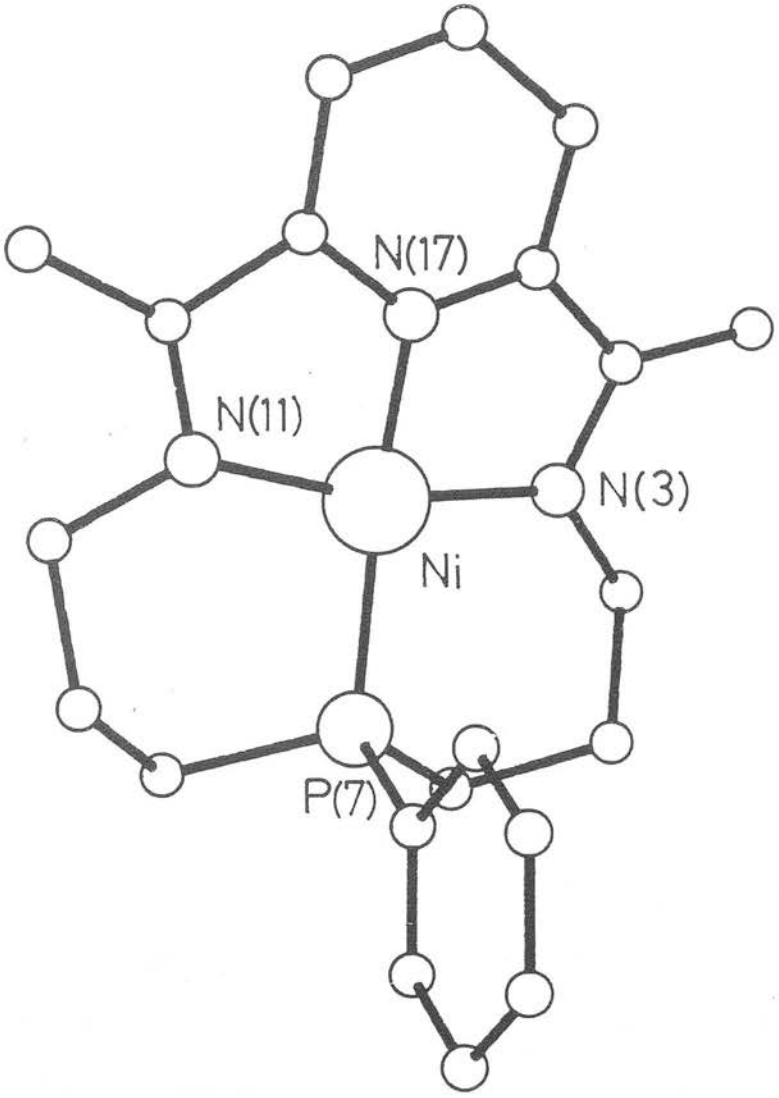

5.3.3 The Single Crystal X-Ray Structure of $[Ni(n_3p)Cl]PF_6$

In order to complete the structural investigation of the series $[Ni(n_3X)(Hal)]^+$ (X = n,p,s, Hal = Cl or Br) and to compare with the square planar $[Ni(n_3p)](PF_6)_2$, the single crystal X-ray structure was undertaken. A purple slightly flattened needle (1.4x0.3x0.2mm) suitable for X-ray analysis was obtained by slow evaporation of an ethanol solution.

Crystal Data

$C_{21}H_{26}ClN_3NiP^+.PF_6^-$ M = 590.52, Monoclinic, space group $P2_1/a$: a = 14.432(10), b = 12.220(7), c = 13.737(7)Å; β = 105.20(5)°, U = 2338Å^3, Dc = 1.558 g cm^{-3}, Z = 4, $F(000)$ = 1208, μ(Mo-Kα) = 10.96 cm^{-1}, λ(Mo-Kα) = 0.71069Å. At convergence R,Rw = 0.0513, 0.0721 for 2169 observed data.

Selected bond lengths and angles are given in Table 5.3.I and two views of the cation are shown in Figs.5.3.III and 5.3.IV.

The structure shows a distorted square based pyramidal coordination geometry of the nickel centre. The bound axial chloride (Ni-Cl = 2.4124(19)Å) is on the opposite face of the macrocycle to the phenyl group. The phenyl group is again orthogonal to the macrocyclic triaza plane, the dihedral angle between Ni, N(3), N(11), N(17) and N(17), Ni, P(7), C(21) is 89.44°. The square pyramidal distortion is a manifestation of the partially folded nature of the macrocycle. The diiminopyridine fragment is again coplanar but the phosphorus atom is displaced by 0.93Å from the 'NiN_3' plane (<N(17)-Ni-P(7) = 153.12(17)°). To relieve the strain the chloride is

Figure 5.3.III View of the Single Crystal X-ray Structure of $[Ni(n_3p)Cl]^+$

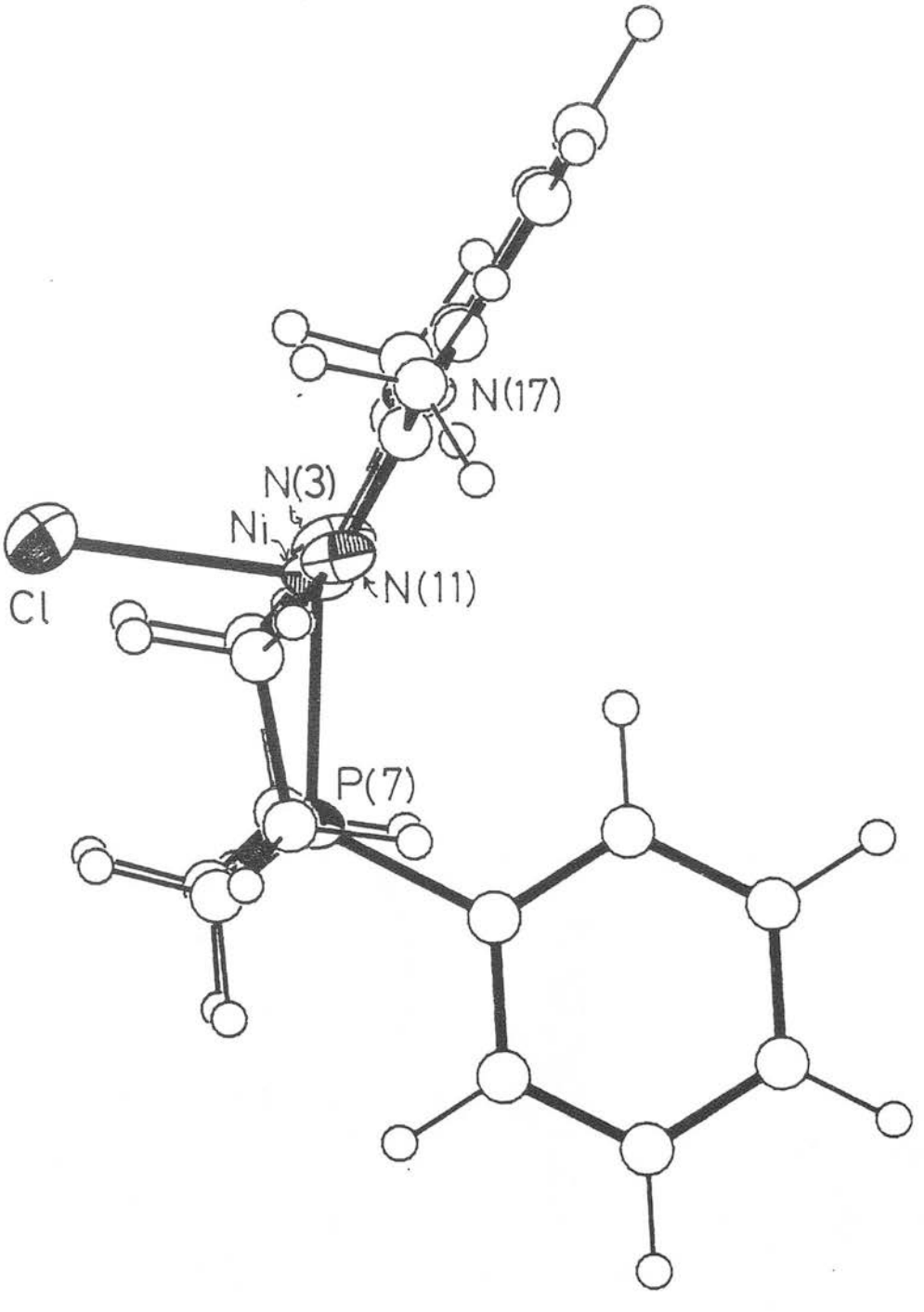

Figure 5.3.IV View of the Single Crystal X-ray Structure of $[Ni(n_3p)Cl]^+$

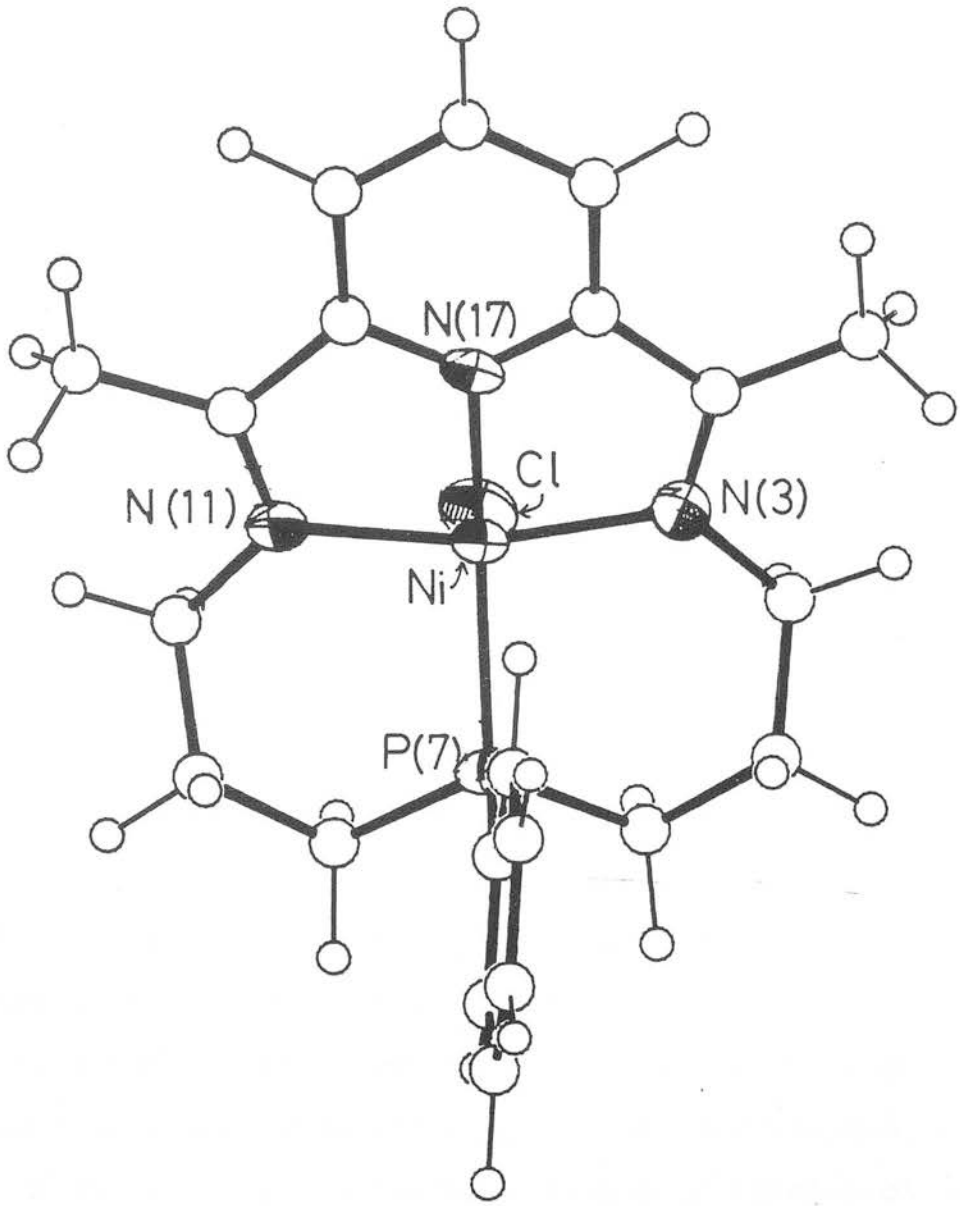

bent away from the macrocyclic plane (<N(17)-Ni-Cl = 110.92(16)°). The addition of the chloride to the nickel coordination sphere has minimal effect on other bond lengths (<0.01Å) and bond angles (<0.5°) when compared with the equivalent parameters of the $[Ni(n_3p)]^{2+}$ structure (Table 5.3.I).

5.3.4 The Single Crystal X-ray Structure of $[Ni(n_3s)Cl]_2(BF_4)_2$

The dimeric structure shows a distorted octahedral geometry around each nickel centre that are related through a centre of inversion[141]. (Figure 5.3.V). Each nickel centre is coordinated to three nitrogen atoms of the diimino pyridine macrocyclic fragment in an approximately planar fashion (Ni-N(3) = 2.032(13) Ni-N(11) = 2.054(12), Ni-N(17) = 1.976(10)Å) with the sulphur donor bent away to occupy an axial position (Ni-S(7) = 2.367(5)Å, <N(17)-Ni-S(7) = 97.1(3)°). The two remaining sites are occupied by *cis* bridging chlorides (Ni-Cl = 2.366(5)Å) in a *trans* geometry to the pyridine moiety (<N(17)-Ni-Cl = 170.3(3)°). Distortion from octahedral geometry illustrated by the inter-bond angles of <(N(17)-Ni-N(11) = 77.3(4), <N(17)-Ni-N(3) = 77.0(5)°, <Cl-Ni-N(11) = 104.1(4)°. In accommodating the strained geometry about nickel all Ni-N bond lengths are *ca.* 0.1Å longer than the corresponding bond lengths of the nickel complexes with the n_3p or n_4 macrocycles.

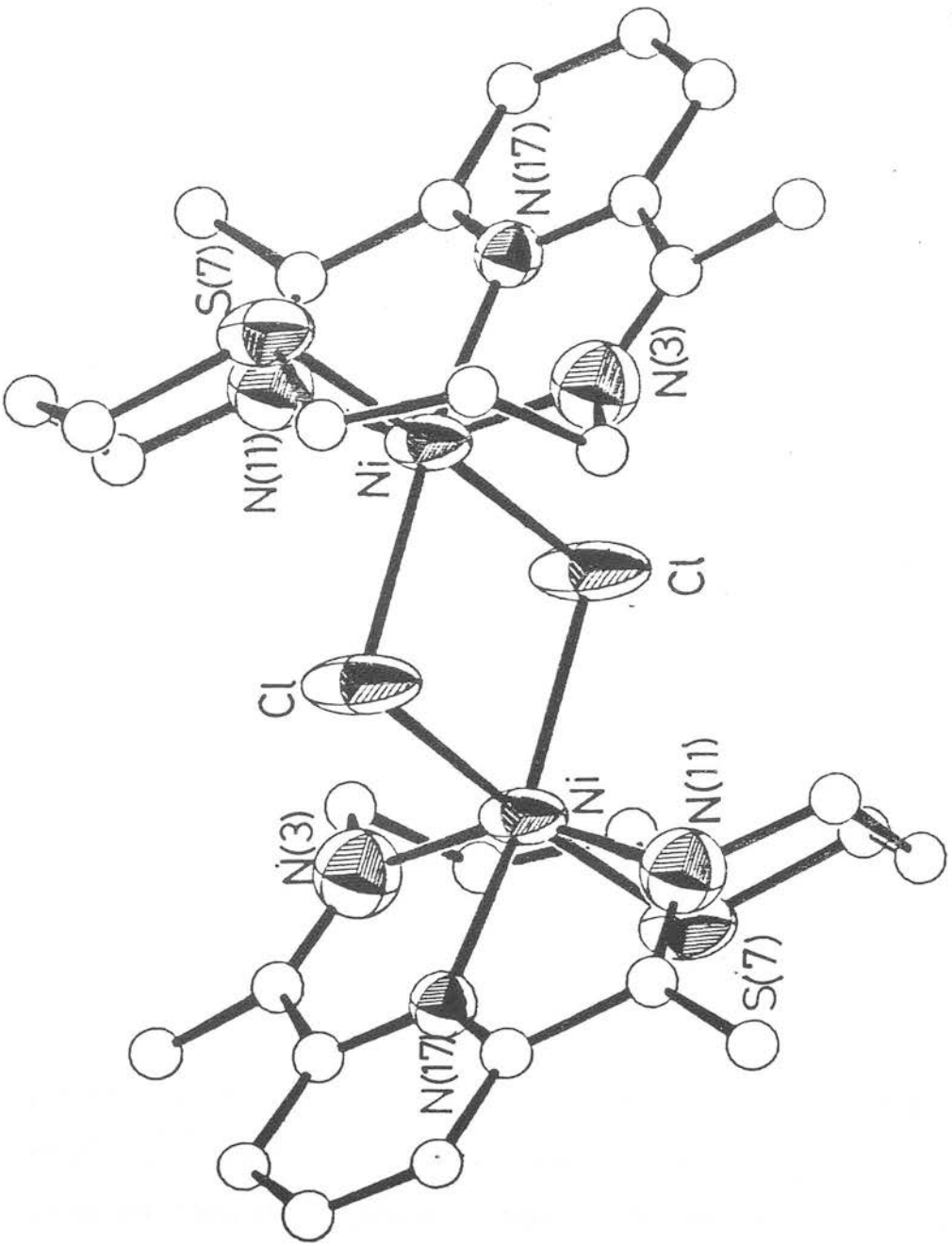

Figure 5.3.V. View of the Single Crystal X-ray Structure of $[Ni(n_3s)Cl]_2^{2+}$

5.3.5 Discussion

A summary of selected structural parameters is presented in Table 5.3.VI . The effect of introducing the larger, softer second row elements phosphorus and sulphur into the tetraaza ligand is clearly demonstrated. For the $[Ni(n_4)Br]^+$ complex the coordination geometry around Ni(II) is square based pyramidal. Maximum deviation of the nitrogen donor from the best 'NiN_4' plane is 0.14Å. For $[Ni(n_3p)Cl]^+$ a distorted square based pyramidal geometry with the P donor 0.93Å from the 'NiN_3' plane is observed. The sulphur derivative gives a dimeric structure, $[Ni(n_3s)Cl)]_2^{2+}$, with dichloro bridges between octahedral Ni(II) centres, with the sulphur atom 2.01Å from the 'NiN_3' plane. This trend may be rationalised by the increase in the Ni-X(7) bond length (Table 5.3.VI). An increase of 20% from Ni-N(7) = 1.932Å for $[Ni(n_4)Br]^+$ to Ni-S(7) = 2.367(5)Å for $[Ni(n_3s)Cl]_2^{2+}$ is a manifestation of the larger second row element incorporated into the macrocyclic donor set. As the diiminopyridine fragment is held rigid and cannot accommodate this increase, to relieve the strain the hetero group (P,S) is forced to bend away from planarity resulting in a folded macrocyclic structure. Hancock[119], in molecular mechanics calculations for the related tetraaza cyclam ligand calculated that a planar macrocyclic conformation was expected for Ni-N bond lengths of less than 2.05Å. Above 2.09Å octahedral geometry with a folded macrocyclic conformation leaving vacant *cis* coordination sites in the coordination sphere is predicted. The folded macrocyclic *cis* stereochemistry represents a coordination mode not previously characterized for

Table 5.3.VI . Summary of Crystallographic Data for $[Ni(n_3X)(Hal)]^+$ (X = n,p,s, Hal = Cl,Br)

Complex	Ni geometry	Ni-X(7)/Å	<N(17)-Ni-Hal	<N(17)-Ni-X(7)	Distance of X(7) best 'NiN_3' plane/Å	Ni-N(17)/Å
$[Ni(n_4)Br]^+$	square based pyramid	1.932(10)	103.2(4)°	163.7(6)°	0.14	1.808(4)
$[Ni(n_3p)Cl]^+$	distorted square based pyramid	2.1498(19)	110.92(16)°	153.12(17)°	0.93	1.828(5)
$[Ni(n_3s)Cl]_2^{2+}$	distorted octahedral (with *cis* dichloride) dimeric	2.367(5)	170.26(32)°	97.1(3)°	2.01	1.977(10)

diiminopyridyl macrocycles. It demonstrates a greater flexibility for the unsaturated tetradentate macrocycle than was previously predicted from reference to the crystal structures of square planar nickel[146] and copper[147] complexes.

5.4 Comparison of the Electrochemistry of $[Ni(n_4)]^{2+}$ and $[Ni(n_3p)]^{2+}$

The electrochemistry of the two nickel(II) macrocyclic complexes was investigated in acetonitrile solution with 0.1M $TBAPF_6$ as supporting base electrolyte. Cyclic voltammetric and e.s.r. data of products formed by electrosynthesis of the first reduction potential are listed in Table 5.4.I.

Table 5.4.I

Complex	1st reduction $^1E_{\frac{1}{2}}$/V (ΔEp/mV)	2nd reduction $^2E_{\frac{1}{2}}$/V (ΔE/mV)	oxidation $^1E_{\frac{1}{2}}$ (ΔE/mV)	E.s.r. of first reduction product
$[Ni(n_3p)]^{2+}$	-0.81(71)	-1.34(72)	-	g_{11}=2.236 g_1 =2.118
$[Ni(n_4)]^{2+}$	-0.92(68)	-1.49(61)	+1.08(70)	g_{iso}=2.002

Inspection of the data listed above illustrates the major effect on the redox properties by the introduction of the π acid phosphorus atom into the macrocyclic donor set. On scanning to +2.0V a Ni(II)/(III) redox couple is observed only

for the $[Ni(n_4)]^{2+}$ macrocycle. Both complexes show two reversible one electron reductions separated by *ca.* 550mV on scanning to -2.0V. Tentative evidence for a second ligand reduction is suggested on scanning to -3.0V. Irreversible reductions of -2.68 and -2.73V for $[Ni(n_3p)]^{2+}$ and $(Ni(n_4)]^{2+}$ respectively are assigned to reduction of the pyridine ring (*cf.* -3.1V for pyridine in MeCN)[148].

E.s.r. evidence outlined below suggests that the first reduction for $[Ni(n_3p)]^{2+}$ is metal based whereas for $[Ni(n_4)]^{2+}$ it is a ligand based reduction.

i. $[Ni(n_3p)]^{2+}$

Reduction at a platinum gauze of an acetonitrile solution of $[Ni(n_3p)]^{2+}$ (λ_{max}=444nm) by controlled potential electrolysis at -0.95V yielded an intense inky maroon solution (λ_{max}=516nm). At 77K this species as an acetonitrile glass shows an anisotropic e.s.r. signal with g_{11}=2.236, $g_{\perp}$=2.118 (Figure 5.4.II). Axial symmetry with $g_{11}>g_{\perp}$ is consistent with a Ni(I) species. Evidence that the second reduction occurred on a ligand centre to form $[Ni(n_3p^{\cdot})]$, a Ni(I) ligand radical species rather than on the nickel to form $[Ni(o)(n_3p)]$ was obtained by quantitative electroreduction at the secondary reduction potential. The e.s.r. spectrum at 77K was rather more complex due to some coupling of the two paramagnetic centres in the complex. A ligand reduction is clearly indicated by the formation of a new isotropic signal, g_{iso}=2.004. Interaction with the metal centre is suggested as the anisotropic nickel g tensors are shifted (g_{11}=2.241, $g_{\perp}$=2.156).

Figure 5.4.II. E.s.r. Spectrum of $[Ni(n_3p)]^+$ Generated Electrochemically Measured at 77K in CH_3CN/0.1M $TBAPF_6$

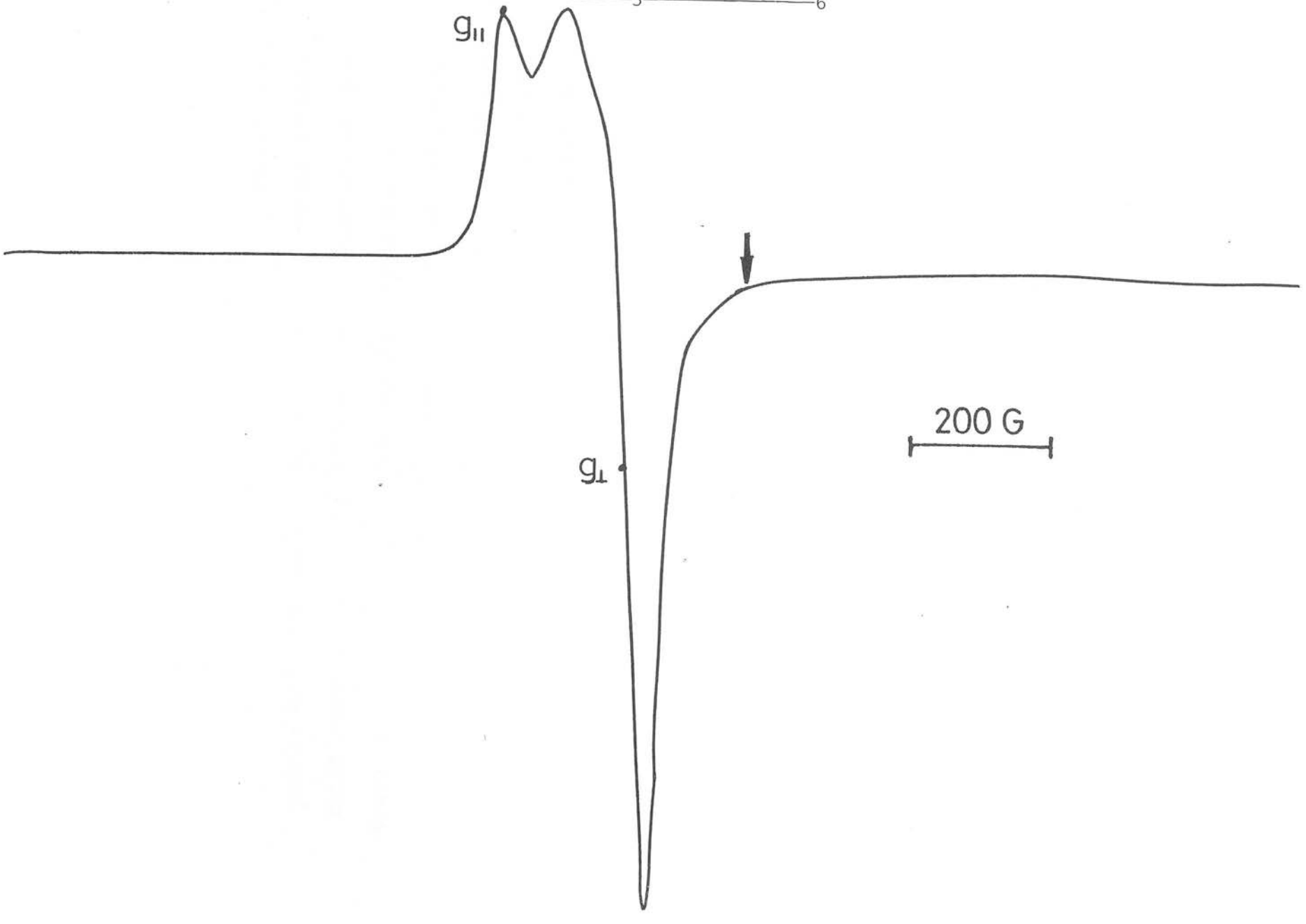

ii. $[Ni(n_4)]^{2+}$

Confirmation of an initial ligand based reduction of $[Ni(n_4)]^{2+}$, in agreement with results from previous studies [18,142], was obtained by electrochemical reduction at the first reduction potential. Controlled potential electroreduction at -1.00V in acetonitrile yields a dark green solution (λ_{max}=640nm), the e.s.r. of which at 77K as an acetonitrile glass shows a single isotropic signal at g_{iso}=2.002 indicative of the formation of $[Ni(n_4^{\cdot-})]^{+}$, a nickel(II)-ligand radical species. Reduction at the secondary reduction potential has been previously shown to produce the nickel(I) ligand radical species $[Ni(n_4^{\cdot-})]$, as characterised by e.s.r. (g_{av}=2.188, g_{iso}=2.002) [142].

iii. Discussion

From the direct comparison of the two diiminopyridine macrocycles, the effect of one equatorial phosphorus atom substituted into the tetraaza macrocycle can be assessed. Comparison of the redox potentials shows that the Ni(II)/(I) redox couple is significantly stabilized whereas the Ni(II)/(III) couple is destabilized and not observed. The formal Ni(II)/(I) redox couple for $[Ni(n_3p)]^{2+}$ of -0.81V therefore compares very favourably with other neutral tetraaza macrocycles. Under equivalent conditions their redox couples range between -1.72V for $[Ni(cyclam)]^{2+}$ to -1.00V for $[Ni(38)]^{2+}$ [19].

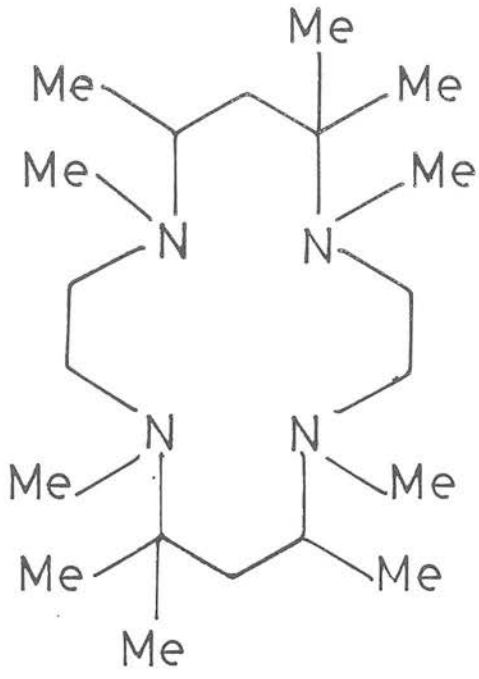

(38)

The significant stabilization of the Ni(I) oxidation state is attributed mostly to the superior π acceptor ability of P over N, but a contribution due to the more structurally accommodating nature of the n_3p macrocycle over the n_4 macrocycle may be involved.

With the Ni-P bond bent away so that the phosphorus atom is 0.44Å out of the 'NiN_3' plane, the larger Ni(I) centre can be more readily accommodated within the macrocyclic cavity than the planar n_4 macrocycle. It is well documented that anodic shifts in the Ni(II)/(I) redox couple are found with an increase in the macrocyclic cavity or 'hole' size[18,19].

The superior σ donor properties of N in comparison to P allow for the stabilization of $[Ni(n_4)]^{3+}$. The analogous n_3p complex is unobserved due to the destabilizing influence of phosphorus on Ni(III).

5.5 Comparison of the Electrochemistry of $[Ni(n_3p)Cl]^+$ and $[Ni(n_3s)Cl]_2^{2+}$

Preliminary studies have been undertaken on the n_3s macrocycle as its nickel complex $[Ni(n_3s)Cl]_2(BF_4)_2$. Results are compared with the monochloro n_3p complex $[Ni(n_3p)Cl]^+$, under similar experimental conditions, and tabulated in Table 5.5.I.

Table 5.5.I

Complex	1st reduction $^1E_{\frac{1}{2}}$/V (ΔEp/mV)	2nd reduction $^2E_{\frac{1}{2}}$/V (ΔE/mV)	Oxidation $^1E_{\frac{1}{2}}$/V	E.s.r. of first reduction product
$[Ni(n_3p)Cl]^+$	-0.95(112)	-1.33(88)	-	g_{av}=2.108
$[Ni(n_3s)Cl]_2^{2+}$	-0.88(120)	-1.44(112)	+0.90irrev	a

a, complex decomposed on electrogeneration.

i. $[Ni(n_3p)Cl]^+$

Two reversible one electron reductions are observed on scanning to -2.0V. In common with the square planar n_3p complex, no oxidation was detected to the anodic limit of the solvent. A shift of 140mV to a more cathodic potential is noted for the first reduction when compared with the corresponding reduction of $[Ni(n_3p)]^{2+}$, with a negligible change between the two second reduction potentials. The

more cathodic potential would be expected with the π donor chloride anion bound to the nickel centre. This strongly suggests that the first reduction of the complex is metal based. Confirmation was achieved by electrosynthesis at -1.05V. An anisotropic e.s.r. signal with non axial symmetry with overlapping g_{11} and $g_{\perp}$ features (g_{av}=2.108) clearly suggests coordinated chloride attached to a nickel(I) centre.

ii. $[Ni(n_3s)Cl]_2^{2+}$

Two quasi-reversible one electron reductions and one irreversible oxidation at +0.90V were recorded for the octahedral sulphur analogue. The large peak to peak separation for the first reduction species (E_{pc} = -0.94, E_{pa} = -0.82V, ΔE_p = 120mV) suggests that in common with the phosphorus analogue the first reduction is metal based. Attempts to electrogenerate at the first reduction potential were unsuccessful due to the rapid decomposition of the reduced product. Of note is the irreversible oxidation at a moderate anodic potential, reflecting the better donor properties of S over P to stabilize the Ni(III) oxidation state.

5.6 The Interaction of Small Molecules with Nickel(I) Macrocycles

The interaction of small molecules with $[Ni(n_3p)]^+$ has been investigated using a combination of electrochemical and e.s.r. techniques and compared with results from the

previously characterized $[Ni(n_4^{\cdot-})]^+$ complex.

In the presence of a large stoichiometric excess of axial π acid ligands CO, $PMePh_2$, EPh_3 (E = P,As,Sb) and PR_3 (R = OMe, ^nBu), reductive cyclic voltammetry of $[Ni(n_3p)]^{2+}$ shows the reduction wave to shift to a more anodic potential with a concomitant shift to more cathodic potentials for the secondary reduction potential (Figure 5.6.I). The magnitudes of these interactions are tabulated in Table 5.6.II. To stabilize Ni(I) a proposed five coordinate species is believed to be formed[142,143]. The strongest π acids, in general, are therefore able to stabilize low oxidation states (resulting in the largest shifts), due to their ability to accept electron density from the electron rich metal centre. For $[Ni(n_3p)]^{2+}$, largest interactions were associated with the addition of a large stoichiometric excess of $P(OMe)_3$.

A shift of *ca.* 245mV in the cathodic and anodic waves of the primary reduction potential to a more positive (favourable) potential leads to an extremely anodic value of the formal reduction potential to Ni(I) of $^1E_{\frac{1}{2}}$ = -0.56V (ΔE_p = 80mV). No shift for the poorer π acid $SbPh_3$ was observed while the intermediate strength π acid $PMePh_2$ gave shifts of *ca.* 115mV (Figure 5.6.I). Larger interactions were observed for the secondary reduction potential. Shifts of 5-600mV to a more cathodic potential were measured for the strongest π acceptors. In contrast, for $[Ni(n_4^{\cdot-})]^+$, shifts of *ca.* 200mV were observed for the corresponding axial ligand under equivalent conditions. This trend of a weaker interaction with the n_4 macrocycle was followed for all ligands studied.

Figure 5.6.I. Reductive Cyclic Voltammetry of $[Ni(n_3p)]^{2+}$ in CH_3CN/0.1M $TBAPF_6$ in the Presence of $PMePh_2$

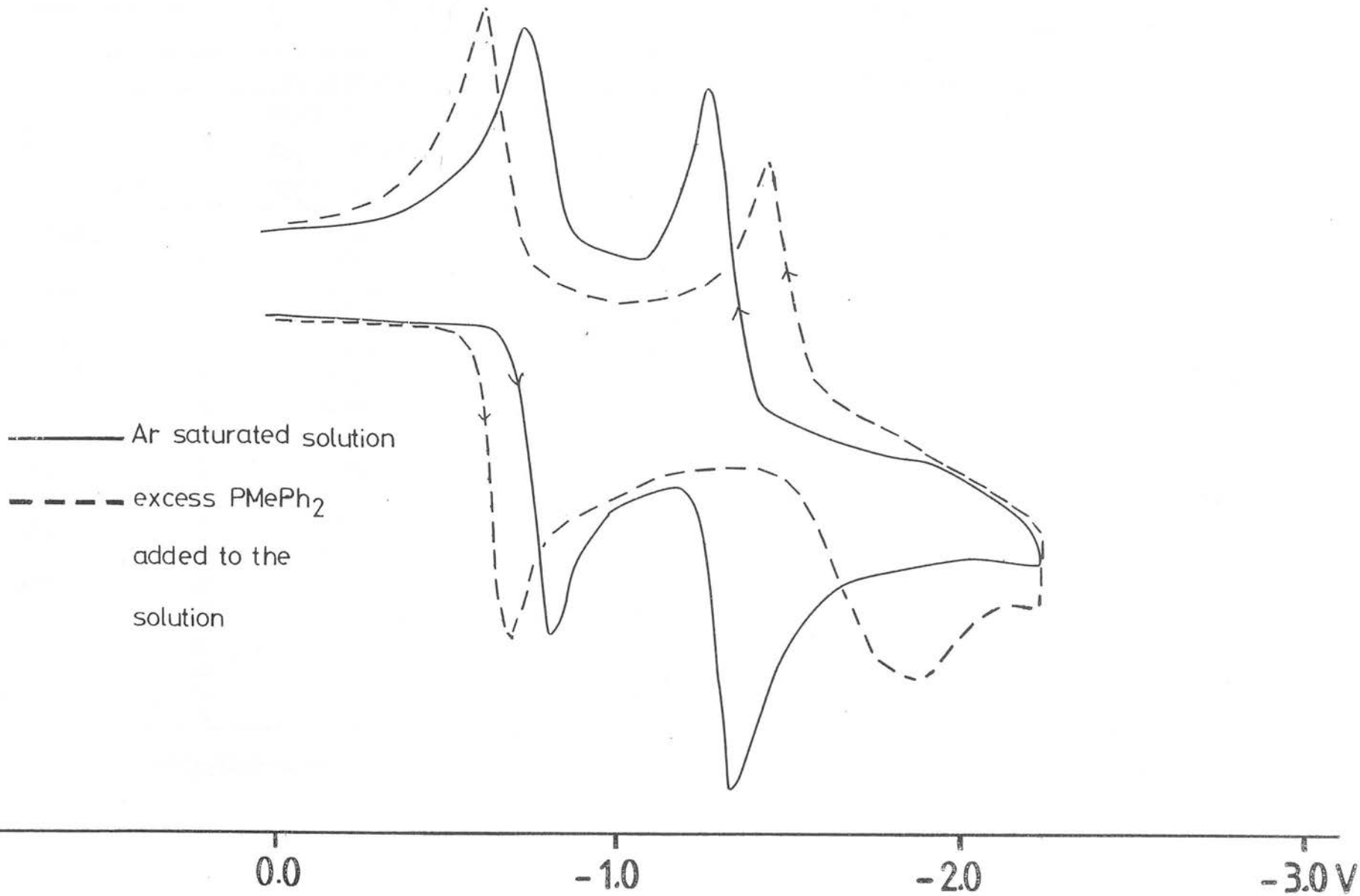

Table 5.6.II. Reductive Cyclic Voltammetry of $[Ni(n_3X)]^{2+}$, X = n,p in the presence of π acceptor ligands[+]

Ligand	‡	$[Ni(n_3p)]^{2+}$ 1st Reduction	$[Ni(n_3p)]^{2+}$ 2nd Reduction	$[Ni(n_4)]^{2+}$ 1st Reduction	$[Ni(n_4)]^{2+}$ 2nd Reduction
		Shift(mV) in redox potentials from:		Shift (mV) in redox potentials from:	
		^1Ep_c = -0.846V	^2Ep_c = -1.366V	^1Ep_c = -0.954V	^2Ep_c = -1.520V
		^1Ep_a = -0.774V	^2Ep_a = -1.294V	^1Ep_a = -0.866V	^2Ep_a = -1.460V
$P(OMe)_3$	C	+243	-629	+135	-220
	A	+248	n.obs.	+275	-200
$P(^nBu)_3$	C	+144	-605	+162	-182
	A	+160	n.obs.	+258	-174
$PMePh_2$	C	+115	-540	+195	-210
	A	+123	-173	+224	-184
CO	C	+72	-325	+54	-59
	A	+345	-113	+54	-48
PPh_3	C	+35	-375	+9	-67
	A	+167	-111	+99	-58
C_2H_4	C	+12	-16	-9	0
	A	+14	-12	-9	0
$AsPh_3$	C	0	-8	0	0
	A	+8	-8	0	0
$SbPh_3$	C	0	0	0	0
	A	0	0	0	0
CO_2	C	0	0	0	0
	A	0	0	0	0

[+] large stoichiometric excess. ‡ C = cathodic wave A = anodic wave n.obs. anodic wave not observed

With the strong binding of phosphines to $[Ni(n_3p)]^+$, it was hoped that the gases CO, CO_2, and C_2H_4 could be activated on interaction with an electron rich centre. Stabilization of Ni(I) in a CO saturated acetonitrile solution was achieved (E_{pa} = -0.38V). For an ethylene saturated acetonitrile solution negligible shifts (*ca.* 12mV) suggested little or no interaction. In aqueous acetonitrile solutions a report suggested that $[Ni(n_4)]^{2+}$ was an electrocatalyst for CO_2 reduction[149]. In dry acetonitrile solution neither $[Ni(n_3p)]^{2+}$ or $[Ni(n_4)]^{2+}$ showed any shifts in redox potentials or increases in current density expected for an electrocatalytic CO_2 reduction.

Further evidence for the coordination of axial substrates to monovalent nickel was obtained from e.s.r. studies. The effect of a range of axial ligands on e.s.r. g tensors is tabulated in Table 5.6.III. On electrogeneration of $[Ni(n_3p)]^+$ in the presence of a stoichiometric excess of a ligand such as $P(OMe)_3$, shifted g tensors are observed when compared to the e.s.r. spectrum of $[Ni(n_3p)]^+$ with no added substrate. The identical e.s.r. spectrum can also be generated by addition of $P(OMe)_3$ to a solution of $[Ni(n_3p)]^+$ electrogenerated at its primary reduction potential. Shifts towards free spin of 107G in g_{11} and 22G in the $g_\perp$ region suggest the formation of a 5 coordinate Ni(I) species, consistent with the proposed structure of other Ni(I) macrocyclic complexes[142,143]. For ligands with little or no interaction with the metal centre (from C.V. experiments), negligible shifts in g tensors are observed. In contrast, electrogeneration of $[Ni(n_3p)Cl]^+$ shows a significant shift

Table 5.6.III. E.s.r. Data[a] of products formed by reduction of $[Ni(n_3X)]^{2+}$, X=n,p, at the first reduction potential in the presence of π acceptor ligands

Complex	Ligand	E.s.r. Spectrum	
		g_{11}	$g_{\perp}$
$[Ni(n_3p)]^{2+}$	-	2.236	2.118
	$P(OMe)_3$	2.159	2.102
	PPh_3	2.254	2.092
	C_2H_4	2.233	2.115
	$AsPh_3$	2.234	2.114
$[Ni(n_4)]^{2+}$	-	$g_{iso}=2.002$[b,c]	
	$P(OMe)_3$	2.190	2.065
	$P(^nBu)_3$	2.209	2.104
	PPh_3	2.206	2.068
	CO	2.211	2.050[c]

a Measured in acetonitrile at 77K

b Isotropic signal

c ref. 142

of both g tensors giving overlapping g_{11}, $g_{\perp}$ features (g_{av} = 2.108) due to the proposed 5 coordinate Ni(I) species generated.

5.7 Conclusions

A combination of e.s.r. and electrochemical techniques has shown the ability to 'tune' the redox behaviour of a metal centre over a wide potential range. Within the diiminopyridine macrocyclic framework the redox potential for the Ni(II)/(I) couple can be varied by *ca.* 1.0V when comparing the structurally similar n_4 and n_3p macrocycles under certain conditions. The n_3p macrocycle stabilizes Ni(I) at the anodic potential of -0.81V. In the presence of $P(OMe)_3$ this potential is further reduced to -0.56V. In comparison the n_4 macrocycle stabilizes the nickel(I) ligand radical, $[Ni(n_4^{\cdot-})]$ at -1.49V.

Although this investigation has produced a large variation in the redox potential of the radical Ni(I) species, no interaction with the industrially important gases CO_2 or C_2H_4 was detected under the conditions employed. A significant stabilization of the nickel(I) oxidation state was however noted in the presence of the π acceptors CO, PR_3 (R = OMe, ^nBu, Ph). In conclusion, a variation in experimental conditions to include protic solvents is envisaged in order to obtain electrocatalytic activity with small molecules.

5.8 Experimental

Microanalyses, infrared and n.m.r. spectra and conductivity measurements were obtained as described in earlier

chapters. Cyclic voltammetric and electrosynthetic studies were carried out using the apparatus described in Chapter 4.

Reagents

Bis(3-aminopropyl)phenyl phosphine (Strem) was used without further purification. $[Ni(n_4)](ClO_4)_2$ was prepared by the method of Busch and Tait[126] (n_4 = 2,12-dimethyl-3,7,11,17-tetraazabicyclo[11.3.1]heptadecapent-1(17),2,11,13,15-ene). $[Ni(n_3s)Cl]_2(BF_4)_2$ was prepared by Dr. R.C.Sharma, University of Edinburgh[141], (n_3s = 2,12-dimethyl-3,11,17-triaza-7-thia-bicyclo[11.3.1]heptadecapent-1(17),2,11,13,15-ene).

$[Ni(n_3p)](PF_6)_2$, (n_3p = 2,12-dimethyl-7-phenyl-3,11,17-triaza-7-phospha-bicyclo[11.3.1]heptadecapent-1(17),2,11,13,15-ene).

$Ni(NO_3)_2.6H_2O$ (200 mg, 0.69 mmol) was dissolved in ethanol (80 cm^3) and distilled water (60 cm^3) at 50°C under nitrogen. Bis(3-aminopropyl)phenyl phosphine (150 mg, 0.69 mmol) in ethanol, (10 cm^3) was added over a period of 5 minutes. 2,6-Diacetylpyridine (110 mg, 0.69 mmol) in ethanol (10 cm^3) was then added and the resulting dark wine-red solution was maintained at 50°C for one hour. After continued stirring for 6 hours at room temperature excess NH_4PF_6 was added. On cooling an orange-brown solid was collected which was recrystallized from water/ethanol, washed with ethanol and diethyl ether and dried *in vacuo*. Yield 340 mg, 0.48 mmol, (70%).

Analysis: Required for $C_{21}H_{26}F_{12}N_3NiP_3$:

C 36.0 H 3.7 N 6.0%

Found C 35.8 H 3.7 N 5.8%

Equivalent conductivity, slope of $\Lambda_o-\Lambda_e$ vs $Ce^{\frac{1}{2}}$ plot in CH_3NO_2 = 373.

I.r. ν_{max} = 3100 pyridyl ν(C-H); 1608, 1590 cm^{-1} pyridyl ν(C=C), ν(C=N).

Electronic spectrum: (in CH_3CN 900-186nm) 444 (ε=1650) 331(3180) 283(5680) 217(22600 $dm^3mol^{-1}cm^{-1}$)

F.a.b. mass spectrum. Calculated for ^{58}Ni (Found) $[Ni(n_3p)(PF_6)]^+$ 554 (not observed), $[Ni(n_3p)]^+$, 409(409).

$[Ni(n_3p)Cl]PF_6$

$NiCl_2.6H_2O$ (278 mg, 1.02 mmol) and NH_4PF_6 (167 mg, 1.02 mmol) were dissolved in ethanol (100 cm^3) under nitrogen. Bis(3-aminopropyl)phenyl phosphine (230 mg, 1.02 mmol) in ethanol (10 cm^3) and 2,6-diacetylpyridine (167 mg, 1.02 mmol) in ethanol (10 cm^3) were successively added, and the resulting mixture was heated for 7 hours at 60°C to give a maroon solution. Cooling gave a dark purple crystalline solid which was recrystallized from ethanol. Yield 300 mg, 0.51 mmol, (50%).

Analysis: Required for $C_{21}H_{26}ClF_6N_3NiP_2$

C 42.7 H 4.4 N 7.1%

Found C 42.5 H 4.2 N 7.0&

Equivalent conductivity, slope of $\Lambda_o-\Lambda_e$ vs $Ce^{\frac{1}{2}}$ plot in CH_3NO_2 = 267.

I.r. ν_{max} = 3060 pyridyl ν(C-H); 1606, 1574 pyridyl ν(C=C), ν(C=N); 458 cm^{-1} ν(Ni-Cl).

Electronic spectrum: (in CH_3CN 900-186nm) 520 (ε=3450), 360(2250)sh 284(6425)sh 219(28,700 $dm^3mol^{-1}cm^{-1}$).

F.a.b. mass spectrum: Calculated for ^{58}Ni (Found) $[Ni(n_3p)Cl]^+$ 445(444), $[Ni(n_3p)]^+$ 409(409).

C H A P T E R 6

The Reaction of Dioxygen and Superoxide with the Nickel Tetraaza Macrocycles $[NiL]^{+/2+}$ L=TMC, C-*rac*-HMC

6.1.1 The Reaction of Dioxygen with Transition Metal Macrocycles

Dioxygen complexes of metalloporphyrins have been of great interest in relation to the elucidation of the mechanism of transport and storage of dioxygen by hemoglobin and myoglobin, of activation of dioxygen by cytochrome P450 and of the *in vivo* four electron reduction of dioxgen by cytochrome oxidase[150-152]. The four electron reduction of dioxygen to water by dimeric cofacial metalloporphyrin electrocatalysts has received considerable study due to its potential importance in fuel cells and air batteries[24,25].

Dioxygen adducts formed by the reaction of molecular dioxygen with Fe(II), Co(II), Cr(III), Ru(II), Rh(II), and Ti(III) porphyrins have been reported[151,152]. With the exception of the Fe(II) case the dioxygen ligand is considered to adopt the electronic configuration of superoxide with end on binding by a formal oxidation of the metal centre by one electron with a concomitant reduction of the coordinated O_2. For Fe(II) porphyrins used as model systems for hemoglobin and myoglobin, an irreversible oxidation to Fe(III) is observed unless specially designed synthetic ligands such as the "picket fence porphyrins"[16] or "lacunar macrocycles"[14] are used. Investigators have employed the reactions of dioxygen with other metals or have studied non-redox active molecules such as CO in order to circumvent this irreversible iron oxidation process while investigating substrate binding reactions[152].

Reactions of transition metal non-porphyrinoid macrocyclic species with dioxygen have also served as useful model systems. Kimura and coworkers[153,154] have recently reported a reaction of a Ni(II) pentadentate macrocycle, (39) with dioxygen to form a formally [Ni(III)-O_2^-] species.

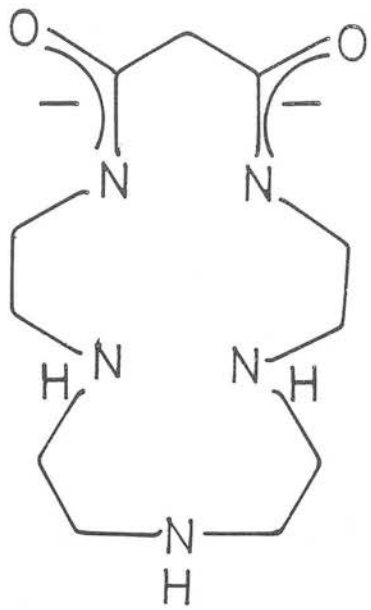

(39)

This system is proposed as a model for biological monooxygenases, as dioxygen bound to the nickel centre can be directly incorporated into a non activated aromatic ring as a hydroxy group [40].

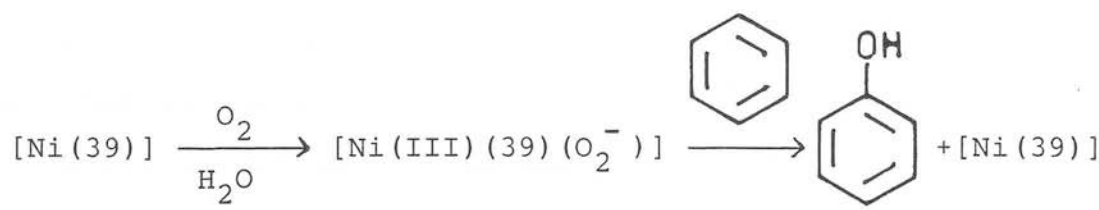

[40]

Anson and coworkers[155] and Endicott and coworkers[156] have observed μ-peroxo bridged cobalt cyclam complexes, $[[Co(cyclam)]_2O_2]^{4+}$, which are regarded as a model for the intermediates formed in the reduction of O_2 using dimeric

cofacial Co(II) porphyrins. Coordination of the cobalt macrocycle at both ends of the peroxo dianion did not result in activation of the O-O bond to enable a 4 electron reduction to occur; H_2O_2 was the only product detected on reduction of the μ-peroxo dimer.

Reaction of dioxygen with the first row metals Cr→Cu are generally mechanistically well understood with the notable exception of Ni. Contradicting reports of the reaction of Ni(I) macrocycles with O_2 are discussed in Section 6.1.2. In an attempt to clarify the mechanism the interaction of O_2 in MeCN solution with $[NiL]^+$, L=C*rac*HMC,TMC, was investigated. Further impetus for the study of reactions of Ni(I) macrocycles is gained from the characterization of Factor F430 found in methane forming bacteria as a Ni complex of an unsaturated tetraaza macrocycle[12]. Preliminary results implicate both the Ni(I) and Ni(III) oxidation states in their mechanism[157].

6.1.2 The Reaction of Ni(I) Macrocycles with Dioxygen

Several conflicting and ill defined reports of the interaction of dioxygen with Ni(I) macrocycles have been described in the literature[39,111,158,159,160].

Balac and Espenson[39] in the preparation of $[Ni(TMC)]^+$ in aqueous solution electroreduced the Ni(II) precursor to only *ca.* 50% completion to avoid contamination with O_2. A reaction of O_2 with $[Ni(TMC)]^+$ forming unidentified yellow products believed to be oxo- or peroxo nickel species was observed if electrolysis was prolonged.

Hayon *et al.*[158] monitored the rapid reaction ($K_{obs}=1.6\times10^{9}M^{-1}s^{-1}$) of $[Ni(HMC)]^{+}$, generated by pulse radiolysis in neutral aqueous solution, with dioxygen. Results indicated that the reaction proceeded via an outer sphere electron transfer path generating O_2^- [41]

$$[Ni(I)(HMC)]^{+} + O_2 \rightarrow [Ni(II)(HMC)]^{2+} + O_2^- \qquad [41]$$

Any reaction of O_2^- with Ni(II) was not competitive and had a rate constant of $<10^{6}M^{-1}s^{-1}$. From pulse radiolysis experiments Meyerstein produced results in agreement with the above findings. No Ni(III) complexes were detected for the final products of the reaction[111].

In contrast Pletcher[160] proposed that the reaction of Ni(I) Schiff base complexes eg. $[Ni(42)]^{+}$ with dioxygen in acetonitrile is not a simple electron transfer reaction. In the presence of low concentrations of dioxygen the reduced species reacted very rapidly as indicated by distinctive colour changes. Cyclic voltammetric experiments showed that the precursor Ni(II) complexes were only reformed in low yield. Using polarography and spectrophotometry Olson and Vasilevskis[159] characterized a green to blue colour change with the unusual stoichiometry, [43].

$$[Ni(HMC)]^{+} + {}^{1}/_{3}O_2 \rightarrow \text{products} \qquad [43]$$

A pale purple species isolated gave analysis figures consistent with a 1:1 nickel-dioxygen complex, $[Ni(HMC)(O_2)]BF_4$.

In comparison with the rapid and often uncontrolled

reactions mentioned above, the effective stabilization of Ni(I) macrocyclic species by careful selection of macrocyclic ligand has been achieved by the Meyerstein and Sauvage groups[110,111,161]. Using a decamethyl substituted cyclam derivative, (38), Meyerstein stabilized Ni(I) in an oxygen free aqueous solution. The combined steric bulk of the ten hydrophobic methyl groups effects stabilization of the low oxidation state. Using two interlocking coordinating rings, each cycle containing the 2,9-diphenyl-1,10-phenanthroline fragment, (44), Sauvage[161], prepared an air stable Ni(I) complex, $[Ni(44)_2]^+$. Its unique redox stability of $E_{\frac{1}{2}}$ = -0.55V vs ferrocene/ferrocinium for the Ni(II)/(I) redox couple in CH_2Cl_2, is ascribed to the topological effect of the tetrahedral geometry around Ni(I) interlinked by the catenand macrocycle.

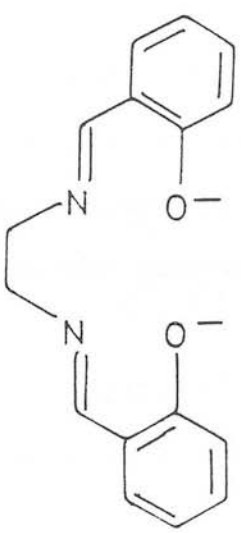

(42)

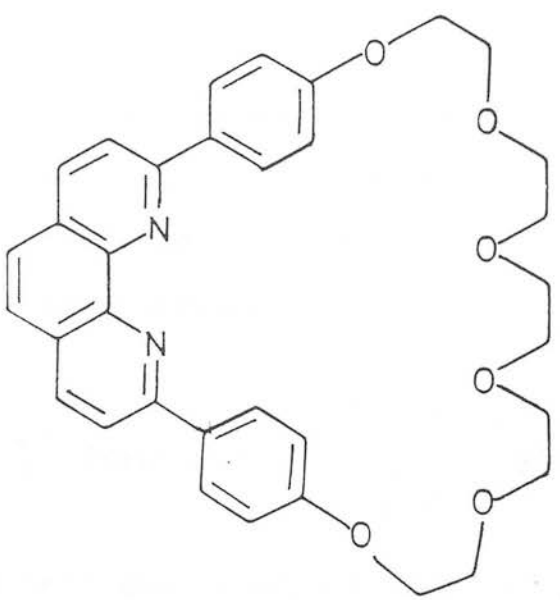

(44)

In the light of the extensive variation in experimental results observed, a reinvestigation into the reaction of Ni(I) with dioxygen was instigated. An extension of this to include the potentially isoelectronic reactions of superoxide with Ni(II) macrocycles was also undertaken. As many of the proposed intermediates are paramagnetic, e.s.r. spectroscopy was extensively used in their characterization.

6.1.3 The Reaction of Ni(II) Macrocycles with Superoxide

Simic and Hoffman[162] were able to prove from a pulse radiolytic study that the initial product formed by the reaction of superoxide with the d^7, Co(II) tetraaza macrocycle $[Co(11)]^{2+}$ was the same product as from the isoelectronic reaction of d^8, $[Co(11)]^{+}$ with dioxygen [45].

$$\left.\begin{array}{l}[Co(I)(11)]^{+} + O_2 \\ [Co(II)(11)]^{2+} + O_2^{-}\end{array}\right\rangle \longrightarrow [Co(11)(O_2)]^{+} \qquad [45]$$

With similar rationale, it was proposed to study the potentially isoelectronic reactions of d^8, Ni(II) with superoxide and d^9, Ni(I) with dioxygen in order to investigate the proposed nickel-dioxygen species [46].

$$\left.\begin{array}{l}[Ni(I)L]^{+} + O_2 \\ [Ni(II)L]^{2+} + O_2^{-}\end{array}\right\rangle \longrightarrow [NiL(O_2)]^{+} \qquad [46]$$

Several other studies into the reactions of superoxide with transition metal macrocycles and porphyrins have been reported[163-167].

Ozawa and Hanaki found that in dmso [Ni(TPP)] and [Pd(TPP)] did not produce adducts with superoxide[164]. Using the nickel(II) Schiff base complexes [Ni(42)] and $[Ni(47)]^{2+}$ Jager[165,166] and Cros[167] have monitored their reaction with superoxide.

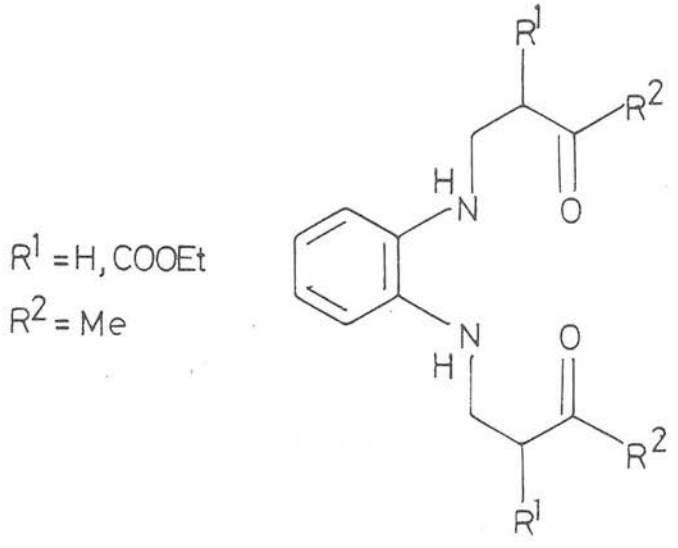

(47)

Addition of [Ni(42)] to O_2^- in acetonitrile at 240K slightly alters the e.s.r. g tensors of superoxide. The shifted g values, g_{11}=2.101, $g_{\perp}$=2.009 are due to the proposed formation of a Ni(II) superoxo complex $[Ni(42)(O_2)]^-$. A similar e.s.r. spectrum was obtained on allowing a trace amount of dioxygen into a sample of $[Ni(I)(42)]^-$, a ligand to metal electron transfer is proposed forming $[Ni(II)(42)-(O_2)]^-$. [167]

6.1.4 Characterization of Paramagnetic Nickel Species using E.s.r. Spectroscopy

E.s.r. spectroscopy can establish whether an unpaired

electron in a transition metal complex belongs primarily to the metal or to the ligand. In certain cases further information such as the electronic ground state, complex geometry and mode of coordination of ligand substrates can be inferred. E.s.r. has proven to be a particularly useful probe for the relatively long lived d^7, Ni(III) and d^9, Ni(I) radical species[18,168,169].

For low spin d^7, Ni(III) with neutral, saturated quadridentate macrocyclic ligands, spectra can be interpreted using the assumption of a tetragonal distorted octahedral coordination around Ni(III) (D_{4h} symmetry). With the macrocycle occupying four equatorial positions and two solvent molecules in axial sites the ground state configuration is usually $(d_{z^2})^1(d_{x^2-y^2})^0$. According to Maki *et al.*[170] the g factors are given by [48].

$$g_{\perp} = 2 - \left(6\lambda/\Delta\right)$$
$$g_{\parallel} = 2 \qquad [48]$$

Where λ = the spin orbit coupling constant (-715 cm^{-1} for the free ion) and Δ = energy gap between d_{z^2}-d_{yz} (or d_{z^2}-d_{xz}).

Since λ is negative $g_{\perp} > g_{\parallel}$. Many paramagnetic d^9, Ni(I) species have $g_{\parallel} > g_{\perp}$ suggesting an axial field with a $(d_{x^2-y^2})^1$ ground state.

Caution must however be employed in the interpretation of spectra on several accounts. Ni(I) species can be diamagnetic due to the presence of a Ni-Ni bond in a dimeric

structure[124,129]. Several examples of Ni(III) spectra with $g_{\perp} < g_{\parallel}$ are known. Neutral polydentate macrocyclic ligands with very large, 18-, or small, 12- membered polyaza rings, eg. (49) and (24), give $g_{\perp} < g_{\parallel}$ due to a respective tetragonal compression or folding of the macrocycle[127]. Dianionic macrocycles with π electrons delocalized over the ligand framework such as the Jager macrocycles (50) also give $g_{\perp} < g_{\parallel}$ [18].

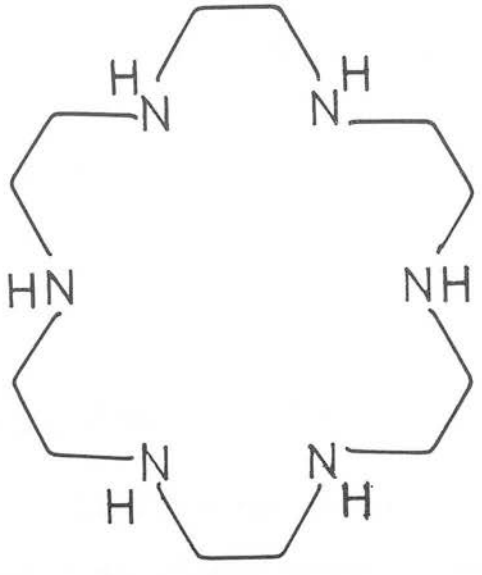

(49)

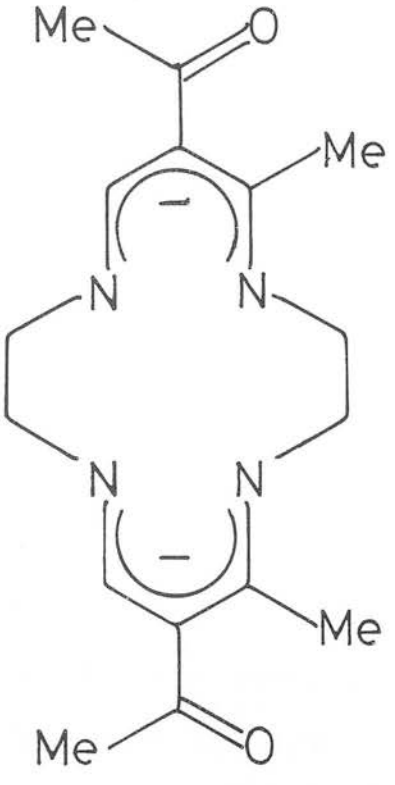

(50)

Results and Discussion

6.2 Reactions Using C-*rac*-$[Ni(HMC)]^{2+/+}$

6.2.1 Electrochemistry

(i) Cyclic voltammetry

The cyclic voltammogram of C-*rac*-$[Ni(HMC)]^{2+}$ in acetonitrile shows two quasi reversible one electron redox processes. A quasi reversible one electron oxidation at Epa = +1.14V, Epc = +0.98V, $^{1}E_{\frac{1}{2}}$ = +1.06V, ΔEp = 160mV and a quasi reversible one electron reduction Epc = -1.63V Epa = -1.49V, $^{1}E_{\frac{1}{2}}$ = -1.56V, ΔEp = 140mV were recorded. The large peak to peak separations have been noted and discussed previously[18,171].

(ii) Electrosynthesis

Electrogeneration of C-*rac*-$[Ni(HMC)]^{2+}$ at a platinum gauze at -1.60V under a constant stream of argon gives a pale green solution of $[Ni(HMC)]^{+}$. The Ni(I) species generated at this extreme cathodic reduction potential is very reactive. On all occasions contamination by small

amounts of extraneous dioxygen containing species was observed in the e.s.r. spectrum.

Electrogeneration of C-*rac*-$[Ni(HMC)]^{2+}$ at a platinum gauze at +1.50V gives the stable Ni(III) species, C-*rac*-$[Ni(HMC)(MeCN)_2]^{3+}$, first fully characterized by Busch and coworkers[18]. The yellow/green solution (λ_{max} = 401, 340nm) as an acetonitrile glass at 77K gives an axially symmetric e.s.r. signal $g_{\perp}$=2.199, $g_{\parallel}$=2.031, with coupling to two equivalent nitrogen atoms from axially coordinated acetonitrile solvent molecules to give a 1:2:3:2:1 intensity quintet, A_{1I}=20G (Figure 6.2.I).

6.2.2 The Reaction of C-*rac*-$[Ni(HMC)]^{+}$ with Dioxygen

Reaction of dioxygen with C-*rac*-$[Ni(HMC)]^{+}$ at 230K produces a pale green solution. Although thermally unstable at temperatures above 230K, this reactive species was consistently formed in repeated reactions. The e.s.r. spectrum of the green solution shows an anisotropic signal, $g_{\perp}$=2.19, $g_{\parallel}$=2.05 (Figure 6.2.II) suggestive of a Ni(III) complex (*cf.* $[Ni(HMC)(MeCN)_2]^{3+}$ $g_{\perp}$=2.199 $g_{\parallel}$=2.031, $A_{\parallel}$=20G). No hyperfine structure is observed from either the first or second derivative e.s.r. spectrum in the $g_{\parallel}$ region of Figure 6.2.II, suggesting no coordination of solvent acetonitrile molecules. The e.s.r. spectrum may be tentatively assigned to the formation of a Ni(III) species in which O_2 is bound to two vacant sites of the nickel centre with a proposed η_2 coordination. A two electron metal to ligand electron transfer reaction is proposed to occur to give a formal Ni(III)-peroxo species, [50].

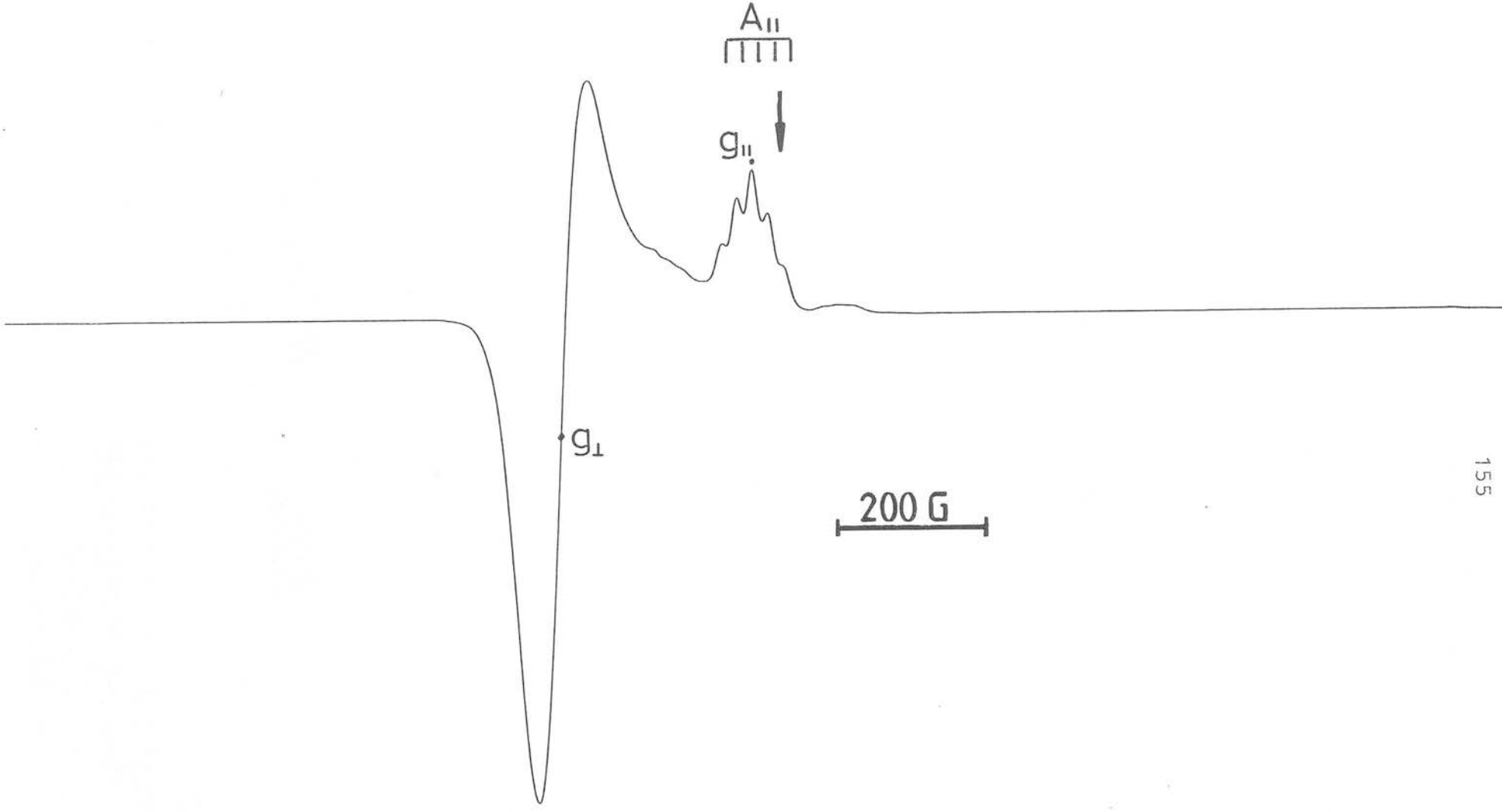

Figure 6.2.I E.s.r. spectrum of C-*rac*-$[Ni(HMC)((MeCN)_2]^{3+}$ generated electrochemically, measured at 77K in CH_3CN/0.1M $TBAPF_6$

Figure 6.2.II E.s.r. spectrum of the product of the reaction of C-*rac*-[Ni(HMC)]$^{+}$ with O_2, measured at 77K in CH_3CN/0.1M $TBAPF_6$

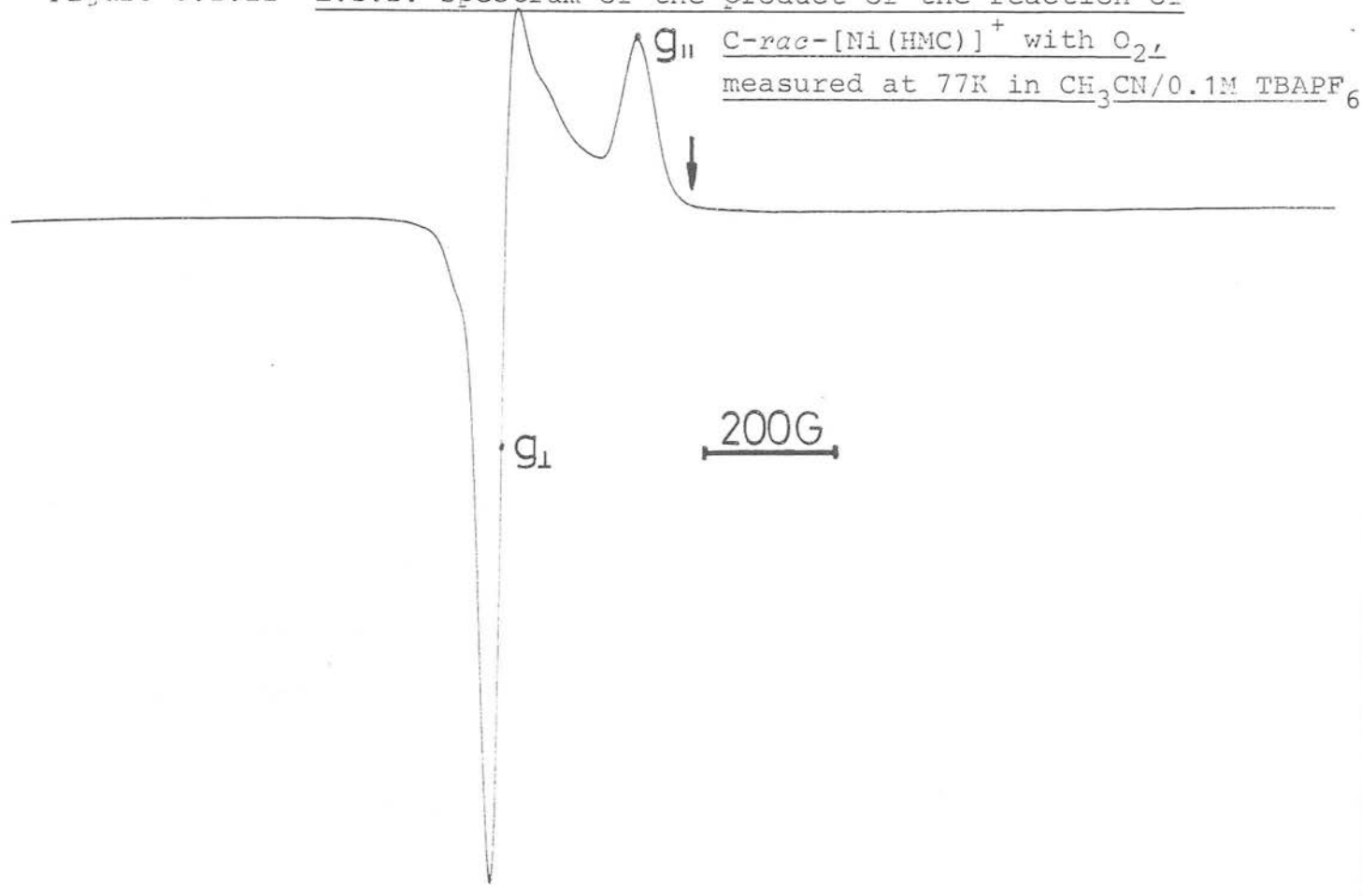

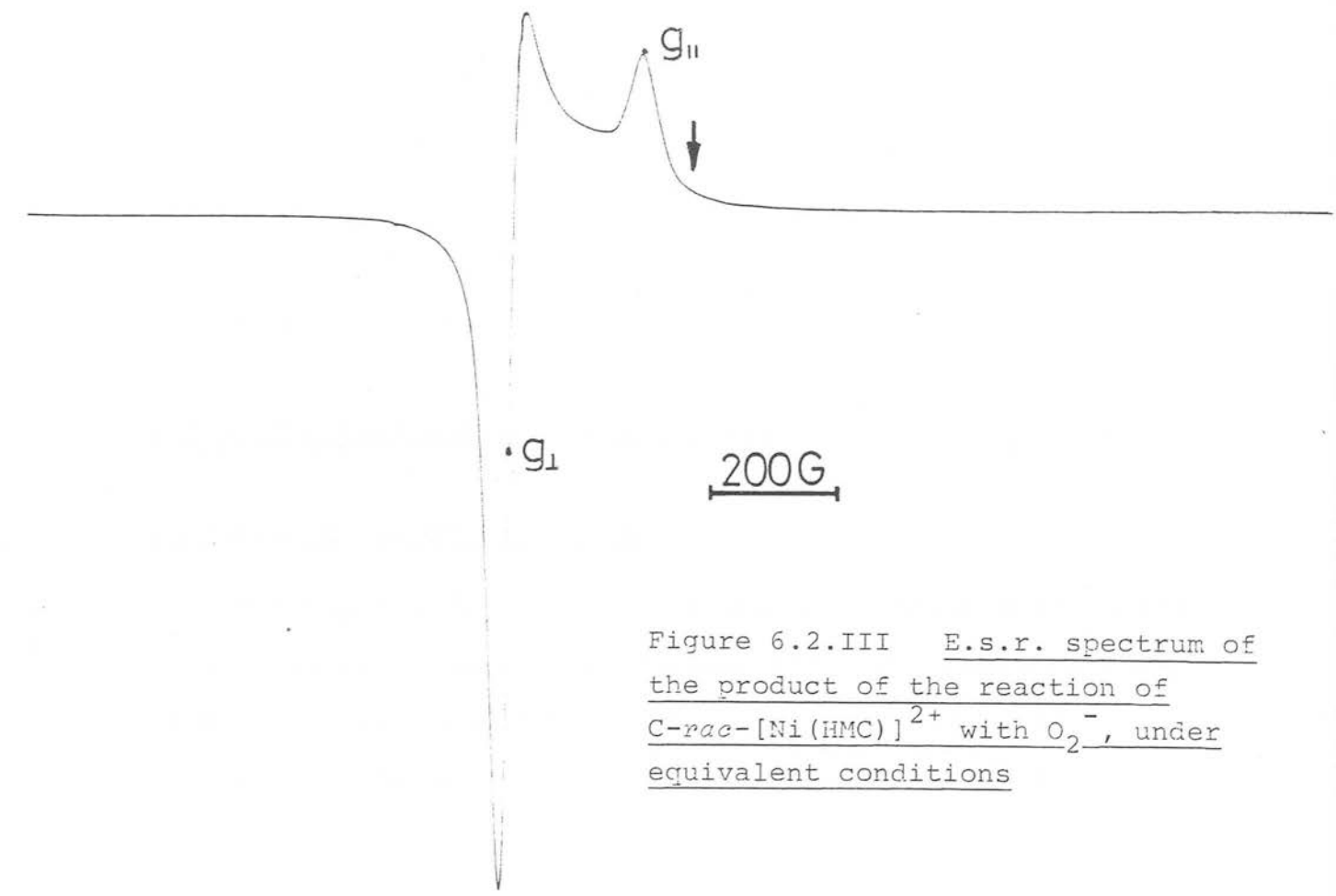

Figure 6.2.III E.s.r. spectrum of the product of the reaction of C-*rac*-[Ni(HMC)]$^{2+}$ with O_2^{-}, under equivalent conditions

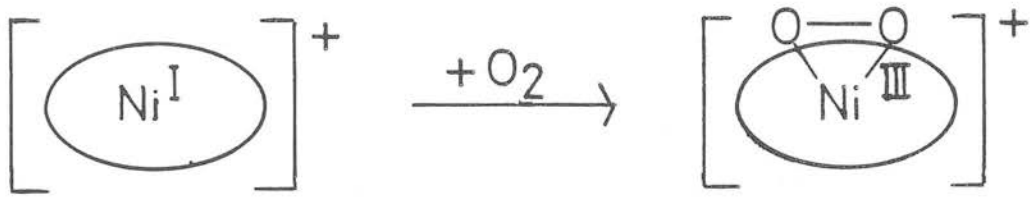

[50]

Further characterization of this product is hampered by its reactive nature and therefore reactions of superoxide with nickel macrocycles were investigated in a parallel study (Section 6.2.3).

The two electron Ni(I)/(III) redox couple proposed for the reaction of dioxygen with Ni(I) has also been suggested to be involved in the addition of alkyl bromides with Ni(I) tetraaza macrocycles[36,160] [51].

$$[Ni(I)L]^{+} + RBr \rightarrow [RNi(III)L(Br)]^{+} \qquad [51]$$

The ability of nickel to function as a multi electron redox centre has been demonstrated in the nickel enzyme hydrogenase isolated from *Chromatium vinosum*. E.s.r. studies have implicated the III, II, I and possibly zero-valent oxidation states in its mechanism[157].

6.2.3 The Reaction of C-*rac*-$[Ni(HMC)]^{2+}$ with Superoxide

(i) Generation of Superoxide

The superoxide ion, O_2^-, is readily generated at -1.60V at a platinum gauze by electrogeneration of a constant stream of dioxygen in acetonitrile containing 0.1M $TBAPF_6$ as supporting base electrolyte. The species is stable for

several hours in aprotic solvents at room temperature[164] and can be characterized by UV/vis spectrophotometry, λ_{max} = 251nm, and e.s.r. spectrometry, g_{11}=2.107 $g_{\perp}$=2.006 in acetonitrile/0.1M $TBAPF_6$ solution at 77K.

(ii) Reaction of C-*rac*-$[Ni(HMC)]^{2+}$ with Superoxide

On mixing degassed acetonitrile solutions of C-*rac*-$[Ni(HMC)]^{2+}$ with O_2^- at 230K results in an almost immediate formation of a pale green solution which is stable at 273K for several minutes. The e.s.r. spectrum shows the total loss of the initial characteristic superoxide spectrum and the formation of a new anisotropic signal, $g_{\perp}$=2.194, g_{11}=2.056, with no discernible hyperfine coupling to either the g_{11} or $g_{\perp}$ features (Figure 6.2.III). Comparison with Figure 6.2.II, the reaction of $[Ni(HMC)]^+$ with dioxygen shows the two spectra to be essentially identical.

$$\begin{array}{l} [Ni(I)(HMC)]^+ + O_2 \\ \qquad\qquad\qquad\qquad \searrow \\ \qquad\qquad\qquad\qquad\quad [Ni(HMC)O_2]^+ \\ [Ni(II)(HMC)]^{2+} + O_2^- \nearrow \end{array} \qquad [52]$$

pale green

$g_{\perp}$=2.19 g_{11}=2.056

The fact that other investigators have found only small shifts in superoxide e.s.r. g tensors on reaction with nickel(II) complexes to form proposed nickel(II)-superoxo species[165-167] suggest that the pale green solution, [52], is not due to an analogous species. An inner sphere electron transfer reaction is therefore proposed to form a formal nickel(III)-peroxo species.

Figure 6.2.III E.s.r. spectrum of the product of the reaction of C-*rac*-$[Ni(HMC)]^{2+}$ with O_2^-, measured at 77K in CH_3CN/0.1M $TBAPF_6$

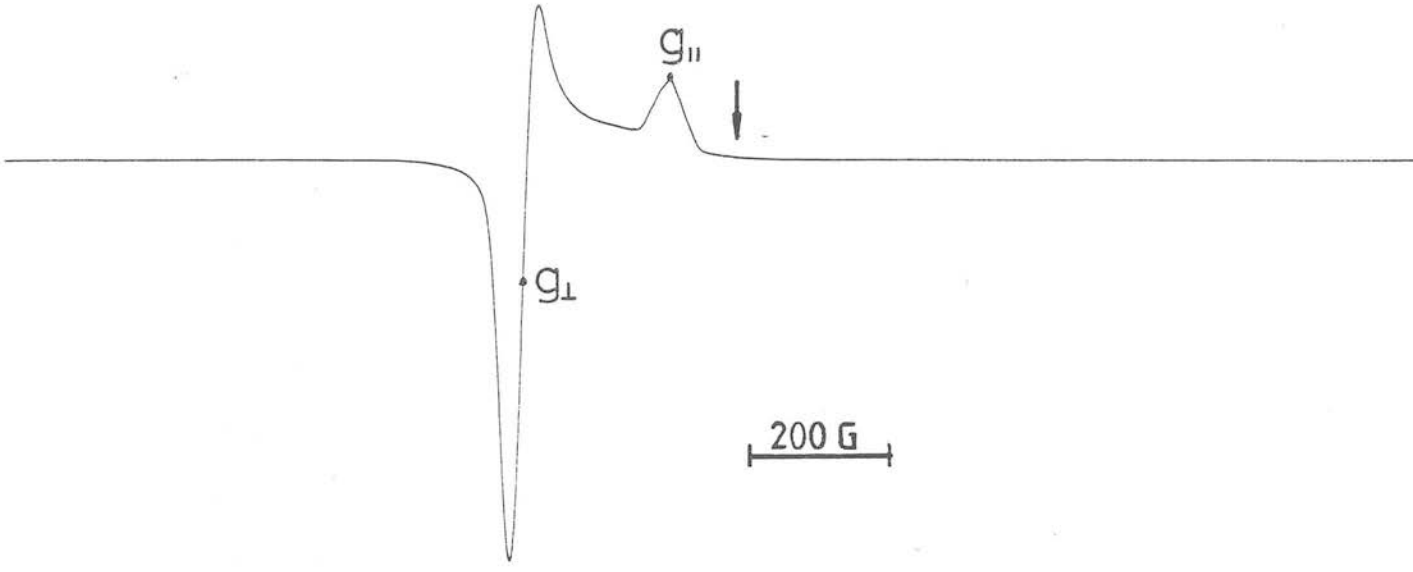

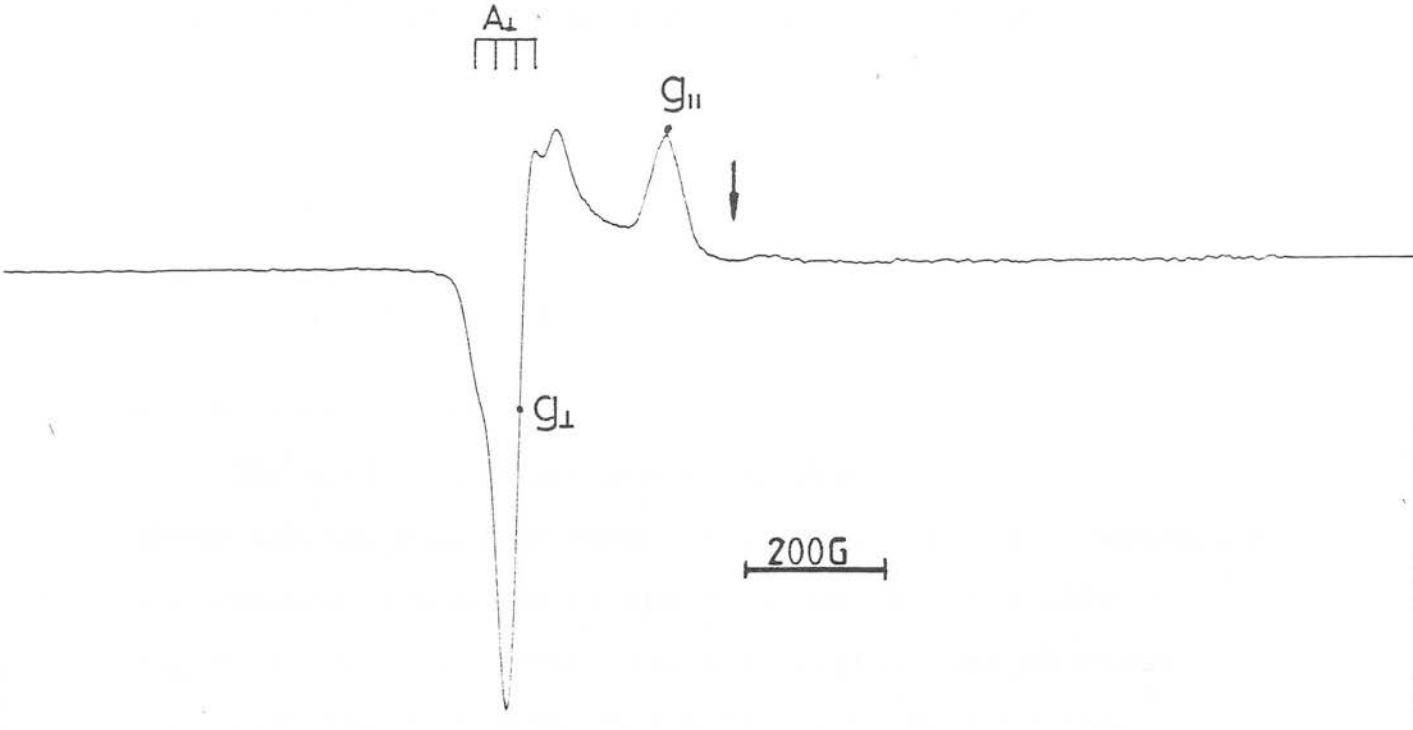

Figure 6.3.IV E.s.r. spectrum of the product of the reaction of C-*rac*-$[^{61}Ni(HMC)]^{2+}$ with O_2^-, under equivalent conditions

For further confirmation of the proposed predominantly metal centred radical species, the reaction of a sample isotoptically enriched to 62% with ^{61}Ni was studied. Reaction of C-*rac*-$[^{61}Ni(HMC)]^{2+}$ with O_2^- gave an e.s.r. spectrum with identical g tensors to that obtained with the unenriched sample.

Additional coupling due to ^{61}Ni, $I=^3/_2$ was observed in the $g_\perp$ region. The first and fourth features are discernible giving $A_\perp$=37G (Figure 6.2.IV). Although a general broadening of the g_{11} signal is noted, no clear hyperfine coupling is observed. A similar result was obtained for $[^{61}Ni(4)_2]^{3+}$ where $A_\perp$=37G and the A_{11} feature remained unresolved[172]. Broadening of the $g_\perp$ and g_{11} features has been also observed by McAuley and coworkers[173] for $[^{61}Ni(7)_2]^{3+}$; neither resolution of A_{11} or $A_\perp$ was possible.

6.3 Reactions Using $[Ni(TMC)]^{2+/+}$

6.3.1 Electrochemistry

(i) Cyclic voltammetry

The cyclic voltammogram of $[Ni(TMC)]^{2+}$ in acetonitrile shows two one electron redox processes. A quasi reversible one electron oxidation at Epa = +1.38V, Epc = +1.28V, $^1E_{\frac{1}{2}}$ = +1.33V ΔEp = 106mV and a reversible one electron reduction Epc = -1.205V, Epa = -1.135V $^1E_{\frac{1}{2}}$ = -1.17V, ΔEp = 70mV were recorded in agreement with previous studies[19, 36]. Separation of the two redox potentials by 2.50V is similar to that of other neutral tetraaza macrocyclic nickel complexes.

(ii) Electrosynthesis

Electrogeneration of $[Ni(TMC)]^{2+}$ at a platinum gauze at -1.20V under a constant stream of argon gas gives a pale green solution, the e.s.r. spectrum at 77K as an acetonitrile glass shows an anisotropic signal due to a d^9, Ni(I) species, g_{11}=2.319, $g_{\perp}$=2.074 (Figure 6.3.I). A repeated electrogeneration using an enriched sample of ^{61}Ni gives equivalent g tensors to the unenriched sample with additional hyperfine coupling due to $^{61}Ni(I=^3/_2)$, A_{11}=62G, $A_{\perp}$=27G (Figure 6.3.II), confirming the predominantly metal centred nature of the reduction.

Attempts to bulk electrogenerate significant amounts of the $[Ni(TMC)]^{3+}$ species were unsuccessful. A highly reactive orange coloured solution was formed at a platinum gauze at +1.50V which decomposed to diamagnetic products. With a rapid syringing technique an e.s.r. spectrum of a dilute sample was obtained. A complex anisotropic signal was detected at high sensitivity. Clearly evident in the g_{11} region was a 1:1:1 intensity triplet, A_{11}=18G, indicative of one nitrogen, (I=1), of a coordinated solvent acetonitrile molecule bound in a five coordinate complex. The failure to stabilize the Ni(III) oxidation state by several related N-alkyl substituted tetraaza macrocycles has also been noted by other workers[19].

6.3.2 The Reaction of $[Ni(TMC)]^+$ with Dioxygen

On addition of dioxygen to an evacuated e.s.r. tube of $[Ni(TMC)]^+$ at 230K gives no noticeable solution colour change.

Figure 6.3.I E.s.r. spectrum of $[Ni(TMC)]^+$ generated electrochemically measured at 77K in CH_3CN/0.1M $TBAPF_6$

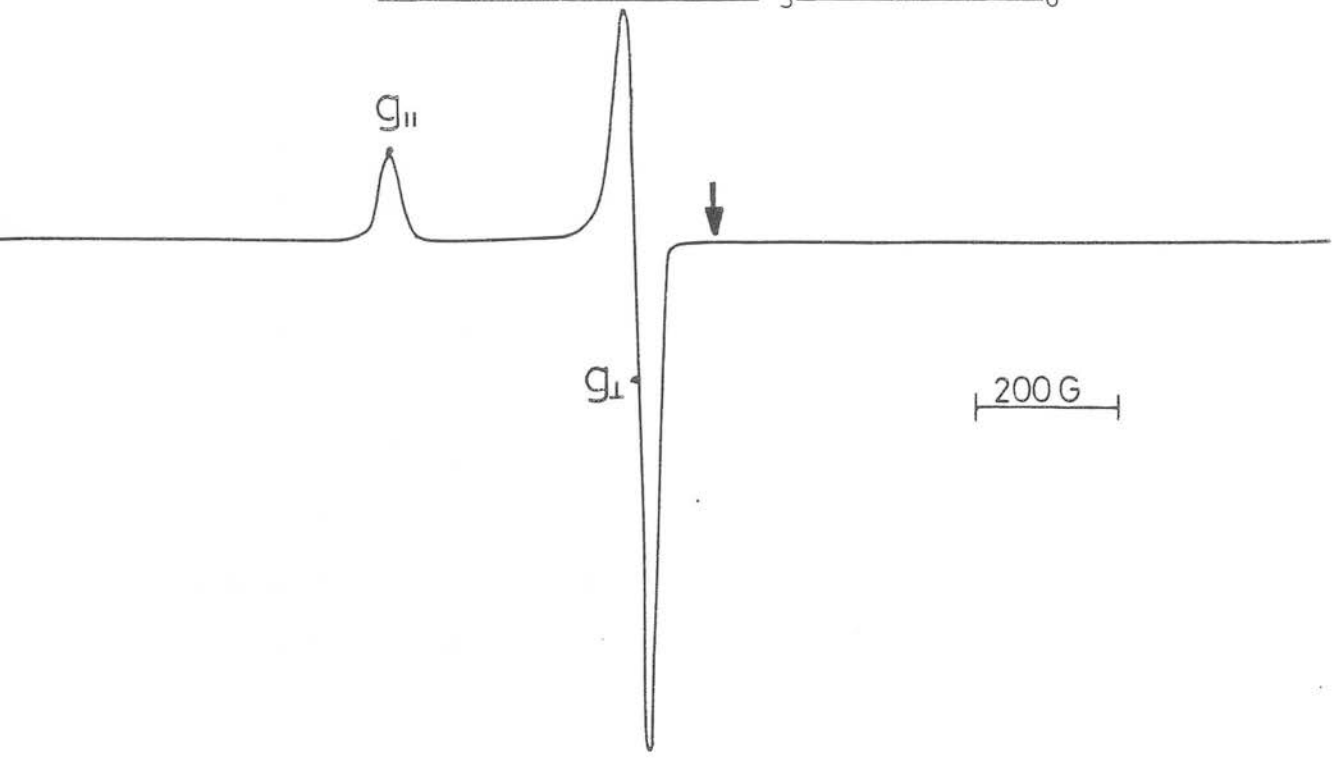

Figure 6.3.II E.s.r. spectrum of 62% enriched $[^{61}Ni(TMC)]^+$ under equivalent conditions

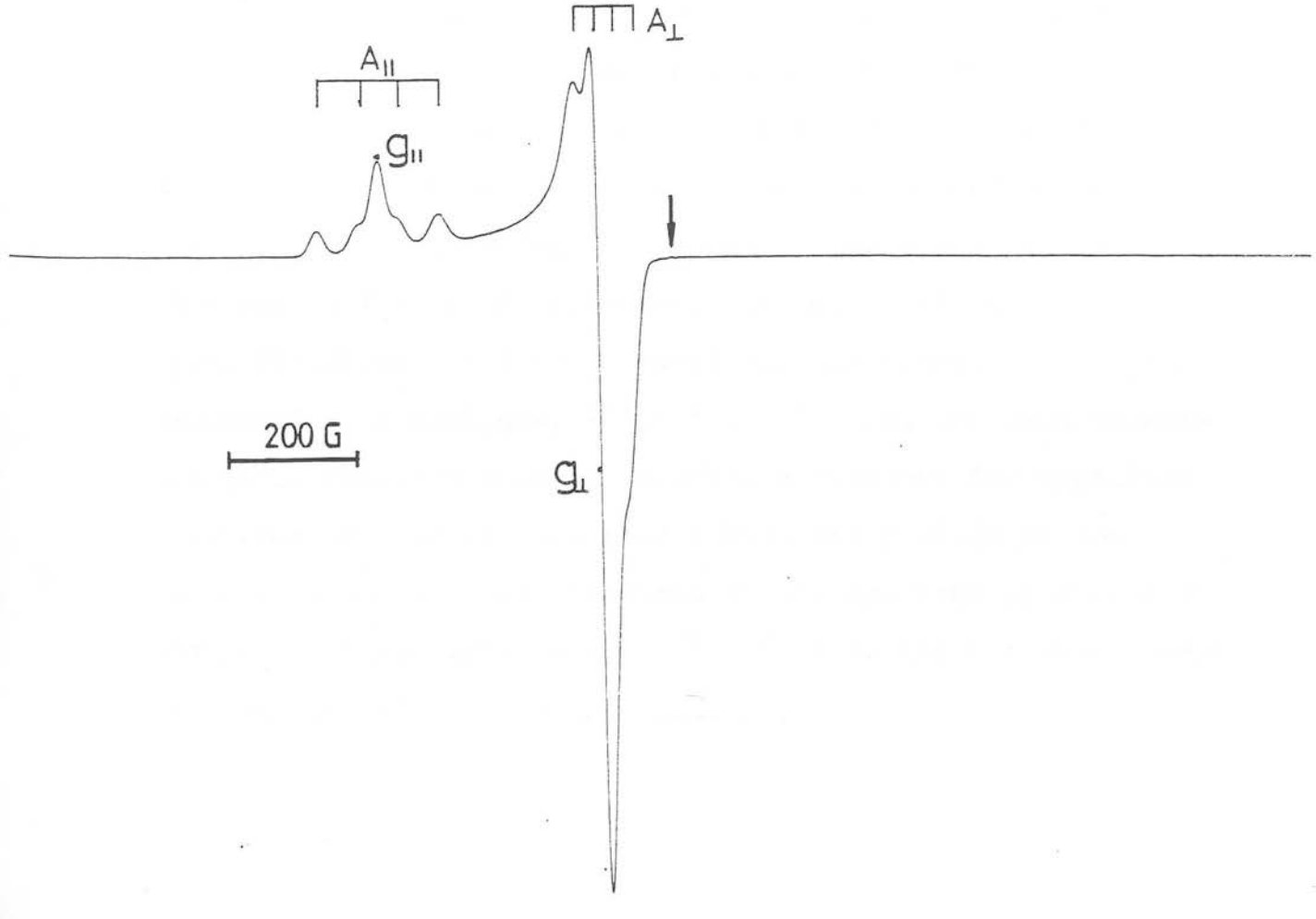

The characteristic d^9 axial symmetric spectra of $[Ni(TMC)]^+$ changes to a spectrum of rhombic symmetry, g_1=2.294, g_2=2.214, g_3=2.095 (Figure 6.3.III). These three features are consistently obtained on repeating the reaction. An unassigned further feature at g=2.04 is apparent in several spectra. It appears to be at a maximum intensity on initial mixing, diminishing over a period of time at 230K. Repeating the reaction with $[^{61}Ni(TMC)]^+$ gives an e.s.r. spectrum with equivalent g tensors although all features are slightly broadened. Indications of hyperfine coupling of ^{61}Ni are apparent around the g_1=2.29 region (A_1=33G), of similar magnitude to the $[^{61}Ni(HMC)O_2]^+$ labelling experiment (Figure 6.3. V).

6.3.3 The Reaction of $[Ni(TMG)]^{2+}$ with Superoxide

Addition of $[Ni(TMC)]^{2+}$ to a degassed acetonitrile solution of superoxide ion at 230K results in an immediate green solution colour on mixing, stable for several minutes at 230K in a similar manner to that found for C-*rac*-$[Ni(HMC)]^{2+}$. The e.s.r. spectrum of the green solution showed a non axially symmetric species with equivalent g tensors observed for the $[Ni(TMC)]^+ + O_2$ reaction, with g_1=2.288, g_2=2.209, g_3=2.091 (Figure 6.3.IV). Repeating the reaction using the enriched ^{61}Ni analogue, $[^{61}Ni(TMC)]^{2+}$, gave the same tensors to those obtained above. Tentative evidence for hyperfine coupling of ^{61}Ni was observed around the g_1=2.29 region (Figure 6.3.VI). All features of the spectrum broadened in common with previous results[172,173] hindering the measurement of ^{61}Ni hyperfine coupling constants.

Figure 6.3.III E.s.r. spectrum of the product of the reaction of $[Ni(TMC)]^{+}$ with O_2, measured at 77K in CH_3CN/0.1M $TBAPF_6$

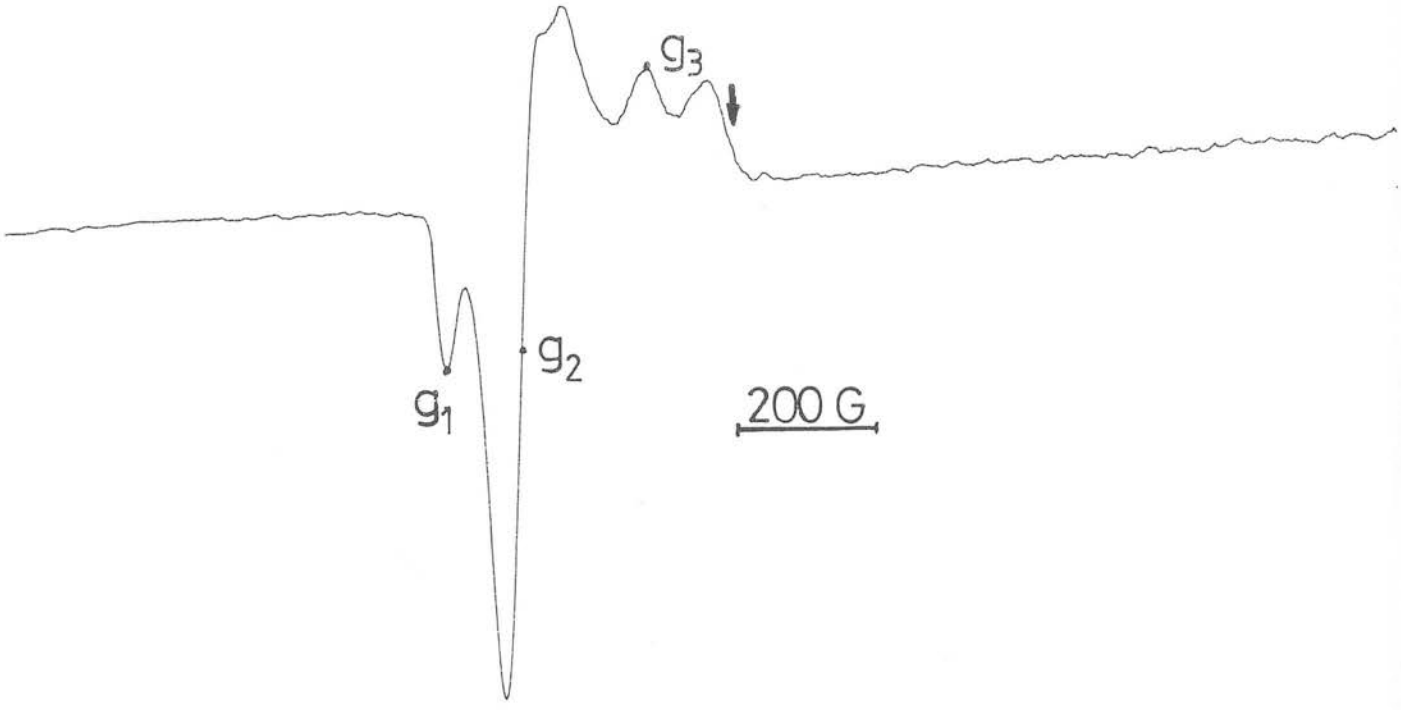

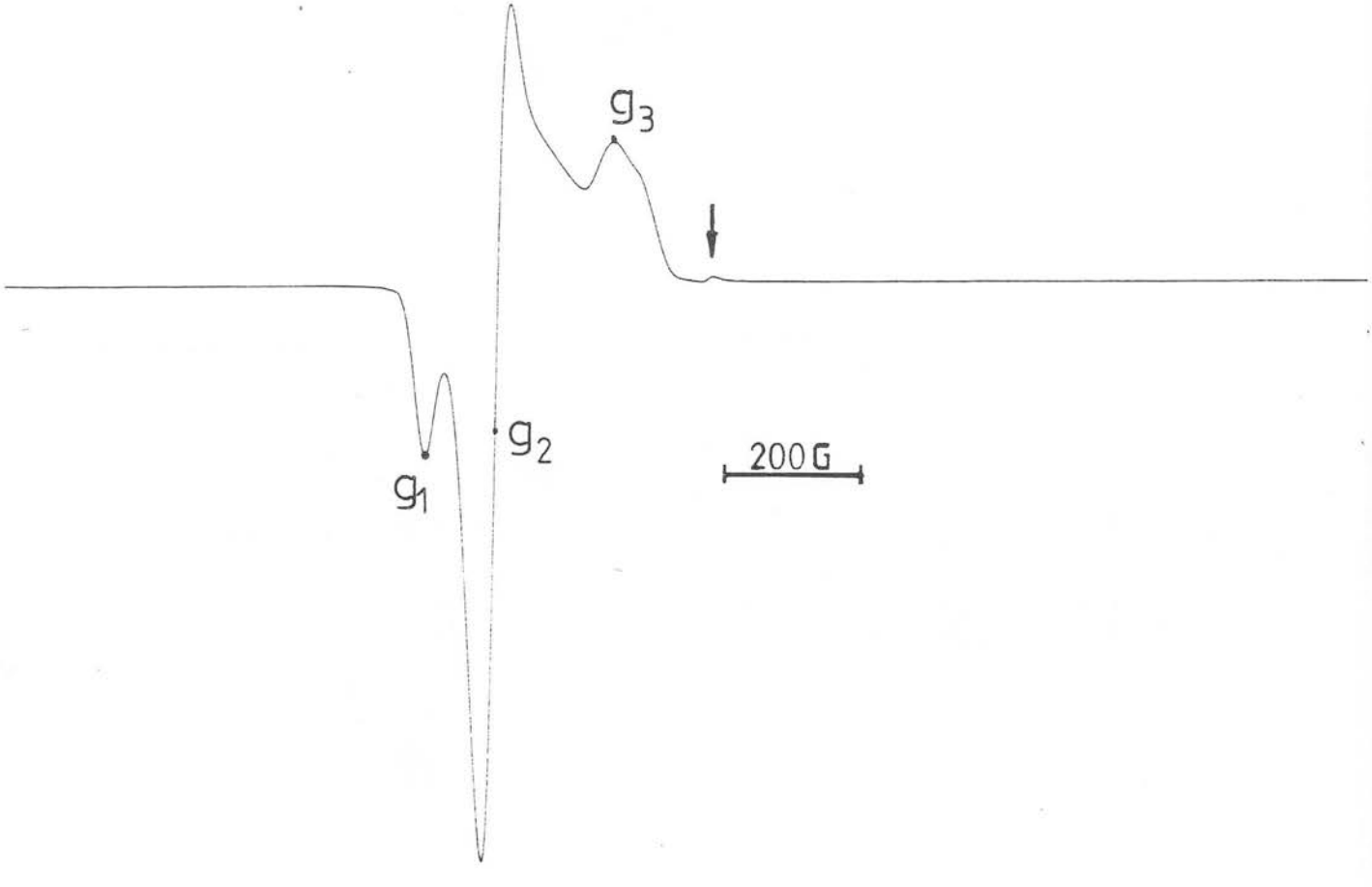

Figure 6.3.IV E.s.r. spectrum of the product of the reaction of $[Ni(TMC)]^{2+}$ with O_2^-, under equivalent conditions

Figure 6.3.V E.s.r. spectrum of the product of the reaction of $[^{61}Ni(TMC)]^{+}$ with O_2, measured at 77K in CH_3CN/0.1M $TBAPF_6$

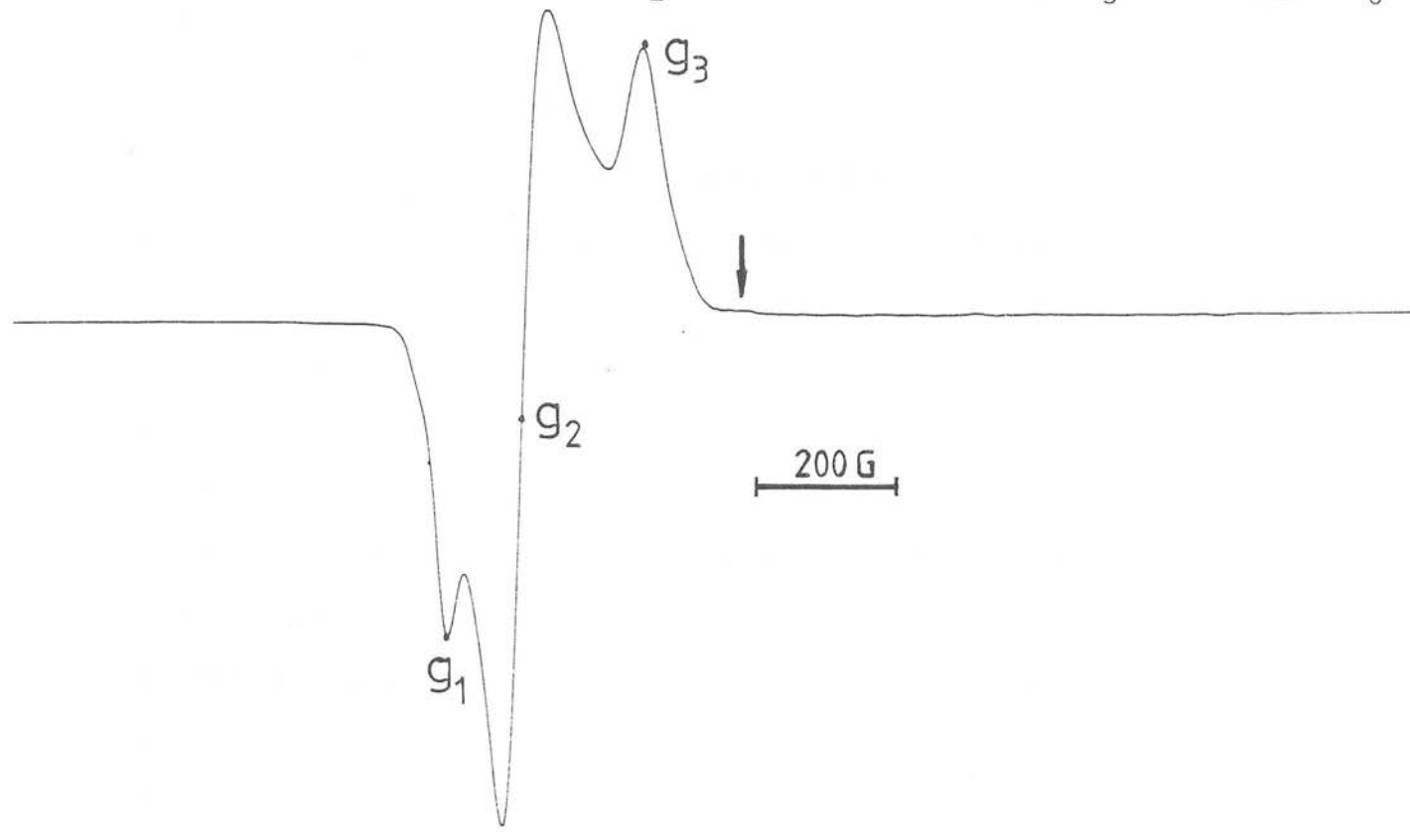

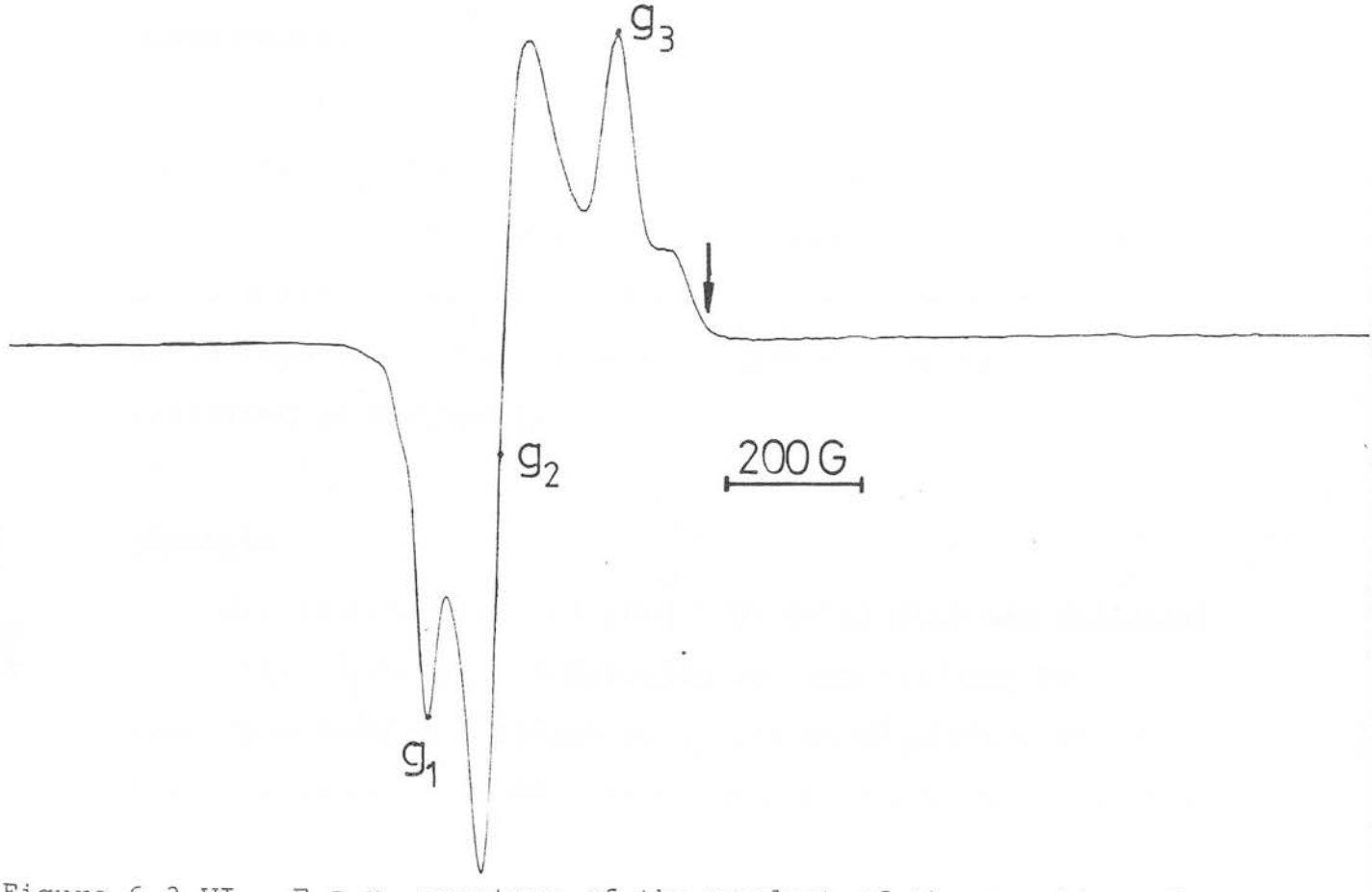

Figure 6.3.VI E.s.r. spectrum of the product of the reaction of $[^{61}Ni(TMC)]^{2+}$ with O_2^-, under equivalent conditions

6.4 Conclusion

Tentative assignments for the formal Ni(III)-peroxo species $[NiL(O_2)]^+$, L = C-*rac*-HMC or TMC are proposed from experiments using the two isoelectronic reactions, [52], and ^{61}Ni isotropic labelling experiments. Of note is the apparent ability of $[Ni(TMC)]^{2+/+}$ to form a formal Ni(III) species on reaction with dioxygen or superoxide, while the attempted bulk electrogeneration of "$[Ni(TMC)]^{3+}$" leads to a reactive, unstable orange coloured species in acetonitrile. Due to the very reactive nature of the precursor Ni(I) complexes and also the nickel-dioxygen products, difficulties are encountered in further characterization of the species formed. To aid in the establishment of a nickel dioxygen interaction it is proposed to use labelled $^{17}O_2$ and $^{17}O_2^-$ ($I = {}^5/_2$) in combination with ^{61}Ni in further e.s.r. experiments.

6.5 Experimental

Microanalyses, infrared and n.m.r. spectra were obtained as described in earlier chapters. Cyclic voltammetric and electrosynthetic studies were carried out using apparatus described in Chapter 4.

Reagents

62% isotopically enriched ^{61}Ni metal foil was obtained from AERE, Harwell. Superoxide ion was produced by electrogenerating a stream of O_2 gas in CH_3CN/0.1M $TBAPF_6$ for 10 minutes at -1.60V, degassed and stored in e.s.r. tubes

frozen at 77K. The species is characterized by its e.s.r. signal at 77K (g_{11}=2.107, $g_{\perp}$=2.006).

The free ligands C-*rac*- and C-*meso*-5,5,7,12,12,14-hexamethyl-1,4,8,11-tetraazacyclotetradecane (C-*rac*- and C-*meso*-HMC) and the nickel complexes. C-*rac*- and C-*meso*-$[Ni(HMC)](BF_4)_2$ were prepared by the method of Busch and Tait[126].

$^{61}Ni(NO_3)_2.6H_2O$

^{61}Ni foil (80 mg, 1.31 mmol) was dissolved in 70% w/w nitric acid (5 cm^3). After *ca.*15 minutes all the metal was in solution. After gently boiling off most of the solution the product was allowed to slowly crystallize out. The green solid was washed with ethyl acetate and dried *in vacuo*. Yield 362 mg (*ca.*95%).

$[^{61}Ni(TMC)](PF_6)_2$

$^{61}Ni(NO_3).6H_2O$ (100 mg, 0.34 mmol) and TMC (86 mg, 0.34 mmol) were refluxed for 9 hours in ethanol (100 cm^3). Addition of NH_4PF_6 gave a pale pink precipitate that was recrystallized from methanol to give a pale purple microcrystalline solid. Yield 190 mg, 0.31 mmol,(92%).

Analysis: Required for $NiC_{14}H_{32}N_4P_2F_{12}$

C 27.8 H 5.3 N 9.3%

Found C 28.3 H 5.3 N 9.6%

$^{61}Ni(O_2CMe)_2.4H_2O$

$^{61}Ni(NO_3)_2.6H_2O$ (100 mg, 0.34 mmol) was dissolved in

H_2O (5 cm^3). An aqueous solution of Na_2CO_3 was added until precipitation was complete. The resulting solid was filtered and air dried. Dilute acetic acid (3 cm^3) was added and the solution was boiled for 30 minutes. On cooling the product was allowed to slowly crystallize out. The pale green solid was washed with cold ethanol and dried *in vacuo*. Yield 50 mg, 0.2 mmol , (58%).

C-*rac*-$[^{61}Ni(HMC)](BF_4)_2$

$^{61}Ni(O_2CMe)_2.4H_2O$ (50 mg, 0.2 mmol) and C-*rac*-HMC.H_2O (61 mg, 0.2 mmol) were dissolved in methanol (20 cm^3) and refluxed for 13 hours to give a blue solution. Addition of $NaBF_4$ and 40% HBF_4 (2 ml) gave an intense yellow solution from which a yellow solid was isolated on standing. The product was recrystallized from water. Yield 25 mg, 0.05 mmol , (25%).

References

1. D.K. Cabbiness and D.W. Margerum, J.Amer.Chem.Soc., 91, 6540 (1969).
2. L. Fabbizzi, P. Paoletti and A.B.P. Lever, Inorg.Chem., 15, 1502 (1976).
3. M. Kodama and E. Kimura, J.Chem.Soc.,Dalton Trans., 116 (1976).
4. F. Hinz and D.W. Margerum, Inorg.Chem., 13, 2941 (1974).
5. A. Dei and R. Gori, Inorg.Chim.Acta, 14, 157 (1975).
6. L. Fabbizzi, P. Paoletti, A. Anichini and R.M. Clay, J.Chem.Soc.,Dalton Trans., 577 (1978)
7. L. Fabbizzi, P. Paoletti and R.M. Clay, Inorg.Chem., 17, 1042 (1979).
8. R.M. Clay, personal communication.
9. D.K. Cabbiness and D.W. Margerum, J.Amer.Chem.Soc., 92, 2151 (1970).
10. D.H. Busch, Y. Hung, L.Y. Martin, S.C. Jackels and A.M. Tait, J.Amer.Chem.Soc., 99, 4029 (1977).
11. V.L. Goedken in 'Coordination Chemistry of Macrocyclic Compounds', Ed. G.A. Melson, Plenum, New York, 1979, pp.603-654.
12. B. Jaun and A. Pfaltz, J.Chem.Soc., Chem.Commun., 1327 (1986).
13. N. Herron, J.H. Cameron, G.L. Neer and D.H. Busch, J.Amer.Chem.Soc., 105, 298 (1983).
14. N. Herron, M.Y. Charan and D.H. Busch, J.Chem.Soc., Dalton Trans., 1491 (1984).
15. J. Almog, J.E. Baldwin and J. Huff, J.Amer.Chem.Soc., 97, 227 (1975).

16. J.P. Collman, R.R. Gagné, T.R. Halbert, J.C. Marchon and C.A. Reed, J.Amer.Chem.Soc., 95, 7868 (1973).

17. J.T. Groves and T.E. Nemo, J.Amer.Chem.Soc., 105, 5786 (1983).

18. D.H. Busch, E.S. Gore and F.V.Lovecchio, J.Amer.Chem. Soc., 96, 3109 (1974).

19. E.K. Barefield, G.M. Freeman and D.G. Van Derveer, Inorg.Chem., 25, 552 (1986).

20. A.J. Blake, R.O. Gould, A.J. Holder, T.I. Hyde, M.O. Odulate, A.J. Lavery and M. Schröder, J.Chem.Soc., Chem.Commun., 118 (1987).

21. A.J. Blake, R.O. Gould, A.J. Holder, T.I. Hyde, Y.V. Roberts, A.J. Lavery and M. Schröder, J.Organometal. Chem., in press.

22. A.J. Blake, A.J. Lavery and M. Schröder, Angew.Chem., 98, 282 (1986); Angew.Chem.,Int.Ed.Engl., 25, 274 (1986).

23. L. Fabbizzi and D.M. Prosperpio, Abstract A44, XI International Symposium on Macrocyclic Chemistry, Florence, 1986.

24. R.R. Durrand, C.S. Bencosme, J.P. Collman and F.C. Anson, J.Amer.Chem.Soc., 105, 2710 (1983).

25. J.P. Collman, M. Marrocco, P. Denisevich, C. Koval and F.C. Anson, J.Electroanal.Chem., 101, 117 (1979).

26. B.B. Wayland and A.R. Newman, Inorg.Chem., 20, 3093 (1981).

27. D. Pletcher and D.J. Pearce, J.Electroanal.Chem., 197, 317 (1986).

28. J.P. Sauvage, M. Beley, J.P. Collin and R. Ruppert, J.Chem.Soc., Chem.Commun., 1315 (1984).

29. J.P. Sauvage, M. Beley, J.P. Collin and R. Ruppert, J.Amer.Chem.Soc., 108, 7461 (1986).

30. B. Fischer and R. Eisenberg, J.Amer.Chem.Soc., 102, 2361 (1980).

31. M.J. Camenzind, D. Dolphin and B.R. James, J.Chem.Soc., Chem.Commun., 1137 (1986).

32. J.P. Collman and K. Kim, J.Amer.Chem.Soc., 108, 7847 (1986).

33. J.Y. Becker, B. Vainas, R. Eger and L. Kaufman, J.Chem.Soc.,Chem.Commun., 1471 (1985).

34. I. Taniguchi, N. Nakashima and K. Yasukouchi, J.Chem. Soc.,Chem.Commun., 1814 (1986).

35. B.B. Wayland and H.W. Bosch, J.Chem.Soc.,Chem.Commun., 900 (1986).

36. D. Pletcher, R. Rosas, J.Y. Becker and J.B. Kerr, J.Electroanal.Chem., 117, 87 (1981).

37. D.H. Busch, W.D. Lenke, K.E. Travis and N.E. Tokvoryan, Adv.Chem.Ser., 150, 358 (1977).

38. J.P. Collman, J.I. Brauman and A.M. Madonik, Organometallics, 5, 311 (1986).

39. J.H. Espenson and A. Balac, J.Amer.Chem.Soc., 108, 713 (1986).

40. J.P. Collman, P.J. Brothers, E. Rose, L.J. Wright and L. McElwee-White, J.Amer.Chem.Soc., 107, 4570 (1985).

41. J.P. Collman and P.J. Brothers, Acc.Chem.Res., 19, 209 (1986).

42. B.B. Wayland and K.J. Del Rossi, J.Chem.Soc.,Chem. Commun., 1653 (1986)

43. B.B. Wayland and A.R. Newman, J.Amer.Chem.Soc., 101, 6472 (1979).

44. N.F. Curtis and D.A. House, Chem.Ind., 42, 1708 (1961).

45. D.H. Busch and M.C. Thompson, Chem.Eng.News (Sept.17) 57 (1962).

46. L.J. Boucher in "Coordination Chemistry of Macrocyclic Compounds" Ed. G.A. Melson, Plenum, New York, 1979, pp.461-516.

47. D.H. Busch and J.L. Karn, Inorg.Chem., 8, 1149 (1969).

48. E.K. Barefield, D.G. Van Derveer and K.A. Foster, J.Chem.Soc.,Chem.Commun., 680 (1986).

49. C. K. Poon, C. M. Che and T. W. Tang, J.Chem.Soc., Dalton Trans., 1697 (1981).

50. L.J. Boucher in "Coordination Chemistry of Macrocyclic Compounds", Ed. G.A. Melson, Plenum, New York, 1979, pp.517-536.

51. D.H. Busch and E. Ochiai, Inorg.Chem., 8, 1474 (1969).

52. P. Moore, N.W. Alcock and H.A.A. Hadi, J.Chem.Soc., Dalton Trans., 985 (1986).

53. D.H. Busch, J.C. Dabrowiak, F.V. Lovecchio and V.L. Goedken, J.Amer.Chem.Soc., 94, 5502 (1972).

54. F.R. Keene, M.D. Ridd and M.R. Snow, J.Amer.Chem.Soc., 105, 7075 (1985).

55. T.A. Kaden and T.J. Lotz, Helv.Chim.Acta, 61, 1376 (1978).

56. P. Moore, N.W. Alcock, H.A.A. Omar and C. Pierpoint, J.Chem.Soc.,Dalton Trans., 219 (1985).

57. P. Moore, N.W. Alcock and K.P. Balakrishnan, J.Chem. Soc.,Chem.Commun., 1731 (1985).

58. D.E. Fenton and G. Rossi, Inorg.Chim.Acta, 98, L29 (1985).

59. T.A. Kaden and H. Haflinger, Helv.Chim.Acta, 62, 683 (1979).

60. E. Fleischer and D. Dewar, Nature, 222, 372 (1969).

61. R.N. Icke, B.B. Wisegarver and G.A. Alles in "Organic Synthesis", Wiley, New York, 1955, Collected Volumes III, p.723.

62. P. Moore, N.W. Alcock and K.F. Mok, J.Chem.Soc., Perkin II, 1186 (1980).

63. M.G.B. Drew, P.A. Rice, S.bin Silong and P.C. Yates, J.Chem.Soc.,Dalton Trans., 1081 (1986).

64. J.W. Krajewski, Z. Urbanczyk-Lipowska and P.Gluzinski, Crystal.Str.Comm., 6, 817 (1977).

65. D.D. Perrin, D.R. Perrin and W.L.F. Arma in "Purification of Laboratory Chemicals", 2nd Ed. Pergamon.

66. S.M. Nelson, Pure and Appl.Chem., 52, 2461 (1980).

67. K.B. Mertes and S. Brawner, J.Inorg.Nucl.Chem., 41, 764 (1979).

68. C.K. Poon, and C.M. Che, J.Chem.Soc.,Chem.Commun., 861 (1979).

69. "Advanced Inorganic Chemistry", Eds. F.A. Cotton and G.Wilkinson, 4th Ed., Wiley, New York, 1980, Chapter 22.

70. P.K. Bhattacharya, J.Chem.Soc.,Dalton Trans., 810 (1980).

71. T.P. Dasgupta, R.M. Milburn and L. Damrauer, Inorg. Chem., 9, 2789 (1970).

72. J.P. Collman and P.W. Schneider, Inorg.Chem., 5, 1380 (1966).

73. A.J. Blake and G. Reid, personal communication.

74. R.W. Hay and P.M. Gidney, J.Chem.Soc.,Dalton Trans., 974 (1976).

75. N.F. Curtis and D.F. Cook, J.Chem.Soc.,Dalton Trans., 691 (1972).

76. C.K. Poon, C.M. Che and T.W. Tang, J.Chem.Soc.,Dalton Trans., 1647 (1983).

77. C.K. Poon, C.M. Che, T.C.W. Mak, T.F. Lai and S.S. Kwong, Inorg.Chem., 24, 1359 (1985).

78. C.K. Poon, C.M. Che and S.S. Kwong, Inorg.Chem., 24, 1601 (1985).

79. C.K. Poon, C.M. Che and T.C.W. Mak, J.Chem.Soc.,Chem. Commun., 546 (1985).

80. C.K. Poon, C.M. Che and T.C.W. Mak, J.Chem.Soc.,Chem. Commun., 988 (1985).

81. C.K. Poon, C.M. Che and T.C.W. Mak, J.Chem.Soc.,Chem. Commun., 986 (1985).

82. C.M. Che and W.K. Cheng, J.Amer.Chem.Soc., 108, 4644 (1986).

83. C.M. Che and W.K. Cheng, J.Chem.Soc.,Chem.Commun, 1519 (1986).

84. T. Ito, H. Ito, M. Yamashita and K. Toriumi,Inorg. Chem., 22, 1566 (1983).

85. E. Kimura, Y. Lin, R. Machida and H. Zenda, J.Chem.Soc., Chem.Commun., 1020 (1986).

86. R.D. Feltham and R.G. Hayter, J.Chem.Soc.A 4587 (1964).

87. A.J. Blake, T.I. Hyde, R.S.E. Smith and M. Schröder, J.Chem.Soc.,Chem.Commun., 334 (1986).

88. C.K. Poon, C.M. Che and S.S. Kwong, Inorg.Chem., 24, 1601 (1985).

89. M.M. Doeff and D.A. Sweigart, Inorg.Chem., 20, 1683 (1981).

90. J.M. Clear, J.M. Kelly, C.M. O'Connell, C.J. Cardin, S.R. Costa and A.J. Edwards, J.Chem.Soc.,Chem.Commun., 750 (1980).

91. S.M. Nelson, M.G.B. Drew, S.G. McFall and C.P. Walters, J.Chem.Res.(S), 16 (1979).

92. R.D. Shannon, Acta Cryst.,Sec.A, 32, 751 (1976).

93. D.D. Walker and H. Taube, Inorg.Chem., 20, 2828 (1981).

94. J.M. Kelly, C.M. O'Connell and J.G. Vos, J.Chem.Soc., Dalton Trans., 253 (1986).

95. H. Ishida, K. Tanaka, M. Morimoto and T. Tanaka, Organometallics, 5, 724 (1986).

96. M.G.B. Drew and S. Hollis, Acta Cryst.Sec.B, 36, 718 (1980).

97. K. Nakamoto in "Infrared and Raman Spectra of Inorganic and Coordination Compounds", 3rd Ed., Wiley, New York, 1978.

98. E.R. Birnbaum, J.Inorg.Nucl.Chem., 33, 3031 (1971).

99. J.M. Jenkins and B.L. Shaw, J.Chem.Soc., 6789 (1965).

100. J.A. Ibers and B.A. Coyle, Inorg.Chem., 11, 1105 (1972).

101. "Advanced Inorganic Chemistry" Eds. F.A. Cotton and G. Wilkinson, 4th Ed., Wiley, New York, 1980, p.946.

102. H.D. Kaesz and R.B. Saillant, Chem.Rev., 72, 231 (1972).

103. B.R. James, R.H. Morris and P. Kvintovics, Can.J.Chem., 64, 897 (1986).

104. B. B. Wayland, B.A. Woods and M.D. Farnos, J.Amer. Chem.Soc., 108, 3659 (1986).

105. S.M. Nelson and A.J. Lavery, J.Chem.Soc., Dalton Trans., 615 (1984).

106. J.M. Millar, J.Organometal.Chem., 249, 299 (1983).

107. J.D. Gilbert, D. Rose and G. Wilkinson, J.Chem.Soc.A, 2765 (1970).

108. C.K. Poon, C.M. Che and K.Y. Wong, Inorg.Chem., 24, 1797 (1985).

109. D. Meyerstein, Y. Koresh, H. Cohen and N. Jubran, J.Chem.Soc.,Chem.Commun., 1683 (1984).

110. D. Meyerstein, G. Ginzberg, H. Cohen and N. Jubran, J.Chem.Soc.,Chem.Commun., 517 (1982).

111. D. Meyerstein, G. Ginzberg, H. Cohen and N. Jubran, Inorg.Chem., 24, 251 (1985).

112. A.J. Blake, R.O. Gould, T.I. Hyde and M. Schröder, J.Chem.Soc.,Chem.Commun, in press.

113. B. Bosnich, C.K. Poon and M.L. Tobe, Inorg.Chem., 4, 1102 (1965).

114. E.K. Barefield and F. Wagner, Inorg.Chem., 12, 2435 (1973).

115. P. Moore, J. Sachinidis and G.R. Willey, J.Chem.Soc., Chem.Commun., 522 (1983).

116. T.W. Hambley, J.Chem.Soc., Dalton Trans., 565 (1986).

117. S.F. Lincoln,J.H. Coates, D.A. Hadi and D.L. Pisaniello, Inorg.Chim.Acta, 81, L9 (1984).

118. L.G. Warner and D.H. Busch, J.Amer.Chem.Soc., 91, 4092 (1969).

119. R.D. Hancock, V.J. Thöm, C.C. Fox and J.C.A. Baeyens, J.Amer.Chem.Soc., 106, 5955 (1984).

120. E.K. Barefield, P. Paoletti, A. Bianchi, E.J. Billo, P.J. Connolly and J.S. Summers, Inorg.Chem., 25, 4197 (1986).

121. K. Broadley, G.A. Lane, N.G. Connelly and W.E. Geiger, J.Amer.Chem.Soc., 105, 2486 (1983).

122. P.M. Maitlis, P. Espinet and M.J.H. Russell in "Comprehensive Organometallic Chemistry", Eds. G. Wilkinson, F.G.A. Stone and E.W. Abel, Pergamon, 1982, p.265.

123. J.R. Boehm and A.L. Balch, Inorg.Chem., 16, 778 (1977).

124. A.W. Addison, B. Walts and M. Wicholas, Inorg.Chem., 23, 813 (1984).

125. E.P. Talsi, V.P. Babenko, V.A. Likholobov, V.M. Nekipelov and V.D. Chinakov, J.Chem.Soc.,Chem.Commun., 1786 (1985).

126. D.H. Busch and A.M. Tait, Inorg.Synth., 18, 10

127. L. Fabbizzi, A. Poggi and A. Bencini, Inorg.Chem., 20, 2544 (1981).

128. L. Fabbizzi and A. Poggi, Inorg.Chim.Acta, 39, 207 (1980).

129. E. Zeigerson, G. Ginzberg, J.Y. Becker, L.J. Kirschenbaum, H. Cohen and D. Meyerstein, Inorg.Chem., 20, 3988 (1981).

130. L. Fabbizzi and L. Sabatini, Inorg.Chem., 18, 438 (1979).

131. E. Kimura, T. Koike, H. Nada and Y. Iitaka, J.Chem.Soc., Chem.Commun., 1322 (1986).

132. C.L. Bailey, R.D. Bereman, D.P. Rillema and R. Nowak, Inorg.Chem., 23, 3956 (1984).

133. S.M. Nelson, S.G. McFall, C. Cairns and M.G.B. Drew, J.Chem.Soc.,Dalton Trans., 2020 (1980).

134. N.W. Alcock, D.C. Liles, M. McPartlin and P.A. Tasker, J.Chem.Soc.,Chem.Commun., 727 (1974).

135. K.P. Balakrishnan, T.A. Kaden, L. Siegfried and A.D. Zuberbühlor, Helv.Chim.Acta, 67, 1061 (1984).

136. L. Siegfried and T.A. Kaden, Helv.Chim.Acta, 67, 29 (1984).

137. C.W.G. Ansell, M.K. Cooper, K.P. Dancey, P.A. Duckworth, K. Henrick, M. McPartlin and P.A. Tasker, J.Chem.Soc., Chem.Commun., 439 (1985).

138. L.G. Scanlon, Y.Y. Tsao, K. Toman, S.C. Cummings and D.W. Meek, Inorg.Chem., 21, 1215 (1982).

139. D.W. Meek and J. Riker-Nappier, J.Chem.Soc.,Chem.Commun., 442 (1974).

140. D.A. Stotter and H. Keypor, Inorg.Chim.Acta, 33, L149 (1979).

141. A.J. Blake, R.C. Sharma and M. Schröder, unpublished results.

142. J. Lewis and M. Schröder, J.Chem.Soc., Dalton Trans., 1085 (1982).

143. R.R. Gagné and D.M. Ingle, Inorg.Chem., 20, 420 (1981).

144. R.R. Gagné, D.M. Ingle and G.C. Lisensky, Inorg.Chem., 20, 1991 (1981).

145. C.W.G. Ansell, M.C. Liptrot, P.R. Raithby, J. Lewis and M. Schröder, J.Chem.Soc., Dalton Trans., 1593 (1982).

146. E.B. Fleischer and S.W. Hawkinson, Inorg.Chem., 7, 2313 (1968).

147. R. Louis B. Metz and R. Weiss, Acta Cryst.Sec.B, 30, 774 (1974).

148. J. Nadra, H. Givadinovitch and M. Devand, J.Chem.Res. (S), 192 (1983).

149. A.H.A. Tinnemans, T.P.M. Koster, D.H.M.W. Thewissen and A. Mackor, Recl.Trav.Pays-Bas, 103, 288 (1984).

150. R.D. Jones, D.A. Summerville and F. Basolo, Chem.Rev., 79, 139 (1979).

151. K. Hasegawa, T. Imamura and M. Fujimoto, Inorg.Chem., 25, 2154 (1986).

152. J.P. Collman, T.R. Halpert and K.S. Suslick in "Metal Ion Activation of Dioxygen", Ed. T.G. Spiro, Wiley, New York, 1980, pp.1-72.

153. E. Kimura and R. Machida, J.Chem.Soc.,Chem.Commun., 499 (1984).

154. E. Kimura, R. Machida and M. Kodama, J.Amer.Chem.Soc., 106, 5497 (1984).

155. F.C. Anson and T. Geiger, J.Amer.Chem.Soc., 103, 7489 (1981).

156. J.F. Endicott, C.L. Wong, J.A. Switzer and K.P. Balakrishnam, J.Amer.Chem.Soc., 102, 5511 (1980).

157. J.W. van der Zwaan, S.P.J. Albracht, R.D. Fontijin and E.C.Slater, F.E.B.S. 179, 271 (1985).

158. M.Z. Hoffman, E. Hayon and A.M. Tait, Inorg.Chem., 15, 934 (1976).

159. D.C. Olson, J. Vasilevskis and K. Loos, J.Chem.Soc., Chem.Commun., 1718 (1970).

160. D. Pletcher, G. Gosden, J.B. Kerr and R. Rosas, J.Electroanal.Chem., 117, 101 (1981).

161. C.O. Dietrich-Buchecker, J.M. Kern and J.P. Sauvage, J.Chem.Soc., Chem.Commun., 760 (1985).

162. M.G. Simic and M.Z. Hoffman, J.Amer.Chem.Soc., 99, 2370 (1977).

163. M. Nappa, J.S. Valentine, A.R. Miksztal, R.J. Schugar and S.S. Isied, J.Amer.Chem.Soc., 101, 7744 (1979).

164. H. Ozawa and A. Hanaki, Inorg.Chim.Acta, 80, 33 (1983).

165. E.G. Jager and M. Rudolph, Z.Chem., 21, 371 (1981).

166. E.G. Jager and M. Rudolph, Z.Chem., 22, 66 (1982).

167. G. Cros, J.P. Costes and D. de Montauzon, Polyhedron, 3, 585 (1984).

168. R.I. Haines and A. McAuley, Coord.Chem.Rev., 39, 77 (1981).

169. K. Nag and A. Chakravorty, Coord.Chem.Rev., 33, 87 (1980).

170. A.H. Maki, N. Edelstein, A. Davidson and R.H. Holm, J.Amer.Chem.Soc., 86, 4580 (1964).

171. D.C. Olson and J. Vasilevskis, Inorg.Chem., 8, 1611 (1969).

172. A.J. Holder, T.I. Hyde and M. Schröder, unpublished results.

173. A. McAuley, M. Olubuyide and P.R. Norman, Inorg.Chem., 23, 1938 (1984).

Abbreviations

^{n}Bu	normal butyl
Bz	benzyl
D.E.P.T.	distortionless enhancement by polarization transfer
dmf	dimethylformamide
dmso	dimethyl sulphoxide
e.s.d.	estimated standard deviation
e.s.r.	electron spin resonance
e.i.	electron impact
Et	ethyl
f.a.b.	fast atom bombardment
Hz	Hertz
i.r.	infrared
MHz	megaHertz
Me	methyl
$MeNO_2$	nitromethane
MeCN	acetonitrile
MeOH	methanol
M.pt.	melting point
M	molecular weight
n.m.r.	nuclear magnetic resonance
Ph	phenyl
p.p.m.	parts per million
$TBAPF_6$	tetra-^{n}butyl ammonium hexafluorophosphate, $[^{n}Bu_4N]PF_6$
thf	tetrahydrofuran
UV/vis	ultra violet/visible

List of Courses Attended

Aspects of Structural Chemistry, by Dr. C. Glidewell.

Organometallic Chemistry, by Dr. M. Schröder.

Electro-analytical Methods, by Dr. G A. Heath.

The Use of Microcomputers with Instrumentation, by Dr. A. Rowley, Mr. King.

Chemical Technology and Industrial Chemistry, by Dr. Nichols, Dr. Mustoe and Dr. Sinclair.

Current Topics in Inorganic Chemistry, by Dr. M. Schröder, Dr. G.A. Heath, Dr. A.J. Welch and Professor E.A.V. Ebsworth.

Nuclear Magnetic Resonance, by Dr. I.H. Sadler.

Recent Developments in Electrochemistry, by Dr. G.A. Heath, and Dr. H. Girault.

University of Strathclyde Inorganic Club Conferences, 1984, 1985, 1986.

2nd International Platinum Metals Conference, Edinburgh, 1984.

3rd European Symposium on Macrocyclic Compounds, Stirling, 1984.

XXIV International Conference on Coordination Chemistry, Athens, 1986.

XI International Symposium on Macrocyclic Chemistry, Florence, 1986.

Synthesis of Platinum Metal Macrocyclic Complexes incorporating a Pyridine-2,6-diyl Moiety. The Single Crystal *X*-Ray Structure of *cis*-[$Ru^{II}Cl(CO)(L)](BPh_4$) {L = 2,7,12-trimethyl-3,7,11,17-tetra-azabicyclo[11.3.1]heptadeca-1,(17),13,15-triene}

Alexander J. Blake, Timothy I. Hyde, Rodney S. E. Smith, and Martin Schröder*

Department of Chemistry, University of Edinburgh, West Mains Road, Edinburgh EH9 3JJ, Scotland, U.K.

The single crystal *X*-ray structure of [$Ru^{II}Cl(CO)(L)](BPh_4$) {L = 2,7,12-trimethyl-3,7,11,17-tetra-azabicyclo[11.3.1]heptadeca-1,(17),13,15-triene} shows octahedral Ru^{II} co-ordinated to the pyridine-2,6-diyl macrocycle and to mutually *cis* chloro and carbonyl ligands; the syntheses of the related complexes *trans*-[$MCl_2(L)]^+$ (M = Rh^{III} or Ir^{III}) and $[M(L)]^{2+}$ (M = Pd^{II} or Pt^{II}) are reported.

Reprinted from the Journal of The Chemical Society
Chemical Communications 1986

Synthesis of Platinum Metal Macrocyclic Complexes incorporating a Pyridine-2,6-diyl Moiety. The Single Crystal *X*-Ray Structure of *cis*-[$Ru^{II}Cl(CO)(L)](BPh_4$) {L = 2,7,12-trimethyl-3,7,11,17-tetra-azabicyclo[11.3.1]heptadeca-1,(17),13,15-triene}

Alexander J. Blake, Timothy I. Hyde, Rodney S. E. Smith, and Martin Schröder*

Department of Chemistry, University of Edinburgh, West Mains Road, Edinburgh EH9 3JJ, Scotland, U.K.

The single crystal *X*-ray structure of [$Ru^{II}Cl(CO)(L)](BPh_4$) {L = 2,7,12-trimethyl-3,7,11,17-tetra-azabicyclo[11.3.1]heptadeca-1,(17),13,15-triene} shows octahedral Ru^{II} co-ordinated to the pyridine-2,6-diyl macrocycle and to mutually *cis* chloro and carbonyl ligands; the syntheses of the related complexes *trans*-[$MCl_2(L)]^+$ (M = Rh^{III} or Ir^{III}) and [$M(L)]^{2+}$ (M = Pd^{II} or Pt^{II}) are reported.

Metal macrocyclic complexes are generally highly thermodynamically stable and kinetically inert systems. The macrocycle can therefore be regarded as a protecting group for the metal centre controlling its stereochemical, electronic, and redox properties. The binding of platinum group metals to macrocyclic ligands, to form stabilised species with specific labile sites for substrate co-ordination and activation, is an area of great potential in the development of new catalytic systems.[1,2] As part of a general study of the binding of platinum metals to macrocyclic species, we have investigated the complexation of pyridine-2,6-diyl-containing macrocycles to a range of metal centres, and report here the single crystal *X*-ray structure of a

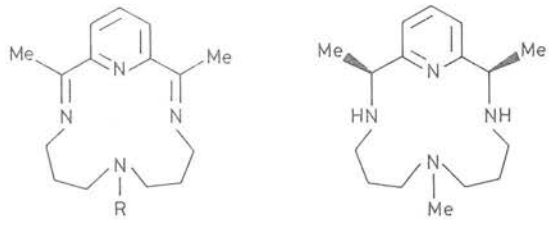

Ru^{II} carbonyl product, together with the synthesis of some related platinum metal species.

The majority of ruthenium macrocycles are based on porphyrin and phthalocyanine ligands.[3] More recently complexation to saturated tetra-aza macrocycles has been developed leading to the stabilisation of new, high-oxidation-state complexes.[2,4,5] Poon and Che, however, have reported[6] an unusual template synthesis of the π-acceptor di-imino ligand (**1**) around ruthenium to give a low valence species $[Ru(\mathbf{1})(OH_2)]^{2+}$. We have attempted to resynthesise this complex by the published procedure, but have been unable to prepare pure samples of $[Ru(\mathbf{1})(OH_2)]^{2+}$, the major product isolated showing bands in the i.r. spectrum assignable to ν_{NH} and ν_{CO} stretching vibrations indicative of only partial condensation of the macrocyclic product. Therefore, we have undertaken a study of metal insertion reactions into the related tetra-aza macrocycle (**2**),[7] leading towards an alternative synthesis of low valence complexes of (**1**).

$[RuCl_2(NCMe)_4]$ was treated with one equivalent of (**2**) in refluxing ethanol under CO for 24 h. Further reflux for 24 h under N_2 gave a dark orange solution and addition of NH_4PF_6 or $NaBPh_4$ yielded the corresponding salts of $[RuCl(CO)(\mathbf{2})]^+$ (by elemental analysis; 1 : 1 electrolyte in $MeNO_2$; ν_{CO} 1930 cm^{-1}, KBr disc) in up to 60% yield. Recrystallisation from $MeNO_2$ yielded red-brown crystals of $[RuCl(CO)(\mathbf{2})](BPh_4)$, a single crystal *X*-ray structural analysis of which was undertaken to confirm the co-ordination and conformation of the complex.†

Figure 1 shows the structure of the $[RuCl(CO)(\mathbf{2})]^+$ cation. The structure shows ruthenium(II) co-ordinated to all four nitrogen donors of (**2**), with three nitrogen donors bound equatorially, Ru–N(3) 2.116(9), Ru–N(11) 2.106(9), Ru–N(17) 2.038(8) Å, and the fourth donor, N(7), bent away to bind at an axial position, Ru–N(7) 2.138(8) Å. This leads to a unique folded conformation being adopted by (**2**) (Figure 1b). Mutually *cis* chloro and carbonyl ligands, Ru–Cl 2.422(3), Ru–C 1.830(10) Å, ∠Ru–C–O 175.2(9)°, complete the essentially octahedral co-ordination around ruthenium(II) with the carbonyl ligand *trans* to the pyridyl N(17) donor, and Cl *trans* to N(7); ∠N(17)–Ru–C 174.4(4), Cl–Ru–N(7)

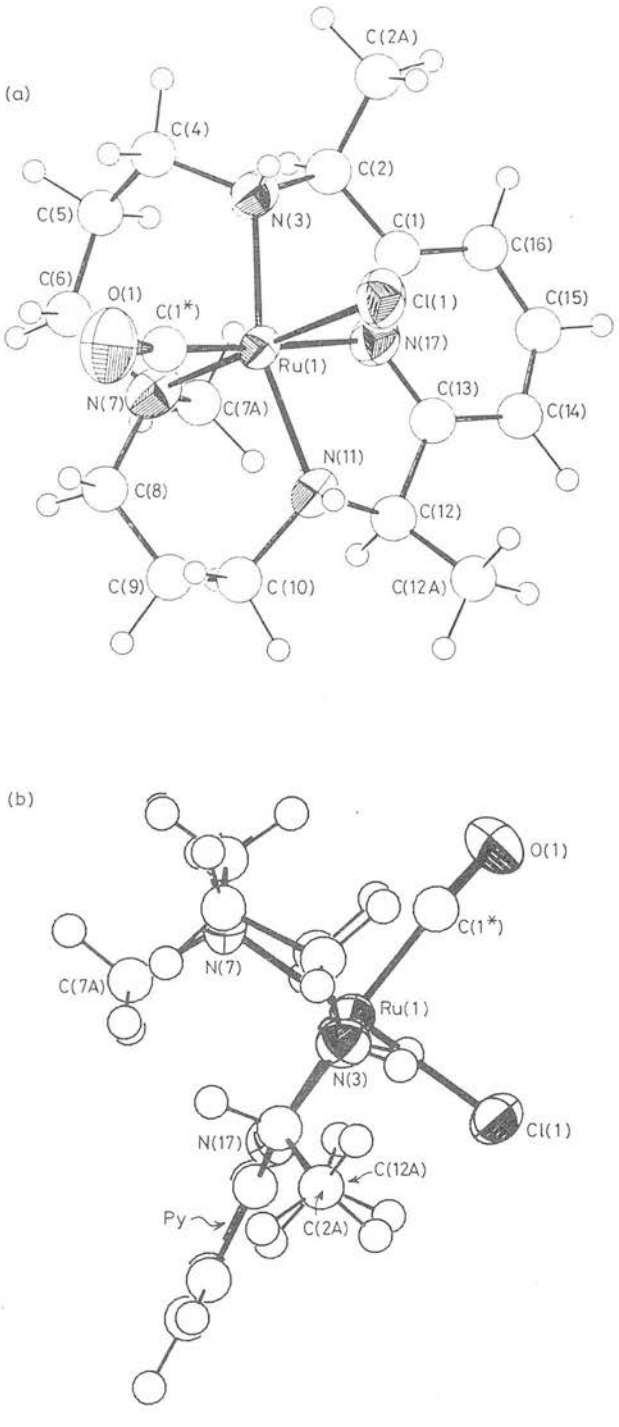

Figure 1. Views of the crystal structure of $[RuCl(CO)(\mathbf{2})]^{2+}$. In (b), N(11) is eclipsed by N(3) and C(12A) by C(2A).

† *Crystal data:* $C_{17}H_{28}ClN_4ORu^+ \cdot C_{24}H_{20}B^-$, M = 760.2, triclinic, space group $P\bar{1}$, a = 9.9854(17), b = 11.6723(22), c = 16.558(3) Å, α = 72.124(19), β = 89.210(15), γ = 82.200(15)°; U = 1818.9 Å^3, D_c = 1.388 g cm^{-3}, Z = 2, 4767 data measured to θ = 22.5°, refinement based on 3757 data with $F \geq 6.0\sigma(F)$. At convergence R and R_W = 0.0670 and 0.0948 respectively for 227 parameters. For structure solution, a Patterson synthesis yielded the Ru position and successive least-squares and difference Fourier syntheses gave the remaining atomic positions.[8] Unusually, the BPh_4^- groups are disordered, the disorder being readily modelled with the B atom and one phenyl ring ordered and each atom of the three remaining phenyl rings occupying two sites equally. For refinement,[8] hydrogen atoms were included at fixed, calculated positions; at convergence, the difference electron density map showed no feature above 0.84 e Å^{-3}.

The atomic co-ordinates for this work are available on request from the Director of the Cambridge Crystallographic Data Centre, University Chemical Laboratory, Lensfield Road, Cambridge CB2 1EW. Any request should be accompanied by the full literature citation for this communication.

179.2(2), Cl–Ru–N(17) 85.9(2), Cl–Ru–N(11) 87.5(2), Cl–Ru–N(3) 86.6(2), Cl–Ru–C 88.6(3)°. This complex represents the first example of ruthenium binding to a pyridyl macrocycle and also incorporates mutually *cis* chloro and carbonyl ligands which is a co-ordination mode not observed previously for ruthenium macrocycles, although related species have been proposed, but not confirmed, for ruthenium phthalocyanine and porphyrin complexes.[9] Interestingly, *cis*-co-ordination has been found also for the products $[RuCl_2(L)]^+$ (L = cyclam)[5] and $[RuCl_2(L)]$ (L = 1,4,8,11-tetrathiacyclotetradecane)[10] suggesting that such co-ordination may be more readily available for ruthenium macrocycles than is assumed currently.

The above work has been extended to the insertion of other platinum group metals into (**2**). Thus reaction of MCl_3 (M = Rh^{III} or Ir^{III}) with (**2**) in refluxing ethanol for 6 and 24 h respectively, followed by addition of PF_6^- counter-ion yielded the complexes $[MCl_2(\mathbf{2})](PF_6)$ while the complexes of type $[M(\mathbf{2})]^{2+}$ (M = Pd^{II} or Pt^{II}) have been prepared by reaction of (**2**) with $Pd(OAc)_2$ and $PtCl_2$ in dichloromethane for 24 h and ethanol for 72 h respectively.

The substitution chemistry and redox and electronic properties of this new range of platinum group metal macrocyclic complexes are under investigation.

We thank the S.E.R.C. for support, the S.E.R.C. and B.P. Chemicals for a C.A.S.E. award (to T. I. H.), and Johnson-Matthey P.L.C. for loans of platinum metals.

Received, 31st October 1985; Com. 1534

References

1 For examples of Ru-based catalysts see: G. Domazetis, B. Tarpey, D. Dolphin, and B. R. James, *J. Chem. Soc., Chem. Commun.*, 1980, 939; M. Pawlik, M. F. Hog, and R. E. Shepherd, *ibid.*, 1983, 1467; T. Leung, B. R. James, and D. Dolphin, *Inorg. Chim. Acta*, 1983, **79**, 180.
2 J. T. Groves and R. Quinn, *Inorg. Chem.*, 1984, **23**, 3844; C-M. Che, K-Y. Wong, and T. C. M. Mak, *J. Chem. Soc., Chem. Commun.*, 1985, 988.
3 D. Dolphin, B. R. James, and P. D. Smith, *Coord. Chem. Rev.*, 1981, **39**, 31; L. J. Boucher, 'Coordination Chemistry of Macrocyclic Compounds,' ed. G. A. Melson, pp. 461—536, Plenum, New York, 1979; K. Kasuga and M. Tsutsui, *Coord. Chem. Rev.*, 1980, **32**, 67.
4 D. D. Walker and H. Taube, *Inorg. Chem.*, 1981, **20**, 2828; C-M. Che, T-W. Tang, and C-K. Poon, *J. Chem. Soc., Chem. Commun.*, 1984, 641; T. C. W. Mak, C-M. Che, and K-Y. Wong, *ibid.*, 1985, 986; C-M. Che, K-Y. Wong, and T. C. W. Mak, *ibid.*, 1985, 546; C-M. Che, S-S. Kwong, and C-K. Poon, *Inorg. Chem.*, 1985, **24**, 1601, and references therein.
5 C-M. Che, S-S. Kwong, C-K. Poon, T-F. Lai, and T. C. W. Mak, *Inorg. Chem.*, 1985, **24**, 1359.
6 C-K. Poon and C-M. Che, *J. Chem. Soc., Chem. Commun.*, 1979, 861.
7 J. L. Karn and D. H. Busch, *Inorg. Chem.*, 1969, **8**, 1149.
8 G. M. Sheldrick, SHELX 76, Program for Crystal Structure Refinement, University of Cambridge, 1976.
9 M. M. Doeff and D. A. Sweigert, *Inorg. Chem.*, 1981, **20**, 1683; L. J. Boucher and P. Rivera, *ibid.*, 1980, **19**, 1816; E. B. Fleischer, R. Thorp, and D. Venerable, *Chem. Commun.*, 1969, 475.
10 T. F. Lai and C-K. Poon, *J. Chem. Soc., Dalton Trans.*, 1982, 1465.

Stabilisation of Trivalent Platinum by Structurally Accommodating Thiamacrocycles

Alexander J. Blake, Robert O. Gould, Alan J. Holder, Timothy I. Hyde, Aidan J. Lavery, Mobolanle O. Odulate, and Martin Schröder*

Department of Chemistry, University of Edinburgh, West Mains Road, Edinburgh EH9 3JJ, Scotland, U.K

The complex cation $[Pt(\mathbf{1})_2]^{2+}$ [(**1**) = 1,4,7-trithiacyclononane] shows a quasi square based pyramidal structure with one non-bonding sulphur donor atom; electrochemical oxidation at +0.5 V. *vs.* Fc^0/Fc^+ (Fc = ferrocene) at 20 °C in MeCN affords a paramagnetic platinum(III) species.

The majority of platinum(III) compounds are diamagnetic Pt–Pt dimers.[1,2] Few monomeric platinum(III) species have been generated, the well-documented examples including $[Pt(C_6Cl_5)_4]^-$,[3] $[Pt(L)_2]^+$ (L = diphenylglyoximate),[4] and [Pt(diamsar)]$^{3+}$ (diamsar = 1,8-diamino-3,6,10,13,16,19-hexa-azabicyclo[6.6.6.]icosane).[5] In view of the ability of macrocyclic ligands to stabilise unusual, otherwise unstable metal oxidation states, we undertook a study of the redox chemistry of platinum(II) macrocyclic complexes and report here structural and electrochemical results on the homoleptic bis-macrocyclic species $[Pt(\mathbf{1})_2]^{2+}$ [(**1**) = 1,4,7-trithiacyclononane].

Reaction of $PtCl_2$ or $K_2[PtCl_4]$ with two molar equivalents of (**1**) gives, on addition of NH_4PF_6, the complex $[Pt(\mathbf{1})_2](PF_6)_2$ in 70% yield. A single crystal *X*-ray structure† of the product shows two independent cations and four PF_6^- anions per asymmetric unit of the monoclinic cell. Views of

† *Crystal data* for $[Pt(\mathbf{1})_2](PF_6)_2$: $C_{12}H_{24}PtS_6^{2+}2PF_6^-$ monoclinic, $P2_1$, a = 11.848(4), b = 17.817(6), c = 11.750(11) Å, β = 98.06(4)°, U = 2456 Å^3, $D_{calc.}$ = 1.77 g cm^{-3}, Z = 4; 3515 data measured to θ = 22.5°, refinement based on 2721 data with $F \geq 6\sigma(F)$. At convergence, R,R_w = 0.044, 0.048 respectively for 354 parameters. Reflections with $h + l = 2n$ were much stronger than others, indicating that the two independent Pt atoms are related by a pseudo B-centring. Approximate positions derived from a Patterson synthesis were used as input to D.I.R.D.I.F.[6] which fixed both the origin and the enantiomorph of the structure, and two subsequent rounds located the other 64 non-hydrogen atoms in the structure. The data were corrected for absorption using D.I.F.A.B.S.,[7] hydrogen atoms were included in calculated positions, and Pt, P, and S atoms were refined anisotropically.[8] At convergence, the difference map showed no feature above 0.7 e Å^{-3}. Atomic co-ordinates, bond lengths and angles, and thermal parameters have been deposited at the Cambridge Crystallographic Data Centre. See Notice to Authors, Issue No. 1.

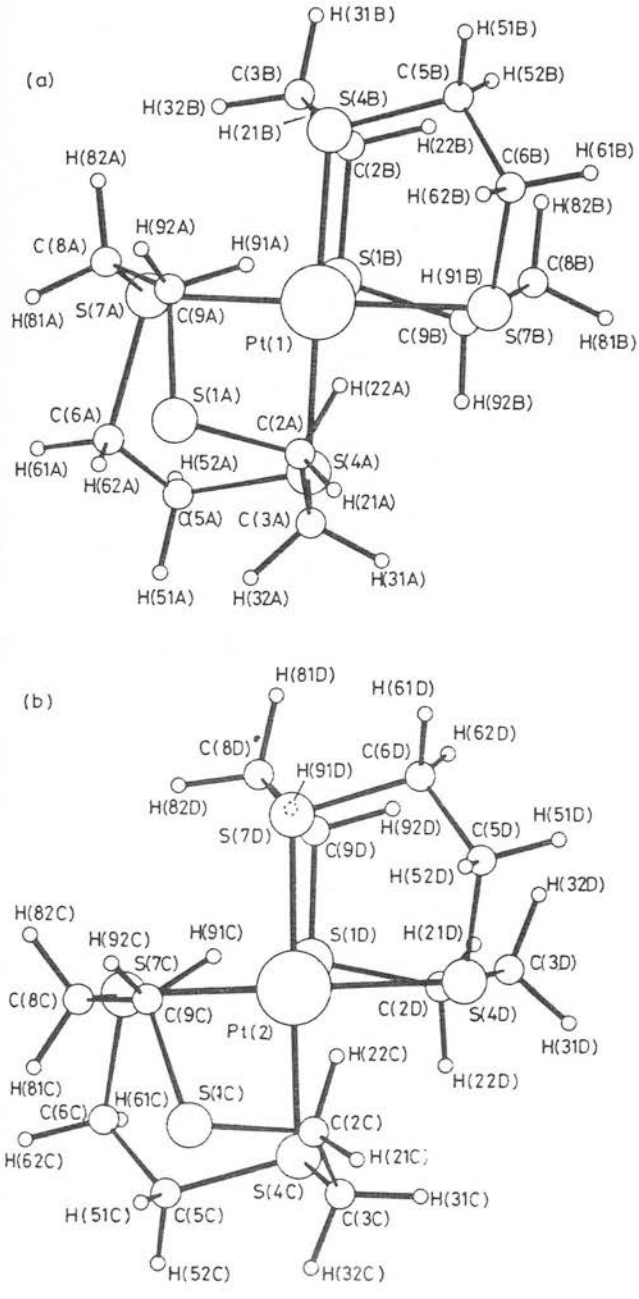

Figure 1. Single crystal *X*-ray structure of $[Pt(\mathbf{1})_2]^{2+}$ with numbering scheme adopted.

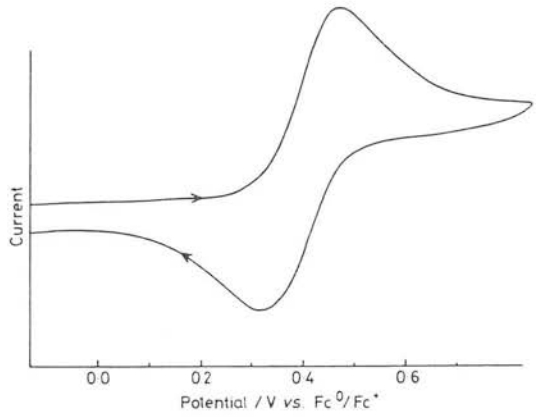

Figure 2. Cyclic voltammogram of $[Pt(\mathbf{1})_2](PF_6)_2$ in MeCN (0.1 M $Bu^n_4NPF_6$) at 20 °C at platinum electrodes. Scan rate = 100 mV s^{-1}. Fc = ferrocene.

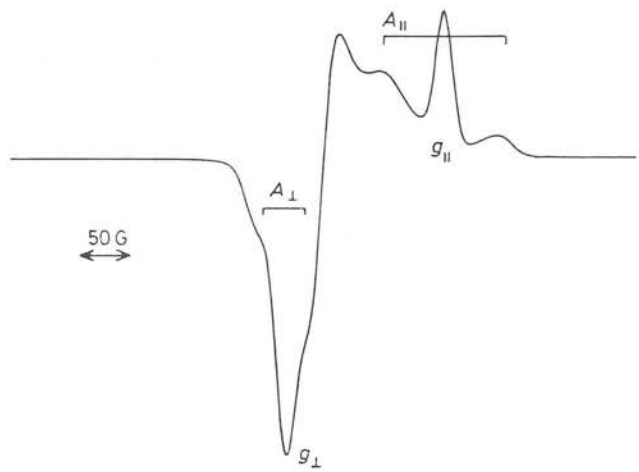

Figure 3. E.s.r. spectrum of $[Pt(\mathbf{1})_2]^{3+}$ at 77 K in MeCN glass. (1 G = 10^{-4} T.)

the two independent cations are shown in Figure 1. In both cases the Pt atoms are co-ordinated by four sulphur atoms from two ligands in a square plane (Pt–S = 2.25—2.30 Å; ∠SPtS = 88.1—91.5°). An elongated square pyramidal co-ordination is achieved in both cases by the third sulphur donor in one of the macrocycles co-ordinating apically (Pt–S′ = 2.88, 2.93 Å; ∠SPtS′ = 84.0—97.2°). The final sulphur atom is not co-ordinated with S · · · Pt = 4.04, 4.18 Å. This unusual stereochemistry around platinum(II) contrasts markedly with that observed for the 1,4,7-triazacyclononane analogue which is centrosymmetric with two dangling nitrogen donors and a square planar metal centre.[9]

Cyclic voltammetry of $[Pt(\mathbf{1})_2](PF_6)_2$ in MeCN (0.1 M $Bu^n_4NPF_6$) shows a one electron oxidation E_{pa} = +0.46 V, with a return wave at E_{pc} = +0.315 V *vs.* Fc^0/Fc^+, ΔE_p = 145 mV, I_{pa}/I_{pc} = 1.0 at a scan rate of 100 mV s^{-1} (Figure 2). Oxidation of the metal-free ligand (**1**), and of the complex cation $[Ni(\mathbf{1})_2]^{2+}$ occurs near +1.0 V[10] suggesting that the oxidation of $[Pt(\mathbf{1})_2]^{2+}$ might be occurring predominantly at the metal centre. Controlled potential electrolysis of $[Pt(\mathbf{1})_2]^{2+}$ ($\lambda_{max.}$ = 432 nm, ε = 95 dm^3 mol^{-1} cm^{-1}) at +0.5 V under N_2 (20 °C, MeCN) affords a stable oxidised product ($\lambda_{max.}$ = 401 nm, ε = 3500 dm^3 mol^{-1} cm^{-1}), the e.s.r. spectrum (77 K, MeCN glass) of which shows an anisotropic signal with $g_\perp$ = 2.044, $g_\parallel$ = 1.987 with coupling to ^{195}Pt (33.8%), $A_\perp$ = 30 G, $A_\parallel$ = 85 G (1 G = 10^{-4} T) (Figure 3). A similar e.s.r. spectrum has been reported previously for $[Pt(diamsar)]^{3+}$, prepared by γ-radiolysis of the platinum(IV) tetracation at 77 K, and assigned to a transient, octahedral platinum(III) species.[5] The co-ordination geometry of $[Pt(\mathbf{1})_2]^{3+}$ is likely therefore to be distorted octahedral with the trithia macrocycles adapting to the stereochemical and electronic requirements of d^7 platinum(III) and positive charge being delocalised onto the thia donors.

The importance of the ability of (**1**) to adjust its mode of co-ordination in response to the oxidation state of the metal is

reflected by the relative stability of the platinum(III) product, and by the oxidative inactivity of the related homoleptic species $[Pt(L)]^{2+}$ (L = 1,4,8,11-tetrathiacyclotetradecane,[11] 1,4,7,10,13,16-hexathiacyclo-octadecane[12]). The inactivity of the hexathia ligand to stabilise the higher valent state may reflect the inability of the two unbound sulphur donor atoms in the complex cation to complete octahedral or pyramidal co-ordination around the metal centre,[12] while for the tetrathia complex, co-ordination is restricted to square planarity. Interestingly, Wieghardt and coworkers have shown[9] that platinum(IV) can be readily stabilised using the corresponding triaza ligand system; this clearly reflects the electronic differences between poly-aza and -thia donors and suggests that homoleptic sulphur macrocycles may indeed be useful ligands for selective metal redox activation and control. The stabilisation of related d^7 palladium(III) and rhodium(II) species has also been achieved using (**1**), while work on the corresponding iridium(II) system is in progress.

We thank B.P. Chemicals and the S.E.R.C. for a CASE Award (to T. I. H.), the S.E.R.C. for support, Johnson-Matthey plc for generous loans of platinum metals, and Dr. R. J. Nelmes for data collection facilities.

Received, 14th July 1986; Com. 985

References

1 J. D. Woolins and P. F. Kelly, *Coord. Chem. Rev.*, 1985, **65**, 115.
2 T. V. O'Halloran and S. J. Lippard, *Isr. J. Chem.*, 1985, **25**, 130.
3 R. Usón, J. Forniés, M. Tomás, B. Menjón, K. Sünkel, and R. Bau, *J. Chem. Soc., Chem. Commun.*, 1981, 751.
4 H. Endres, H. J. Keller, H. van de Sand, and V. Dong, *Z. Naturforsch., Teil B*, 1978, **33**, 843.
5 H. A. Boucher, G. A. Lawrance, P. A. Lay, A. M. Sargeson, A. M. Bond, D. F. Sangster, and J. C. Sullivan, *J. Am. Chem. Soc.*, 1983, **105**, 4652.
6 P. T. Beurskens, W. P. Bosman, H. M. Doesbury, Th. E. M. van den Hark, P. A. J. Prick, J. H. Noordik, G. Beurskens, R. O. Gould, and V. Parthasarathia, D.I.R.D.I.F., Applications of Direct Methods to Difference Structure Factors, University of Nijmegen, Netherlands, 1983.
7 N. Walker and D. Stuart, *Acta Crystallogr., Sect. A*, 1983, **39**, 159.
8 G. M. Sheldrick, SHELX76, Program for Crystal Structure Refinement, University of Cambridge, 1976.
9 K. Wieghardt, M. Köppen, W. Swiridoff, and J. Weiss, *J. Chem. Soc., Dalton Trans.*, 1983, 1869.
10 K. Wieghardt, H-J. Kuppers, and J. Weiss, *Inorg. Chem.*, 1985, **24**, 3067.
11 A. J. Blake, R. O. Gould, A. J. Holder, and M. Schröder, to be published.
12 A. J. Blake, R. O. Gould, A. J. Lavery, and M. Schröder, *Angew. Chem.*, 1986, **98**, 282; *Angew. Chem., Int. Ed. Engl.*, 1986, **25**, 274.